Facultad de Ciencias Biológicas
Programa de Doctorado en Biomedicina y Biotecnología

Utilización de microRNAs como dianas terapéuticas en Distrofia Miotónica

Tesis Doctoral

Estefanía Cerro Herreros
Julio 2018

Trabajo dirigido por:

Dr. Rubén D. Artero Allepuz
Dra. M. Beatriz Llamusi Troisi

Departamento de Genética

Dr. **RUBÉN D. ARTERO ALLEPUZ**, Profesor Titular del Departamento de Genética de la Facultad de Ciencias Biológicas de la Universitat de València

Dra. **MARIA BEATRIZ LLAMUSI TROISI**, Doctora en Bioquímica e Investigadora del Instituto de Investigación Sanitaria INCLIVA,

INFORMAN

Que Doña Estefanía Cerro Herreros, licenciada en Biología por la Universidad de Alicante, ha realizado bajo nuestra supervisión el trabajo de investigación original recogido en la presente memoria y artículos adjuntos titulada "Utilización de microRNAs como dianas terapéuticas en Distrofia Miotónica"

Revisado el presente trabajo, expresan su conformidad para la presentación del mismo en el Departamento de Genética de la Universidad de Valencia, por considerar que reúne los requisitos necesarios para ser sometido a discusión ante el Tribunal correspondiente, para optar al grado de Doctor por la Universidad de Valencia dentro del Programa Oficial de Doctorado en Biomedicina y Biotecnología.

En Valencia, a 24 de abril de 2018

Dr. Rubén D. Artero Allepuz

Dra. M. Beatriz Llamusí Troisi

-Agradecimientos-

La verdad es que siempre imaginé que este día estaba aún muy lejos y sin embargo, aquí estoy, escribiendo los agradecimientos de mi tesis.

Quisiera empezar estos agradecimientos por mis raíces, porque soy lo que soy gracias a mi familia. Gracias al esfuerzo de mis padres, en los que he visto lo que es realmente la capacidad de sacrificio y el respeto por el trabajo, por su confianza en mí, por estar siempre a mi lado y ayudarme y apoyarme en todo lo que me he propuesto desde siempre. Gracias también a mi hermana Silvia, por ser tan especial en mi vida y demostrarme cada vez que voy a Lezuza lo mucho que me echa de menos; te quiero.

Me gustaría agradecer a Rubén, por la oportunidad de trabajar en su laboratorio y conocer así, de primera mano, lo que significa la investigación. Sin esa confianza depositada en mí, esto no habría sido posible. A mi co-directora de tesis, Bea, por enseñarme a trabajar en mis inicios en el laboratorio, por confiar en mí para este trabajo y por insistir en que yo sí que podía con todo lo propuesto.

Gracias a Piotr, por ser mi mejor amigo dentro y fuera del laboratorio, porque estos años de tesis sin ti no hubieran sido lo mismo. Espero que, aunque la ciencia nos separe, permanezcas siempre en mi vida. A Anna, mi italiana favorita, mi hermana mayor, mi compañera de cotilleos y de viajes. A María por ser una luchadora, por ser mi confidente y por ayudarme tanto en laboratorio. A Nerea mi "esclava" favorita, por estar siempre ahí para cualquier cosa y ser tan positiva. A Sarah "con h", por ser mi Queen of Winter, eres un amor, sigue así siempre. A Ari, porque nuestras fiestas de los primeros años de tesis, siempre quedaran en nuestro recuerdo.

Por supuesto, también quiero dar las gracias al consejo de sabios del laboratorio, a Amparo, Juanma y Vero quienes me vieron dar mis primeros pasos en el laboratorio y me han ayudado a subsanar más de un problema. A las jovencitas del laboratorio Mouli, Estela y Irene, por la ayuda prestada. A Rocío, Sandra, Sarah "la francesa" y Marta por dejar huella en mí, en su paso por el laboratorio. También quiero dar las gracias a los Moleculares y a los Bioquímicos por hacer que las comidas y los almuerzos sean más entretenidos.

Agradecer a todos los miembros del PAS, Javi, Paco, Edgar, Jota y Fede, por hacer que nuestro trabajo sea un poco más fácil. Pero, en especial a Carmen de Cultivos y a Nuria de secretaria por toda la ayuda prestada y por hacer que mi trabajo en la Universidad estos años sea infinitamente más fácil.

Me gustaría dar las gracias también a los que han hecho que todo sea más fácil fuera del laboratorio, al grupo de los Polacios y en especial a Josep, Noelia, Javi, Carmen, soy los mejores compañeros de fiesta. A María y Anabel, mis zumberas favoritas. A las Sara´s y a Diego por ser los mejores compañeros de piso del mundo.

Gracias a Almudena y a Vicky por todos estos años de amistad y de apoyo, porque siempre estáis ahí para escucharme cuando algo va mal; la Biología os puso en mi camino pero ya formáis parte de mi vida y mi familia. A Aingeru, Fabián, Zaragoza, Óscar y Lamia, porque los años en la carrera con vosotros fueron geniales. A Willy, Ecu, José Carlos y Alberto porque no concibo el Carnaval si no estáis vosotros. También quiero dar las gracias a mi primo Ernesto, por sacarme siempre una sonrisa y hacer que los momentos contigo sean geniales.

A mis amigos de Lezuza, porque aunque nunca haya sido capaz de explicarles que hacía con las moscas y los ratones nunca han dejado de preguntar y de interesarse por lo que hacía. En especial a Inma, por responder al teléfono cada vez que la he necesitado y por ser mí amiga desde que la memoria me alcanza a recordar.

Por último, gracias a Fran, por ayudarme tanto en estos años, por acompañarme al laboratorio sin quejarse cuando me tocaba trabajar en fin de semana y ayudarme a cambiar las moscas o poner etanol a las cosas. Gracias también, por aguantar mis malos momentos y haber sido parte de todos los buenos. Eres muy importante en mi vida. Te quiero.

En definitiva, a todos y a todas que ayudaron, confiaron en mí y estuvieron a mi lado durante toda esta etapa.

“La ciencia más útil

es aquella cuyo fruto es el más comunicable”

-Leonardo Da Vinci-

A mis abuelos

-Introducción General- 11

1. Distrofia miotónica 13

1.1. Mecanismo molecular de patogénesis 15

2. Las proteínas Muscleblind 19

2.1. Implicación de las proteínas Muscleblind en el metabolismo de RNAs 20

2.2. Papel de las proteínas Muscleblind en DM 20

3. Patogénesis muscular y espliceopatía 21

4. MicroRNAs 23

4.1. Biogénesis de microRNAs 23

4.2. Mecanismos de silenciamiento génico mediado por microRNAs 24

4.3. miRNAs alterados en DM 24

5. Modelos animales de DM 25

5.1. *Drosophila melanogaster* 25

5.2. *Mus musculus* 26

6. Medicina basada en RNA 27

7. Estrategias terapéuticas en DM1 28

7.1. Degradación del RNA mutante. 29

7.2. Inhibición de las interacciones patogénicas RNA-MBNL y regulación positiva de MBNL. 30

7.3. Corrección de las alteraciones moleculares aguas abajo del RNA tóxico 31

-Objetivos- 33

-Artículos- 37

-Artículo 1-: Expanded CCUG repeat RNA expression in *Drosophila* heart and muscle trigger Myotonic Dystrophy type 1-like phenotypes and activate autophagocytosis genes 39

-Artículo 2- Derepressing muscleblind expression by miRNA sponges ameliorates myotonic dystrophylike phenotypes in *Drosophila* 55

-Artículo 3- *miR-23b* and *miR-218* silencing increase Muscleblind-like expression and alleviate myotonic dystrophy phenotypes in mammalian models 71

-Resultados principales- 87

1. Caracterización funcional y molecular de un modelo muscular en *Drosophila* de Distrofia miotónica tipo 2 89

1.1. La expresión de expansiones de repeticiones CCUG en el músculo de la mosca provoca el secuestro de Muscleblind en foci, afectando al *splicing* alternativo y al proceso autofágico 90

1.2. La expresión de expansiones CCUG en el músculo de mosca reduce el área muscular, la función motora y la supervivencia media. 90

2. Desrepresión de Muscleblind mediante silenciamiento de miRNAs represores en un modelo en *Drosophila* de Distrofia miotónica tipo 1: Prueba de concepto 91

2.1. El silenciamiento de *dme-miR-277* o *dme-miR-304* desreprime la expresión de Muscleblind en el músculo de *Drosophila* 92

2.2. *dme-miR-277* y *dme-miR-304* regulan diferentes isoformas de Muscleblind 93

2.3. El silenciamiento de *dme-miR-277* y *dme-miR-304* potencia la expresión de Muscleblind y rescata cambios en la expresión génica de transcritos definidos en moscas modelo de DM1..... 94

2.4. El silenciamiento de *dme-miR-277* o *dme-miR-304* mejora la atrofia muscular, la locomoción y la supervivencia de las moscas modelo de DM1 94

3. Silenciamiento de miRNAs represores específicos de la expresión de MBNL1 y MBNL2 en un modelo celular y murino de DM1 95

3.1. Identificación de miRNAs reguladores de *MBNL1* y *MBNL2* 95

3.2. Mapeo de los sitios de unión miRNA-mRNA al 3'UTR de *MBNL1 / 2*..... 96

3.3. El silenciamiento de *miR-23b* y *miR-218* estabiliza los transcritos de *MBNL1/2* y rescata los defectos en el *splicing* en mioblastos DM1..... 96

3.4. Los AntagomiRs-23b y -218 restauran la distribución subcelular normal de las proteínas MBNL..... 97

3.5. La administración sistémica de AntagomiRs en ratones HSA^{LR} aumenta la expresión muscular de Mbnl..... 98

3.6. Los AntagomiRs rescatan los defectos en el *splicing* muscular en ratones HSA^{LR} .. 98

3.7. El silenciamiento de *miR-23b* y *miR-218* rescata la histopatología muscular y reduce la miotonía en ratones HSA^{LR} 99

3.8. El tratamiento con AntagomiRs rescata a largo plazo fenotipos funcionales y no produce efectos deletéreos 99

-Discusión general-..... 101

1. Las moscas modelo de DM2 son una importante herramienta in vivo donde probar nuevos enfoques terapéuticos para la distrofia miotónica tipo 2 103

2. El silenciamiento de *dme-miR-277* y *dme-miR-304* potencia la expresión de Muscleblind y rescata alteraciones moleculares y funciones típicas de DM1 en *Drosophila*.....104

3. El silenciamiento de *miR-23b* y *miR-218* incrementa la expresión de las proteínas MBNL rescatando fenotipos característicos de DM1 en modelos mamíferos. 106

-Conclusiones-..... 109

-Bibliografía -..... 113

-Introducción General-

1. Distrofia miotónica

La distrofia miotónica (DM) es la forma de afección muscular más común de aparición en el adulto y la segunda forma más habitual de enfermedad del músculo esquelético tras la Distrofia muscular de Duchenne. La DM es una enfermedad de herencia autosómica dominante y multisistémica con un patrón clínico complejo que incluye miotonía progresiva, degeneración y debilidad muscular, pérdida muscular, defectos en la conducción cardíaca, cataratas iridiscentes y trastornos endocrinos (Harper 2001, Ranum et al. 2004, Schara et al. 2006). A pesar de considerarse una enfermedad rara, la prevalencia de DM a nivel mundial es de 1/8000 y dada la existencia de formas moderadas o asintomáticas de la enfermedad se estima que la incidencia real sea mayor (Udd et al. 2012).

Actualmente se conocen dos tipos genéticamente distintos de DM de comienzo en la edad adulta, la distrofia miotónica tipo 1 (DM1, OMIM #160900) y la distrofia miotónica tipo 2 (DM2, OMIM #602668). Ambas son enfermedades clínicamente parecidas pero con causas genéticas distintas (Tabla I1). La distrofia miotónica tipo 1 o enfermedad de Steinert, fue descrita por primera vez en 1909 por el médico alemán Hans Steinert y se origina por una expansión del triplete CTG en la región 3´ no traducida (UTR) del gen de la *Proteína quinasa DM* (*DMPK*, Entrez 1760) localizado citogenéticamente en la región cromosómica 19q13.3 (Brook et al. 1992, Fu et al. 1992, Harley et al. 1992, Mahadevan et al. 1992) (Figura I-1). Posteriormente, al descubrimiento de la mutación causante de la DM1, en 1994, se describieron tres casos de pacientes con manifestaciones clínicas de la DM1 pero no presentando la expansión patológica del trinucleótido CTG en el gen DMPK (Ricker et al. 1994, Thornton et al. 1994, Meola et al. 1996, Udd et al. 1997). Esta enfermedad se denominó en Europa como miopatía miotónica proximal (PROMM Meola et al. 1996) mientras que, en los Estados Unidos, se denominó distrofia miotónica tipo 2 (Thornton et al. 1994). Estudios posteriores demostraron que la DM2 se originaba por una mutación dinámica en la región cromosómica 3q21.3 (Ranum et al. 1998, Liquori et al. 2001). Esta mutación consiste en la expansión de repeticiones CCTG en el intrón 1 del gen de *CCHC-type zinc finger nucleic acid binding protein* (*CNBP*, Entrez 7555, también conocido como ZNF9) (Figura I1).

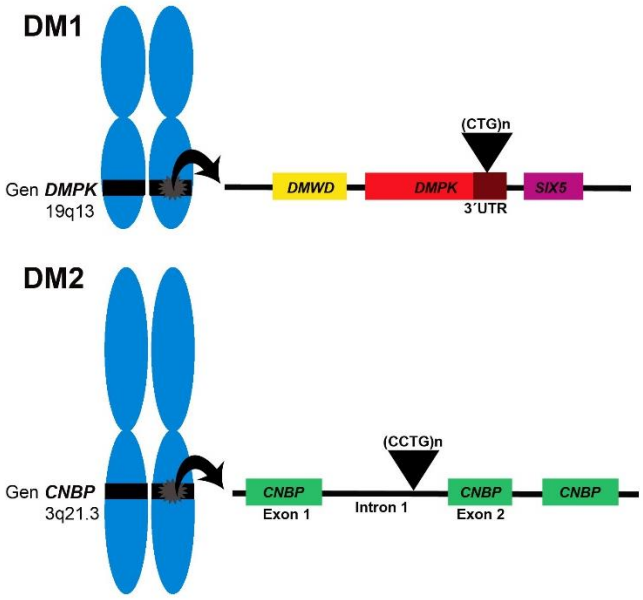

Fig. I-1. Representación esquemática de las mutaciones causantes de la DM: (Parte superior) Se muestra el contexto genómico de la DM1, donde se indica la localización cromosómica de la mutación genética y el tipo de mutación (CTG) dentro del 3´UTR del gen *DMPK* (caja roja). La región flanqueante a *DMPK* contiene los genes *DMDW* y SIX 5 (cajas amarilla y violeta, respectivamente). (Parte inferior) Contexto genómico de la DM2, donde se indica la localización cromosómica de la mutación (CCTG) causante de la enfermedad situada dentro del intrón 1 del gen *CNBP* (cajas verdes).

En individuos sanos, el gen *DMPK* presenta de 5 a 35 copias de este trinucleótido, mientras que, en pacientes de la DM1 este gen contiene más de 50 copias del trinucleótido CTG. Generalmente, el número de repeticiones en células sanguíneas está correlaccionado con la gravedad de los síntomas y la edad a la que comienzan a manifestarse. Así, en la forma adulta de la enfermedad, que suele manifestarse en la segunda década de la vida, el rango de repeticiones oscila entre 50 y 4000 (Harley et al. 1992, Meola et al. 2015). En los casos en el que el número de repeticiones alcanza los miles de copias, la enfermedad se manifiesta desde el nacimiento en forma de distrofia miotónica congénita (DMC). En la DM1, el número de repeticiones CTG aumenta de generación en generación. Por consiguiente, la edad de aparición desciende y la gravedad de la enfermedad aumenta de padres a hijos, lo cual se conoce como anticipación genética. Esto es debido a que la longitud de las expansiones está relacionada con la inestabilidad de estas secuencias tanto en células somáticas como germinales, de forma que a mayor número de repeticiones mayor inestabilidad (Monckton et al. 1995, Martorell et al. 1998, Meola et al. 2015). La inestabilidad meiótica se observa como una variación intergeneracional del número de repeticiones, y es la explicación molecular del fenómeno de la anticipación que se observa en las familias afectadas. La inestabilidad mitótica se refleja con un elevado mosaicismo somático y una heterogeneidad en el número de repeticiones entre y dentro de los tejidos del mismo individuo, que irá incrementando a lo largo de la vida del individuo (Higham et al. 2012, Morales et al. 2012).

En la DM2, el rango patológico va desde 75 hasta 11.000 repeticiones CCTG. Los síntomas de este tipo de distrofia miotónica son similares a los de la DM1 aunque suelen ser más leves y de progresión más lenta en DM2 (Liquori et al. 2001, Schara et al. 2006). En el gen *CNBP*, los individuos sanos tienen menos de 26 repeticiones mientras que los alelos con un numero de repeticiones entre 27-74 se consideran como ‘‘gray-zone’, desconociéndose si son patológicos o no (Kamsteeg et al. 2012). Al igual que las expansiones CTG, el tamaño de las expansiones CCTG parece aumentar con el tiempo y estas repeticiones son inestables en las células somáticas. Contrariamente a lo que ocurre en la DM1, en la DM2, el tamaño de las expansiones CCTG no parecen marcar ninguna diferencia en la edad de aparición o en la gravedad de la enfermedad, al igual que la anticipación genética que parece ser poco significativa (revisado en Meola et al. 2017).

Las distrofias miotónicas tipo 1 y 2 muestran un espectro clínico muy amplio (Tabla I-1), donde ambas enfermedades se consideran afecciones degenerativas de desarrollo lento, que en general es más leve para la distrofia miotónica tipo 2. Clínicamente DM1 es más diversa que DM2, pues nos encontramos subtipos como la forma congénita grave de la enfermedad (DMC) presente desde el desarrollo en la DM1 y que no se ha encontrado en la DM2.

Tabla I-1: Aspectos moleculares y clínicos de la DM1 y la DM2

Aspectos	DM1	DM2
Herencia	Autosómica dominante	Autosómica dominante
Tipo de expansión	CTG	CCTG
Tamaño normal repeticiones	≥37	≥27
Tamaño patológico repeticiones	>50	>75
Rango patológico repeticiones	50-4000	75-11000
Edad de inicio	Infancia – edad adulta	Infancia – edad adulta avanzada
Anticipación	Si	No (?)
Forma congénita	Presente	Ausente
Cataratas	Presente	Presente
Atrofia Muscular	Presente	Presente
Debilidad muscular	Presente	Presente
Miotonía clínica	Presente	Presente en <50%
Miotonía EMG	Siempre presente	Ausente o variable
Trastornos del sueño	Presente	Infrecuente
Deterioro cognitivo	Prominente	No es aparente
Arritmia cardíaca	Presente	De ausente a grave en algunos grupos de pacientes
Hipogonadismo masculino	Presente	Presente
Esperanza de vida	Reducido	Normal

1.1. Mecanismo molecular de patogénesis

El hecho de que dos mutaciones dinámicas en genes diferentes causen enfermedades con sintomatología similar sugiere un mecanismo de patogénesis común basado en la toxicidad de RNAs que contienen las expansiones CUG y CCUG (Mankodi et al. 2000, Osborne et al. 2006, revisado en Gomes-Pereira et al. 2011) como un factor necesario y suficiente para causar la DM1 y la DM2. En el año 2000, Mankodi y colaboradores describieron el primer ratón transgénico que expresaba RNAs con 250 repeticiones CTG en un contexto génico independiente de *DMPK*. Estos ratones transgénicos desarrollaban miotonía, miopatía y eventos de *splicing* alterados característicos de la DM1 (Mankodi et al. 2000, Lin et al. 2006), lo que demostraba que las repeticiones CUG son tóxicas *per se*.

En el núcleo, el RNA que contiene las expansiones CUG o CCUG se pliega formando una estructura en horquilla “imperfecta” (con desapareamientos “U-U”) capaz de unir y secuestrar a proteínas de unión a doble cadena de RNA (dsRNA). Consecuentemente, se forman grandes agregados ribonucleares, también conocidos como foci ribonucleares (Michalowski et al. 1999, Miller et al. 2000, Tian et al. 2000, Mooers et al. 2005). Estas expansiones interfieren por secuestro u otros mecanismo en la actividad de un número creciente de proteínas cuyas funciones son la regulación del *splicing* alternativo, transcripción, traducción, poliadenilación, biogénesis de miRNA, estabilidad y localización intracelular de mRNA (Liquori et al. 2001, Timchenko et al. 2001, Krol et al. 2007, Lee et al. 2009, Rau et al. 2011, Fernandez-Costa et al. 2013, Batra et al. 2014, Kalsotra et al. 2014, resvisado en Meola et al. 2015 y Konieczny et al. 2017). De modo, que estas moléculas dejan de estar presentes en sus localizaciones subcelulares correspondientes y su función resulta alterada.

Entre los reguladores del *splicing* secuestrados por CUG y CCUG, están las proteínas Muscleblind-like 1-3 (MBNL1-3) (Miller et al. 2000, Fardaei et al. 2002, Mankodi et al. 2003, Kino et al. 2004), las ribonucleoproteínas heterogéneas nucleares hnRNP F y hnRNP H (Jiang et al. 2004, Kim et al. 2005, Paul et al. 2006) y Staufen1 (Ravel-Chapuis et al. 2012). Por otro lado, los niveles de la proteína CELF1 (del inglés CUGBP Elav-like family member 1) están aumentados en mioblastos, músculo esquelético y corazón de pacientes DM1 debido a la hiperfosforilación de dos regiones de la proteína, una mediada por la proteína quinasa C (PCK) y la otra por la activación de la ruta Akt/GSK3β (Kuyumcu-Martinez et al. 2007, Jin et al. 2009). Estas fosforilaciones provocan la estabilización de la proteína en los núcleos celulares (Timchenko et al. 2001, Salisbury et al. 2008). MBNL1 y CELF1 regulan el *splicing* alternativo de manera antagónica de forma que el balance entre ambas proteínas determina la exclusión o inclusión de exones específicos (Figura I2). El desequilibrio de este balance en la DM1 origina defectos en el *splicing* de un gran número de transcritos (Tabla I2). Por ejemplo, en la regulación del exón 5 del transcrito de la troponina cardíaca (cTNT), mientras MBNL1 reprime su inclusión, CELF1 la promueve. Ambas proteínas reconocen regiones diferentes en los transcritos inmaduros por lo que su antagonismo no se debe a fenómenos de competencia por el sitio de unión (Ho et al. 2004, Ho et al. 2005).

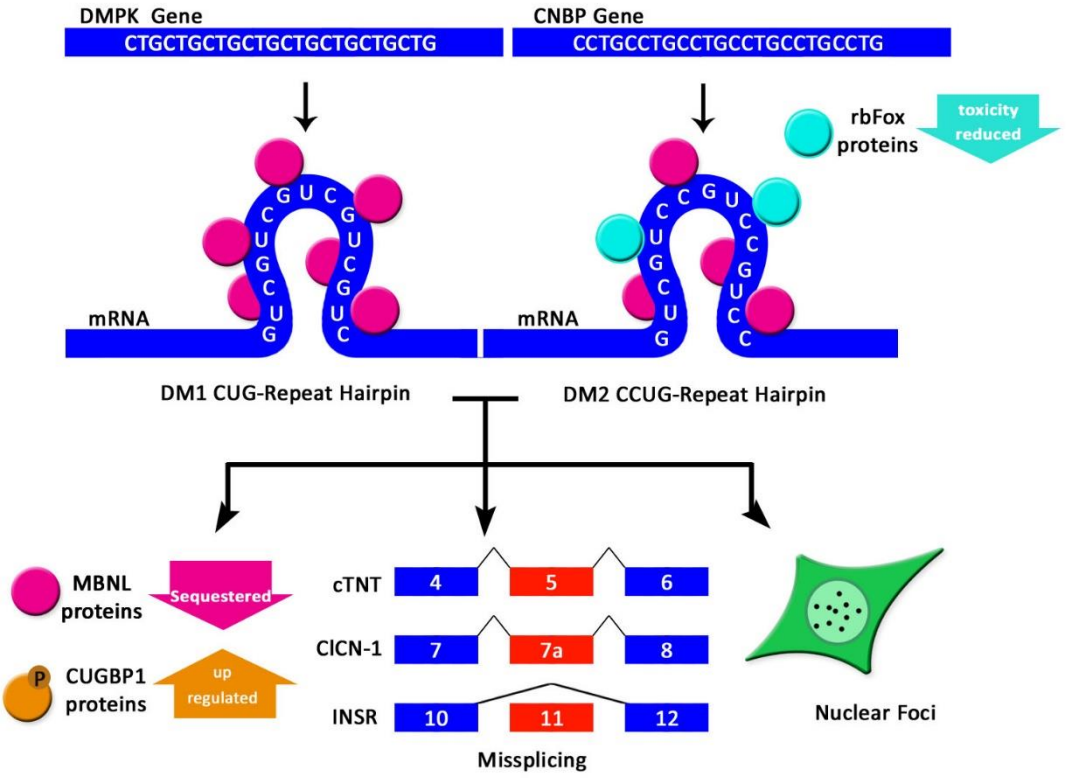

Fig. I-2. Modelo de RNA tóxico para la DM1 y la DM2. En células normales, con transcritos *DMPK* y *CNBP* con pocas repeticiones CUG y CCUG, existe un equilibrio entre las proteínas MBNL y CELF, el cual mantiene patrones de *splicing* adultos para una serie de transcritos como *INSR*, *CLC-1* y *cTNT*. Las expansiones CUG en células DM1 (izquierda) y CCUG en células DM2 (derecha) se pliegan en horquillas, lo cual tiene al menos dos consecuencias patogénicas: secuestro de MBNL en inclusiones nucleares (foci) y activación de proteína kinasa C (PKC), la cual hiperfosforila y estabiliza CELF en el núcleo. Estas alteraciones tienen un efecto sinérgico ya que MBNL1 y CELF1 regulan de forma antagónica muchos transcritos, produciendo patrones *splicing* característicos de estadíos fetales. En el caso de la DM2 las proteínas rbFox se unen a las expansiones CCUG compitiendo con las proteínas MBNL, siendo las proteínas rbFox un posible modulador de la toxicidad en la patología.

Como ya se ha mencionado anteriormente, la DM2 sigue un curso clínico más favorable que la DM1, sin embargo, son múltiples los estudios moleculares que sugieren que los síntomas de la DM2 deberían ser más graves que los de la DM1, en vez de suceder al contrario (Liquori et al. 2001, Kino et al. 2004, Wu et al. 2016). Por ejemplo, las proteínas MBNL se unen con mayor afinidad a las expansiones CCUG que a las CUG de modo que, en igualdad de condiciones, se esperaría mayor secuestro de las proteínas en la DM2 que en la DM1. Dicha paradoja sugiere la existencia de modificadores específicos que puedan modular la gravedad de la DM2. En este sentido un artículo recientemente publicado, apunta a las proteínas de unión al RNA rbFOX como posibles moduladoras (Figura I-2). Dichas proteínas compiten con MBNL1 por la unión a las repeticiones CCUG expandidas en células musculares DM2, pero no a las repeticiones CUG típicas de DM1 (Sellier et al. 2018).

Además de los errores en el *splicing* de transcritos, proceso que se conoce como espliceopatía y que se explica más adelante, en la DM1 las proteínas MBNL también se unen a los extremos 3´UTR de transcritos y participan en el control del patrón de poliadenilación. Centenares de transcritos musculares en ratones modelo para la enfermedad, y en biopsias de músculo de pacientes, mantienen un patrón de poliadenilación fetal en vez de los típicos de adulto (Batra et al. 2014). Las proteínas MBNL también participan en la biogénesis de miRNAs, pequeños RNAs no codificantes con función reguladora. MBNL1 se une a un motivo UGC localizado en el bucle del pre-miR-1, facilitando el procesado por Dicer que genera el miRNA maduro. En condiciones patológicas, el secuestro de MBNL1 conduce a una reducción en los niveles de *miR-1* en músculo cardíaco de pacientes y biopsias de músculo de pacientes (Rau et al. 2011, Fernandez-Costa et al. 2013). Sin embargo, estudios independientes han encontrado *miR-1* sobreexpresado en bíceps de pacientes (Perbellini et al. 2011), sin aclarar el origen de estas diferencias.

Tabla I-2: Ejemplos de eventos de *splicing* alternativo desregulados en DM1

Pre-mRNA	Exón/Intrón desregulado	Tipo de desregulación	Referencia
Músculo esquelético y cardíaco			
INSR	Exón 11	Exclusión	(Savkur et al. 2001)
CLCN-1	Intrón 2	Inclusión	(Mankodi et al. 2002)
	Exón 7a	Inclusión	(Charlet et al. 2002)
BIN1	Exón 11	Exclusión	(Fugier et al. 2011)
Cav1.1	Exón 29	Exclusión	(Tang et al. 2012)

cTNT	Exón 5	Inclusión	(Ho et al. 2004)
TNNT3	Exón fetal	Inclusión	(Kanadia et al. 2003)
RyR1	Exón 70	Exclusión	(Kimura et al. 2005)
SERCA1	Exón 22	Exclusión	
SERCA2	Intrón 19	Inclusión	
ZASP	Exón 11	Inclusión	(Lin et al. 2006)
Titin	Exón Zr4	Inclusión	
	Exón Zr5	Inclusión	
CAPN3	Exón 16	Exclusión	
FHOS	Exón 11a	Exclusión	
GFPT1	Exón 10	Exclusión	
MBNL1	Exón7	Inclusión	(Lin et al. 2006)
	Exón 6	Inclusión	(Yamashita et al. 2012)
MBNL2	Exón7	Inclusión	(Lin et al. 2006)
	Exón8	Inclusión	(Yamashita et al. 2012)
SMYD1	Exón 39	Inclusión	(Du et al. 2010)
Antígeno 9 asoc. Esperma	Exón 39	Inclusión	
MTMR1	Exón 2.1, 2.3	Exclusión	(Buj-Bello et al. 2002)
DTNA	Exón 11a, 12	Inclusión	(Nakamori et al. 2008)
MYOM1	Exón 17a	Inclusión	(Koebis et al. 2011)
ATPG2	Exón 1	Inclusión	(Yamashita et al. 2012)
MXRA7	Exón 4	Inclusión	
NCOR2	Exón 10	Inclusión	
NEB	Exón 116	Inclusión	
TTN	Exón 45	Inclusión	
PKM	Exón 10	Inclusión	(Gao et al. 2013)
SOS1	Exón 25	Exclusión	(Nakamori et al. 2013)
ATP2A1	Exón 22	Exclusión	
ALPK3	Exón 2	Inclusión	
NFIX	Exón 7	Inclusión	
LDB3	Exón 11	Inclusión	(Yamashita et al. 2014)
Cerebro			
TAU	Exón 2, 3	Exclusión	(Sergeant et al. 2001)
	Exón 6	Exclusión6c, inclusión 6d	(Leroy et al. 2006)
	Exón 10	Exclusión	(Sergeant et al. 2001, Jiang et al. 2004)
NMDAR1	Exón 5	Inclusión	(Jiang et al. 2004)
APP	Exón 7	Exclusión	
GRIN1	Exón 4	Inclusión	(Suenaga et al. 2012)
MAPT	Exón 3, 12	Exclusión	
SORBS1	Exón 26	Exclusión	
DCLK1	Exón 19	Exclusión	
CAMK2D	Exón 14, 15	Exclusión	

2. Las proteínas Muscleblind

Las proteínas Muscleblind (Mbl) fueron identificadas inicialmente en *Drosophila* (Begemann et al. 1997, Artero et al. 1998). El gen *mbl*, en *Drosophila* se encuentra localizado en el cromosoma 2R y mediante *splicing* alternativo a partir de un único gen, se generan al menos catorce isoformas diferentes. La mayoría de los transcritos comparten una región común en 5´, pero difieren en la región 3´, generando proteínas de diferente longitud y región carboxilo terminal (Begemann et al. 1997, Irion 2012). En *Drosophila*, Mbl es una proteína con expresión principal en el sistema nervioso central (SNC) embrionario y en musculatura somática y visceral (Artero et al. 1998, Llamusi et al. 2013, Bargiela et al. 2014).

A diferencia de invertebrados donde existe un único gen *mb*l, en humanos y ratón existen tres homólogos Muscleblind: *MBNL1*, *MBNL2* y *MBNL3* (Miller et al. 2000, Fardaei et al. 2002, Kanadia et al. 2003). En mamíferos, los tejidos en los que se expresan MBNL1 y MBNL2 coinciden e incluyen músculo esquelético adulto, corazón, cerebro, intestino, hígado, pulmón, riñón y placenta. Sin embargo, MBNL3 se expresa únicamente durante el desarrollo embrionario en placenta y en adulto de forma transitoria en músculo esquelético cuando existe regeneración muscular debido a un daño (Fardaei et al. 2002, Kanadia et al. 2003, Lee et al. 2007, Poulos et al. 2013).

Una de las características estructurales de las proteínas Mbl es la presencia de motivos de tipo dedo de zinc (ZnF) CCCH en su extremo N-terminal, que se encuentran conservados a lo largo de la evolución (Vicente-Crespo et al. 2008, Irion 2012, Oddo et al. 2016, Hale et al. 2018). Dichos motivos participan en el reconocimiento de las dianas de Muscleblind a través de la unión a horquillas de RNA que contienen desapareamientos entre pirimidinas (Warf et al. 2007, Goers et al. 2008). MBNL1 interacciona con el RNA mediante cuatro ZnF que se pliegan en dos dominios compactos en tándem (ZF1-2 y ZF3-4)(Teplova et al. 2008) que se unen a motivos YGCY del pre-mRNA, los cuales, además, son necesarios para la actividad como factor de *splicing* de MBNL1 (Goers et al. 2010).

Además de los ZnF, otra región altamente conservada en las proteínas Muscleblind es el motivo KRAEK que se encuentra en la región C-terminal de la proteína. Este motivo no es necesario para la actividad como regulador del *splicing* de Muscleblind, pero sí lo es para su correcta localización nuclear (Vicente-Crespo et al. 2008, Fernandez-Costa et al. 2010, Kino et al. 2015). La mutación del motivo KRAEK en células S2 de *Drosophila*, reduce la localización nuclear de MblC, una isoforma de Muscleblind, pero no de otras isoformas con localizaciones diferentes como son MblA de localización periplásmica y MblB en citoplasma (Fernandez-Costa et al. 2010). Estudios de localización subcelular en cultivos celulares de mamífero demostraron que para la correcta localización nuclear de MBNL1 es necesaria la participación de un segundo motivo similar a KRAEK presente en el exón 7 del pre-mRNA (Terenzi et al. 2010, Tran et al. 2011, Kino et al. 2015). La inclusión de este exón en el mRNA maduro está regulada por la misma MBNL1 (Gates et al. 2011) de manera que la actividad de MBNL1 está autoregulada mediante el acoplamiento del control de la localización nuclear y el *splicing* alternativo.

2.1. Implicación de las proteínas Muscleblind en el metabolismo de RNAs

Aunque algunos estudios recientes señalan a las proteínas MBNL como reguladores de la poliadenilación alternativa (Batra et al. 2014, Goodwin et al. 2015), estabilidad de mRNAs (Masuda et al. 2012), localización (Adereth et al. 2005) o de la biogénesis de miRNA en el citoplasma (Rau et al. 2011), la función más conocida y caracterizada de estas proteínas es la de regulación del *splicing* alternativo. Dichas proteínas en cerebro, corazón y músculo esquelético regulan el *splicing* alternativo de los transcritos de diversos genes, que codifican para proteínas estructurales del sarcómero muscular, proteínas implicadas en la adhesión celular y componentes del citoesqueleto, moléculas de señalización y proteínas relacionadas con la excitación y contracción muscular (Machuca-Tzili et al. 2006, Vicente et al. 2007, Vicente-Crespo et al. 2008, Wang et al. 2012, Picchio et al. 2013). En humanos, MBNL1 regula los cambios de patrones de *splicing* durante el desarrollo muscular y del corazón (Lin et al. 2006, Kalsotra et al. 2008), mientras que MBNL2 tiene un papel similar en el sistema nervioso central (Charizanis et al. 2012, Goodwin et al. 2015). Además, MBNL2 puede complementar funcionalmente a su parálogo MBNL1 y así regular el *splicing* alternativo de transcritos de forma semejante a este último, pues tiene un patrón de expresión en gran parte solapante (Ho et al. 2004, revisdo en Fernandez-Costa et al. 2011, Lee et al. 2013). El papel de MBNL3 como regulador del *splicing* es más dudoso ya que no se ha demostrado su actividad *in vivo*, aunque es capaz de controlar el *splicing* de determinados exones in vitro (Ho et al. 2004, Poulos et al. 2013).

Se ha propuesto un modelo posicional de la actividad de las proteínas MBNL sobre el *splicing*, pudiendo actuar como activadoras o represoras del *splicing.* Basándose en aproximaciones bioinformáticas y en los motivos de unión ZnF de MBNL1 a sus transcritos regulados, se determinó que MBNL1 se unía corriente arriba de los exones que reprimía y aguas abajo de los exones en los que promovía su inclusión (Du et al. 2010, Goers et al. 2010, Sen et al. 2010, revisado en Fernandez-Costa et al. 2011). El modelo de represión mediada por MBNL1 está basado en la caracterización de la unión de MBNL1 a la troponina cardíaca humana (*TNNT2*) (Warf et al. 2007). En este modelo, MBNL1 se une a los motivos YGCY aguas arriba del sitio de *splicing* 3' del exón 5, estabilizando a una horquilla en el tracto de pirimidinas. El tracto de pirimidinas no es reconocido por la subunidad 65 del factor U2AF y como consecuencia el exón se excluye del transcrito maduro (Warf et al. 2009). Aunque el mecanismo de activación del *splicing* no está del todo claro, se ha demostrado que la activación del *splicing* mediada por MBNL1 es dependiente de factores activadores (proteínas SR) (Sen et al. 2010), por lo que se ha sugerido que MBNL1 puede actuar favoreciendo el reconocimiento de las regiones de activación del *splicing* (ESEs), reprimiendo el de las regiones inhibidoras (ISSs) o ayudando al reconocimiento del sitio de *splicing* 5' por la maquinaria basal de *splicing* (Fernandez-Costa et al. 2011).

2.2. Papel de las proteínas Muscleblind en DM

En los últimos años, se han generado un número importante de modelos animales para DM1 así como mutantes para miembros de la familia Muscleblind. Estudios con ratones transgénicos modelo para la enfermedad mostraron que existían 156 transcritos cuyo *splicing* se encontraba alterado por las expansiones CUG. El mismo experimento realizado con ratones *knock-out* (KO) de *Mbnl1* dejó de manifiesto que más del 80% de los sucesos de *splicing* alternativo alterados anteriormente también lo estaban en estos ratones. Estos datos sugieren que el secuestro y la consiguiente pérdida de función de MBNL1 tiene un papel crucial en el

desarrollo de la enfermedad (Du et al. 2010). Los ratones KO para *Mbnl1* permitieron demostrar la función clave de las proteínas MBNL para el desarrollo de la DM1 y la DM2 ya que reproducían muchos de los síntomas presentes en los pacientes tales como cataratas iridiscentes, miotonía y defectos histológicos en tejido muscular (Kanadia et al. 2003). Además, recientemente se ha descrito que los ratones mutantes *Mbnl1* desarrollan problemas cardiacos prominentes en la DM1 (hipertrofia cardíaca, fibrosis intersticial, alteraciones en el *splicing* alternativo de transcritos) con tan solo dos meses de edad, fenotipos que empeoran notablemente tras seis meses de vida, lo cual sugiere un papel clave en la iniciación de los problemas cardiacos en la patología (Dixon et al. 2015). No obstante, los KO para *Mbnl1* no recapitulan el rango completo de síntomas de la DM1, pudiendo estar Mbnl2 compensando la falta de función de Mbnl1 en estos ratones. Por ello se generó un ratón KO para *Mbnl1* en el que la función *Mbnl2* está adicionalmente reducida (*Mbnl1*(-/-) ; *Mbnl2*(+/-)), estos ratones son viables y desarrollan aspectos cardinales de la enfermedad, incluyendo vida media reducida, bloqueo de la conducción cardíaca, miotonía grave, fibras atróficas y debilidad muscular esquelética progresiva, espliceopatía y defectos en la poliadenilación de transcritos en el SNC (Lee et al. 2013, Goodwin et al. 2015). Como demostración de la hipótesis de la compensación, los niveles de Mbnl2 estaban elevados en ratones KO Mbnl1(-/-) y Mbnl2 regulaba exones normalmente regulados por Mbnl1 (Lee et al. 2013). De forma similar a ratón, en *Drosophila* la pérdida de función de Mbl causaba defectos en las uniones entre músculo y epidermis así como alteraciones en las bandas Z en los sarcómeros musculares (Artero et al. 1998).

La demostración definitiva del papel clave de Muscleblind en la DM1 se consiguió mediante la sobrexpresión de la proteína en modelos animales de DM1. La sobrexpresión de Mbnl1 o MBNL1 en un ratón que expresa 250 repeticiones CUG revertió tanto la espliceopatía como la miotonía (Kanadia et al. 2006, Chamberlain et al. 2012). De manera similar, la sobrexpresión de MBNL1 humano y de la isoforma C de Muscleblind (MblC) en moscas que expresaban repeticiones CTG consiguió rescatar parcialmente la atrofia muscular, los defectos cardíacos y los fenotipos de ojo rugoso característicos de moscas modelo DM1 (de Haro et al. 2006, Garcia-Lopez et al. 2008, Bargiela et al. 2015, Chakraborty et al. 2018). Por tanto, el análisis de fenotipos en estos modelos a diferentes niveles ha determinado que los niveles críticamente bajos de proteínas MBNL en DM1 son la principal contribución al fenotipo final.

3. Patogénesis muscular y espliceopatía

El músculo esquelético es el principal tejido afectado en la DM, pues es donde se manifiestan la miotonía, la debilidad muscular y la degeneración; síntomas definitorios de la patología (Cho et al. 2007). La miotonía, característica de ambas enfermedades, se define como un retraso en la relajación de los músculos después de la contracción voluntaria o la estimulación eléctrica. Sin embargo, la principal causa de minusvalía en los pacientes no es la miotonía sino la debilidad muscular causada por una degeneración muscular progresiva, lo que se define como distrofia. Aunque el patrón inicial de debilidad muscular es notablemente diferente entre DM1 y DM2 (distal vs proximal), las biopsias musculares muestran una histología similar de nucleación central (Figura I-3) y un aumento en el tamaño de las fibras (Meola et al. 2004). La degeneración muscular o atrofia, también es diferente entre ambos tipos DM, pues como se muestra por la

tinción con ATPasa, se produce preferentemente en fibras de tipo 1 en DM1 y en fibras de tipo 2 en DM2 (Vihola et al. 2003).

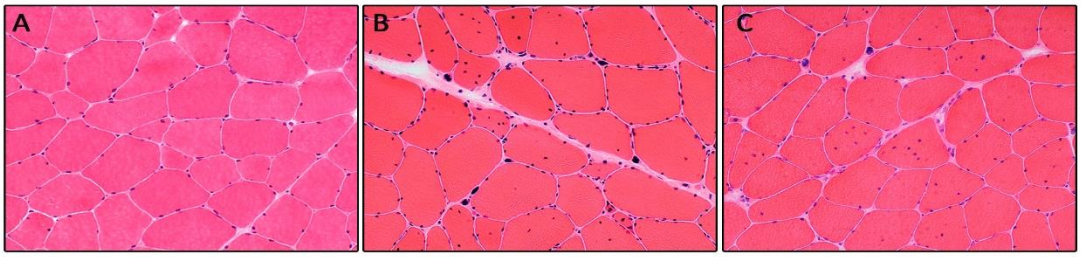

Fig. I-3. Histopatología en músculo esquelético. Secciones histológicas de músculo esquelético de un control (A), de un paciente con DM1 (B) y de un paciente con DM2 teñidas con hematoxilina eosina. Las fibras musculares de los pacientes presentan incrementado el número de núcleos centrales en comparación con el control.

Los síntomas musculares a nivel molecular, se han relacionado con errores en la regulación del *splicing* alternativo que provocan la presencia de variantes de *splicing* fetales de algunos transcritos en tejidos adultos; es por ello que a la DM, a nivel molecular se la conoce como una espliceopatía. En concreto se ha relacionado directamente la espliceopatía muscular con la miotonía, la debilidad muscular y la resistencia a la insulina. La miotonía se ha relacionado con errores en el procesado del exón 7a del gen del canal de cloro tipo 1, *CLCN1* (Charlet et al. 2002, Mankodi et al. 2002). Este exón presenta un codón de parada prematuro y su inclusión en el transcrito final genera una proteína truncada no funcional. Además estos transcritos son degradados por la vía NMD (del inglés non-sense mediated decay). En individuos sanos, esta variante solo está presente en el feto, sin embargo en los pacientes se expresa durante toda la vida. La expresión de esta variante no funcional junto a la reducción en la transcripción del gen en el músculo de los pacientes (Ebralidze et al. 2004), se traduce en una reducción en la conductancia del cloruro, causando despolarización y desestabilización de los potenciales de membrana en las fibras musculares, lo que provoca la miotonía. Al igual que el empalme alternativo desregulado del *CLCN1* detectado en los tejidos musculares de la DM1 y la DM2, el *splicing* alterado del exón 22 de *ATP2A1* (*SERCA1*) puede alterar la señalización intracelular de Ca2+ afectando a la excitabilidad sarcolemal en los miotubos DM1 y DM2 e influir en la miotonía (Santoro et al. 2014).

Otro ejemplo de espliceopatía relacionada con síntomas en la DM1 se encuentra en la debilidad muscular. La eliminación del exón 11 en los transcritos maduros del gen de la Anfifisina 2 (*BIN1*) en el músculo esquelético de pacientes de DM1 se ha correlacionado con la debilidad muscular (Fugier et al. 2011). Los transcritos de la proteína BIN1 en pacientes carecen del exón 11 y la presencia de dicha isoforma se correlaciona directamente con la gravedad de la enfermedad y la alteración en la organización de la red de túbulos T, lo que se traduce en debilidad muscular. Al igual que el caso anterior los defectos detectados en el procesado del exón 29 en transcritos del *calcium channel voltage-dependent* (*CACNA1s*) que codifica para el canal de calcio Cav1.1.1 también se han visto relacionados con la debilidad muscular (Tang et al. 2012, Santoro et al. 2014).

La resistencia a la insulina que presentan los pacientes tanto de DM1 como de DM2 se debe a la expresión en músculo esquelético adulto de una isoforma fetal del gen del receptor de insulina, INSR. En los pacientes de DM el exón 11 es preferentemente excluido lo que da lugar a la conservación de la isoforma INSR-A de baja señalización en enfermos adultos. Estos defectos en el *splicing* y la baja respuesta metabólica asociada a la menor capacidad de señalación del receptor de la insulina, predisponen a los pacientes a padecer diabetes (Savkur et al. 2001, Savkur et al. 2004).

4. MicroRNAs

Los microRNAs (miRNAs, miRs) son RNAs monocatenarios no codificantes de pequeño tamaño (20 – 24 pares de bases) cuya función es regular la expresión a nivel post-transcripcional. Esta regulación se lleva a cabo mediante la modificación de la estabilidad de los mensajeros y de la traducción de los mismos (Bartel 2009, Cech et al. 2014). Esta forma de regulación es generalmente negativa, ya que promueve la degradación de los mRNA y el bloqueo de su traducción (Guo et al. 2010).

4.1. Biogénesis de microRNAs

En animales los transcritos primarios (pri-miRNAs) producidos por la RNA polimerasa II son procesados por la RNasa tipo III, Drosha, en el núcleo. El precursor generado de unos 70 nt posee una estructura de horquilla (pre-miRNA) que es exportada al citoplasma, en un proceso mediado por exportina 5 (EXP5). En el citoplasma, el pre-miRNA es procesado por otra RNasa tipo III, Dicer, de modo que se genera un miRNA de doble hebra de unos 20-21 nt. En el último paso en la maduración una de las hebras del RNA se integra en el complejo miRISC que contiene proteínas Argonauta (Ago). Esta hebra constituye el miRNA maduro y es utilizada por el complejo RISC (*RNA-induced silencing complex*) para seleccionar sus mRNAs diana por complementariedad de secuencia con el miRNA maduro (Figura I-4) (Hammond et al. 2001, Bohnsack et al. 2004, Lee et al. 2004, Lee et al. 2004, Gregory et al. 2005, Bouhour et al. 2007).

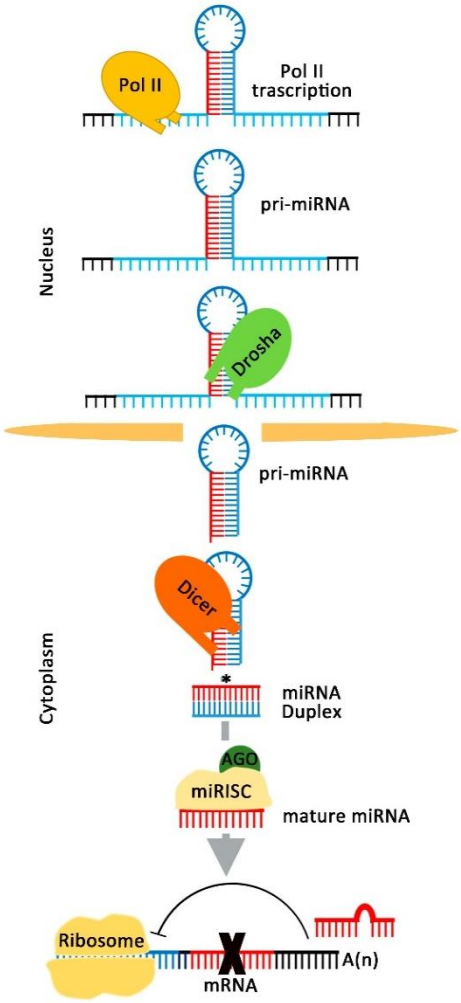

Figura I-4. Ruta de biogénesis de miRNAs. En la ruta canónica de biogénesis, los miRNAs se transcriben como transcritos precursores primarios (pri-miRNAs) que son procesados en el núcleo por Drosha para generar una o más horquillas precursoras (pre-miRNAs). Dicer procesa las horquillas en el citoplasma generando el miRNA maduro que se incorpora al complejo RISC para silenciar la expresión génica de sus mRNAs diana.

La mayoría de miRNAs siguen la ruta de biogénesis canónica. Sin embargo se han descrito mecanismos alternativos que generan miRNAs maduros. Estos mecanismos se pueden agrupar en dos grupos principales: las rutas independientes del Microprocesador también conocida como ruta de los miRtrones y las rutas independientes de Dicer (Revisado en Creugny et al. 2018)

4.2. Mecanismos de silenciamiento génico mediado por microRNAs

En las últimas dos décadas, una variedad de estudios bioquímicos, genéticos y bioinformáticos han determinado el mecanismo por el cual los miRNAs reconocen sus mensajeros diana. La mayoría de los mRNAs dianas de miRNAs, son reconocidos por medio de la complementariedad que existe entre la región 3' no traducida de los mRNAs y la región semilla del microRNA situada entre los nucleótidos 2-8 del extremo 5' del miRNA (Lewis et al. 2003, Ambros 2004, Bartel 2009, Carthew et al. 2009). Estudios *in vitro* determinaron que los nucleótidos de la región semilla por si solos son capaces de reprimir la expresión de sus dianas y que cambios en la secuencia de la región semilla alteran esta represión (Obad et al. 2011). Puesto que la zona requerida para la unión miRNA:mRNA es tan pequeña, un único miRNA puede silenciar una gran variedad de transcritos y un mRNA puede ser regulado por diferentes miRNAs a la vez (Lim et al. 2005, Peter 2010, Wu et al. 2010). Aunque la unión de la región semilla es fundamental para la represión de sus dianas, el apareamiento de nucleótidos en posición 13 y 16, la presencia de bases A y U cerca de la región semilla o la proximidad de varios sitios de unión del miRNA en el 3' del mensajero diana, aumentan la especificidad y la estabilidad de la unión mejorando la eficiencia en la represión de transcritos mediada por miRNAs (Lai 2002, Brennecke et al. 2005, Grimson et al. 2007, Nielsen et al. 2007).

Los miRNA no pueden actuar por sí solos, deben formar parte del complejo ribonucleoproteico RISC para ejercer su función represora. El componente principal del miRISC es una proteína de la familia Argonauta la cual provee una plataforma única para el reconocimiento del mRNA diana y su silenciamiento (Figura I-4). Una vez formado el complejo miRNA:mRNA, el miRISC induce el silenciamiento mediante varios procesos moleculares que incluyen la represión traduccional por medio de la inhibición del inicio de la traducción o desestabilización del mRNA mediante degradación de la cola poli A (Filipowicz et al. 2008, Djuranovic et al. 2010). Por tanto, el resultado de la interacción entre el miRISC y el mRNA es una disminución en la producción de la proteína diana (Guo et al. 2010), afectando de esta forma a los distintos procesos biológicos en los que ésta participa.

4.3. miRNAs alterados en DM

Los miRNAs juegan un papel crucial en la mayoría de los procesos biológicos, lo que explica que la alteración de miRNAs específicos o de sus dianas se haya asociado a diferentes enfermedades humanas como el cáncer (Melo et al. 2011, Peng et al. 2016), cardiopatías (Latronico et al. 2009), enfermedades musculares (Eisenberg et al. 2007), metabólicas (Deiuliis 2016) y neurodegenerativas (Hebert et al. 2009, Lee et al. 2011).

Según algunos estudios, queda demostrado que los miRNAs se encuentran también implicados en el mecanismo de patogénesis de DM1. A partir de biopsias de músculo de pacientes y homogeneizados de músculo de moscas modelo para DM1, se demostró que la expresión de algunos miRNAs, o su localización subcelular, se encontraban alteradas. Estos

resultados mostraron que la expresión de *miR-206* y *miR-335* estaba aumentada mientras que la expresión de *miR-7*, *miR-10*, *miR-29b*, *miR-29c* y *miR-33* se veía disminuida en comparación con su expresión en el músculo de individuos sanos. En el caso de *miR-1*, a partir de estudios independientes se demostró que su expresión aumentaba, que cambiaba de localización subcelular e incluso que disminuía según el estudio (Gambardella et al. 2010, Perbellini et al. 2011, Rau et al. 2011, Fernandez-Costa et al. 2013). La disparidad de los resultados indica que la desregulación de *miR-1* es particularmente sensible al contexto celular lo cual incluye factores tales como número de repeticiones CTG, tipo de tejido o edad de los pacientes. Este miRNA es de particular interés en el mecanismo de patogénesis de DM1 ya que en músculo cardíaco MBNL1 está directamente implicado en la biogénesis de *miR-1*, conduciendo el secuestro de MBNL1 por las repeticiones CTG a la disminución de los niveles de *miR-1* (Rau et al. 2011).

Otros estudios recientes realizados en plasma de pacientes han demostrado que existen nueve miRNAs alterados, ocho sobreexpresados (*miR-133a*, *miR-193b*, *miR-191*, *miR-140-3p*, *miR-454*, *miR-574*, *miR-885-5p*, *miR-886-3p*) y uno disminuido (*miR-27b*) (Perfetti et al. 2014). Estando la expresión de *miR-193b* también aumentada en pacientes de DM2 (Greco et al. 2012). Este hallazgo presenta a los miRNAs como posibles biomarcadores humorales de la enfermedad. Estas evidencias sugieren que las expansiones CTG y CCTG alteran también la función de los miRNAs y la reversión de estas variaciones podría formar parte de una posible terapia para la enfermedad.

5. Modelos animales de DM

La generación de animales modelo para la DM1 ha sido clave para caracterizar los mecanismos de patogénesis de esta enfermedad tan compleja y determinar los elementos implicados y asociarlos a síntomas concretos. Para modelizar la enfermedad se ha utilizado tanto animales invertebrados como vertebrados. En invertebrados se ha utilizado el gusano, *Caenorhabditis elegans* (Chen et al. 2007,Wang et al. 2007) y la mosca, *Drosophila melanogaster* (de Haro et al. 2006, Garcia-Lopez et al. 2008, Picchio et al. 2013), mientras que en vertebrados se ha utilizado principalmente el ratón, *Mus musculus* (Mankodi et al. 2000, Seznec et al. 2000, Seznec et al. 2001, Mahadevan et al. 2006), aunque también se han creado modelos en el pez cebra, *Danio rerio* (Todd et al. 2014). En todos los casos los modelos de DM1 se han conseguido mediante la expresión de RNAs tóxicos CUG o CCUG en diferentes tejidos implicados en la patología y se han obtenido fenotipos típicos de la de la DM1 y la DM2.

5.1. *Drosophila melanogaster*

En nuestro laboratorio y en paralelo con otros grupos de investigación, se generó un modelo de DM1 en *Drosophila* por expresión de 480 repeticiones CTG en el contexto de un RNA no traducible, cuyo transgén estaba formado por repeticiones sintéticas interrumpidas cada 20 tripletes por el pentanucleótido CTCGA (de Haro et al. 2006, Garcia-Lopez et al. 2008). La expresión de estas repeticiones CTG en los precursores del ojo generaba fenotipos de ojo rugoso y neurodegeneración de los fotorreceptores (Haro et al. 2006). Mientras que la expresión de las 480 repeticiones CTG en músculo de *Drosophila* reproducía varios aspectos de la enfermedad en humanos como el secuestro de las proteínas Muscleblind en los foci ribonucleares, la degeneración progresiva de los músculos indirectos del vuelo (IFM del inglés), alteraciones en el *splicing*, reducción de la vida media y alteración en la biogénesis de miRNAs (Garcia-Lopez et al. 2008, Fernandez-Costa et al. 2013). Posteriormente, en estas moscas se ha observado como la

reducción significativa en el área media de los músculos IFM es concomitante con la activación de las rutas de apoptosis y autofagia, activadas en modelos celulares de DM1 (Loro et al. 2010, Bargiela et al. 2015). Por tanto, este modelo reproduce aspectos moleculares, genéticos e histológicos de la enfermedad y ha sido utilizado como herramienta para descubrir nuevos componentes en la ruta de patogénesis de la enfermedad, así como fármacos potenciales para el tratamiento de la misma (Garcia-Lopez et al. 2008, Garcia-Lopez et al. 2011, Fernandez-Costa et al. 2013, Llamusi et al. 2013, Garcia-Alcover et al. 2014). Posteriormente, se describió un modelo inducible en el que se expresaban 240, 600 o 900 repeticiones CTG interrumpidas con la idea de simular la progresión o gravedad de la enfermedad ya que los fenotipos observados en las moscas modelo se correlacionaban con la longitud de las expansiones. En la musculatura somática de larvas que expresaban las repeticiones CTG se detectó la presencia de foci ribonucleares, secuestro de Mbl, defectos en la división y tamaño de fibras musculares, baja movilidad, hipercontracción muscular y defectos en la fusión de los mioblastos (Picchio et al. 2013).

De igual forma que en DM1 el grupo de Nancy Bonini generó el primer modelo en ojo de *Drosophila* para DM2 que expresaba de 16 a 720 repeticiones CCUG puras. Este modelo de moscas DM2 recapitula características clave de la patología, incluida la toxicidad inducida por la repeticiónes de RNA, la formación de foci ribonucleares y los cambios en *splicing* alternativo (Yu et al. 2015). Recientemente, se ha descrito un modelo de DM2 en el que se expresaban 106 repeticiones CCUG, dicho modelo presenta además de los fenotipos anteriormente mencionados en ojo, una fuerte respuesta apoptótica en este tejido, mientras que en músculo estas repeticiones producen defectos en el *splicing*, pero no fenotipo atrófico (Yenigun et al. 2017).

5.2. *Mus musculus*

Se han descrito distintos modelos murinos de la enfermedad como son HSA^{LR}, EpA960, DM300, DMSXL y DMPK-GFP-$(CTG)_5$ (revisado en Gomes-Pereira et al. 2011), de los cuales el modelo HSA^{LR} merece destacarse por su relevancia para este proyecto de tesis. El modelo HSA^{LR} expresa 250 repeticiones CTG en el contexto de la región 3´UTR del gen de la actina esquelética humana (HSA), siendo su control ratones con el mismo fondo genético (cepa FVB). Este modelo desarrolla miotonía, miopatía, foci ribonucleares, secuestro de Mbnl1 y alteraciones en el *splicing* de transcritos musculares. Sin embargo, este modelo tiene la limitación de la expresión exclusiva en musculatura esquelética y que no reproduce algunas de las características típicas de la enfermedad como la inestabilidad somática e intergeneracional de las expansiones, la debilidad, el desgaste muscular y los niveles de Celf1 aumentados(Mankodi et al. 2000).

Otro modelo murino a destacar de DM1 en el cual las repeticiones CTG se encuentran en su contexto humano (>45 kb locus genómico del gen humano *DMPK* completo) es el nombrado como DMSXL, por tener un número superior a 1300 repeticiones CTG. Estos ratones presentaban foci ribonucleares en diversos tejidos, alta mortalidad, retraso del crecimiento, alteraciones en el *splicing* de transcritos expresados en músculo, corazón y SNC, así como defectos musculares a nivel histológico y funcional (Gomes-Pereira et al. 2007, Huguet et al. 2012). Sin embargo, este modelo cuenta con ciertas desventajas respecto al HSA^{LR} entre las que destacan la gran variabilidad interindividual existente entre los ratones y una mayor complejidad a nivel de generación y mantenimiento, ya que para la obtención de ratones DMSXL

homocigotos es necesario el cruce entre individuos de la misma cepa, aumento el tiempo y el costo en la cría de los ratones. (Revisado en Gomes-Pereira et al. 2011).

De forma análoga a los ratones HSA^{LR}, los ratones DM2-HSAtg modelo para DM2, expresan 121 repeticiones de la expansión intronica CCTG. Dichos ratones muestran foci ribonucleares, regulación positiva de CELF1 en hígado y recapitulan algunos de los aspectos de la patología muscular de DM2, pero no presentan defectos en el *splicing* (Udd et al. 2011).

6. Medicina basada en RNA

Las terapias basadas en el metabolismo del RNA, son un tipo de terapia génica que tiene como diana secuencias especificas del mRNA. En este sentido, el desarrollo de técnicas basadas en la interferencia del RNA (RNAi) y oligonucleótidos antisentido (ASO), entre otros, ha permitido corregir defectos genéticos específicos que acontecen en algunas enfermedades (Burnett et al. 2012, Chery 2016).

Se han descrito dos clases de moléculas pequeñas de RNA que desencadenan de forma natural en la célula el proceso de RNAi a nivel post-transcripcional, los RNA interferentes pequeños (siRNA) y los microRNA (Kubowicz et al. 2013). Los siRNAs son moléculas que tienen un tamaño de unos 21 a 25 nucleótidos y son producidas a partir de precursores de RNA de doble cadena (dsRNA). Estos precursores son procesados por Dicer, que los corta en fragmentos más cortos del RNA. Los pequeños dúplex de RNA resultantes son incorporados al complejo siRISC uniéndose a uno de sus componentes conocido como Ago2. La incorporación del siRNA al siRISC desencadena la separación de las dos cadenas en cadenas sencillas, sólo una de las cuales, conocida como cadena guía, se mantiene asociada al complejo y sirve para identificar el mRNA complementario. Cuando las moléculas de mRNA complementarias son encontradas, la interacción entre el siRNA y este mRNA desemboca en el corte del mRNA y su posterior degradación (Matranga et al. 2005, recisado en Garber 2017). Atendiendo a una finalidad terapéutica, estos siRNAs pueden ser sintetizados químicamente y ser utilizados para silenciar genes específicos. Los mecanismos de síntesis y silenciamiento mediados por microRNAs se describen previamente en los apartados 4.1 y 4.2. Los miRNAs pueden ser modulados *in vivo* mediante la administración de oligonucleótidos sintéticos tanto para reducir su actividad (anti-miRs) como para aumentarla (Ago-miRs o miRNAs miméticos) de manera que estos moduladores afectan directamente a la expresión génica de las dianas de miRNAs específicos. Es evidente que el potencial terapéutico del RNAi es enorme y esto ha provocado que una gran variedad de grupos de investigación y empresas farmacéuticas se hayan embarcado en el desarrollo de tratamientos para diversas enfermedades basados en el RNA interferente como modulador de la expresión génica (Wallace et al. 2011, Kubowicz et al. 2013).

Los oligonucleótidos antisentido son pequeñas moléculas de DNA monocatenario complementarias a determinadas secuencias específicas de un mRNA diana. Estos ASOs entran a la célula mediante endocitosis y se unen al mRNA diana. La formación del heteroduplex ASO-mRNA desencadena el bloqueo de la traducción proteica, a través de mecanismos que incluyen: (1) inducción de la actividad RNasa-H , endonucleasa que degrada el mRNA, (2) interferencia de la traducción por impedimento estérico de la actividad ribosomal e (3) interferencia de la maduración del mRNA por inhibición del *splicing* o desestabilización del pre-mRNA en el núcleo (Chan et al. 2006).

Sin embargo, para su uso como terapia génica los RNAi y los ASOs deben superar una serie de problemas relacionados con la estabilidad, biodistribución y selectividad por mRNA. Estos problemas pueden resolverse, al menos en parte, mediante el uso de modificaciones químicas, las cuales se incorporan al ácido nucleico durante su síntesis (revisado en Geary et al. 2015, Dowdy 2017, Garber 2017 y Khvorova et al. 2017). Una modificación química básica para combatir la degradación por nucleasas es la introducción en el esqueleto químico del oligonucleótido enlaces fosforotioato (PT), mientras que las modificaciones en la ribosa por adición de grupos 2'-metoxi (2'-O-metil: 2'-OMe) o 2'-Ometoxietil (2'-MOE) mejoran la afinidad de la unión y la estabilidad del oligonucleótido por su diana. Una segunda generación de modificaciones químicas usadas para mejorar sustancialmente la afinidad y disminuir la degradación por nucleasas son las de tipo LNA (locked nucleic acids) y BNAs (bridged nucleic acid), en las que un residuo de la ribosa está modificado con un puente extra que conecta el oxígeno en 2' y el carbono 4', bloqueando a la ribosa en la conformación 3'-endo. Las modificaciones químicas más actuales o de tercera generación incluyen: (1) a los oligonucleótidos de tipo PMO (phosphorodiamidate morpholino oligomer) donde la ribosa del ácido nucleico ha sido sustituida por un grupo morfolino; (2) los de tipo PNAs (peptide nucleic acid) donde el grupo ribosa-fosfato se sustituye por un residuo aminoacídico, de forma que el oligonucleotido tiene por esqueleto una estructura de unidades repetidas de N-(2-aminoetil)-glicina unidas por enlaces peptídicos y (3) los oligonucleótidos conjugados con colesterol, mejorando estos residuos lipídicos su afinidad por las membrana celular y así su entrada a la célula. Sin embargo, estas modificaciones en los grupos azúcar no son compatibles con actividad de la RNasa-H. Para eludir este impedimento, se puede agregar un espacio en la región central del oligonucleótido que carezca de estas modificaciones 2'-OMe, 2'-MOE, LNA o BNA dejando así hueco para que proteína RNasa-H pueda actuar. Los ASOs de esta naturaleza se denominan *gapmers* (Soutschek et al. 2004, revisado en Chan et al. 2006 y Khvorova et al. 2017).

En 2016, la FDA aprobó el uso dos ASOs para su uso clínico, Eteplirsen (comercializado como Exondys 51) como tratamiento de la distrofia muscular de Duchenne (Cirak et al. 2011, Mendell et al. 2013, Exondys 51 FDA 2016) y Nusinersen (comercializado como Spinraza) para el tratamiento de la atrofia muscular espinal (Zanetta et al. 2014, Spinraza FDA 2016).

7. Estrategias terapéuticas en DM1

La disponibilidad de modelos de la enfermedad en *Drosophila*, ratones y células, ha permitido el diseño de numerosos enfoques terapéuticos que se pueden agrupar en términos generales como (revisado en Gomes-Pereira et al. 2011, Konieczny et al. 2017, Thornton et al. 2017 y Overby et al. 2018); (1) estrategias terapéuticas antisentido o farmacológicas que bien provoquen la degradación de los transcritos mutantes o impidan su plegamiento en horquillas; ya sea a nivel transcripcional (Coonrod et al. 2013, Siboni et al. 2015) o a nivel de silenciamiento post-transcripcional (Mulders et al. 2009, Francois et al. 2011, Lee et al. 2012, Wheeler et al. 2012, Gonzalez-Barriga et al. 2013, Sobczak et al. 2013, Pandey et al. 2015, Batra et al. 2017, Jauvin et al. 2017). (2) Estrategias de inhibición farmacológica del secuestro de MBNL1 por expansiones (Warf et al. 2009, Garcia-Lopez et al. 2011, Parkesh et al. 2012, Leger et al. 2013, Hoskins et al. 2014, Ketley et al. 2014, Nakamori et al. 2016) y (3) estrategias de corrección de las alteraciones moleculares aguas abajo del RNA tóxico (Wheeler et al. 2007, Wang et al. 2009).

7.1. Degradación del RNA mutante.

En los últimos años, numerosos trabajos han centrado sus esfuerzos en reducir la expresión de las repeticiones tóxicas a través de la inhibición de la transcripción. Aunque la inhibición a este nivel no se considera una estrategia robusta, Coonrod y colaboradores demostraron como algunas pequeñas moléculas de la familia de los antibióticos pueden unirse a las repeticiones CTG.CAG reduciendo así la expresión del RNA que porta las expansiones CUG (Coonrod et al. 2013).

Sin embargo, es la estrategia post-transcripcional basada en ASOs y siRNAs para destruir el RNA tóxico causante de la DM1, la que ha obtenido mayor atención (Figura I-5 Overby et al. 2018). Para que los ASOs de este tipo sean eficaces como terapia deben ser capaces de llegar a los RNAs tóxicos e hibridar con los mismos y así potenciar su degradación. Esta degradación de los trascritos patológicos por los ASOs se centra en la localización nuclear de los transcritos DMPK y en la activación de las vías de degradación del RNA mediadas por la RNasa-H. En este sentido, la estrategia más avanzada en desarrollo clínico que emplea ASOs activos por RNasa-H es el de Wheeler y colaboradores donde este tipo de ASOs administrados a ratones HSA^{LR} desencadenan una reducción marcada del RNA tóxico en el músculo esquelético, la liberación de las proteínas MBNL de foci ribonucleares, corrige los defectos en el *splicing*, elimina la miotonía y produce una mejora en la arquitectura del músculo (Wheeler et al. 2012).

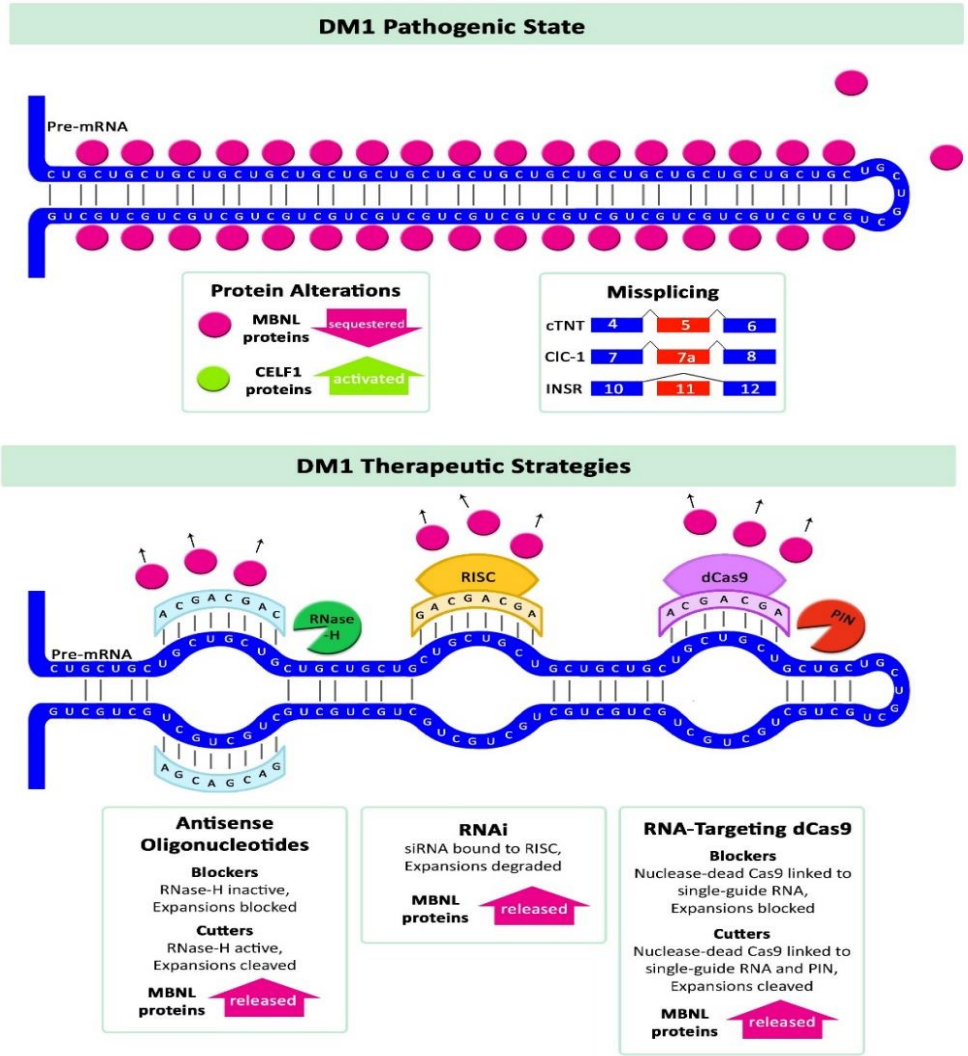

Figura I-5. Terapias basadas en oligonucleótidos en la distrofia miotónica. (Arriba) Estado patogénico de DM1 donde se incluye el secuestro de proteínas MBNL a los transcritos tóxicos de DMPK, la activación de proteínas CELF y patrones de *splicing* de tipo fetal alterados. (Abajo) Las estrategias terapéuticas dirigidas a los transcritos expandidos CUG en DM1, donde se incluyen ASOs, RNAi y la Nucleasa de muerte celular-Cas9. Los ASO pueden funcionan a través de la ruta RNasa-H o por otras rutas que implican un bloqueo estérico o la unión de la caperuza 5´. Del mismo modo, dCas9 puede funcionar mediante escisión del mRNA activada por PIN o mediante bloqueo estérico (Tomado de (Overby et al. 2018).

Pero son los ASOs de tipo *gapmer* (*gapmer*-ASO) que desencadenan la degradación específica de los transcritos *DMPK* los que han llegado a fase clínica (IONIS-DMPK-2.5Rx ensayo clínico NCT02312011 (Madsen A 2017)) tras haber funcionado de forma muy efectiva en mioblastos DM1, ratones DMSXL y monos (Pandey et al. 2015, Jauvin et al. 2017). Brevemente, una vez que estos *gapmers* entran en la célula se unen al mRNA endógeno dando como resultado un dúplex de g*apmer*-mRNA. El dúplex de g*apmer*-mRNA es reconocido por la enzima celular RNasa-H, que corta el mRNA diana e inhibe la expresión génica de los transcritos de *DMPK* de forma específica (Castanotto et al. 2015, Pandey et al. 2015). A pesar de los resultados relevantes logrados al usar este gapmer-ASO IONIS-DMPKR-2.5x en modelos murinos, el ensayo clínico para este fármaco se suspendió debido a un beneficio terapéutico inadecuado en los pacientes con DM1, pues se observó que llegaba de forma insuficiente al músculo de los pacientes (Madsen A 2017).

7.2. Inhibición de las interacciones patogénicas RNA-MBNL y regulación positiva de MBNL

Los grupos de investigación que han seguido este enfoque alternativo para tratar los fenotipos relacionados con la enfermedad, han realizado rastreos de alto rendimiento para identificar pequeñas moléculas que inhiban la interacción CUGexp:MBNL o que regulen positivamente a MBNL (Rzuczek et al. 2015, Konieczny et al. 2017). En este tipo de rastreos han surgido cientos de moléculas (Warf et al. 2009, Garcia-Lopez et al. 2011, Parkesh et al. 2012, Leger et al. 2013, Hoskins et al. 2014, Ketley et al. 2014, Nakamori et al. 2016) entre ellas 4 son las que han generado mayor expectación; (1) la pentamidina, por ser la primera en ser identificada, siendo esta una pequeña molécula capaz de competir con MBNL1 por la unión a horquillas CUG, sin embargo presenta una ventana terapéutica estrecha (Warf et al. 2009). Por otro lado, en el laboratorio se identificó el (2) hexapéptido abp1, el cual estabiliza las expansiones CUG en su conformación de cadena sencilla evitando el secuestro de MBNL1 y demostrando que la formación de esta estructura secundaria es en sí misma es una diana terapéutica válida en moscas modelo DM1 y ratones HSA^{LR} (Garcia-Lopez et al. 2011). Otro tipo de moléculas que impiden la unión de MBNL a las repeticiones es (3) la eritromicina un antibiótico natural que mejora la miotonía y las alteraciones en el *splicing* en un modelo murino de la enfermedad (Nakamori et al. 2016). Un último fármaco es (4) la fenilbutazona un antiinflamatorio no esteroideo anti-DM1 con actividad dual, pues no solo actúa inhibiendo la unión de MBNL a CUGexp sino que también aumenta la transcripción de Mbnl1 mediante la supresión de la metilación de una región potenciadora definida (Chen et al. 2016). Muchas de estas moléculas permiten su reposicionamiento, ya que son fármacos con indicaciones terapéuticas previas.

7.3. Corrección de las alteraciones moleculares aguas abajo del RNA tóxico

Otro enfoque terapéutico llevado a cabo en modelos de DM1 es corregir alteraciones moleculares corriente abajo del RNA tóxico, por ejemplo corregir sucesos de *splicing* responsables de síntomas concretos de la enfermedad. Un estudio de este tipo es la inclusión del exon 7a en los transcritos del canal de cloro muscular para corregir la miotonía, mediante el uso de morfolinos de tipo ASO (Wheeler et al. 2007, Koebis et al. 2013). Otro ejemplo de abordaje aguas abajo, es la normalización de la vía AMPK / TOR mediante la administración de 5-aminoimidazol-4-carboxamida ribonucleótido (AICAR) (Brockhoff et al. 2017) o la inhibición la PKC (Wang et al. 2009). La inhibición de PKC por pequeñas moléculas reduce la hiperfosforilación de CELF1 rescatando la degeneración muscular en ratones modelo. En esta aproximación es Tideglusib, un inhibidor de GSK-3B, el único que ha llegado a fase clínica II (ensayo clínico NCT02858908) como tratamiento para la DM1 (Konieczny et al. 2017).

-Objetivos-

El intenso trabajo de investigación de la última década, ha aclarado muchos aspectos del mecanismo de fisiopatogénesis de la DM1 y la DM2 y ha permitido experimentar con tratamientos potenciales. Sin embargo, no se ha transferido a la práctica clínica una terapia efectiva para la enfermedad. Por ello, existe la necesidad de explorar nuevos conceptos terapéuticos con potencial translacional. La mayoría de las aproximaciones terapéuticas que se han planteado hasta el momento contra la DM se basan en impedir la unión de las proteínas MBNL1 a los RNA que contienen las repeticiones expandidas y su degradación específica (revisado en Konieczny et al. 2017, Thornton et al. 2017 y Overby et al. 2018). Una alternativa poco explorada para la DM1, es la modulación terapéutica de la expresión génica (TGM), que persigue aumentar o disminuir la expresión endógena de un gen para aliviar un determinado estado patológico. Sobre este tipo de terapia encontramos algunos ejemplos como son la inhibición de CD44 en cáncer de próstata metastásico (Liu et al. 2011), o la potenciación farmacológica de utrophin para compensar la falta de distrofina en la distrofia muscular de Duchenne (Guiraud et al. 2015).

Para la DM la estrategia se centra en potenciar la expresión endógena de MBNL1/2 (Chen et al. 2016), cuya actividad es limitante en la enfermedad. Una de los abordajes utilizados para modular los niveles de expresión endógenos son las terapias basadas en miRNAs, las cuales han despertado un gran interés en los últimos tiempos, gracias a su eficacia en modelos animales de distintas patologías humanas, al desarrollo de químicas especializadas que permiten un eficaz silenciamiento de su diana, y unos parámetros farmacocinéticos compatibles con su desarrollo como medicamento (Liu et al. 2011, Liu et al. 2012, Schober et al. 2014, Fiorillo et al. 2015). El fármaco probablemente más avanzado de este tipo es Miravirsen, un anti-miRNA contra un miRNA específico de hígado, *miR-122*, que es imprescindible para la replicación del virus de la hepatitis (Ottosen et al. 2015).

Para la DM1 la estrategia de desrepresión se podía validar *in vivo* en nuestro modelo de *Drosophila*, pero no para la DM2, debido a la ausencia de un modelo animal para esta enfermedad al inicio de esta tesis. Por ello, en el contexto de esta tesis doctoral se hizo necesario plantear el desarrollo de un modelo de DM2 en *Drosophila*.

Con todo lo anteriormente expuesto, los objetivos que se persiguieron durante el desarrollo de la presente tesis doctoral son los siguientes:

-**Objetivo 1**- Generación de un modelo muscular en *Drosophila* de DM2, donde desreprimir la expresión *muscleblind* mediante silenciamiento de miRNAs represores.

-Objetivo 2- Desrepresión de *muscleblind* mediante silenciamiento de miRNAs represores en un modelo de *Drosophila* para Distrofia miotónica tipo 1: Prueba de concepto

-Objetivo 3- Silenciamiento de miRNAs represores específicos de la expresión de *MBNL1* y *MBNL2* en modelos mamíferos de DM1.

-Artículos-

-Artículo 1-

SCIENTIFIC REPORTS

OPEN

Expanded CCUG repeat RNA expression in *Drosophila* heart and muscle trigger Myotonic Dystrophy type 1-like phenotypes and activate autophagocytosis genes

Received: 31 October 2016
Accepted: 19 April 2017
Published online: 06 June 2017

Estefania Cerro-Herreros[1,2,3], Mouli Chakraborty[1,2,3], Manuel Pérez-Alonso[1,2,3], Rubén Artero[1,2,3] & Beatriz Llamusí[1,2,3]

Myotonic dystrophies (DM1–2) are neuromuscular genetic disorders caused by the pathological expansion of untranslated microsatellites. DM1 and DM2, are caused by expanded CTG repeats in the 3′UTR of the *DMPK* gene and CCTG repeats in the first intron of the *CNBP* gene, respectively. Mutant RNAs containing expanded repeats are retained in the cell nucleus, where they sequester nuclear factors and cause alterations in RNA metabolism. However, for unknown reasons, DM1 is more severe than DM2. To study the differences and similarities in the pathogenesis of DM1 and DM2, we generated model flies by expressing pure expanded CUG ([250]×) or CCUG ([1100]×) repeats, respectively, and compared them with control flies expressing either 20 repeat units or GFP. We observed surprisingly severe muscle reduction and cardiac dysfunction in CCUG-expressing model flies. The muscle and cardiac tissue of both DM1 and DM2 model flies showed DM1-like phenotypes including overexpression of autophagy-related genes, RNA mis-splicing and repeat RNA aggregation in ribonuclear foci along with the Muscleblind protein. These data reveal, for the first time, that expanded non-coding CCUG repeat-RNA has similar *in vivo* toxicity potential as expanded CUG RNA in muscle and heart tissues and suggests that specific, as yet unknown factors, quench CCUG-repeat toxicity in DM2 patients.

Myotonic dystrophy type 1 (DM1) and type 2 (DM2) are dominantly-inherited multi-systemic genetic disorders. DM1 (OMIM: 160900) is caused by an unstable expansion of a CTG trinucleotide repeat motif located in the 3′ untranslated region (UTR) of the *dystrophia myotonica protein kinase* (*DMPK*) gene[1]. Unaffected individuals carry fewer than 37 triplet-repeats, whereas expansions ranging between 50 and 4000 CTG repeats have been found in affected individuals. DM2 (OMIM: 602668), initially named proximal myotonic myopathy due to the greater weakness of proximal compared to distal muscles[2], is caused by a tetranucleotide (CCTG) expansion in intron 1 of the CCHC-type zinc finger nucleic acid binding protein gene (*CNBP*, *also known as ZNF9*)[3]. Healthy individuals carry fewer than 30 tetra-nucleotide repeats, whereas repeat lengths found in affected patients are significantly longer than in DM1 (between 55 and 11000)[3]. In contrast to DM2, which does not have a congenital form, very large (>1,000 repeat) *DMPK* CTG mutations also cause congenital DM1 (CDM) characterized by neonatal hypotonia (floppy baby) and intellectual disability[4]. The expansions are transcribed into (CUG)n and (CCUG)n-containing RNA, respectively, which form secondary structures and sequester RNA-binding proteins, such as the RNA processing factors Muscleblind-like proteins (MBNL1-3 in vertebrates, Muscleblind in *Drosophila*), forming nuclear aggregates known as foci[5–11]. Additional splicing factors, such as CUGBP Elav-like family member 1 (CELF1), are also disrupted, leading to the mis-splicing of a large number of downstream genes[12–14]. Among them, the alteration in the splicing pattern of *CLCN1*, *INR*, *PKM*, *CACNA1S*, and *BIN1*

[1]Translational Genomics Group, Incliva Health Research Institute, Valencia, Spain. [2]Department of Genetics and Interdisciplinary Research Structure for Biotechnology and Biomedicine (ERI BIOTECMED), University of Valencia, Valencia, Spain. [3]CIPF-INCLIVA joint unit, Valencia, Spain. Estefania Cerro-Herreros and Mouli Chakraborty contributed equally to this work. Correspondence and requests for materials should be addressed to R.A. (email: ruben.artero@uv.es)

pre-mRNAs has been associated with myotonia, insulin resistance, perturbed glucose metabolism and muscle weakness, respectively, which are all symptoms of DM[15–19]. Importantly, the repeat-length extensively correlated with disease severity in DM1[20] and with the amount of MBNL sequestered in both types of DM[5,21]. Although for DM2 the correlation between repeat length and disease severity in humans is less clear-cut, expression of non-coding CCUG-expanded RNA in flies has been shown to cause length-dependent toxicity in *Drosophila* eyes[22].

Clinically, DM2 patients generally experience a milder phenotype than DM1 patients, including slower and less severe progression of the disease, reduced severity of the cardiac involvement with a significant reduction in arrhythmicity and prophylactic pacing requirements, lack of prominent late respiratory or facial and bulbar muscle weakness, less evocable myotonia, and preserved social and cognitive abilities[23–26]. However, the molecular origin of these milder phenotypes in DM2 is unknown. Indeed, several studies have reported that DM2 individuals tend to carry significantly more (75 to approximately 11,000, with a mean of 5,000 CCTG) repeats in mutant alleles compared to patients with CTG expansions (classic DM1 range is 100–1000 repeats)[3] and, according to different sources *CNBP* is 4 to 8-fold more expressed in human muscles than the *DMPK* gene[27–29]. In addition, MBNL binds to CCUG with higher affinity than to CUG repeats[6,30], resulting in larger ribonuclear inclusions in DM2 patients, which sequester more MBNL[21]. Considering that CNBP is expressed at higher levels than DMPK in muscles, and that expanded alleles tend to carry more CTG repeats, as well as the fact that MBNL proteins have higher affinity for CCUG repeats than for CUG RNA, DM2 symptoms should be more severe, rather than milder, than DM1.

To investigate this paradox, we reasoned that the phenotypes brought about by both expansion types in *Drosophila* tissues might be informative. Significantly, weaker phenotypes are expected for CCUG expansions should they be intrinsically less toxic than CUG repeats, whereas similar phenotypes are expected if toxicity is modulated in humans by CCUG-specific factors. With this aim, we generated and characterized *Drosophila* models of DM1 and DM2 expressing pure CUG or CCUG repeats, respectively, in muscular and cardiac tissues. We found common pathogenic events between CUG and CCUG repeat toxicity, such as Mbl sequestration in foci, mis-splicing and increased autophagy in both tissues. Importantly, the severity of the phenotypes in the DM2 flies reveals that CCUG repeat expansions are potentially as toxic as CUG repeats in muscle and heart. Our study therefore suggests that unknown molecular RNA-toxicity modifiers account for the milder symptoms of DM2.

Results

Expression of either CUG or CCUG-expanded repeats sequester Muscleblind in ribonuclear foci in muscle and cardiac tissue. To accurately model DM1 and DM2 in flies, we generated *UAS-CTG* and *UAS-CCTG* transgenic fly lines carrying either 250 CTG (CTG (250)×) or 1100 CCTG (CCTG (1100)×) pure repeats, which are within the pathological range of repeat lengths and mimic the, at least 4 times longer, expansion size in DM2 patients compared with DM1[25,31]. As controls, we generated flies carrying short versions of the repeats (CTG (20)× or CCTG (20)×). In order to express the repeats in different tissues, we crossed the UAS fly lines with the muscle-specific driver myosin heavy chain *Mhc-Gal4*[32] or the cardiac-specific driver *GMH5–Gal4*[33]. The expression level of the repeats was assessed by qPCR using primers against the common SV40 terminator contained in these vectors (Fig. S1).

Fluorescent *in-situ* hybridization (FISH) to detect ribonuclear foci showed that they were present in the nuclei of indirect flight muscle (IFM) and heart cells expressing long CUG or CCUG repeats, but not in flies expressing the short versions of the repeats (Figs 1 and S2). Because Muscleblind sequestration is one of the main features of the disease, we studied Muscleblind subcellular localization in our model flies. As we previously reported, *Drosophila* Muscleblind is found in sarcomeric bands in adult muscle tissue and dispersed throughout the nuclei of cardiomyocytes[34,35]. Muscleblind immunodetection in muscle and heart tissue in flies expressing the short versions of the CUG or CCUG repeats showed that Muscleblind localization was the same as that described in control samples. In contrast, Muscleblind was concentrated in CUG or CCUG ribonuclear foci in muscle and heart cells from flies expressing long CUG or CCUG repeats (Fig. 1). Thus, both expanded CUG and CCUG arrays originate ribonuclear foci and Muscleblind sequestration in *Drosophila* muscle and heart tissue, which are both histological hallmarks of DM.

Muscleblind-dependent splicing is altered in flies expressing expanded CUG or CCUG repeats. To test whether the confirmed Muscleblind retention in foci was enough to cause splicing misregulation, we studied the percentage of exon retention ("*percentage spliced in*", PSI) of the *Drosophila formin* (*Fhos*) gene exon 16′, which has a highly conserved ortholog in human, with altered splicing in DM1 patients[36]. *Fhos* has 19 exons, which produce nine different transcripts (Ensembl Genome browser, release 83). We recently reported that exon 16′ (132 nt) is preferentially included in DM1 model flies expressing 480 interrupted CUG repeats (i(CUG)480) in muscle[37]. Importantly, this splicing event was shown to be Muscleblind-dependent. In control flies, the PSI of *Fhos* exon 16′ was around 50%. However, in flies expressing i(CUG)480 in muscle, this percentage increased to nearly 95%. Consistent with the milder toxic effects reported in DM1 individuals and in animal models with shorter CUG repeats, the inclusion percentage dropped to close 75% in flies expressing 250 CUG repeats in muscle. In the case of flies expressing expanded CCUG repeats in muscle, we also observed increased *Fhos* exon 16′ inclusion, which reached 85%. Importantly, flies expressing short versions of either CUG or CCUG repeats, showed no significant changes in exon usage (Fig. 2A and C). In cardiac tissue, the 50% exon inclusion found in control or short-repeat-expressing flies, increased to 75% in both expanded CUG and CCUG-expressing flies (Fig. 2B and D). We also quantified the inclusion of exon 13 of the Mbl-dependent *Serca* gene, which decreased 50% in the flies expressing the long repeats in muscle, while in heart, resulted into a 50% increase. Accordingly, in previous studies the expression of 480 interrupted CUG repeats in adult flies using the

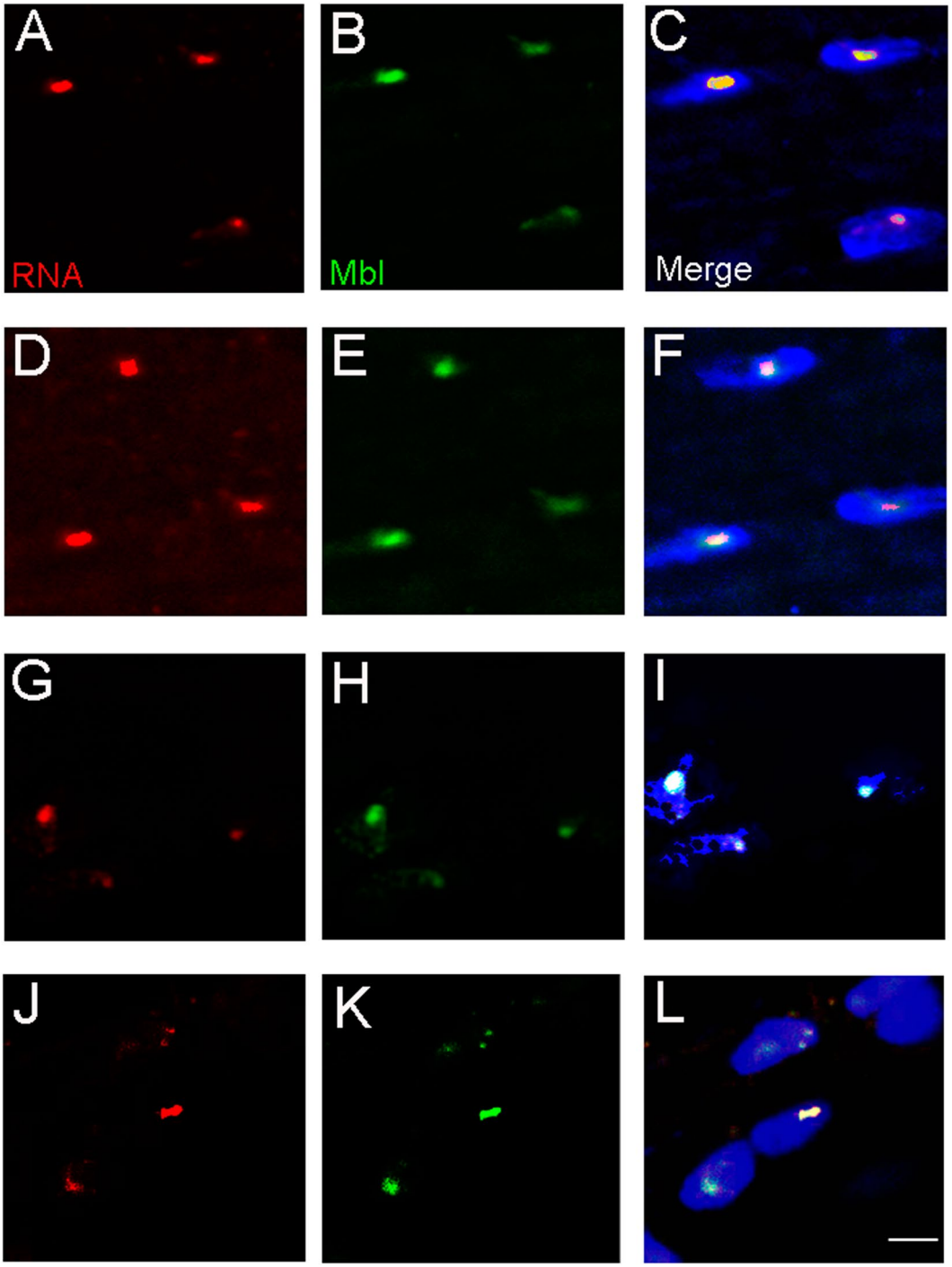

Figure 1. Muscleblind is retained in ribonuclear foci in flies expressing expanded CUG or CCUG repeats. Representative fluorescent confocal images of IFMs (**A**–**F**) and heart cells (**G**–**L**) from flies expressing expanded CUG (**A**–**C** and **G**–**I**) or CCUG (**D**–**F** and **J**–**L**) repeats under the control of the Mhc-Gal4 and GMH5-Gal drivers, respectively. Ribonuclear foci retaining Muscleblind were present in flies expressing long CUG or CCUG repeats. Merged images in (**C**,**F**,**I** and **L**) include DAPI (blue) counterstaining of the nuclei. Scale bar = 10 μm.

late muscle driver Mhc-Gal4 induced a 2.4-fold reduction of *Serca* transcripts with exon 13[37], while the expression of 960 CUG repeats using the Mef-Gal4 driver resulted in increased expression[38], suggesting a remarkable developmental-dependent regulation of this event in flies (Fig. 2E and F).

These data confirmed that the Muscleblind sequestration in ribonuclear foci observed in fly models of DM1 and DM2, led to a functional depletion of Muscleblind in adult muscle and heart tissue.

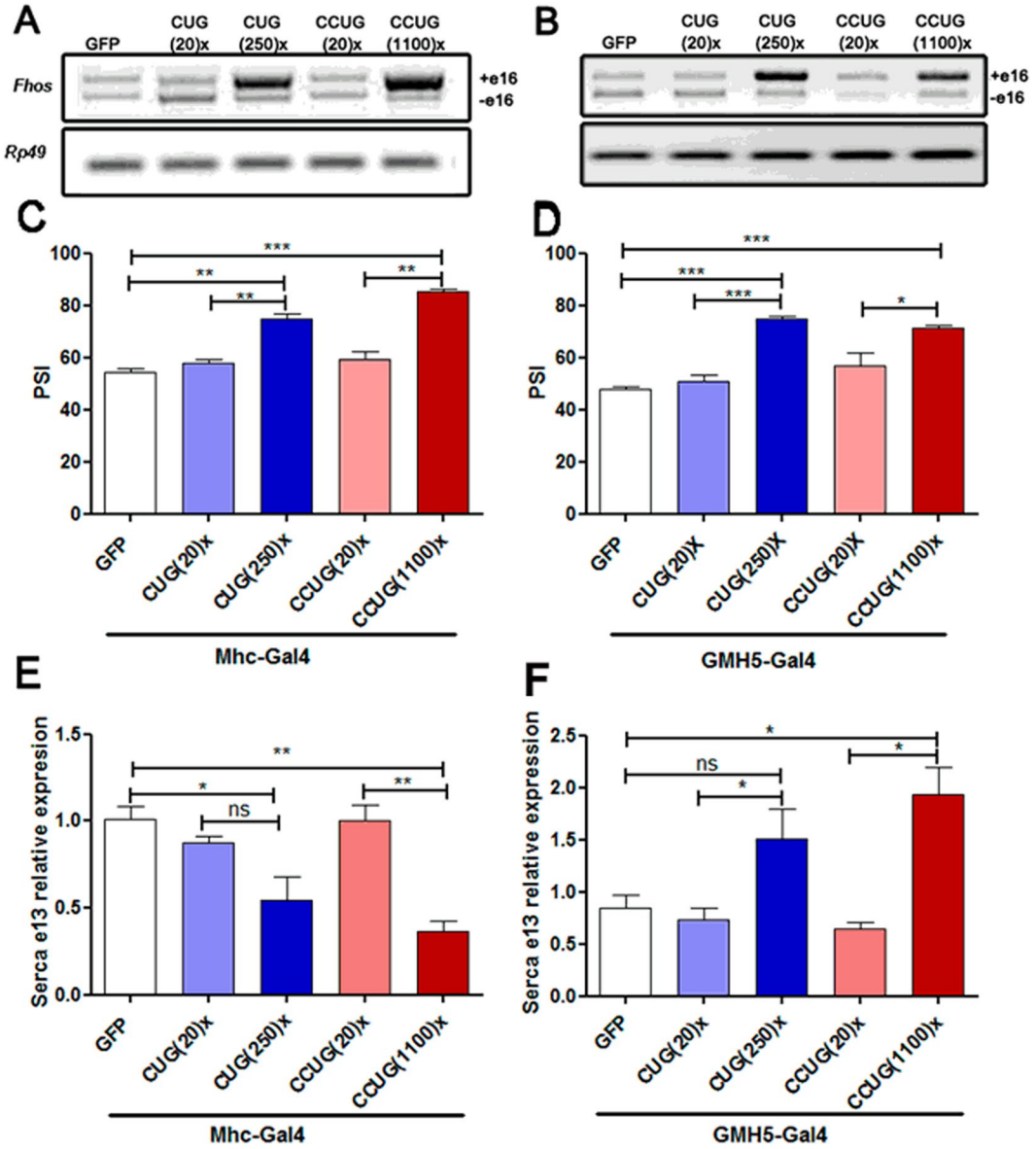

Figure 2. CUG and CCUG expansions cause Muscleblind-dependent missplicing. (**A**,**B**) Representative semi-quantitative RT-PCR showing inclusion of *Fhos* exon 16′ in flies expressing the indicated constructs in muscle (**A**) or heart (**B**) under the control of Mhc-Gal4 or GMH5-Gal4, respectively. Endogenous *Rp49* was used for normalization. Percentage of exon 16′ inclusion, revealed that expression of long CUG or CCUG repeats in the fly muscle (**C**) or heart (**D**), favored increased use of this exon. qRT-PCR results of *Serca* exon 13 expression relative to *Rp49 expression*, confirmed that the use of this exon in the flies expressing the expanded repeats and the control flies is significantly different in muscle (**E**) and heart tissues (**F**). The histograms show the mean ± SEM. $*p < 0.05$, $**p < 0.01$, $***p < 0.001$ (Student's t-test).

The expression of autophagy-related genes is increased in muscular and cardiac tissues in DM1 and DM2 model flies. Several studies have reported a pathological over-activation of the autophagy-lysosome pathway in DM1 models. Apoptotic activation and increased presence of autophagy markers has been reported in primary human cell lines from adult-onset DM1 patients[39,40] and in human DM1 embryonic stem cells-derived neural stem cells[41]. In addition, pathway analysis on global PolyA-seq studies of human DM skeletal muscle[42] and brain[43] identified enriched terms associated with ubiquitin-mediated proteolysis and the mTOR pathway. More recently, studies performed in a murine model of DM1 have reported that targeting deregulated AMPK/mTORC1 pathways improves muscle function in DM1[44]. Accordingly, we have previously demonstrated over-activation of apoptosis and autophagy by inducible expression of 480 interrupted CUG repeats in *Drosophila* adults and a rescue of muscle atrophy by silencing the expression of the autophagy-related genes Atg4, Atg7, Atg8a and Atg9[34]. To study the expression of autophagy-related genes in our DM1 and DM2 *Drosophila* models, we performed qPCRs with cDNAs from heart and thorax samples of flies expressing short and long versions of the CUG or CCUG repeats in heart and muscle (Fig. 3). In general, we found that expression of Atg4,

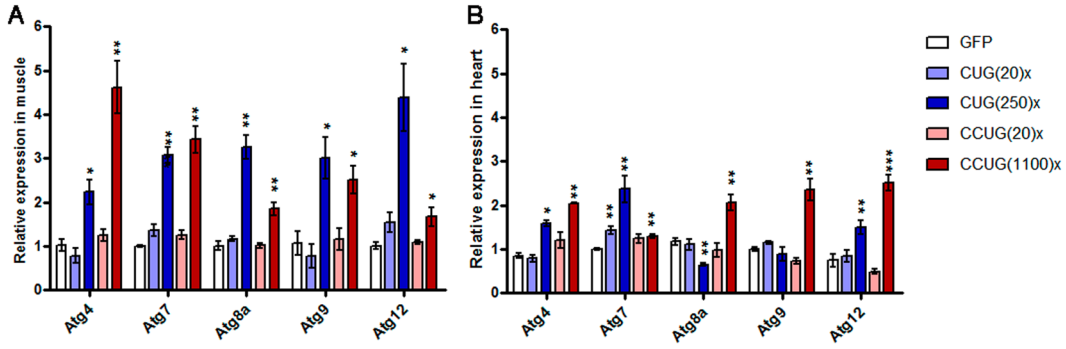

Figure 3. The expression of autophagy-related genes is upregulated in flies expressing expanded CUG or CCUG repeats in muscle or heart. Relative expression levels of *Atg4*, *Atg7*, *Atg8a*, *Atg9* and *Atg12* measured by qRT-PCR in muscle (Mhc-Gal4 driver; **A**) and heart samples (GMH5-Gal4 driver; **B**), showed a significant upregulation of these autophagy-related genes in flies expressing expanded CUG (CUG(250)×) or CCUG repeats (CCUG(1100)×). The histograms show the mean ± SEM. $*p < 0.05$, $**p < 0.01$, $***p < 0.001$ (Student's t-test).

Atg7, Atg8a, Atg9 and Atg12 were significantly upregulated in flies expressing either expanded CUG or CCUG repeats in muscle, compared to control flies expressing GFP or short repeats. Of note, the expression levels of these genes in flies expressing short CUG or CCUG repeats were similar to the levels in control flies that did not express the repeats (Fig. 3A). In comparison, the expression of the repeats in heart caused a moderate upregulation of *Atg* genes expression, in the case of flies expressing the long repeats. Upregulation of Atg genes mediated by the repeats was higher in the flies expressing CCUGs compared to those expressing CUG repeats (Fig. 3B). Consistent with these findings, we observed upregulation of *AKT2*, *AKT1S1* and *ATG4* mRNAs in human patient skeletal muscle[34]. These data support a role of autophagy activation in DM pathogenesis not only in DM1, as we previously reported, but also in DM2. In addition, our results highlight the relevance of the activation of this pathway in different tissues affected by repeat expression.

Both expanded CUG and CCUG repeat RNA reduced cross-sectional muscle area and fly survival. Despite the fact that MBNL1 is sequestered in CCUG foci and it is expected that the longer CCUG repeat expansions will have a greater inhibitory effect on MBNL1 in DM2 cells, visible muscle atrophy in DM2 muscle is actually milder than in DM1 patients[45]. To investigate how *Drosophila* muscle responds to expanded CCUG repeat RNA, we quantified the cross-sectional muscle area of IFMs from adult flies at different ages that expressed 250 CUG or 1100 CCUG repeats, or controls expressing 20 units or the GFP reporter, under the control of the Mhc-Gal4 driver. We observed a significant reduction in muscle area in 3-day-old flies expressing long CUG or CCUG repeat RNA, whereas cross-sectional muscle area in flies expressing the short versions of the repeats were not significantly different from control GFP-expressing flies. Importantly, flies expressing either long CUG or CCUG repeats showed similar muscle phenotype, which reached up to a 50% reduction in muscle area in both cases (Fig. 4A–E and K). Similarly, muscle area in aged flies (30-day-old flies) expressing expanded repeats was reduced in comparison to aged GFP flies. The decrease in the muscle area in young and aged flies was similar in all the genotypes studied (around 20%) suggesting that the strong muscle reduction observed in the model flies had an important developmental component. Nevertheless, we observed vacuolization, splitting muscles and occasional absence of muscle packages, characteristic of degenerating muscles[46], which were only present in aged flies expressing the expanded CUG or CCUG repeats (Fig. 4F–K). Taken together, these results suggests that toxic RNAs interfere with both muscle development and muscle maintenance.

Population studies have reported higher mortality and morbidity rates, and a positive correlation between the age at onset of DM1 and age at death in patients[47,48]. Similarly, we observed that the lifespan and mean survival of flies expressing expanded CUG or CCUG repeat RNA was significantly reduced in comparison to control flies expressing only GFP, whereas the lifespan of flies expressing 20 units of the repeats was not significantly different from the control flies (Fig. 5A). These results are consistent with our previous description of muscle loss, degeneration and reduced viability of flies expressing i(CTG)480 throughout the fly musculature[34,49]. Taken together our data indicate that the expression of expanded CUG or CCUG repeats in muscle causes similar defects in the IFMs of young and aged flies, and in the viability of *Drosophila*.

Locomotor performance is compromised in flies expressing expanded CUG or CCUG repeat RNA in muscle. To test whether the muscle loss observed in the model flies was of functional relevance, we assessed the flight and climbing ability of flies expressing the expanded repeats and compared them to control flies expressing GFP or short repeats. Climbing velocity and landing distance were only reduced in flies expressing the expanded versions of the repeats and no significant differences were observed between DM1 and DM2 model flies. Of note, these functional parameters were not altered in flies expressing the short versions of the repeats compared to the controls. In the case of climbing velocity, flies expressing the long CUG or CCUG repeats retained 70% of the control-fly climbing speed, and there was no significant difference in velocity between these two genotypes (Fig. 5B). The average landing height was reduced to 25% compared to control flies expressing

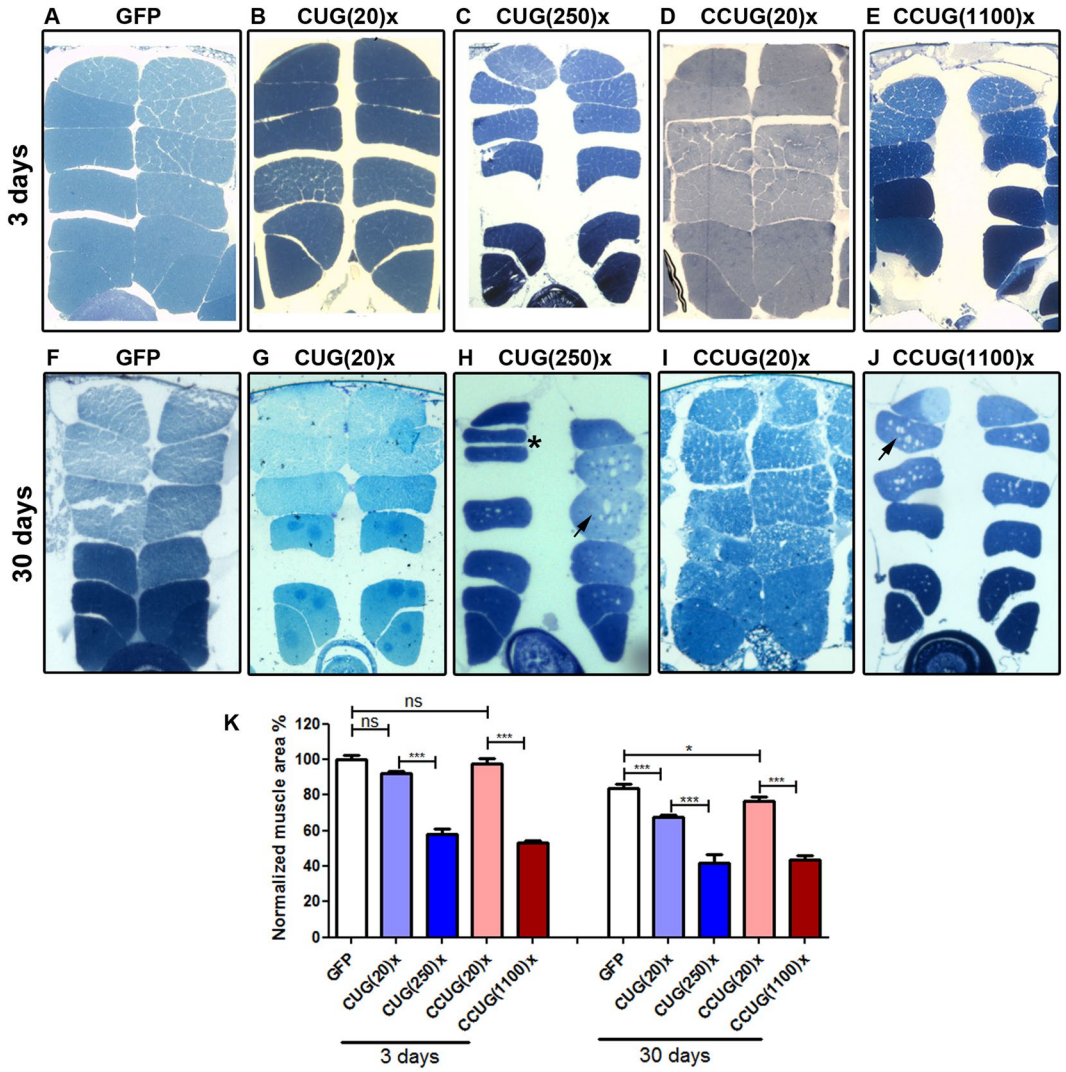

Figure 4. Expression of expanded CUG or CCUG repeats in muscle induces similar levels of muscle area reduction and degeneration. (**A**–**J**) Dorsoventral sections of resin-embedded fly thoraces. In all images the dorsal side is displayed at the top. Mhc-Gal4 was used to drive the expression of the indicated constructs in muscle. (**K**) Quantification of the mean percentage of muscle area per genotype relative to the muscle area of the control flies (GFP), which is considered as 100%. While young flies (3 day-old, in **A**–**E**) expressing 20 CUG or CCUG repeats were not different from control flies expressing GFP, flies expressing expanded CUG or CCUG repeats have a 50% reduction in IFM muscle area. All aged flies (30 day-old, in **F**–**J**) displayed reduced muscle area compared to young flies of the same genotype. However, vacuolization (arrows) and occasional muscle splitting (asterisk) characteristic of degenerating muscles were present only in muscles expressing expanded repeats. The graph shows the means ± *SEM*. *$p < 0.05$, **$p < 0.01$, ***$p < 0.001$ (Student's t-test).

GFP or 20 units of the repeats, and was similar in flies expressing either expanded CUG or CCUG repeat RNA (Fig. 5C). Thus, in contrast to human patients, where DM2 muscle disability is milder than in DM1, these data indicate that expression of long CUG or CCUG repeat RNA in muscle tissue has a similar effect on locomotion in flies.

Heart dysfunction in both DM1 and DM2 model flies includes systolic and diastolic alterations, arrhythmia, and contractility defects. Cardiac alterations, characterized by conduction delays, arrhythmia, and heart blockage are the second most common cause of death in DMs[50]. In DM2, cardiac abnormalities have been reported to be similar to those described in DM1 but less frequent and severe[24]. To study heart function in the *Drosophila* DM models, adult fly hearts were dissected in artificial hemolymph and recorded with a high-speed video camera. Cardiac contractions were analyzed using a semi-automatic optical heartbeat analysis (SOHA) method to quantify the fly heart functional parameters[51]. The study of heart function in DM2 model flies revealed that expression of long CCUG repeats in fly heart caused lengthening of the heart period (HP), and extension of the systolic and diastolic intervals (SI and DI, respectively). Heart contraction, measured as a percentage of fractional shortening (%FS), and arrhythmicity measured using the arrhythmia index (AI), were

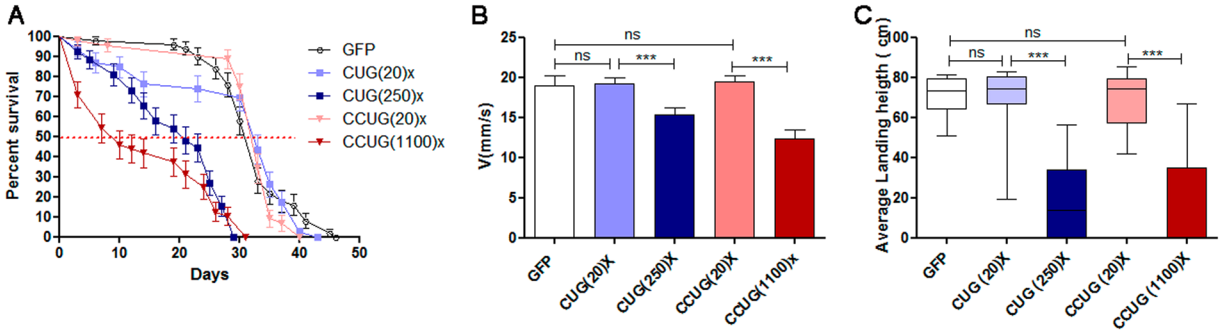

Figure 5. Survival and locomotor function were reduced in flies expressing expanded CUG or CCUG repeats in muscle. (**A**) Average percentage of live flies versus age (in days). The Mhc-Gal4 driver was used to induce the expression of the indicated constructs in muscle. The horizontal dotted line marks the median survival. Whereas control and short-repeat-expressing flies had similar median survival (GFP; n = 90, CUG(20)×, n = 100 and CCUG(20)×, n = 95), long CUG and CCUG-expressing flies have reduced survival (CUG(250)×; n = 95 and CCUG(1100)×; n = 100). Differences in the survival curves were highly significant ($p < 0.0001$, log-rank test). (**B**) Histogram showing the climbing speed as the mean speed ± *SEM* in mm/s. Flies expressing long CUG or CCUG repeats had reduced climbing velocity compared to control flies or flies expressing the short versions of repeats. (**C**) Notched box plot showing the median and the distribution of the average landing height data obtained in the flight assay with the relevant genotypes. Flight disability was observed in flies expressing long CUG or CCUG repeats. *$p < 0.05$, **$p < 0.01$, ***$p < 0.001$ (Student's t-test).

significantly altered compared to controls. In these model flies, the %FS was reduced to 20% and AI increased by around 3-fold (Fig. 6D,E). Importantly, the expression of short CCUG repeats did not affect %FS or AI but it increased the SI compared to controls, and resulted in a significantly increased HP (Fig. 6A–C). Similarly, we previously reported, that overexpression of expanded CUG repeats *in Drosophila* heart results in an increased HP with prolonged DI and SI, a reduction in %FS, and increased AI. In contrast, the expression of short CUG repeats only produced a slight increase in the SI duration[35].

Expression of expanded CUG or CCUG repeat RNA in fly heart reduces survival but does not affect locomotion. We previously reported that overexpression of long CUG repeats in fly heart results in a reduction in mean survival and lifespan[35]. The mean survival in control flies expressing GFP was 29 days which was reduced to about half in the DM1 model flies. The survival curve for flies expressing CCUG repeats in heart tissue was also significantly reduced compared to the GFP control flies. Of note, the survival curve of flies expressing short CUG or CCUG repeats was similar to that of control flies (Fig. 7A). These data suggest that the cardiac alterations in our DM1 and DM2 models affect the survival of flies.

To assess whether the expression of repeats in heart affects locomotor performance in flies, we analyzed the climbing velocity and landing distance of flies expressing CUG or CCUG repeats and found that neither the expression of short nor long versions of CUG or CCUG repeats affected these abilities (Fig. 7B,C). Thus, the reduction in %FS did not affect acute workload demands (flight, and climbing), but did have an accumulative detrimental effect on survival.

Materials and Methods

Drosophila strains. Pure expanded CTG and CCTG repeats were generated by PCR amplification of self-priming single-stranded CTG and CAG or CCTG and CAGG oligonucleotides as previously described[52]. Synthesized DNA duplexes were electrophoresed, size fractionated, purified using a DNA gel extraction kit (Qiagen), 5′-phosphorylated with T4 polynucleotide kinase, and cloned into the *Eco*RV site of pUAST. The recombinant plasmids containing uninterrupted stretches of CTG or CCTG repeats were amplified in STBL3 *E. coli* (Invitrogen) at 20 °C. Plasmid DNA was purified using a Qiagen plasmid DNA purification kit and sequenced from both ends to ensure the sequence integrity of the clones. Transgenic flies were generated by injecting the plasmids into w^{1118} embryos by BestGene Inc. following the method described in ref. 53. UAS-GFP strain was obtained from the Bloomington *Drosophila* Stock Center (Indiana University, Bloomington, IN). The cardiomyocyte-specific driver *GMH5–Gal4* was kindly provided by Dr. Bodmer from the Sanford Burnham Institute, California, USA[33]. The Mhc-GAL4 line was previously described[32]. Mhc-Gal4 drives expression in terminally differentiated muscle under the control of endogenous myosin heavy chain regulatory regions, while GMH5-Gal4 is expressed in cardiomyocytes initially driven by a 900 nt *tinman* heart enhancer and later maintained by a *UAS-Gal4* autoregulatory loop[33]. All the fly lines were maintained in standard *Drosophila* food. The flies were grown at 25 °C to study the effect of expressing repeats throughout the musculature and at 29 °C to study the cardiac defects. Expression levels of the different transgenes were assessed as previously described[35].

Cardiac physiological analysis. For the physiological analysis, female flies were collected just after eclosion and were maintained for 7 days at 29 °C. For the heart-beat recordings, semi-intact heart preparations were made as previously described[54,55]. An Leica DFC 450C microscope, connected to an ORCA Flash (Hamamatsu)

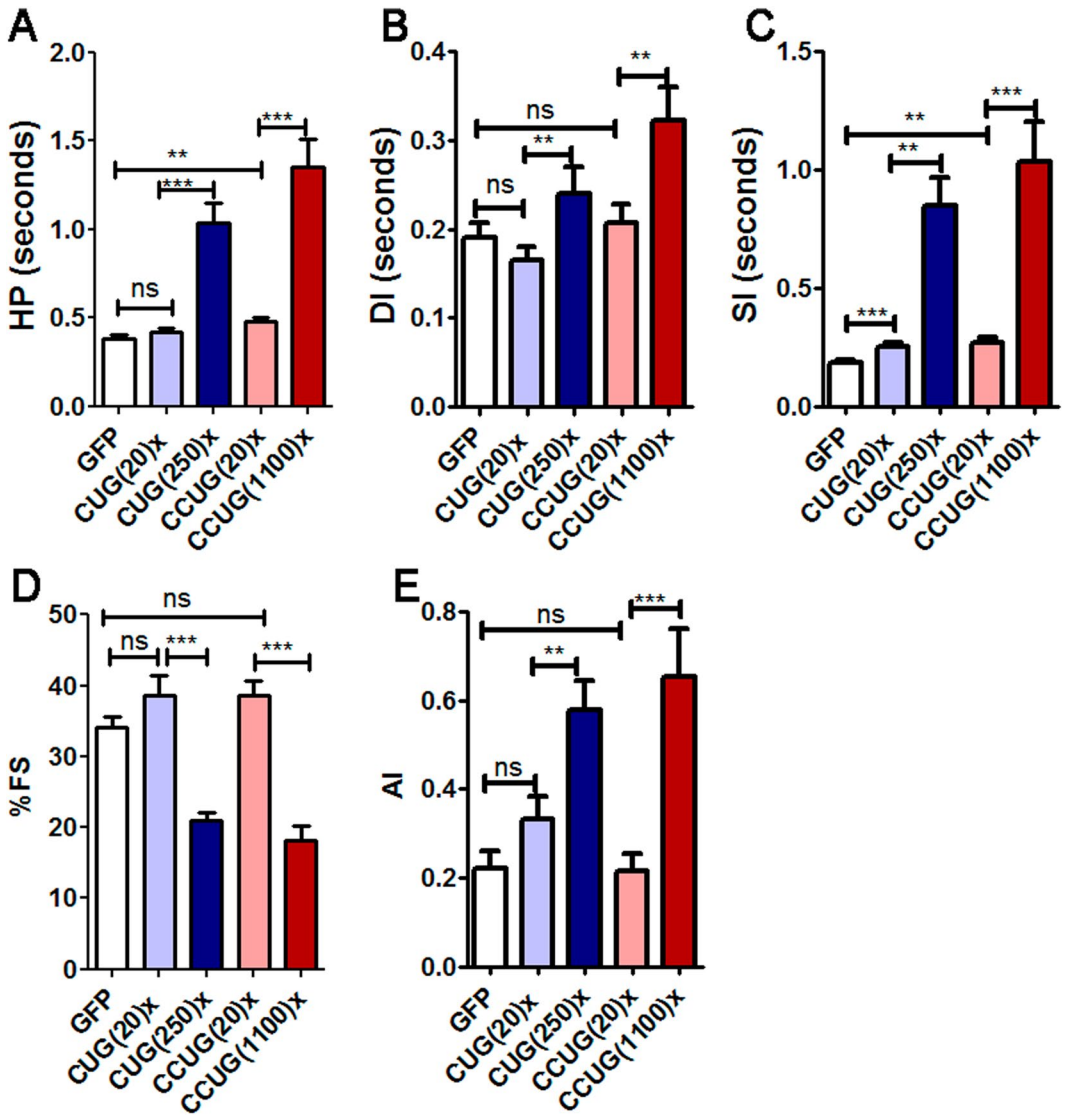

Figure 6. Cardiac dysfunction in DM1 and DM2 model flies includes diastolic and systolic elongation, increased arrhythmicity, and reduced contractility. The mean heart period (HP, in **A**) was significantly increased in flies expressing expanded CUG or CCUG repeats in heart. This increase was caused by a prolongation of both diastolic and systolic intervals (DI, in **B** and SI, in **C**) in the model flies. Heart tube contractility and cardiac rhythm were also affected in these flies, because the percentage of fractional shortening (%FS in **D**) was reduced to only 20% and arrhythmia, measured as the arrhythmicity index (AI in **E**), was significantly increased to similar levels in both DM1 and DM2 model flies. Graph bars show the mean values and their standard errors (n = 18 to 29). *p < 0.05, **$p < 0.01$, ***$p < 0.001$ (Student's t-test).

high-speed digital camera was used to take 20 s recordings at a minimum speed of 150 frames/s. Different cardiac parameters were measured using SOHA software[51].

Histological analysis. Analysis of the IFM area in *Drosophila* thoraces was performed as previously described[56]. Briefly, six thoraces from three-day or thirty-day-old (aged group) females were embedded in Epon following standard procedures. After drying the resin, semi-thin 1.5 µm-sections were obtained using an ultramicrotome (Ultracut E, Reichert-Jung and Leica). Images were taken at 100× magnification with a Leica DM2500 microscope (Leica Microsystems, Wetzlar, Germany). To quantify the muscle area, five images containing IFMs per fly were converted into binary images. Considering the complete image as 100% of the area, we used ImageJ software to calculate the percentage occupied by pixels corresponding to the IFMs. The percentage of pixels occupied by muscle in the control GFP flies were considered as 100%, and the percentage of muscle area of the rest of genotypes were normalized to these control flies.

For immunofluorescence analysis, dissected fly hearts or *Drosophila* thorax longitudinal sections were fixed for 20 min in 4% paraformaldehyde, and washed in PBT (PBS containing 0.3% Triton X-100) before staining. Muscleblind staining, and FISH to detect ribonuclear CUG foci, were performed as previously described[56]. The

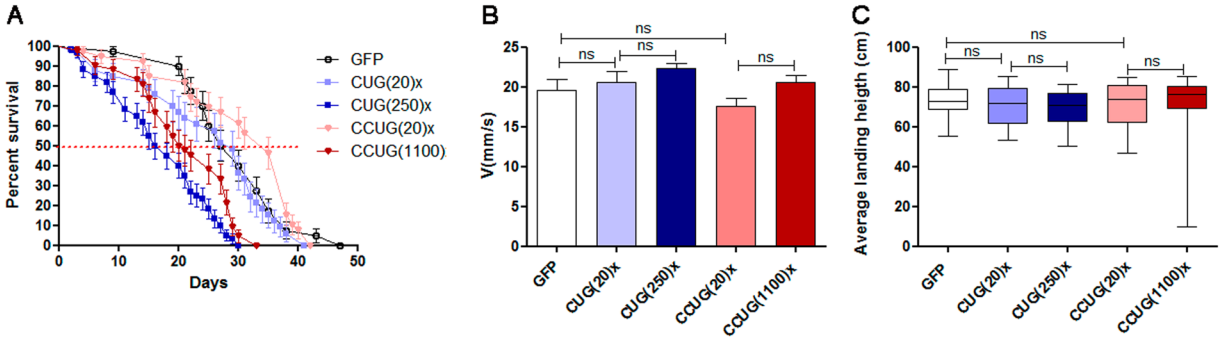

Figure 7. Expression of expanded CUG or CCUG repeats in fly heart alters survival but not locomotion. (**A**) Average percentage of live flies, with the indicated genotypes, versus age (in days). The *GMH5-Gal4* driver was used to induce expression of the indicated genotypes in cardiomyocytes. Horizontal dotted line marks the median survival. Flies expressing expanded CUG (CUG(250)×; n = 100) or CCUG (CCUG(1100)×; n = 97) repeats had a reduced lifespan compared to control flies (GFP; n = 100) or flies expressing the short versions of the repeats (CUG(20)×; n = 95 and CCUG(20)×; n = 99). The differences in survival curves were highly significant ($p < 0.0001$, log-rank test). (**B**) Histogram showing the climbing velocity of flies as the mean speed ± *SEM* in mm/s. Expression of long CUG or CCUG repeats in heart did not modify climbing velocity compared to control flies or flies expressing the short versions of repeats. (**C**) Notched box plot showing the median and the distribution of the average landing height data obtained in the flight assay using flies with the genotypes indicated. *$p < 0.05$, **$p < 0.01$, ***$p < 0.001$ (Student's t -test).

specificity of the anti-Mbl antibody has been previously tested in ref. 56. To detect CCUG foci a variation of the FISH protocol was implemented using a locked nucleic acid (LNA) probe with 7 CAGG repeats (Sigma), which was hybridized at 55 °C. All the confocal images were taken with an Olympus FV1000 microscope.

RNA extraction, RT-PCR and qRT-PCR. For each biological replicate, total RNA was extracted using Trizol (Sigma) from 10 five-day old adult males for the muscle studies and 20 seven-day old adult female hearts for the cardiac studies. One microgram of RNA was digested with DNase I (Invitrogen) and reverse-transcribed with SuperScript II (Invitrogen) using random hexanucleotides. 20 ng of cDNA were used in a standard PCR reaction with GoTaq polymerase (Promega) and specific primers to analyze *Fhos* exon 16′ inclusion (Table S1). *Rp49* was used as endogenous control using 0.2 ng of cDNA. qRT-PCR to analyze *Serca* exon 13 and *Atg 4*, *Atg7*, *Atg8a*, *Atg9* and *Atg12* expression levels was carried out from 2 ng of cDNA template with SYBR Green PCR Master Mix (Applied Biosystems) and specific primers (Table S1). For reference gene, *Rp49*, qRT-PCR was carried out from 0.2 ng of cDNA. Thermal cycling was performed in Step One Plus Real Time PCR System (Applied Biosystems). Three biological replicates and three technical replicates per biological sample were carried out. Relative expression to endogenous gene and the control group was obtained by the $2^{-\Delta\Delta Ct}$ method. Pairs of samples were compared using two-tailed t-test ($\alpha = 0.05$), applying Welch's correction when necessary.

Survival curves. Survival experiments were performed independently twice with a minimum of 45 flies each time. Flies were maintained at 25 °C for experiments involving Mhc-Gal4 and at 29 °C for the GMH5-Gal4 driver. The flies were transferred to new fresh nutritive media every second day and scored for deaths daily.

Flight and climbing functional assays. Given the heterogeneity generally found in the functional assays performed with female flies, we only used males in these experiments. Flight assays were performed on day five as described previously[57] using 100 flies per group. To assess climbing velocity, groups of 15, five-day-old males were transferred into 25 cm long, 1.5 cm diameter pipettes, after a period of 24 h without anesthesia. The height reached from the bottom of the vial by each fly in a period of 10 s was recorded with a camera. For each genotype, approximately 30 flies were tested.

Statistical analysis. Statistical analysis was performed using GraphPad Prism5 software. Pairs of samples were compared using a two-tailed Student's t-test ($\alpha = 0.05$), applying Welch correction when necessary. The survival curves used a minimum of 90 individuals and a log-rank test was used to assess whether there were any significant differences between them. The flight assay data are represented as a notched box plot, which includes the median and the distribution of the average landing heights obtained; the horizontal lines inside the boxes represent the median values, the bottom and top edges of the boxes represent the 25th and 75th percentiles, and bottom and top whiskers reach the 10th and 90th percentiles, respectively.

Discussion

A significant feature of DM is that two different microsatellite expansions in two unrelated genes cause a clinically similar disease. The histological features of skeletal muscle biopsies taken from DM1 and DM2 patients are very similar[50,58]. In both diseases, affected muscles show central nuclei, a reduction in the number and diameter of specific fiber types, fibrosis and adipose deposition. DM2 is specifically characterized by the presence of atrophic fibers with nuclear clumps even before the muscle weakness appearance as well as by a predominant type 2 fiber

atrophy[59,60]. In DM2, cardiac abnormalities have also been reported to be similar to those described in DM1, including conduction disturbances, cardiac arrhythmias and sudden death[26,61–63]. Similarly, the characteristic features of DM that we describe in our DM2 (CCUG-repeat bearing) flies, including muscle and locomotor defects, cardiac dysfunction and reduced survival, were very similar to the characteristics of flies expressing CUG repeats. Interestingly, the phenotypic similarities between our DM1 and DM2 model flies go beyond phenotypes to the pathogenesis mechanisms. We showed that Mbl retention in foci resulting in missplicing, and autophagy activation are common to both diseases. We report that autophagy-related genes are upregulated not only in muscle, but also in heart in both models, suggesting that this is not a tissue-specific mechanism of repeat toxicity. Some important differences between both models are also highlighted in our study. The effect of the expression of long CCUG repeats in heart was more pronounced than that of long CUG repeats, and correlated with stronger upregulation of autophagy-related factors. These data suggest the existence of unknown tissue-dependent factors that might modulate the toxicity of CUG and CCUG repeats. The difference between the expression level of autophagy-related factors in control or expanded repeat-expressing flies was higher in muscle compared to heart samples, suggesting that autophagy is importantly involved in pathogenesis in this tissue. The autophagy activation in the DM1 and DM2 model flies coincides in muscle with strong muscle area reduction in the flies expressing the long versions of the repeats. These data are consistent with our previous results in the model flies expressing 480 CUG repeats[34]. Moreover, our experiments with young and aged flies have shown that muscle defects caused by expanded CCUG repeats have not only a developmental contribution but may also impinge on adult muscle maintenance and/or degeneration, as we have previously shown with heat-shock-induced expression of CUG expansions exclusively in adult muscle[34]. Importantly, this is the first DM2 animal model showing obvious muscle phenotypes.

As a result of expanded repeats expression in heart, we observed systolic and diastolic dysfunction, reduction of the fractional shortening and increased arrhythmicity in DM2 model flies, which resembled the DM1-like phenotype previously described in flies[35] and in DM patients[64]. Importantly, SI and DI were more affected by CCUG repeats than by CUG repeats expression. Accordingly, in heart tissue, the expression of short repeats produced a slight but significant prolongation in the systolic interval, which was more pronounced in the case of CCUG-expressing flies. Remarkably, the expression of short versions of repeats did not induce Muscleblind sequestration in foci in IFM or heart tissue. Therefore, the phenotypes observed in these flies might be independent of Muscleblind, and the factors originating the phenotype seem to be more sensitive to CCUG repeats than to CUG repeats.

An open question in the field of DM is to clarify the pathomechanisms underlying the phenotypic differences between DM1 and DM2. Several studies have confirmed that the frequency and severity of cardiac involvement and of muscle weakness are reduced in DM2 compared to DM1 and that progression is slower and less severe in DM2[24,26]. This suggests that other cellular and molecular pathways are involved besides the shared toxic-RNA gain of function in the human disease phenotype. Three factors have been shown to influence the level of toxicity of expanded repeats in the RNA; expression level, length, and sequence[21,65,66]. Longer sequences tend to cause severe pathogenesis but depending on the sequence, RNA binding factors might be differentially affected. Importantly, in DM2 patients, the severity of the disease has not been directly correlated with the repeat number, only a relationship between repeat lengths and MBNL1 rate of sequestration has been established[21]. In flies, however, a previous report showing the effect in eye of the expression of pure, uninterrupted CCUG-repeat expansions ranging from 16 to 720 repeats in length, has shown a nice correlation between length and toxicity of the CCUG repeats[22]. We believe that this previous observation, and our own reports of similar phenotypes in flies expressing either expanded CUG or CCUG repeats, suggest the existence of unknown modifiers in humans, which might quench RNA toxicity in DM2 patients.

In our flies expressing 250 CUG repeats we observed very similar phenotypes but milder than the ones previously reported by expressing 480 interrupted CUG repeats in muscle[34,49]. Our data suggests that these phenotypes are sensitive to CUG repeat length, a main feature of DM1, and suggest that the phenotypes described in the previous model were not significantly affected by interrupting sequences.

The experiments expressing the CUG or CCUG repeats in a non-human context in *Drosophila* provide evidence of the strong toxicity potential of the CCUG repeats, as the phenotypes we report in the DM2 model flies expressing the repeats in muscle or heart, are as strong as the phenotypes obtained from expressing the CUG repeats. Disease-specific manifestations may then result from factors that are extrinsic to the repeats and previous evidence suggested several hypotheses. Disease-specific manifestations may result from differences in spatial and temporal expression patterns of *DMPK* and *CNBP* genes. Similarly, changes in the expression of neighboring genes may define disease-specific manifestations. It was recently reported that CUGBP1 protein is overexpressed in muscle biopsies from patients affected by the adult classical form of DM1 but not in muscle from DM2 patients, suggesting that CUGBP1 overexpression in DM1 might be an additional pathogenic mechanism not shared by DM2[67]. Another possible explanation for the clinical differences between the two DM forms is the reduction of DMPK or ZNF9 protein levels in DM1 and DM2 respectively[68–70]. However, *Dmpk* knockout young mice do not develop a multisystemic phenotype mimicking myotonic dystrophy[71]. On the contrary, reduction of *CNBP* levels is sufficient to produce multiorgan symptoms resembling those of DM as observed in heterozygous Cnbp +/− knockout mice[72] implying that CNBP may well play a role in DM2 pathology[21]. According to different sources, *CNBP* is 4 to 8-fold more expressed in human muscles than the *DMPK* gene[27–29], which makes it difficult to explain the phenotypic differences between DM1 and DM2 based on the small reductions in *CNBP* expression reported in DM2 patients. Another important difference between CUG and CCUG expansions is that MBNL has been reported to bind CCUG repeats with a stronger affinity compared to CUG repeats[6,30]. In addition, the ribonuclear inclusions in DM2 patients appear to be larger than in DM1 patients, and sequester more MBNL[21]. Accordingly, our results in the DM model flies show that, at least in muscle, flies expressing expanded CCUG repeats tend to have higher levels of missplicing, suggesting a reduced activity of Mbl. However, the muscle

defects in DM1 and DM2 model flies were similar, suggesting that Mbl involvement in muscle phenotype is already limiting in DM1 model flies and decreasing levels of Mbl would not result in stronger phenotype.

In conclusion, through this demonstration of CUG and CCUG repeat-induced toxicity in different fly tissues we have gained a useful insight into the differences and similarities in the mechanism of DM pathogenesis in these tissues. The dual system we report (DM1 vs DM2 fly model) with well-characterized repeat expression, resulting phenotypes and molecular alterations, will also be useful to compare the effect of potential chemical or genetic modifiers of RNA toxicity on each of these diseases. The potential discovery of genetic modifiers that affect only one of the components in flies, either CUG or CCUG toxicity, could explain the clinical differences between both human diseases, contributing to increase the knowledge about their pathogenesis pathways and towards the development of new treatments.

References

1. Brook, J. D. *et al.* Molecular basis of myotonic dystrophy: expansion of a trinucleotide (CTG) repeat at the 3′ end of a transcript encoding a protein kinase family member. *Cell* **69**, 385 (1992).
2. Ricker, K. *et al.* Proximal myotonic myopathy: a new dominant disorder with myotonia, muscle weakness, and cataracts. *Neurology* **44**, 1448–1452, doi:10.1212/WNL.44.8.1448 (1994).
3. Liquori, C. L. *et al.* Myotonic dystrophy type 2 caused by a CCTG expansion in intron 1 of ZNF9. *Science* **293**, 864–867, doi:10.1126/science.1062125 (2001).
4. Meola, G. & Cardani, R. Myotonic dystrophies: An update on clinical aspects, genetic, pathology, and molecular pathomechanisms. *Biochimica et biophysica acta* **1852**, 594–606, doi:10.1016/j.bbadis.2014.05.019 (2015).
5. Miller, J. W. *et al.* Recruitment of human muscleblind proteins to (CUG)(n) expansions associated with myotonic dystrophy. *Embo J* **19**, 4439–4448, doi:10.1093/emboj/19.17.4439 (2000).
6. Kino, Y. *et al.* Muscleblind protein, MBNL1/EXP, binds specifically to CHHG repeats. *Human molecular genetics* **13**, 495–507, doi:10.1093/hmg/ddh056 (2004).
7. Mankodi, A. *et al.* Muscleblind localizes to nuclear foci of aberrant RNA in myotonic dystrophy types 1 and 2. *Human molecular genetics* **10**, 2165–2170, doi:10.1093/hmg/10.19.2165 (2001).
8. Fardaei, M. *et al.* Three proteins, MBNL, MBLL and MBXL, co-localize *in vivo* with nuclear foci of expanded-repeat transcripts in DM1 and DM2 cells. *Human molecular genetics* **11**, 805–814, doi:10.1093/hmg/11.7.805 (2002).
9. Jiang, H., Mankodi, A., Swanson, M. S., Moxley, R. T. & Thornton, C. A. Myotonic dystrophy type 1 is associated with nuclear foci of mutant RNA, sequestration of muscleblind proteins and deregulated alternative splicing in neurons. *Human molecular genetics* **13**, 3079–3088, doi:10.1093/hmg/ddh327 (2004).
10. Cardani, R., Mancinelli, E., Rotondo, G., Sansone, V. & Meola, G. Muscleblind-like protein 1 nuclear sequestration is a molecular pathology marker of DM1 and DM2. *European journal of histochemistry: EJH* **50**, 177–182 (2006).
11. Lukas, Z. *et al.* Sequestration of MBNL1 in tissues of patients with myotonic dystrophy type 2. *Neuromuscular disorders: NMD* **22**, 604–616, doi:10.1016/j.nmd.2012.03.004 (2012).
12. Timchenko, N. A. *et al.* RNA CUG repeats sequester CUGBP1 and alter protein levels and activity of CUGBP1. *J Biol Chem* **276**, 7820–7826, doi:10.1074/jbc.M005960200 (2001).
13. Goodwin, M. & Swanson, M. S. RNA-binding protein misregulation in microsatellite expansion disorders. *Adv Exp Med Biol* **825**, 353–388, doi:10.1007/978-1-4939-1221-6_10 (2014).
14. Wang, E. T. *et al.* Antagonistic regulation of mRNA expression and splicing by CELF and MBNL proteins. *Genome Res* **25**, 858–871, doi:10.1101/gr.184390.114 (2015).
15. Kino, Y. *et al.* MBNL and CELF proteins regulate alternative splicing of the skeletal muscle chloride channel CLCN1. *Nucleic Acids Res* **37**, 6477–6490, doi:gkp681 (2009).
16. Santoro, M. *et al.* Molecular, clinical, and muscle studies in myotonic dystrophy type 1 (DM1) associated with novel variant CCG expansions. *Journal of neurology* **260**, 1245–1257, doi:10.1007/s00415-012-6779-9 (2013).
17. Gao, Z. & Cooper, T. A. Reexpression of pyruvate kinase M2 in type 1 myofibers correlates with altered glucose metabolism in myotonic dystrophy. *Proceedings of the National Academy of Sciences of the United States of America* **110**, 13570–13575, doi:1308806110 (2013).
18. Tang, Z. Z. *et al.* Muscle weakness in myotonic dystrophy associated with misregulated splicing and altered gating of Ca(V)1.1 calcium channel. *Human molecular genetics* **21**, 1312–1324, doi:ddr568 (2012).
19. Fugier, C. *et al.* Misregulated alternative splicing of BIN1 is associated with T tubule alterations and muscle weakness in myotonic dystrophy. *Nat Med* **17**, 720–725, doi:nm.237 (2011).
20. Martorell, L. *et al.* Germline mutational dynamics in myotonic dystrophy type 1 males: allele length and age effects. *Neurology* **62**, 269–274, doi:10.1212/WNL.62.2.269 (2004).
21. Cardani, R. *et al.* Progression of muscle histopathology but not of spliceopathy in myotonic dystrophy type 2. *Neuromuscular disorders: NMD* **24**, 1042–1053, doi:10.1016/j.nmd.2014.06.435 (2014).
22. Yu, Z. *et al.* A fly model for the CCUG-repeat expansion of myotonic dystrophy type 2 reveals a novel interaction with MBNL1. *Human molecular genetics* **24**, 954–962, doi:10.1093/hmg/ddu507 (2015).
23. Milone, M., Batish, S. D. & Daube, J. R. Myotonic dystrophy type 2 with focal asymmetric muscle weakness and no electrical myotonia. *Muscle & nerve* **39**, 383–385, doi:10.1002/mus.21150 (2009).
24. Meola, G. & Moxley, R. T. 3rd Myotonic dystrophy type 2 and related myotonic disorders. *Journal of neurology* **251**, 1173–1182, doi:10.1007/s00415-004-0590-1 (2004).
25. Schoser, B. & Timchenko, L. Myotonic dystrophies 1 and 2: complex diseases with complex mechanisms. *Current genomics* **11**, 77–90, doi:10.2174/138920210790886844 (2010).
26. Sansone, V. A. *et al.* The frequency and severity of cardiac involvement in myotonic dystrophy type 2 (DM2): long-term outcomes. *Int J Cardiol* **168**, 1147–1153, doi:10.1016/j.ijcard.2012.11.076 (2013).
27. Wu, C., Jin, X., Tsueng, G., Afrasiabi, C. & Su, A. I. BioGPS: building your own mash-up of gene annotations and expression profiles. *Nucleic Acids Res* **44**, D313–316, doi:10.1093/nar/gkv1104 (2016).
28. Wu, C., Macleod, I. & Su, A. I. BioGPS and MyGene.info: organizing online, gene-centric information. *Nucleic Acids Res* **41**, D561–565, doi:10.1093/nar/gks1114 (2013).
29. Wu, C. *et al.* BioGPS: an extensible and customizable portal for querying and organizing gene annotation resources. *Genome Biol* **10**, R130, doi:10.1186/gb-2009-10-11-r130 (2009).
30. Warf, M. B. & Berglund, J. A. MBNL binds similar RNA structures in the CUG repeats of myotonic dystrophy and its pre-mRNA substrate cardiac troponin T. *Rna* (2007).
31. Bachinski, L. L. *et al.* Premutation allele pool in myotonic dystrophy type 2. *Neurology* **72**, 490–497, doi:01.wnl.0000333665.01888.33 (2009).
32. Marek, K. W. *et al.* A genetic analysis of synaptic development: pre- and postsynaptic dCBP control transmitter release at the Drosophila NMJ. *Neuron* **25**, 537–547, doi:10.1016/S0896-6273(00)81058-2 (2000).

33. Wessells, R. J. & Bodmer, R. Screening assays for heart function mutants in Drosophila. *BioTechniques* **37**, 58–60, 62, 64 passim (2004).
34. Bargiela, A. *et al*. Increased autophagy and apoptosis contribute to muscle atrophy in a myotonic dystrophy type 1 Drosophila model. *Disease models & mechanisms* **8**, 679–690, doi:8/7/679 (2015).
35. Chakraborty, M. *et al*. Pentamidine rescues contractility and rhythmicity in a Drosophila model of myotonic dystrophy heart dysfunction. *Disease models & mechanisms* **8**, 1569–1578, doi:10.1242/dmm.021428 (2015).
36. Lin, X. *et al*. Failure of MBNL1-dependent post-natal splicing transitions in myotonic dystrophy. *Human molecular genetics* **15**, 2087–2097, doi:10.1093/hmg/ddl132 (2006).
37. Cerro-Herreros, E., Fernandez-Costa, J. M., Sabater-Arcis, M., Llamusi, B. & Artero, R. Derepressing muscleblind expression by miRNA sponges ameliorates myotonic dystrophy-like phenotypes in Drosophila. *Sci Rep* **6**, 36230, doi:10.1038/srep36230 (2016).
38. Picchio, L., Plantie, E., Renaud, Y., Poovthumkadavil, P. & Jagla, K. Novel Drosophila model of myotonic dystrophy type 1: phenotypic characterization and genome-wide view of altered gene expression. *Human molecular genetics* **22**, 2795–2810, doi:ddt127 (2013).
39. Loro, E. *et al*. Normal myogenesis and increased apoptosis in myotonic dystrophy type-1 muscle cells. *Cell Death Differ* **17**, 1315–1324, doi:cdd201033 (2010).
40. Vignaud, A. *et al*. Progressive skeletal muscle weakness in transgenic mice expressing CTG expansions is associated with the activation of the ubiquitin-proteasome pathway. *Neuromuscular disorders: NMD* **20**, 319–325, doi:S0960-8966(10)00111-2 (2010).
41. Denis, J. A. *et al*. mTOR-dependent proliferation defect in human ES-derived neural stem cells affected by myotonic dystrophy type 1. *J Cell Sci* **126**, 1763–1772, doi:jcs.116285 (2013).
42. Batra, R. *et al*. Loss of MBNL leads to disruption of developmentally regulated alternative polyadenylation in RNA-mediated disease. *Mol Cell* **56**, 311–322, doi:S1097-2765(14)00682-0 (2014).
43. Goodwin, M. *et al*. MBNL Sequestration by Toxic RNAs and RNA Misprocessing in the Myotonic Dystrophy Brain. *Cell Rep* **12**, 1159–1168, doi:S2211-1247(15)00789-5 (2015).
44. Brockhoff, M. *et al*. Targeting deregulated AMPK/mTORC1 pathways improves muscle function in myotonic dystrophy type I. *J Clin Invest* **127**, 549–563, doi:10.1172/JCI89616 (2017).
45. Udd, B. & Krahe, R. The myotonic dystrophies: molecular, clinical, and therapeutic challenges. *Lancet Neurol* **11**, 891–905, doi:S1474-4422(12)70204-1 (2012).
46. Chelly, J. & Desguerre, I. Progressive muscular dystrophies. *Handb Clin Neurol* **113**, 1343–1366, doi:10.1016/B978-0-444-59565-2.00006-X (2013).
47. Mathieu, J., Allard, P., Potvin, L., Prevost, C. & Begin, P. A 10-year study of mortality in a cohort of patients with myotonic dystrophy. *Neurology* **52**, 1658–1662, doi:10.1212/WNL.52.8.1658 (1999).
48. Breton, R. & Mathieu, J. Usefulness of clinical and electrocardiographic data for predicting adverse cardiac events in patients with myotonic dystrophy. *The Canadian journal of cardiology* **25**, e23–27, doi:10.1016/S0828-282X(09)70479-9 (2009).
49. Garcia-Lopez, A. *et al*. Genetic and chemical modifiers of a CUG toxicity model in Drosophila. *PLoS ONE* **3**, e1595, doi:10.1371/journal.pone.0001595 (2008).
50. Harper, P. *Myotonic dystrophy*. (Saunders, 2001).
51. Cammarato, A., Ocorr, S. & Ocorr, K. Enhanced assessment of contractile dynamics in Drosophila hearts. *BioTechniques* **58**, 77–80, doi:10.2144/000114255 (2015).
52. Ordway, J. M. & Detloff, P. J. *In vitro* synthesis and cloning of long CAG repeats. *BioTechniques* **21**, 609–610, 612 (1996).
53. Spradling, A. C. & Rubin, G. M. Transposition of cloned P elements into Drosophila germ line chromosomes. *Science* **218**, 341–347, doi:10.1126/science.6289435 (1982).
54. Magny, E. G. *et al*. Conserved regulation of cardiac calcium uptake by peptides encoded in small open reading frames. *Science* **341**, 1116–1120, doi:10.1126/science.1238802 (2013).
55. Ocorr, K. A., Crawley, T., Gibson, G. & Bodmer, R. Genetic variation for cardiac dysfunction in Drosophila. *PLoS One* **2**, e601, doi:10.1371/journal.pone.0000601 (2007).
56. Llamusi, B. *et al*. Muscleblind, BSF and TBPH are mislocalized in the muscle sarcomere of a Drosophila myotonic dystrophy model. *Disease models & mechanisms* **6**, 184–196, doi:dmm.009563 (2013).
57. Babcock, D. T. & Ganetzky, B. An improved method for accurate and rapid measurement of flight performance in Drosophila. *Journal of visualized experiments: JoVE* e51223, doi:10.3791/51223 (2014).
58. Day, J. W. *et al*. Myotonic dystrophy type 2: molecular, diagnostic and clinical spectrum. *Neurology* **60**, 657–664, doi:10.1212/01.WNL.0000054481.84978.F9 (2003).
59. Schoser, B. G. *et al*. Muscle pathology in 57 patients with myotonic dystrophy type 2. *Muscle & nerve* **29**, 275–281, doi:10.1002/mus.10545 (2004).
60. Pisani, V. *et al*. Preferential central nucleation of type 2 myofibers is an invariable feature of myotonic dystrophy type 2. *Muscle & nerve* **38**, 1405–1411, doi:10.1002/mus.21122 (2008).
61. Schmacht, L. *et al*. Cardiac Involvement in Myotonic Dystrophy Type 2 Patients With Preserved Ejection Fraction: Detection by Cardiovascular Magnetic Resonance. *Circulation. Cardiovascular imaging* **9**, e004615, doi:10.1161/CIRCIMAGING.115.004615 (2016).
62. Lau, J. K., Sy, R. W., Corbett, A. & Kritharides, L. Myotonic dystrophy and the heart: A systematic review of evaluation and management. *Int J Cardiol* **184**, 600–608, doi:10.1016/j.ijcard.2015.03.069 (2015).
63. Petri, H., Vissing, J., Witting, N., Bundgaard, H. & Kober, L. Cardiac manifestations of myotonic dystrophy type 1. *Int J Cardiol* **160**, 82–88, doi:S0167-5273(11)00878-3 (2012).
64. McNally, E. M. & Sparano, D. Mechanisms and management of the heart in myotonic dystrophy. *Heart* **97**, 1094–1100, doi:10.1136/hrt.2010.214197 (2011).
65. Mastroyiannopoulos, N. P. *et al*. The effect of myotonic dystrophy transcript levels and location on muscle differentiation. *Biochem Biophys Res Commun* **377**, 526–531, doi:10.1016/j.bbrc.2008.10.031 (2008).
66. Botta, A. *et al*. The CTG repeat expansion size correlates with the splicing defects observed in muscles from myotonic dystrophy type 1 patients. *Journal of medical genetics* **45**, 639–646, doi:10.1136/jmg.2008.058909 (2008).
67. Cardani, R. *et al*. Overexpression of CUGBP1 in skeletal muscle from adult classic myotonic dystrophy type 1 but not from myotonic dystrophy type 2. *PLoS One* **8**, e83777, doi:10.1371/journal.pone.0083777 (2013).
68. Huichalaf, C. *et al*. Reduction of the rate of protein translation in patients with myotonic dystrophy 2. *J Neurosci* **29**, 9042–9049, doi:10.1523/JNEUROSCI.1983-09.2009 (2009).
69. Raheem, O. *et al*. Mutant (CCTG)n expansion causes abnormal expression of zinc finger protein 9 (ZNF9) in myotonic dystrophy type 2. *The American journal of pathology* **177**, 3025–3036, doi:10.2353/ajpath.2010.100179 (2010).
70. Kaliman, P. & Llagostera, E. Myotonic dystrophy protein kinase (DMPK) and its role in the pathogenesis of myotonic dystrophy 1. *Cellular signalling* (2008).
71. Carrell, S. T. *et al*. Dmpk gene deletion or antisense knockdown does not compromise cardiac or skeletal muscle function in mice. *Human molecular genetics* **25**, 4328–4338, doi:10.1093/hmg/ddw266 (2016).
72. Chen, W. *et al*. Haploinsuffciency for Znf9 in Znf9+/− mice is associated with multiorgan abnormalities resembling myotonic dystrophy. *Journal of molecular biology* **368**, 8–17, doi:10.1016/j.jmb.2007.01.088 (2007).

Acknowledgements

We thank Dr. Ocorr and Dr. Bodmer (Sanford Burnham Prebys Medical Discovery Institute, USA) for the development of the freely available SOHA software and Dr. Nicholas Charlet Berguerand (*Institut de Génétique et de Biologie Moléculaire et Cellulaire*, France) for providing us with the different CTG and CCTG plasmid versions. This study was co-funded by grants from the Instituto de Salud Carlos III, Spain (PI13/00386, including funds from ERDF) and the ERA-Net E-Rare framework from ISCIII (PI12/03106 including funds from ERDF) upon the AES (R + D + I) National Plan of Spain awarded to MPA and BL, respectively. Additional financial support was from P73 project "Todos somos raros, todos somos Unicos", RTVE TELEMARATON (FEDER, FUNDACION ISABEL GEMIO and ASEM) to BL and PROMETEOII/2014/067 to RA. ECH was supported by a pre-doctoral fellowship (BES-2013–064522) from the Ministerio de Economia y Competitividad, Spain. MC was the recipient of a Santiago Grisolía award (GrisoliaP/2013/A/044).

Author Contributions

B.L.L., R.A. and M.P.A. conceived and designed the experiments. B.L.L., E.C.H., and M.C. performed the experiments and analyzed the data. B.L.L. and R.A. wrote the paper with contributions from all the authors.

Additional Information

Supplementary information accompanies this paper at doi:10.1038/s41598-017-02829-3

Competing Interests: The authors declare that they have no competing interests.

Publisher's note: Springer Nature remains neutral with regard to jurisdictional claims in published maps and institutional affiliations.

-Artículo 2-

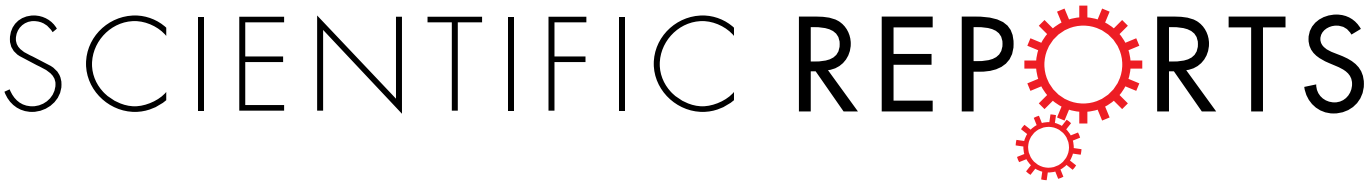

OPEN

Derepressing *muscleblind* expression by miRNA sponges ameliorates myotonic dystrophy-like phenotypes in *Drosophila*

Received: 22 April 2016
Accepted: 12 October 2016
Published: 02 November 2016

Estefania Cerro-Herreros[1,2], Juan M. Fernandez-Costa[1,2], María Sabater-Arcis[1,2], Beatriz Llamusi[1,2] & Ruben Artero[1,2]

Myotonic Dystrophy type 1 (DM1) originates from alleles of the *DMPK* gene with hundreds of extra CTG repeats in the 3′ untranslated region (3′ UTR). CUG repeat RNAs accumulate in foci that sequester Muscleblind-like (MBNL) proteins away from their functional target transcripts. Endogenous upregulation of MBNL proteins is, thus, a potential therapeutic approach to DM1. Here we identify two miRNAs, *dme-miR-277* and *dme-miR-304*, that differentially regulate *muscleblind* RNA isoforms in miRNA sensor constructs. We also show that their sequestration by sponge constructs derepresses endogenous *muscleblind* not only in a wild type background but also in a DM1 *Drosophila* model expressing non-coding CUG trinucleotide repeats throughout the musculature. Enhanced *muscleblind* expression resulted in significant rescue of pathological phenotypes, including reversal of several mis-splicing events and reduced muscle atrophy in DM1 adult flies. Rescued flies had improved muscle function in climbing and flight assays, and had longer lifespan compared to disease controls. These studies provide proof of concept for a similar potentially therapeutic approach to DM1 in humans.

Myotonic dystrophy type 1 (DM1) is an incurable neuromuscular disorder that is caused by an expanded CTG*CAG repeat in the 3′-untranslated region (3′ UTR) of the *dystrophia myotonica-protein kinase* (*DMPK*) gene (for a recent review, see ref. 1). The normal human *DMPK* gene harbors 5–37 copies of the trinucleotide motif, but a dynamic mutation may increase this number to over 5000 repeat copies. Clinically, DM1 is a multisystemic disorder, which mainly affects skeletal muscle, the heart and the nervous system. Severity of disease correlates with the expansion size and typical disease features are myotonia, muscle weakness and atrophy, smooth and cardiac muscle involvement, CNS dysfunction, somnolence, endocrine disorders and reduced life span[2,3].

Expression of expanded alleles in DM1 results in the nuclear retention of mutant *DMPK* mRNA and reduced DMPK protein levels[4]. Mutant transcripts sequester Muscleblind-like (MBNL) splicing factors, leading to the abnormal alternative splicing of a multitude of other transcripts and the expression of fetal forms of their protein products in DM1 adults[5–7]. Spliceopathy is therefore thought to be the major factor underlying the pathogenesis of DM1. However, alternative mechanisms such as additional changes in gene expression, antisense transcripts, translation efficiency, misregulated alternative polyadenylation and miRNA deregulation may also contribute to the pathogenesis of DM1[8–15].

Several therapeutic approaches have been tested in DM1 animal models. Among them, the most exciting results derived from blocking the interaction between MBNL and toxic RNA using small molecules, peptides, morpholinos or antisense oligonucleotides, and gapmers to degrade the mutant transcripts[16–21]. A less explored alternative in DM1 is the therapeutic modulation of MBNL gene expression. Although the expression of CUG expansions triggers different molecular alterations, current evidence points to MBNL depletion as the main cause of disease symptoms. A *Mbnl1* knock-out (KO) mouse model displays myotonia, missplicing of muscular transcripts and cataracts, which are all characteristic symptoms of DM1 disease[22]. More recently, relevant cardiac dysfunction features have been described in 2 month-old *Mbnl1* mutant mice (hypertrophy, interstitial fibrosis

[1]Translational Genomics Group, Incliva Health Research Institute, Valencia, Spain. [2]Department of Genetics and Interdisciplinary Research Structure for Biotechnology and Biomedicine (ERI BIOTECMED), Universitat de València, Valencia, Spain. Correspondence and requests for materials should be addressed to R.A. (email: ruben.artero@uv.es)

miRNA	Miranda	TargetScan	*mbl* isoform
miR-92a	—	—	*mblA*
	—	—	*mblB*
	—	—	*mblC*
	—	—	*mblD*
miR-100	—	—	*mblA*
	—	—	*mblB*
	—	—	*mblC*
	—	—	*mblD*
miR-124	1 site	—	*mblA*
	—	—	*mblB*
	—	—	*mblC*
	1 site	—	*mblD*
miR-277	1 site	—	*mblA*
	2 sites	—	*mblB*
	—	—	*mblC*
	2 sites	1 site	*mblD*
miR-304	—	—	*mblA*
	—	—	*mblB*
	1 site	—	*mblC*
	—	1 site	*mblD*

Table 1. Number of miRNA recognition sites predicted in *muscleblind* 3′ UTR according to different algorithms. -: no predictions.

and splicing alterations), which suggests a role for Mbnl1 reduction in the cardiac problems in DM1[23]. However, *Mbnl1* KO mice do not display the whole set of symptoms of DM1. Therefore, it has been hypothesized that *Mbnl2* could compensate for *Mbnl1* loss of function in these mice. In fact, *Mbnl1* KO mice with reduced expression of *Mbnl2* (*Mbnl1*$^{-/-}$; *Mbnl2*$^{+/-}$), are viable but develop most of the cardinal defects of the disease, including reduced lifespan, cardiac blockage, severe myotonia, atrophic fibers and progressive weakness of skeletal muscles. In support of the compensation hypothesis, levels of *Mbnl2* are increased in *Mbnl1*$^{-/-}$ KO mice and Mbnl2 can regulate the splicing of exons which are normally regulated by Mbnl1[24]. Furthermore, genetic polymorphisms in the human MBNL1 gene promoter have been associated with the severity of the disease[25].

Several observations suggest that MBNL1 overexpression has potential for treating DM1 pathology. Firstly, administration of recombinant Mbnl1 protein to a *HSA*^{LR} mouse model of DM1, rescues myotonia and the splicing alterations characteristic of DM1[26]. Secondly, we showed that the overexpression of a *muscleblind* isoform partially rescues muscle atrophy in a *Drosophila* DM1 model[27]. Finally, MBNL1 overexpression is well tolerated in skeletal muscle in transgenic mice where it causes only relatively minor splicing changes but no effect on longevity[28].

In this proof of concept study, we use the *Drosophila* DM1 model to explore the therapeutic potential of silencing specific microRNAs (miRNAs) and thus boost *muscleblind* (*mbl*) expression. The fundamental roles of miRNAs in the regulation of gene expression have been well-established. These endogenous ~22 nucleotide-long non-coding RNAs act post-transcriptionally and exert their regulatory effects mainly by binding to the 3′ UTR of target mRNAs, which results in mRNA deadenylation and decay, translational suppression or, rarely, mRNA cleavage[29–33]. Starting from a set of miRNAs predicted as *muscleblind* regulators, we confirmed that specific silencing of two of them, using sponge constructs, which sequester the miRNAs, upregulated *muscleblind* mRNA and protein. Similar effects were observed in flies co-expressing 480 CTG interrupted repeats (*i(CTG)480*) and either of the two sponge constructs in muscle. Muscleblind upregulation was sufficient to rescue characteristic DM1 model phenotypes such as missplicing events, reduced lifespan, and muscle atrophy. Importantly, the rescue of muscle atrophy resulted in improved climbing and flight ability in DM1 model flies. These data provide proof-of-principle for the therapeutic potential of Muscleblind upregulation by specific miRNA inhibitors in DM1 patients.

Results

Silencing of *dme-miR-277* or *dme-miR-304* derepresses *muscleblind* in *Drosophila* muscle.

Muscleblind sequestration in RNA foci and subsequent loss of function of the protein is a main triggering factor in DM1 molecular pathology. In order to identify miRNAs that repress *muscleblind* we selected candidate miRNAs and blocked their activity using specific miRNA sponges. We selected *dme-miR-92a*, *dme-miR-100* and *dme-miR-124* based on data generated in our laboratory and their orthology with human miRNAs. To widen the search of miRNA set of candidates, we used TargetScan[34] to analyze miRNA recognition sites in the *muscleblind* 3′UTR and identified sites for two additional miRNAs: *dme-miR-277* and *dme-miR-304* (Table 1). Importantly, profiling of *Drosophila* microRNA expression in dissected thoracic muscles, had previously demonstrated *miR-124, miR-100, miR-277* and *miR-304* expression in these muscles[35].

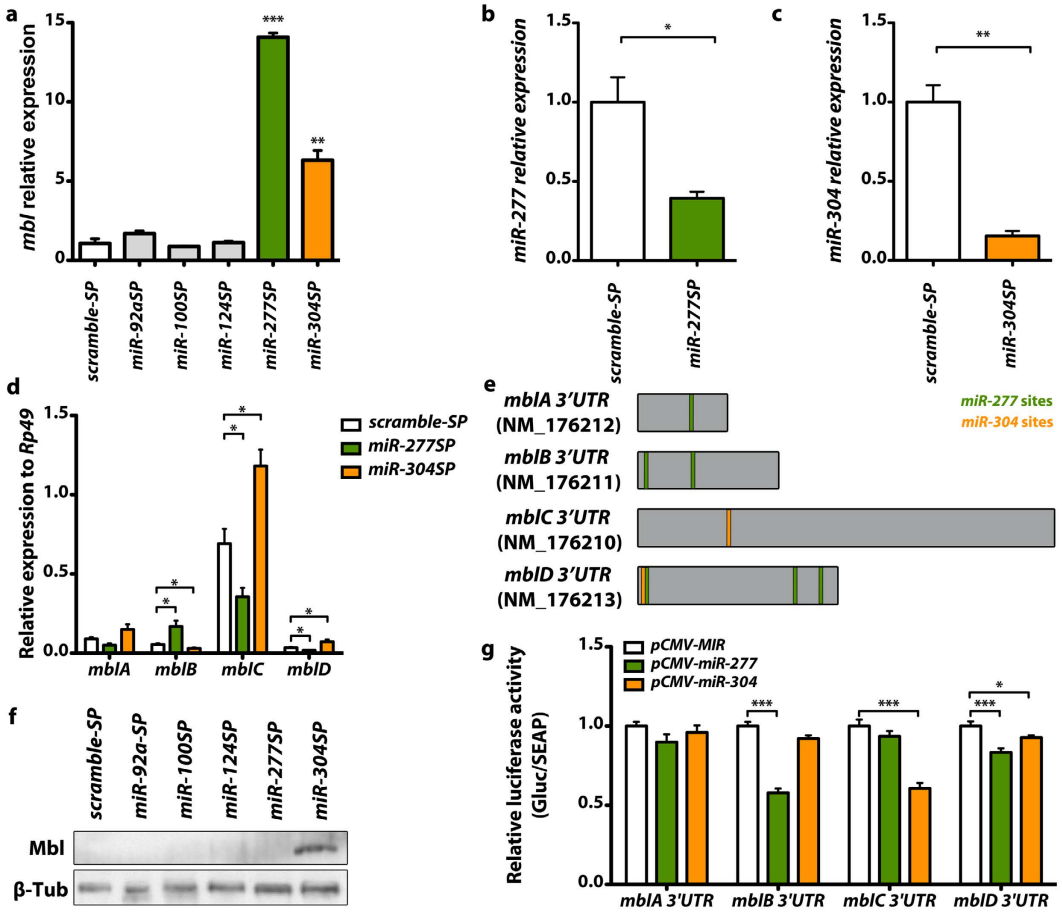

Figure 1. Tissue-specific silencing of *dme-miR-277* and *dme-miR-304* upregulates *muscleblind* mRNA and protein in *Drosophila* muscle. (**a**) qRT-PCR amplification of *muscleblind* from flies expressing miRNA sponge constructs for *dme-miR-92a*, *dme-miR-100*, *dme-miR-124*, *dme-miR-277* and *dme-miR-304* in muscle. *muscleblind* expression levels were strongly upregulated in *miR-277SP* and *miR-304SP* flies. (**b**) Analysis of the levels of *muscleblind* isoforms by qRT-PCR. *dme-miR-277* silencing in muscle caused an upregulation of the *mblB* isoform whilst expression levels of the *mblC* and *mblD* isoforms were reduced in *miR-277SP* flies. Conversely, *mblC* and *mblD* levels were increased and the *mblB* isoform was reduced in *miR-304SP* flies. (**c**) Detection of Muscleblind protein by Western blot. An increase of Muscleblind protein was only detected in *miR-304SP* flies. All the indicated transgenes were driven in muscle using *Mhc-Gal4*. Histogram showing *dme-miR-277* (**d**) and *dme-miR-304* (**e**) relative expression levels according to qRT-PCR data. Both miRNAs were significantly silenced in flies expressing the corresponding sponge constructs under the control of *Mhc-Gal4* compared to flies that expressed *scramble-SP* (control). (**f**) Scheme of the predicted binding sites for *dme-miR-277* and *dme-miR-304* in *muscleblind* 3′ UTRs (*mblA* to *mblD*). Reference sequence accessions and size (in nt) are also included. Representation is to scale. (**g**) Quantification of Gaussian luciferase activity relative to alkaline phosphatase (Gluc/SEAP) of HeLa cells cotransfected with the indicated *mbl* 3′ UTR sensor constructs and plasmids expressing *dme-miR-277* or *dme-miR-304*. Significantly reduced relative luminescence compared to empty vector (pCMV-MIR, control) reveals direct binding of *dme-miR-277* to m*blB* and m*blD* 3′UTRs and of *dme-miR-304* to m*blC* and m*blD* 3′ UTRs. The graphs show means±s.e.m. *$p < 0.05$, **$p < 0.01$, ***$p < 0.001$ (Student's t-test).

To validate that these miRNAs regulate Muscleblind, we targeted the expression of miRNA sponge constructs[35], *UAS-miR-XSP*, to the *Drosophila* muscles using the *Myosin heavy chain* (*Mhc*)-*Gal4* driver line and analyzed *muscleblind* transcript levels by qRT-PCR. We used specific primers to amplify a region in *muscleblind* exon 2, which is shared by all known transcript isoforms[36,37]. As a control, we used a scramble miRNA sponge line (*UAS-scramble-SP*). No significant increase in *muscleblind* expression level was detected in flies expressing *miR-92aSP*, *miR-100SP* or *miR-124SP* under the control of *Mhc-Gal4*. In contrast, *muscleblind* transcripts were significantly increased in flies that expressed *miR-277SP* or *miR-304SP* in muscle compared with *scramble-SP* controls (Fig. 1a). *Muscleblind* levels were 14-fold higher when *dme-miR-277* was inhibited while *dme-miR-304* silencing resulted into a 6-fold increase. Consistently, the quantification of the expression of the mCherry reporter contained in the SP constructs showed that *miR-277*SP and *miR-304SP* were the two SPs with the highest expression in the flies (Fig. S1). Thus, we cannot disprove that *miR-92aSP*, *miR-100SP* or *miR-124SP* regulate *muscleblind* since their SP constructs had comparatively lower expression levels. As we were not interested in a complete

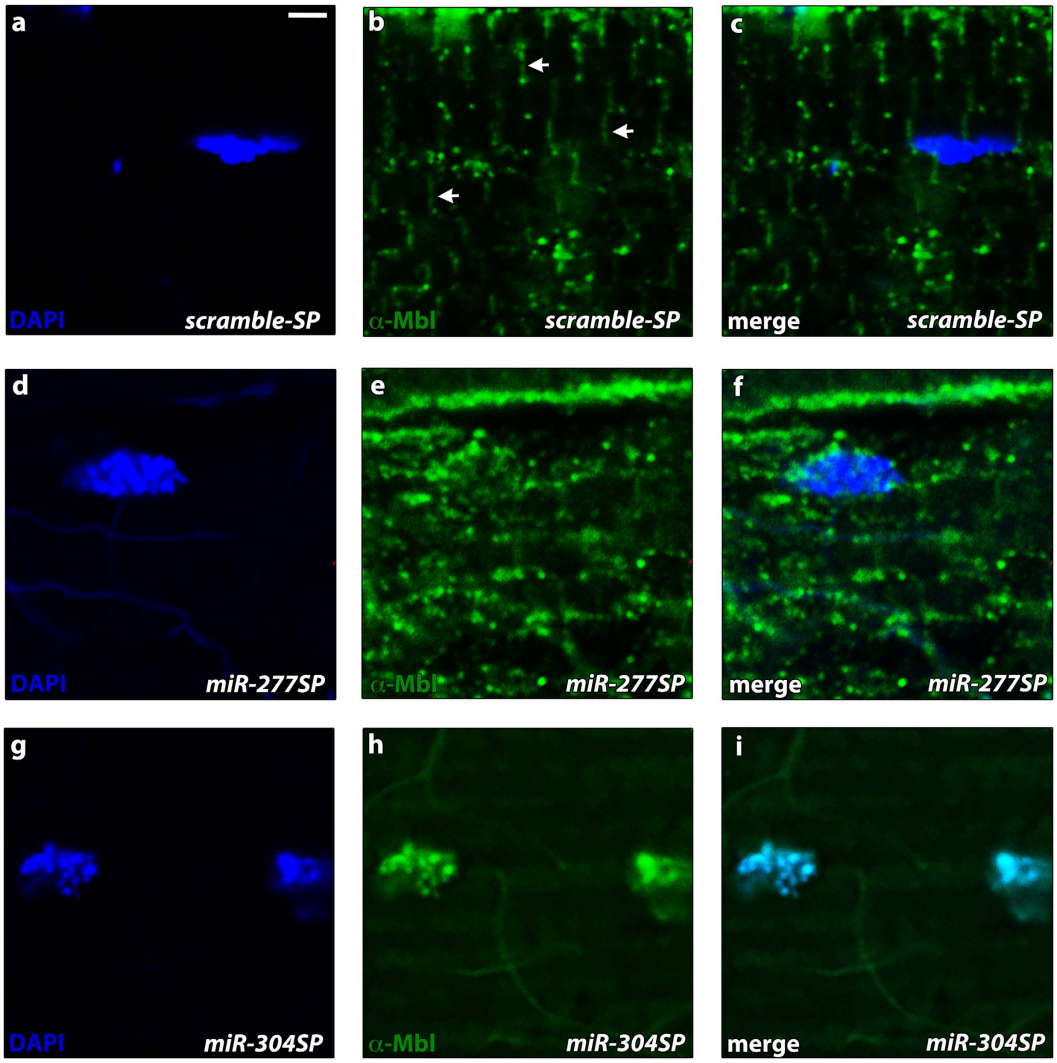

Figure 2. ***dme-miR-277*** **and** ***dme-miR-304*** **silencing upregulates Muscleblind proteins with different subcellular localization.** Representative confocal images of longitudinal sections of IFMs showing anti-Mbl staining (green). Nuclei were counterstained with DAPI (blue) (**a**–**c**) Endogenous Muscleblind expression was preferentially detected in sarcomeric bands while a low signal was detected in some cell nuclei. Arrow-heads in (**b**) point to the sarcomeric bands. (**d**–**f**) An increase in the Muscleblind cytoplasmic signal was detected in *miR-277SP* flies. In contrast, silencing of *dme-miR-304* in IFMs boosted the Muscleblind nuclear signal (**g**–**i**). Scale bar = 2 μm.

description of *muscleblind* regulation by microRNAs but in providing proof of concept of their usefulness as therapeutic targets in DM1, we continued our studies with the two confirmed *muscleblind* regulators; *miR-277* and *miR-304*. To assess the efficiency of miRNA downregulation by driving sponge constructs with the *Mhc*-Gal4 driver, we performed qRT-PCRs to detect the levels of the corresponding RNAs and confirmed that flies expressing *miR-277SP* or *miR-304SP* had reduced levels of the corresponding microRNA (Fig. 1b,c). *dme-miR-277* was silenced ~60% while a robust reduction of ~80% was detected for *dme-miR-304*. Therefore, these results demonstrate that silencing of *dme-miR-277* or *dme-miR-304* derepresses *muscleblind*.

dme-miR-277 and dme-miR-304 regulate different Muscleblind isoforms. *Drosophila muscleblind* is a large gene, spanning more than 110 kb, which gives rise to different 3′ UTRs through the use of alternative 3′ exons[36,37]. Experimental evidence suggests that *muscleblind* isoforms are not functionally redundant[38]. To determine which *muscleblind* isoforms are regulated by *dme-miR-277* or *dme-miR-304*, we used the Miranda algorithm[39] to identify *dme-miR-277* and *dme-miR-304* recognition sites in Muscleblind isoform 3′ UTRs (Table 1, Fig. 1e). Importantly, note that Miranda database allowed the search in *mblA*, *mblB*, *mblC* and *mblD* transcripts named according to[36] but did not include the recently identified isoforms *mblH*, *mblH′*, *mblJ* and *mblK*[37]. We found one potential recognition site for *dme-miR-277* in the *mblA* isoform and two in *mblB* and *mblD*. qRT-PCR analyses revealed that the level of *mblB* significantly increased when *dme-miR-277* was inhibited. *mblD* expression levels were reduced in *Mhc-Gal4 miR-277SP* flies and no significant differences were detected for *mblA* compared

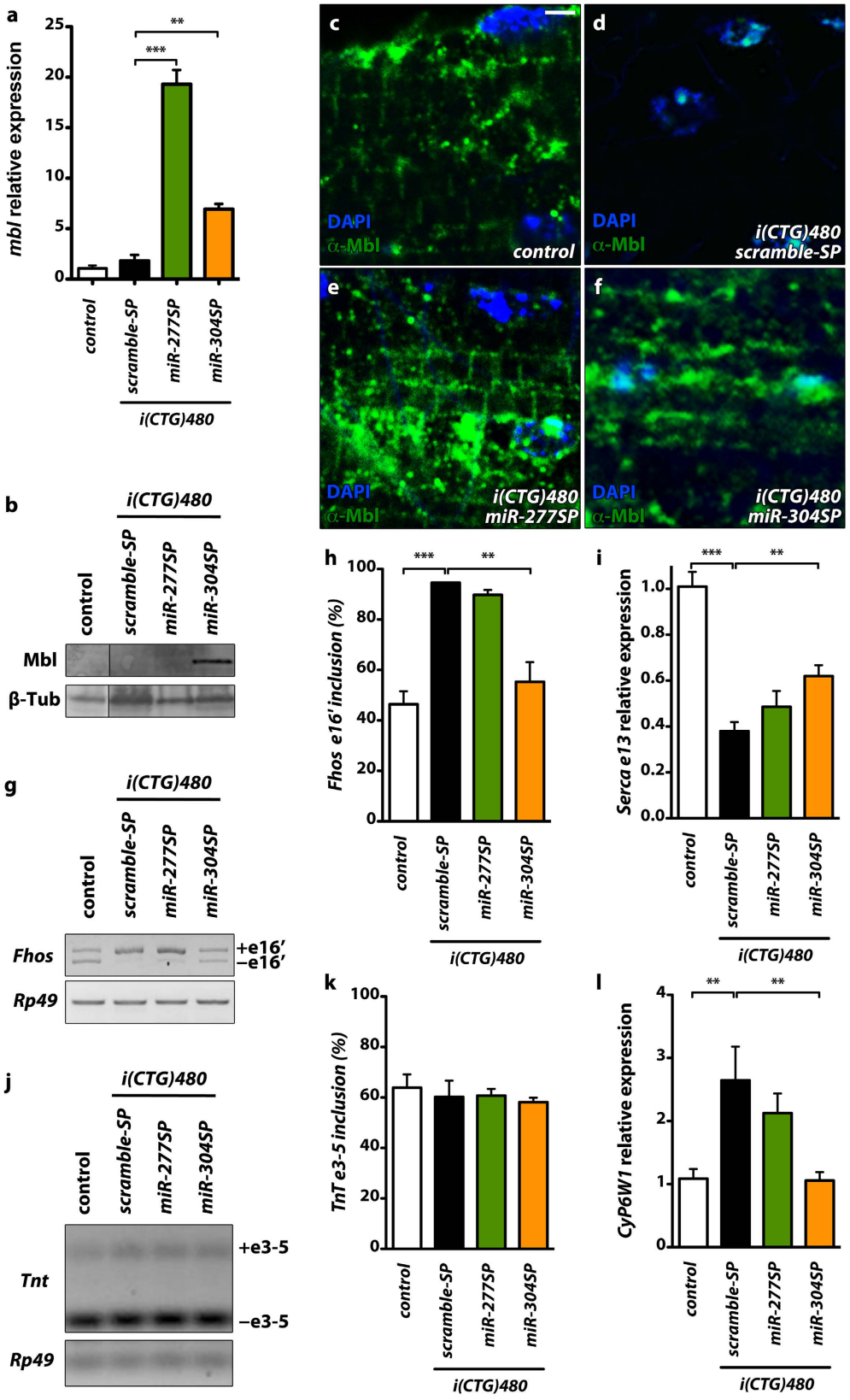

Figure 3. ***dme-miR-277*** **or** ***dme-miR-304*** **silencing enhance** ***muscleblind*** **expression and rescues missplicing events in a DM1 background.** (**a**) Bar graph showing *muscleblind* expression levels qRT-PCR data. *muscleblind* mRNA was significantly upregulated in model flies expressing *miR-277SP* and *miR-304SP* in comparison to flies that did not express the expansions (control, *Mhc-Gal4/+*) or model flies expressing *scramble-SP*. (**b**) Western blot analysis showed additional Muscleblind C only in model flies expressing *miR-304SP*. (**c–f**) Confocal images of longitudinal sections of IFMs reveal Muscleblind (green) distribution to sarcomeric bands in control

flies (**c**). In contrast, Muscleblind was found in nuclear aggregates in IFMs expressing CTG expansions (**d**). Expression of *miR-277SP* in model flies released Muscleblind from aggregates and restored its distribution to sarcomeric bands (**e**). *miR-304SP* expression achieved a dispersed overexpression of Muscleblind in both nuclei and cytoplasm (**f**). Nuclei were counterstained with DAPI (blue). (**g**) RT-PCR to assess inclusion of *Fhos* exon 16′ in flies with different genotypes. *Rp49* transcripts were detected as endogenous control. (**h**) Quantification of percentage of exon inclusion (according to g) confirmed an improvement of *Fhos* missplicing in model flies expressing *miR-304SP*. (**i**,**l**) qRT-PCR results of *Serca* exon 13 and *CyP6W1* expression relative to *Rp49*, confirmed a significant rescue of both events in model flies expressing *miR-304SP*. (**j**) RT-PCR showing inclusion of *TnT* exon 3–5, which did not differ in the studied genotypes. (**k**) Quantification of exon percentage inclusion according to (**j**). All the indicated genotypes were driven to muscle using *Mhc-Gal4*. Scale bar = 2 μm. $^{*}p < 0.05$, $^{**}p < 0.01$, $^{***}p < 0.001$ (Student's t-test).

with *scramble-SP* control flies (Fig. 1d). Intriguingly, expression level of *mblC*, an isoform with no predicted recognition sites for *dme-miR-277,* were significantly reduced in *Mhc-Gal4 miR-277SP* flies. For *dme-miR-304*, we found one recognition site in the *mblC* and *mblD* 3′ UTR and observed a significant upregulation of both isoforms in *Mhc-Gal4 miR-304SP* flies (Fig. 1d). Notably, silencing of *dme-miR-304* in muscle triggered a strong increase in the level of *mblC*, which is the most expressed isoform in adult flies[38]. The fact that *dme-miR-277* and *dme-miR-304* silencing cause isoform-specific changes in *muscleblind* expression levels suggest that these miRNAs directly regulate the *mbl* transcripts. To confirm direct binding of these miRNAs to the corresponding 3′ UTRs of *mbl* transcripts, we performed luciferase reporter gene assays in HeLa cells. In these studies, the 3′ UTR of the different *mbl* transcripts were cloned downstream of Gaussia luciferase and the interaction of the microRNAs to their targets in these regions, was detected as a decrease in the luminescence measurements. These experiments confirmed direct binding of *dme-miR-277* to the 3′ UTR of the *mblB* and *D* isoforms and direct binding of *dme-miR-304* to *mbl* isoforms C and D (Fig. 1e,g).

Given that miRNAs can act either by reducing target transcript levels or blocking their translation, we decided to analyze Muscleblind protein levels to validate the regulatory miRNA candidates. With this aim, we used an anti-Mbl antibody that has previously been optimized to detect overexpression of MblA, MblB and MblC protein, but not their endogenous expression[40,41]. Western blotting analyses revealed an increase in Muscleblind protein levels only in *Mhc-Gal4 miR-304SP* flies (Fig. 1f). Consistently with the qRT-PCR determinations, we only detected one band in the Western blot corresponding to MblC protein. To further analyze the effect of *dme-miR-277* or *dme-miR-304* silencing we stained Muscleblind distribution in longitudinal sections of indirect flight muscles (IFMs). We had previously shown that endogenous Muscleblind protein is localized mainly in sarcomeric Z and H bands of muscle[42]. Consistently, we detected Muscleblind proteins in the bands of muscle sarcomeres in control flies that express the *scramble-SP* construct (Fig. 2a–c). Interestingly, *dme-miR-277* and *dme-miR-304* exhaustion, had different effects on Mbl protein distribution. *dme-miR-277* silencing increased cytoplasmic Mbl, (Fig. 2d–f), while a strong nuclear localization was detected in *Mhc-Gal4 miR-304SP* flies (Fig. 2g–i). Taken together, these results demonstrate that endogenous Muscleblind isoforms can be upregulated by blocking *dme-miR-277* and *dme-miR-304* inhibitory activity.

dme-miR-277 or dme-miR-304 silencing upregulates Muscleblind expression in a *Drosophila* DM1 model. Previous *Drosophila* models of DM1 displayed ribonuclear foci in muscle cells containing Muscleblind proteins[43–45]. To test the effect of specific silencing of the miRNA repressors of *muscleblind* in a *Drosophila* DM1 model, we studied Muscleblind expression in flies expressing 480 interrupted CTG repeats under the control of the muscle-specific driver Myosin heavy chain with simultaneous expression of sponge constructs (*Mhc-Gal4 UAS-i(CTG)480 UAS-miR-XSP*). Analyses of *muscleblind* transcript levels by qRT-PCR showed that silencing of *dme-miR-277* or *dme-miR-304* upregulated *muscleblind* in DM1 flies (Fig. 3a). *muscleblind* transcript levels were 19-fold higher in flies expressing both *i(CTG)480* and *miR-277SP* and 7-fold higher in those expressing *i(CTG)480* and *miR-304SP* compared to controls. Moreover, in agreement with protein analyses in *miR-SP* (Fig. 1c), silencing of *dme-miR-304* triggered an increase of MblC protein levels in DM1 flies (Fig. 3b).

To study the effect of *dme-miR-277* or *dme-miR-304* silencing on Muscleblind subcellular localization in DM1 flies, we examined Muscleblind protein distribution by inmunodetection in IFMs. Expression of either *miR-277SP* or *miR-304SP* in DM1 model flies released Muscleblind from ribonuclear foci and increased the level of protein, both in nuclei and in cytoplasm (Fig. 3c–f). In the case of model flies expressing *miR-277SP*, Muscleblind distribution in sarcomeric bands of muscle, which is characteristic of control flies not expressing the repeats, was significantly rescued. Similarly, expression of *miR-304SP* led to a detectable increase of Muscleblind dispersed in nuclei and cytoplasm. Of note, in flies that did not express the CTG repeats, *dme-miR-304* silencing results in increase of Muscleblind only in nuclei (compare Figs 2i and 3f). The overall greater derepression of *mbl* in a CTG background, compared to wild type, may stem from the higher transcription or stability of *muscleblind* transcripts, perhaps as a compensatory mechanism, in DM1 flies (1.8 fold; Fig. 3a). Hence, when exposed to the same levels of *miR-304SP* sponge, more muscleblind transcripts may be available to translation in a DM1 background. Therefore, silencing of *dme-miR-277* or *dme-miR-304* upregulates Muscleblind levels and rescues its subcellular distribution in DM1 fly muscles.

***dme-miR-304* silencing rescues molecular defects in a *Drosophila* DM1 model.** RNA metabolism alterations are the major biochemical hallmark in DM1. Specifically, spliceopathy is the only molecular alteration that has been directly linked with DM1 symptoms. To test whether Muscleblind increase, triggered by *dme-miR-277* or *dme-miR-304* silencing, was enough to rescue missplicing in the DM1 model flies we studied two altered splicing events (Fig. S2g) and the alteration in the expression level of a specific transcript. First, we

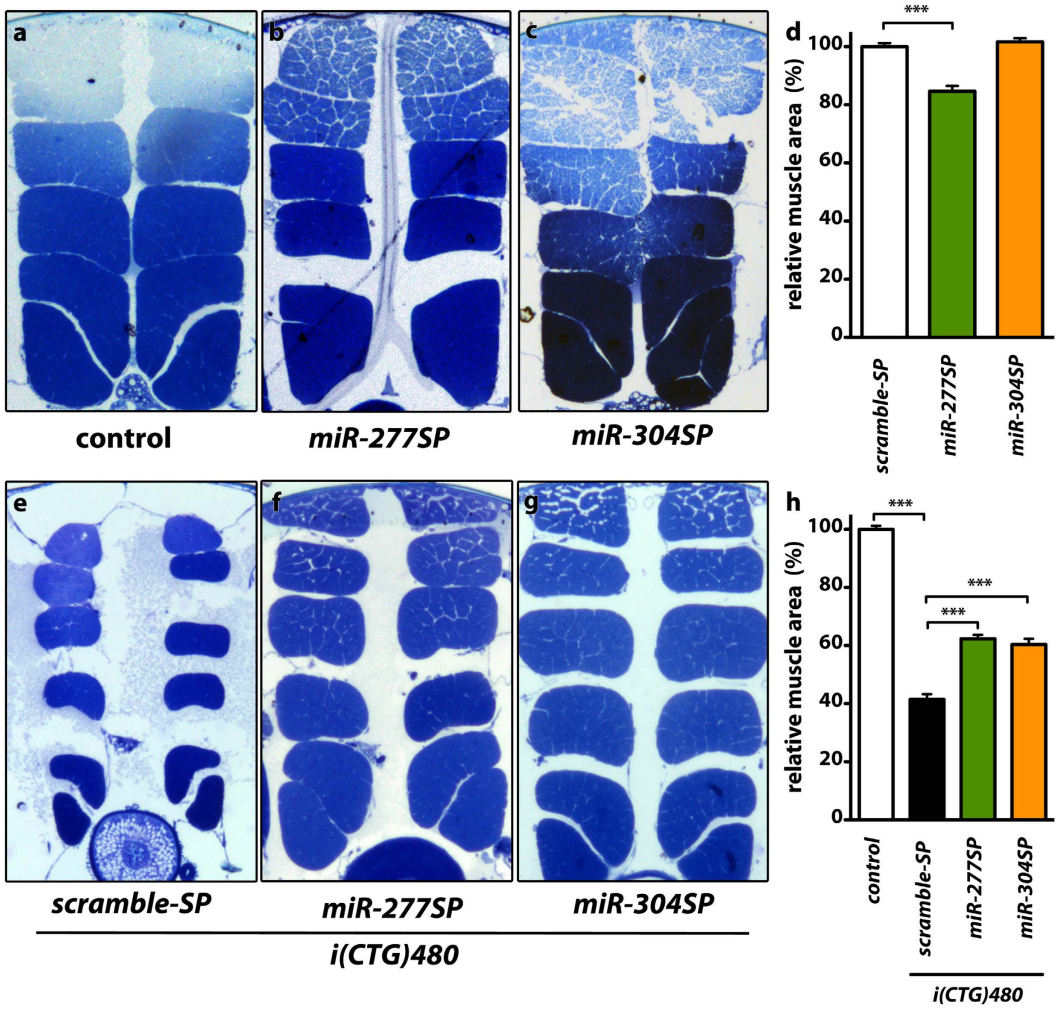

Figure 4. ***dme-miR-277*** **or** ***dme-miR-304*** **silencing rescue muscle atrophy in model flies.** (**a**–**c**,**e**–**g**) Representative dorsoventral sections of resin-embedded thoraces of flies with the indicated relevant genotypes. Compared to control flies (**a**) muscle-specific expression of *miR-277SP* resulted into a significant reduction of indirect flight muscle (IFM) area (**b**) whereas *miR-304SP* expression had no effect on this phenotype (**c**) In DM1 model flies the IFM muscle area was reduced to 40% of normal (**e**) In model flies co-expressing either *miR-277SP* or *miR-304SP* and *i(CTG)480* the muscle area increased to 60% of normal (**f**,**g**). (**d**,**h**) Quantification of the mean percentage of muscle area per genotype. The graphs show means ± s.e.m. All the indicated genotypes were driven to muscle using *Mhc-Gal4*. *$p < 0.05$, **$p < 0.01$, ***$p < 0.001$ (Student's t-test). In all images the dorsal side is on top.

identified *Fhos* exon 16′ missplicing in DM1 flies and demonstrated that this splicing event and Serca exon 13 inclusion, previously identified as altered in the *Drosophila* DM1 model, both are regulated by Muscleblind C (Fig. S2a,b)[45]. Second, we confirmed that the expression level of the *CyP6W1* gene was also dependent on *mblC* expression (Fig. S2c,f). In DM1 model flies, we confirmed a 2-fold increase of *Fhos* exon 16′ inclusion, a 2.4-fold reduction of *Serca* transcripts with exon 13 and a 3-fold increase of *CyP6W1* expression in comparison to control flies not expressing the repeats. Expression of *miR-304SP* in these flies achieved a complete rescue of *Fhos* splicing and *CyP6W1* expression and a significant 20% increase of *Serca* transcripts including exon 13 (Fig. 3g–i,l). Notably, *dme-miR-304* silencing in muscle caused a strong increase in the level of *mblC* (Fig. 3b), which is an isoform previously shown to act as splicing regulator[38]. Conversely, expression of *miR-277SP*, which rescued Muscleblind expression in cytoplasm, and reduced *mblC* expression levels, did not modify these splice events. As a control, we confirmed that the splicing pattern of *Tnt* exons 3–5, which is not altered in DM1 adult flies[44], was neither modified by the expression of the sponge constructs nor by *mbl* expression alterations (Fig. 3j,k; Fig. S2d,e). These results show that the level of *muscleblind* derepression achieved with miRNA sponges is enough to trigger significant molecular rescues.

dme-miR-277 **or** ***dme-miR-304*** **silencing rescues muscle atrophy and motor function in a** ***Drosophila*** **model of DM1.** To assess the functional relevance of Muscleblind increase achieved by the expression of specific sponge constructs, we studied the effect of *dme-miR-277* or *dme-miR-304* silencing on

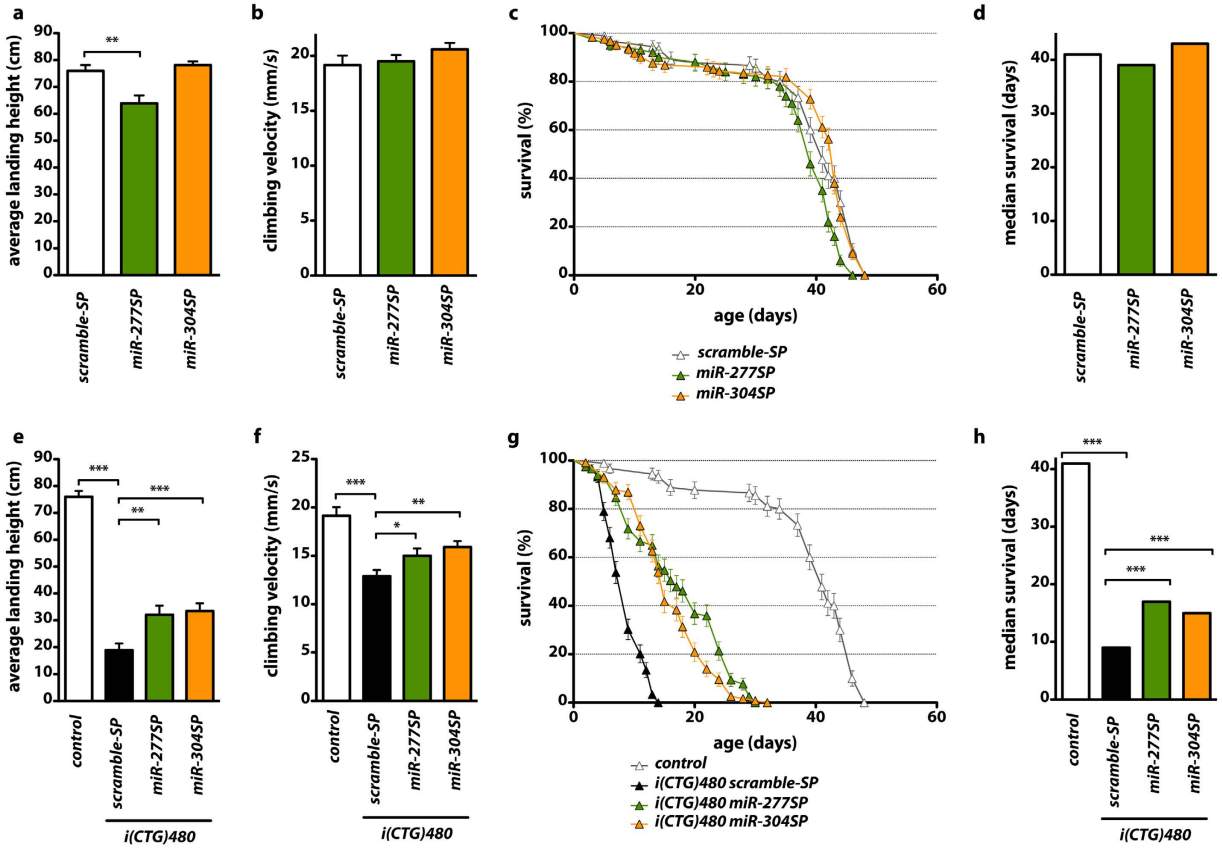

Figure 5. Inhibition of *dme-miR-277* or *dme-miR-304* improved locomotion and survival of DM1 model flies. (**a**,**e**) Average landing height for flies with the indicated relevant genotypes. In control individuals (**a**) *dme-miR-277* silencing decreased landing height while *dme-miR-304* silencing did not affect flight. In DM1 model flies (**e**) expression of *miR-277SP* or *miR-304SP* rescued the reduced flight ability observed. (**b**,**f**) Histograms showing the climbing velocity as mean speed ± SEM in mm/s. In control flies (**b**) silencing of either *dme-miR-277* or *dme-miR-304* had no effect on climbing velocity. However, in DM1 flies (**f**) which have very reduced climbing velocity, expression of *miR-277SP* or *miR-304SP* significantly rescued this phenotype. (**c**,**g**) Survival curves and (**d**,**h**) median survival, showing that expression of *miR-277SP* or *miR-304SP* had no effect on control but improved survival of DM1 model flies. Between 140 and 160 individuals from each genotype were analyzed. All the indicated transgenes were driven in muscle with *Mhc-Gal4*. *$p < 0.05$, **$p < 0.01$, ***$p < 0.001$ (Student's t-test).

muscle atrophy, which is a characteristic alteration in DM1 individuals. To study muscle atrophy we first measured muscle area in dorsoventral sections of IFMs in control flies expressing either *miR-277SP* or *miR-304SP* in muscle (Fig. 4a–d). *dme-miR-277* inhibition induced a reduction of 15% in IFM area, in comparison to flies expressing *scramble-SP* as control. Importantly, *miR-304SP* expression had no effect on this parameter. We have previously reported muscle atrophy in *i(CTG)480* flies[27,44]. In these DM1 model flies, we found that tissue-specific silencing of *dme-miR-277* or *dme-miR-304* was enough to rescue muscle area percentage significantly (Fig. 4e–h). In comparison to control flies that did not express the CUG repeats, the mean area of IFMs in model flies expressing the *scramble-SP* was significantly reduced to 40%. Concomitant expression of CUG repeats and either *miR-277SP* or *miR-304SP* resulted in a 20% increase of muscle area in these flies. These data confirm that derepression of *muscleblind* by miRNA silencing was sufficient to rescue muscle atrophy in *Drosophila*.

To assess the correlation between muscle area and locomotor activity we analyzed the flight and climbing ability in flies of different genotypes. Expression of *miR-277SP* in otherwise wild type muscle resulted in a reduction of the average landing height of around 10% in comparison to control flies expressing the *scramble-SP*, which indicates that the reduction of muscle area observed in these flies has a functional correlation (Fig. 5a). However, the muscle atrophy was apparently specific to IFMs since climbing velocity was unchanged in these flies (Fig. 5b). In contrast, silencing of *dme-miR-304* in muscle did not affect locomotor activity of flies (Fig. 5a,b). In DM1 model flies, in comparison to controls not expressing the repeats, concomitant expression of CUG repeats and the *scramble-SP* construct resulted in a drastic reduction of average landing height and climbing velocity (Fig. 5e,f). However, expression of either *miR-277SP* or *miR-304SP* in model flies resulted in a significant partial rescue of both of these parameters to similar levels (Fig. 5e,f). Thus, these results demonstrate that specific silencing of miRNAs regulating *muscleblind* can rescue the muscle atrophy and functional phenotypes characteristic of DM1.

Functional depletion of *dme-miR-277* or *dme-miR*-304 extends lifespan of DM1 flies. Muscle wasting, particularly in the respiratory system, is the leading cause of death in DM1. We have previously reported that flies expressing *i(CTG)480* in the musculature had a reduced lifespan and median survival compared with control flies[44]. To study whether *dme-miR-277* or *dme-miR-304* silencing rescues lifespan of DM1 flies, we performed survival curves analyses in flies of different genotypes. Importantly, survival curves for flies expressing *miR-277SP* or *miR-304SP* in otherwise wild type muscle were not different to *scramble-SP* control indicating that *dme-miR-277* or *dme-miR-304* silencing did not alter lifespan (Fig. 5c,d). Lifespan of DM1 model flies expressing the *scramble-SP* was significantly reduced compared with control flies that did not express the CTG repeats (Fig. 5g,h). Expression of either *miR-277SP* or *miR-304SP* in model flies increased the median survival. *dme-miR-277* silencing increased median survival by eight days while an increase of six days was detected for DM1 flies expressing *miR-304SP.* Thus, *muscleblind* upregulation triggered by *dme-miR-277* or *dme-miR-304* silencing, improved survival of DM1 model flies. Taken together, our results demonstrate that silencing of specific miRNAs in *Drosophila* triggers an increase of *muscleblind* levels that is sufficient to rescue several molecular and physiological DM1-like features thus supporting miRNA-based derepression of Muscleblind as a potential strategy to treat human DM1.

Discussion

DM1 presents a considerable disease burden as it is the most common adult-onset muscle dystrophy, and includes cognitive dysfunction, malignant heart arrhythmia, and respiratory failure, ultimately leading to shortened life expectancy. Inhibition of MBNL activity due to sequestration by microsatellite expansion RNAs is a major pathogenic event in DM1. Using a *Drosophila* model of this disease, we confirmed that upregulation of endogenous *muscleblind* by specific microRNA silencing, can rescue DM1-like phenotypes. Endogenous gene modulation to alleviate pathology has been successful in breast cancer where estrogen receptor antagonists are regularly used in clinical practice[46]. Furthermore, pharmacological enhancement of *utrophin* expression, a gene exclusively expressed in fetus but that can compensate Dystrophin loss of function in Duchenne Muscular Dystrophy is currently under investigation[47]. One of the most promising therapeutic strategies for endogenous gene regulation is based on miRNA derepression. These strategies have proven to be beneficial in animal models, to be highly efficient in specific target silencing, and to have appropriate pharmacokinetic parameters to be developed as drugs. In this study we aimed to upregulate endogenous *muscleblind* expression by silencing defined miRNAs, which regulate it in muscle. miRNAs have been extensively associated with several neuromuscular disorders in valuable *in-vivo* systems, which highlights the importance of studying miRNA-based regulation of dystrophy-associated genes as potential therapeutic strategy[48–52]. Specifically, we used miRNA sponge constructs, which are transgenes, containing multiple, tandem binding sites of a microRNA of interest, expressed from strong promoters. From our previous studies and TargetScan predictions, we selected a group of microRNAs as potential regulators of *Drosophila muscleblind* and confirmed that sponge constructs for *dme-miR-277* and *dme-miR-304*, which had the highest expression among the sponge constructs tested, reduced the abundance of their respective target miRNAs and achieved upregulation of *muscleblind* at the RNA and protein levels. Isoform-specific quantitative analysis confirmed that each of these sponge construct upregulated different *muscleblind* isoforms and luciferase reporter assays revealed that this regulation was mediated by direct binding of the miRNAs to the 3′ UTR of the different *muscleblind* isoforms. We confirmed direct binding of *dme-miR-277* to the 3′ UTR of the *mbl B* and *D* isoforms and direct binding of *dme-miR-304* to *mbl* isoforms *C* and *D*. Accordingly, the *mblB* and *mblC* isoforms were increased by *miR-277SP* and *miR-304SP*, which reduced the levels of these microRNAs. In the case of *mblD*, we have confirmed direct binding of both microRNAs to its 3′ UTR. Consistently, *miR-304SP* produced an increase of the transcript. However, we have observed a slight but significant decrease of *mblD* transcript as a result of *miR-277SP*, which might be explained by an inter-isoform regulation as *dme-miR-277* also produces a strong upregulation of the *mblB* isoform, which might have a negative effect on *mblD*. Of note, binding sites of *dme-miR-277* and *dme-miR-304* overlap in the *mblD* 3′ UTR, which could explain the difference observed between *in vivo* and luciferase assays for *mblD* regulation by *dme-miR-277*. Interestingly, *miR-304SP* and *miR-277SP* were able to downregulate the expression of *mblB* and *mblC*, respectively, instead of increasing expression, which could also be a consequence of inter-isoform regulation as it has been previously shown for MBNL proteins[53,54].

Since different subcellular localizations, indicative of specific functions, have been reported for different Muscleblind isoforms[38,55], we immunodetected the protein in fly muscle tissue expressing either *miR-277SP* or *miR-304SP*. In both cases we observed Muscleblind overexpression but in different subcellular locations. Whereas *miR-277SP* preferentially increased Muscleblind in sarcomeric bands, *miR-304SP* enhanced Muscleblind expression in nuclei. Consistently, when we analyzed the effects of the sponge constructs on DM1 model flies expressing pathogenic expansions, *miR-277SP* rescued Muscleblind localization in sarcomeric bands and *miR-304SP* increased Muscleblind in nuclei and cytoplasm. Of note, in both cases Muscleblind retention in ribonuclear foci was no longer detectable and protein levels in DM1 flies seemed higher than in normal individuals, suggesting that, in addition to an upregulation of *muscleblind* expression, there might be a release of the protein from foci. Finally, we have shown that MblC localizes to nuclei[55] and, as we show in this study, is preferentially upregulated by *miR-304SP* expression. Supporting a role for MblC in nuclei, we also confirmed that *miR-304SP* expression rescued a number of Muscleblind-dependent molecular events. Taken together, these data confirm that the upregulation of *muscleblind* achieved by silencing specific regulatory miRNAs is sufficient to rescue critical molecular features that are altered in DM1 model flies.

We also checked the effect of *miR-277SP* and *miR-304SP* expression on muscle atrophy, which is a characteristic DM1 phenotype. We have previously reported that muscle atrophy stems, at least in part, from hyperactivation of the autophagy process and that this had a Muscleblind component. Specifically, we showed that MblC overexpression partially rescued muscle atrophy in the DM1 model flies[27] and, consistent with these previous observations, we confirmed that *miR-304SP* expression in model flies also rescued muscle atrophy. However,

processes other than splicing must be involved in triggering this phenotype as *miR-277SP* expression, which preferentially upregulates Muscleblind in sarcomeric bands, was also able to rescue muscle area in the DM1 model flies. Importantly, the increase in IFM muscle area achieved by expression of sponge constructs had a functional correlation, as survival, climbing and flight abilities also improved.

By expressing the sponge constructs with the *Mhc-Gal4* driver we also tested the effects of long-term Muscleblind overexpression. In control flies, we observed that *miR-304SP* expression, caused a 6-fold increase in *muscleblind* relative expression and had no effect on muscle area, survival or locomotor function. However, *miR-277SP* expression, which produced a 15-fold upregulation of *muscleblind* caused a significant reduction in muscle area, which correlated with decreased landing height. In a CTG expressing background, however, expression of either of the sponge constructs brought about beneficial effects suggesting that limited overexpression of additional natural miRNA target transcripts are negligible compared to the positive effects of boosting *muscleblind*. Previous studies have confirmed that long-term overexpression of *MBNL1* in mouse models is well tolerated when limited to skeletal muscle. *MBNL1* overexpression, in a range of 10 to 17 fold, caused no detectable histopathology or functional abnormalities[28]. Deletereous effects of *miR-277SP* could originate from overexpression of several targets in addition to *musclebind*, as *dme-miR-277* is one of the miRNAs with highest expression in muscle[35]. Importantly, we show for the first time functional locomotor defects in DM1 model flies expressing CUG repeats in skeletal muscle and, according to our data, flight assays seem more sensitive than climbing assays as small differences in muscle area translate into detectable differences in flight ability.

Conceptually similar to sponge constructs, several drugs targeting specific miRNAs are currently being developed for the treatment of human diseases. Miravirsen, a drug targeting *hsa-miR-122*, the hepatocyte-specific microRNA that Hepatitis C virus hijacks and uses to self-replicate[56], is one the most advanced. Our study with the *Drosophila* model of DM1 sets the stage for the evaluation of miRNA blockers to de-repress *muscleblind* expression as a valid and powerful therapeutic target for treatment of DM1.

Materials and Methods

***Drosophila* stocks.** *Mhc-Gal4* flies were described in ref. 57. miRNA sponge lines (*UAS-miR-SP*) for *dme-miR-92a*, *dme-miR-100*, *dme-miR-124*, *dme-miR-277, dme-miR-304* and *scramble-SP* (control) were obtained from Dr. T. Fulga[35]. Briefly, *miR-SP* constructs were designed with a silencing cassette of 20 repetitive miRNA complementary sequences separated by variable four-nucleotide linker sequences. The recombinant line *Mhc-Gal4 UAS-i(CTG)480* was generated in ref. 42. *UAS-mblC* flies[58] and *UAS-IR-mbl* flies[42] were previously reported. All crosses were carried out at 25 °C with standard fly food. Transgene doses were the same for control and experimental conditions throughout this work.

RNA extraction, RT-PCR and qRT-PCR. For each biological replicate, total RNA from 10 adult males was extracted using Trizol (Sigma). One microgram of RNA was digested with DNaseI (Invitrogen) and reverse-transcribed with SuperScript II (Invitrogen) using random hexanucleotides. 20 ng of cDNA were used in a standard PCR reaction with GoTaq polymerase (Promega) and specific primers were used to analyze *Fhos* exon 16′ and *Tnt* exon 3–5 splicing (Table S2). *Rp49* was used as endogenous control using 0.2 ng of cDNA. qRT-PCR was carried out on 2 ng of cDNA template with SYBR Green PCR Master Mix (Applied Biosystems) and specific primers (Table S1). For reference gene, *Rp49*, qRT-PCR was carried out on 0.2 ng of cDNA. Thermal cycling was performed with Step One Plus Real Time PCR System (Applied Biosystems). Three biological replicates and three technical replicates per biological sample were carried out. Relative expression to endogenous gene and the control group was obtained by the $2^{-\Delta\Delta Ct}$ method. Pairs of samples were compared using two-tailed t-test ($\alpha = 0.05$), applying Welch's correction when necessary.

Luciferase reporter assay. A luciferase assay using the pEZX-MT05 vector was performed to validate the binding of *dme-miR-277* and *dme-miR-304* to *mblA, mblB, mblC,* and/or *mblD* 3′ UTR regions. pEZX-MT05 vector contains a secreted Gaussia luciferase (GLuc) ORF driven by SV40 promoter as a reporter of the 3′ UTR expression and a secreted Alkaline Phosphatase (SEAP) reporter driven by a CMV promoter as an internal control. Firstly, the 3′ UTR *mbl* isoforms were generated by amplifying genomic *Drosophila* DNA with specific primers using Pfu DNA polymerase (Biotools) (Table S1). The PCR products were cloned into the *Eco*RV site of pBluescript II KS vector. The plasmids containing the 3′ UTR *mbl* isoforms were cut out and subcloned into the pEZX-MT05 vector at the *Xho*I and *Sfa*AI sites. The constructs were verified by sequencing the plasmids from both ends. Secondly HeLa cells were used for the 3′ UTR luciferase assay. Cells were maintained in DMEM supplemented with 10% FBS and 1% penicillin-streptomycin at 37 °C and 5% CO_2. HeLa cells were seeded (5×10^4/well) in 24-well plates. A total of 500 ng/well of pEZX-MT05 vector containing *mblA, mblB, mblC* or *mblD* were cotrasfected with 500 ng/well of pCMVMIR vector (Blue Heron) containing *dme-miR-277* or *dme-miR-304*, using X-tremeGENE TM HP DNA Transfection Reagent (Sigma-Aldrich). 48 h and 72 h after transfection, Gaussia luciferase (GLuc) and alkaline phosphatase (SEAP) activities were measured by luminescence in conditioned medium using the secreted-pair dual luminescence kit (GeneCopoeia). Gaussia luciferase activity was normalized to alkaline phosphatase activity (GLuc/SEAP). The statistical differences were analyzed using the Student's t test ($p < 0.05$) on normalized data.

MicroRNA quantification. *UAS-miR-277SP, UAS-miR-304SP* and *UAS-Scramble-SP* were expressed in flies under the control of a muscle specific *Mhc-Gal4* driver. Total RNA from thoraces was isolated according to the miRNeasy miRNA kit protocol without enrichment for miRNAs (Qiagen). The expression analysis of *dme-miR-277* and *dme-miR-304* was performed by real-time PCRs with specific miRCURY LNA microRNA PCR primers (Exiqon) according to the manufacturer's instructions. As reference genes we used *dme-miR-7* and

dme-miR-8. Expression level determinations were performed using an Applied Biosystems Step One Plus Real Time PCR System and the values were calculated using the $2^{-\Delta\Delta Ct}$.

Western blotting. For total protein extraction 20 female thoraces were homogenized in RIPA buffer (150 mM NaCl, 1.0% IGEPAL, 0.5% sodium deoxycholate, 0.1% SDS, 50 mM Tris-HCl pH 8.0) plus protease and phosphatase inhibitor cocktails (Roche Applied Science). Total proteins were quantified with BCA protein assay kit (Pierce) using bovine serum albumin as standard. 20 μg of samples were denatured for 5 min at 100 °C, resolved in 12% SDS-PAGE gels and transferred onto polyvinylidene difluoride (PVDF) membranes. The membranes were blocked with 5% nonfat dried milk in PBS-T (8 mM Na_2HPO4, 150 mM NaCl, 2 mM KH_2PO4, 3 mM KCl, 0.05% Tween 20, pH 7.4) and immunodetected following standard procedures. For Mbl protein detection anti-Mbl antibody[40] was pre-absorbed against early stage wild type embryos (0–6 h after egg laying) to eliminate non-specific binding of antibody. Membranes were incubated with pre-absorbed primary (overnight, 1:1000) followed by horseradish peroxidase (HRP)-conjugated anti-sheep-IgG secondary antibody (1 h, 1:5000, Sigma-Aldrich). Loading control was anti-Tubulin (overnight, 1:5000, Sigma-Aldrich) followed by incubation with HRP-conjugated anti-mouse-IgG secondary antibody (1 h, 1:3000, Sigma-Aldrich). Bands were detected using ECL Western Blotting Substrate (Pierce). Images were acquired with an ImageQuant LAS 4000 (GE Healthcare).

Histological analysis. Inmunofluorescence detection of Muscleblind in fly muscle and analysis of the IFM area in *Drosophila* thoraces were performed as previously described[42]. Briefly, six adult female thoraces were embedded in Epon following standard procedures. After drying the resin, semi-thin sections of 1.5 μm were obtained using an ultramicrotome (Ultracut E, Reichert-Jung and Leica). Images were taken at 100× magnification with a Leica DM2500 microscope. To quantify muscle area, sections were counterstained with toluidine blue and five images containing IFMs per fly were converted into binary images. Considering the complete image as 100% of the area, we used NIH ImageJ software to calculate the percentage occupied by pixels corresponding to IFMs. P-values were obtained using a two-tailed, non-paired t-test ($\alpha = 0.05$), applying Welch's correction when necessary.

***Drosophila* lifespan analyses.** A total of 120 newly hatched flies with the appropriate genotypes were collected and kept at 29 °C. Flies were transferred to new fresh nutritive media every second day and the decline in number was scored on a daily basis. Survival curves were obtained using the Kaplan-Meier method and statistical analysis was performed with a log-rank (Mantel-Cox) test ($\alpha = 0.05$) using the GraphPad Prism5 software.

Functional assays. Flight assays were performed at day 5 according to ref. 59 using 100 male flies per group. Landing distance was compared between groups using two-tailed t-test ($\alpha = 0.05$). To assess climbing velocity groups of ten 5-day-old males were transferred into disposable pipettes (1.5 cm in diameter and 25 cm height) after a period of 24 h without anesthesia. The height reached from the bottom of the vial by each fly in a period of 10 s was recorded with a camera. For each genotype, two groups of 30 flies were tested. Two-tailed t-test ($\alpha = 0.05$) was used for comparisons of pairs of samples applying Welch's correction whenever necessary.

References

1. Thornton, C. A. Myotonic dystrophy. *Neurol Clin* **32,** 705–719, viii, doi: 10.1016/j.ncl.2014.04.011 (2014).
2. Harper, P. *Myotonic dystrophy*. (Saunders, 2001).
3. Gagnon, C. *et al.* Towards an integrative approach to the management of myotonic dystrophy type 1. *Journal of Neurology, Neurosurgery & Psychiatry* **78,** 800–806 (2007).
4. Davis, B. M., McCurrach, M. E., Taneja, K. L., Singer, R. H. & Housman, D. E. Expansion of a CUG trinucleotide repeat in the 3′ untranslated region of myotonic dystrophy protein kinase transcripts results in nuclear retention of transcripts. *Proc Natl Acad Sci USA* **94,** 7388–7393 (1997).
5. Lin, X. *et al.* Failure of MBNL1-dependent post-natal splicing transitions in myotonic dystrophy. *Hum Mol Genet* **15,** 2087–2097, doi: 10.1093/hmg/ddl132 (2006).
6. Mankodi, A. *et al.* Expanded CUG repeats trigger aberrant splicing of ClC-1 chloride channel pre-mRNA and hyperexcitability of skeletal muscle in myotonic dystrophy. *Mol Cell* **10,** 35–44 (2002).
7. Du, H. *et al.* Aberrant alternative splicing and extracellular matrix gene expression in mouse models of myotonic dystrophy. *Nat Struct Mol Biol* **17,** 187–193, doi: 10.1038/nsmb.1720 (2010).
8. Batra, R. *et al.* Loss of MBNL leads to disruption of developmentally regulated alternative polyadenylation in RNA-mediated disease. *Mol Cell* **56,** 311–322, doi: 10.1016/j.molcel.2014.08.027 (2014).
9. Goodwin, M. *et al.* MBNL Sequestration by Toxic RNAs and RNA Misprocessing in the Myotonic Dystrophy Brain. *Cell Rep* **12,** 1159–1168, doi: 10.1016/j.celrep.2015.07.029 (2015).
10. Kalsotra, A. *et al.* The Mef2 transcription network is disrupted in myotonic dystrophy heart tissue, dramatically altering miRNA and mRNA expression. *Cell Rep* **6,** 336–345, doi: 10.1016/j.celrep.2013.12.025 (2014).
11. Fernandez-Costa, J. M. *et al.* Expanded CTG repeats trigger miRNA alterations in Drosophila that are conserved in myotonic dystrophy type 1 patients. *Hum Mol Genet* **22,** 704–716, doi: 10.1093/hmg/dds478 (2013).
12. Rau, F. *et al.* Misregulation of miR-1 processing is associated with heart defects in myotonic dystrophy. *Nat Struct Mol Biol* **18,** 840–845, doi: 10.1038/nsmb.2067 (2011).
13. Moseley, M. L. *et al.* Bidirectional expression of CUG and CAG expansion transcripts and intranuclear polyglutamine inclusions in spinocerebellar ataxia type 8. *Nat Genet* **38,** 758–769, doi: 10.1038/ng1827 (2006).
14. Cho, D. H. *et al.* Antisense transcription and heterochromatin at the DM1 CTG repeats are constrained by CTCF. *Mol Cell* **20,** 483–489, doi: 10.1016/j.molcel.2005.09.002 (2005).
15. Timchenko, N. A. *et al.* Overexpression of CUG triplet repeat-binding protein, CUGBP1, in mice inhibits myogenesis. *J Biol Chem* **279,** 13129–13139, doi: 10.1074/jbc.M312923200 (2004).
16. Mulders, S. A. *et al.* Triplet-repeat oligonucleotide-mediated reversal of RNA toxicity in myotonic dystrophy. *Proc Natl Acad Sci USA* **106,** 13915–13920, doi: 10.1073/pnas.0905780106 (2009).

17. Garcia-Lopez, A., Llamusi, B., Orzaez, M., Perez-Paya, E. & Artero, R. D. *In vivo* discovery of a peptide that prevents CUG-RNA hairpin formation and reverses RNA toxicity in myotonic dystrophy models. *Proc Natl Acad Sci USA* **108,** 11866–11871, doi: 10.1073/pnas.1018213108 (2011).
18. Wheeler, T. M. *et al.* Targeting nuclear RNA for *in vivo* correction of myotonic dystrophy. *Nature* **488,** 111–115, doi: 10.1038/nature11362 (2012).
19. Warf, M. B., Nakamori, M., Matthys, C. M., Thornton, C. A. & Berglund, J. A. Pentamidine reverses the splicing defects associated with myotonic dystrophy. *Proc Natl Acad Sci USA* **106,** 18551–18556, doi: 10.1073/pnas.0903234106 (2009).
20. Parkesh, R. *et al.* Design of a bioactive small molecule that targets the myotonic dystrophy type 1 RNA via an RNA motif-ligand database and chemical similarity searching. *J Am Chem Soc* **134,** 4731–4742, doi: 10.1021/ja210088v (2012).
21. Lee, J. E., Bennett, C. F. & Cooper, T. A. RNase H-mediated degradation of toxic RNA in myotonic dystrophy type 1. *Proc Natl Acad Sci USA* **109,** 4221–4226, doi: 10.1073/pnas.1117019109 (2012).
22. Kanadia, R. N. *et al.* A muscleblind knockout model for myotonic dystrophy. *Science* **302,** 1978–1980, doi: 10.1126/science.1088583 (2003).
23. Dixon, D. M. *et al.* Loss of muscleblind-like 1 results in cardiac pathology and persistence of embryonic splice isoforms. *Sci Rep* **5,** 9042, doi: 10.1038/srep09042 (2015).
24. Lee, K. Y. *et al.* Compound loss of muscleblind-like function in myotonic dystrophy. *EMBO Mol Med* **5,** 1887–1900, doi: 10.1002/emmm.201303275 (2013).
25. Huin, V. *et al.* MBNL1 gene variants as modifiers of disease severity in myotonic dystrophy type 1. *J Neurol* **260,** 998–1003, doi: 10.1007/s00415-012-6740-y (2013).
26. Kanadia, R. N. *et al.* Reversal of RNA missplicing and myotonia after muscleblind overexpression in a mouse poly(CUG) model for myotonic dystrophy. *Proc Natl Acad Sci USA* **103,** 11748–11753, doi: 10.1073/pnas.0604970103 (2006).
27. Bargiela, A. *et al.* Increased autophagy and apoptosis contribute to muscle atrophy in a myotonic dystrophy type 1 Drosophila model. *Dis Model Mech* **8,** 679–690, doi: 10.1242/dmm.018127 (2015).
28. Chamberlain, C. M. & Ranum, L. P. Mouse model of muscleblind-like 1 overexpression: skeletal muscle effects and therapeutic promise. *Hum Mol Genet* **21,** 4645–4654, doi: 10.1093/hmg/dds306 (2012).
29. Chendrimada, T. P. *et al.* MicroRNA silencing through RISC recruitment of eIF6. *Nature* **447,** 823–828, doi: 10.1038/nature05841 (2007).
30. Lytle, J. R., Yario, T. A. & Steitz, J. A. Target mRNAs are repressed as efficiently by microRNA-binding sites in the 5′ UTR as in the 3′ UTR. *Proc Natl Acad Sci USA* **104,** 9667–9672, doi: 10.1073/pnas.0703820104 (2007).
31. Wu, J. & Xie, X. Comparative sequence analysis reveals an intricate network among REST, CREB and miRNA in mediating neuronal gene expression. *Genome Biol* **7,** R85, doi: 10.1186/gb-2006-7-9-r85 (2006).
32. Giraldez, A. J. *et al.* Zebrafish MiR-430 promotes deadenylation and clearance of maternal mRNAs. *Science* **312,** 75–79, doi: 10.1126/science.1122689 (2006).
33. Guo, H., Ingolia, N. T., Weissman, J. S. & Bartel, D. P. Mammalian microRNAs predominantly act to decrease target mRNA levels. *Nature* **466,** 835–840, doi: 10.1038/nature09267 (2010).
34. Kheradpour, P., Stark, A., Roy, S. & Kellis, M. Reliable prediction of regulator targets using 12 Drosophila genomes. *Genome Res* **17,** 1919–1931, doi: 10.1101/gr.7090407 (2007).
35. Fulga, T. A. *et al.* A transgenic resource for conditional competitive inhibition of conserved Drosophila microRNAs. *Nat Commun* **6,** 7279, doi: 10.1038/ncomms8279 (2015).
36. Begemann, G. *et al.* muscleblind, a gene required for photoreceptor differentiation in Drosophila, encodes novel nuclear Cys3His-type zinc-finger-containing proteins. *Development* **124,** 4321–4331 (1997).
37. Irion, U. Drosophila muscleblind codes for proteins with one and two tandem zinc finger motifs. *PLoS One* **7,** e34248, doi: 10.1371/journal.pone.0034248 (2012).
38. Vicente, M. *et al.* Muscleblind isoforms are functionally distinct and regulate alpha-actinin splicing. *Differentiation* **75,** 427–440, doi: 10.1111/j.1432-0436.2006.00156.x (2007).
39. Enright, A. J. *et al.* MicroRNA targets in Drosophila. *Genome Biol* **5,** R1, doi: 10.1186/gb-2003-5-1-r1 (2003).
40. Houseley, J. M. *et al.* Myotonic dystrophy associated expanded CUG repeat muscleblind positive ribonuclear foci are not toxic to Drosophila. *Hum Mol Genet* **14,** 873–883, doi: 10.1093/hmg/ddi080 (2005).
41. Vicente-Crespo, M. *et al.* Drosophila muscleblind is involved in troponin T alternative splicing and apoptosis. *PLoS One* **3,** e1613, doi: 10.1371/journal.pone.0001613 (2008).
42. Llamusi, B. *et al.* Muscleblind, BSF and TBPH are mislocalized in the muscle sarcomere of a Drosophila myotonic dystrophy model. *Dis Model Mech* **6,** 184–196, doi: 10.1242/dmm.009563 (2013).
43. de Haro, M. *et al.* MBNL1 and CUGBP1 modify expanded CUG-induced toxicity in a Drosophila model of myotonic dystrophy type 1. *Hum Mol Genet* **15,** 2138–2145, doi: 10.1093/hmg/ddl137 (2006).
44. Garcia-Lopez, A. *et al.* Genetic and chemical modifiers of a CUG toxicity model in Drosophila. *PLoS One* **3,** e1595, doi: 10.1371/journal.pone.0001595 (2008).
45. Picchio, L., Plantie, E., Renaud, Y., Poovthumkadavil, P. & Jagla, K. Novel Drosophila model of myotonic dystrophy type 1: phenotypic characterization and genome-wide view of altered gene expression. *Hum Mol Genet* **22,** 2795–2810, doi: 10.1093/hmg/ddt127 (2013).
46. Shiau, A. K. *et al.* The structural basis of estrogen receptor/coactivator recognition and the antagonism of this interaction by tamoxifen. *Cell* **95,** 927–937 (1998).
47. Tinsley, J., Robinson, N. & Davies, K. E. Safety, tolerability, and pharmacokinetics of SMT C1100, a 2-arylbenzoxazole utrophin modulator, following single- and multiple-dose administration to healthy male adult volunteers. *J Clin Pharmacol* **55,** 698–707, doi: 10.1002/jcph.468 (2015).
48. Marrone, A. K., Edeleva, E. V., Kucherenko, M. M., Hsiao, N. H. & Shcherbata, H. R. Dg-Dys-Syn1 signaling in Drosophila regulates the microRNA profile. *BMC Cell Biol* **13,** 26, doi: 10.1186/1471-2121-13-26 (2012).
49. Yatsenko, A. S. & Shcherbata, H. R. Drosophila miR-9a targets the ECM receptor Dystroglycan to canalize myotendinous junction formation. *Dev Cell* **28,** 335–348, doi: 10.1016/j.devcel.2014.01.004 (2014).
50. Yatsenko, A. S., Marrone, A. K. & Shcherbata, H. R. miRNA-based buffering of the cobblestone-lissencephaly-associated extracellular matrix receptor dystroglycan via its alternative 3′-UTR. *Nat Commun* **5,** 4906, doi: 10.1038/ncomms5906 (2014).
51. Fiorillo, A. A. *et al.* TNF-alpha-Induced microRNAs Control Dystrophin Expression in Becker Muscular Dystrophy. *Cell Rep* **12,** 1678–1690, doi: 10.1016/j.celrep.2015.07.066 (2015).
52. Liu, N. *et al.* microRNA-206 promotes skeletal muscle regeneration and delays progression of Duchenne muscular dystrophy in mice. *J Clin Invest* **122,** 2054–2065, doi: 10.1172/JCI62656 (2012).
53. Kino, Y. *et al.* Nuclear localization of MBNL1: splicing-mediated autoregulation and repression of repeat-derived aberrant proteins. *Hum Mol Genet* **24,** 740–756, doi: 10.1093/hmg/ddu492 (2015).
54. Terenzi, F. & Ladd, A. N. Conserved developmental alternative splicing of muscleblind-like (MBNL) transcripts regulates MBNL localization and activity. *RNA Biol* **7,** 43–55 (2010).
55. Fernandez-Costa, J. M. & Artero, R. A conserved motif controls nuclear localization of Drosophila Muscleblind. *Mol Cells* **30,** 65–70, doi: 10.1007/s10059-010-0089-9 (2010).
56. Ottosen, S. *et al. In vitro* antiviral activity and preclinical and clinical resistance profile of miravirsen, a novel anti-hepatitis C virus therapeutic targeting the human factor miR-122. *Antimicrob Agents Chemother* **59,** 599–608, doi: 10.1128/AAC.04220-14 (2015).

57. Marek, K. W. *et al.* A genetic analysis of synaptic development: pre- and postsynaptic dCBP control transmitter release at the Drosophila NMJ. *Neuron* **25,** 537–547 (2000).
58. Garcia-Casado, M. Z., Artero, R. D., Paricio, N., Terol, J. & Perez-Alonso, M. Generation of GAL4-responsive muscleblind constructs. *Genesis* **34,** 111–114, doi: 10.1002/gene.10147 (2002).
59. Babcock, D. T. & Ganetzky, B. An improved method for accurate and rapid measurement of flight performance in Drosophila. *J Vis Exp*, e51223, doi: 10.3791/51223 (2014).

Acknowledgements

We thank Dr. Tudor Fulga for kindly providing miRNA sponge flies. This project was carried out with research grants SAF2012-36854 and SAF2015-64500-R, which include European Regional Development Funds, awarded to R.A. by the Ministerio de Economia y Competitividad. E.C.H. was supported by a predoctoral fellowship (BES-2013-064522) from the Ministerio de Economia y Competitividad.

Author Contributions

R.A. provided the conceptual framework for the study. All the authors conceived and designed the experiments. E.C.H., J.M.F.C., M.S.A. and B.L.L. performed the experiments and analyzed data. J.M.F.C. and B.L.L. prepared the manuscript with input by R.A.

Additional Information

Supplementary information accompanies this paper at http://www.nature.com/srep

Competing financial interests: The authors declare no competing financial interests.

How to cite this article: Cerro-Herreros, E. *et al.* Derepressing *muscleblind* expression by miRNA sponges ameliorates myotonic dystrophy-like phenotypes in *Drosophila*. *Sci. Rep.* **6**, 36230; doi: 10.1038/srep36230 (2016).

Publisher's note: Springer Nature remains neutral with regard to jurisdictional claims in published maps and institutional affiliations.

-Artículo 3-

nature COMMUNICATIONS

ARTICLE

DOI: 10.1038/s41467-018-04892-4 OPEN

miR-23b and *miR-218* silencing increase Muscleblind-like expression and alleviate myotonic dystrophy phenotypes in mammalian models

Estefania Cerro-Herreros[1,2,3], Maria Sabater-Arcis[1,2,3], Juan M. Fernandez-Costa[1,2,3], Nerea Moreno[1,2,3], Manuel Perez-Alonso[1,2,3], Beatriz Llamusi[1,2,3] & Ruben Artero[1,2,3]

Functional depletion of the alternative splicing factors Muscleblind-like (MBNL 1 and 2) is at the basis of the neuromuscular disease myotonic dystrophy type 1 (DM1). We previously showed the efficacy of miRNA downregulation in *Drosophila* DM1 model. Here, we screen for miRNAs that regulate *MBNL1* and *MBNL2* in HeLa cells. We thus identify *miR-23b* and *miR-218*, and confirm that they downregulate MBNL proteins in this cell line. Antagonists of *miR-23b* and *miR-218* miRNAs enhance MBNL protein levels and rescue pathogenic missplicing events in DM1 myoblasts. Systemic delivery of these "antagomiRs" similarly boost MBNL expression and improve DM1-like phenotypes, including splicing alterations, histopathology, and myotonia in the HSA^{LR} DM1 model mice. These mammalian data provide evidence for therapeutic blocking of the miRNAs that control Muscleblind-like protein expression in myotonic dystrophy.

[1] Interdisciplinary Research Structure for Biotechnology and Biomedicine (ERI BIOTECMED), University of Valencia, Dr. Moliner 50, E46100 Burjassot, Valencia, Spain. [2] Translational Genomics Group, Incliva Health Research Institute, Dr. Moliner 50, E46100 Burjassot, Valencia, Spain. [3] Joint Unit Incliva-CIPF, Dr. Moliner 50, E46100 Burjassot, Valencia, Spain. Correspondence and requests for materials should be addressed to B.L. (email: Mbeatriz.Llamusi@uv.es) or to R.A. (email: ruben.artero@uv.es)

Myotonic dystrophy type 1 (DM1) is an autosomal dominant rare genetic disease with variable presentation. It typically involves severe neuromuscular symptoms including cardiac conduction defects, myotonia, and progressive muscle weakness and wasting (atrophy). Neuropsychological dysfunction is also a common symptom of DM1[1]. The cause of DM1 is well known, namely the accumulation of mutant transcripts containing expanded CUG repeats in the 3′UTR of the *dystrophia myotonica protein kinase* (*DMPK*) gene. CUG repeats form the disease's hallmark ribonuclear foci. Mutant *DMPK* RNA triggers toxic gene misregulation events at the level of transcription[2], translation[3–6], gene silencing[7–10], alternative splicing, and polyadenylation of subsets of transcripts[11–13].

RNA toxicity stems from enhanced binding of proteins to expanded CUG RNA, which exists as imperfect hairpin structures. The RNA-binding proteins are thus depleted from their normal cellular targets. Chief among these are the Muscleblind-like proteins (MBNL1–3), whose sequestration contributes to DM1 in several ways. MBNL1 controls fetal-to-adult splicing and polyadenylation transitions in muscle and MBNL2 likely has a similar role in the brain[14,15], whereas *Mbnl3* deficit results in age-associated pathologies that are also observed in myotonic dystrophy[16,17]. No treatment has yet been specifically developed for DM1 despite intensive efforts. Numerous therapeutic approaches have been designed following different approaches[18,19] that can be broadly grouped as: (1) specific targeting of the mutant allele or its RNA product, including preventing MBNL protein sequestration using small molecules[20–23], transcriptional[24,25] and post-transcriptional silencing of *DMPK*[26], and (2) target signaling pathways downstream from CUGexp (CUG expansion) expression[27,28]. Two strategies have reached human trials: Tideglusib, a small molecule non-ATP-competitive glycogen synthase kinase 3 (GSK-3) inhibitor[4] (clinical trial NCT02858908) and IONIS-DMPKRx, an RNase H1-active ASO (antisense oligonucleotide) that target CUGexp RNA[29] (clinical trial NCT02312011). However, in IONIS-DMPKRx clinical trial, drug levels measured in muscle biopsy confirmed that the amount of target engagement was not enough to exert a desired therapeutic effect[30].

There is ample evidence that MBNL1 and MBNL2 functions are the limiting factors in DM1. Therefore, boosting their expression is a potential therapeutic avenue. Indeed overexpression of MBNL1 could rescue disease-associated RNA missplicing and muscle myotonia in a DM1 mouse model that expresses 250 CTG repeat units from a human skeletal actin promoter (HSA^{LR})[31,32]. Consistently, compound loss of Muscleblind-like function reproduces cardinal features of DM1 such as reduced lifespan, heart conduction block, severe myotonia, and progressive muscle weakness[33]. *MBNL1* overexpression was well-tolerated in skeletal muscle and early and long-term *MBNL1* overexpression prevented CUG-induced myotonia, myopathy, and alternative splicing abnormalities in DM1 mice[34]. Targeted expression of *MBNL1* can even rescue eye and muscle atrophy phenotypes in *Drosophila* DM1 models[35–37].

We recently used a *Drosophila* DM1 model to show that Muscleblind could be upregulated by sequestration of repressive miRNAs to improve splicing, muscle integrity, locomotion, flight, and lifespan[38]. Here, we extend these studies to mammalian disease models and demonstrate that *miR-23b* and *miR-218* are endogenous translational repressors of *MBNL1/2* and *MBNL2*, respectively. AntagomiRs transfection upregulates MBNL proteins and rescues alternative splicing in normal and DM1 human myoblasts. Furthermore, systemic administration of antagomiRs in the HSA^{LR} mouse model upregulate Muscleblind-like protein in both gastrocnemius and quadriceps muscles and rescue the molecular, cellular, and functional defects of DM1 muscle.

Results

Identification of miRNAs that regulate *MBNL1* and *MBNL2*. We approached a detailed description of *MBNL1* and *MBNL2* regulation by overexpressing miRNAs in HeLa cells using a commercial kit. The study identified 19 and 9 miRNAs that reduced *MBNL1* or *MBNL2* transcript levels by at least 4-fold, respectively, compared to controls (Supplementary Fig. 1). We ranked the miRNAs according to likelihood of a direct physical interaction with *MBNL1* or *MBNL2* 3′-UTR sequences (Supplementary Table 1). We selected five miRNAs with the best target predictions and also included *miR-146b* in our validation work because it downregulated *MBNL1* the most. Overall, selected miRNAs were: *miR-96* and *miR-181c* as candidate direct repressors of *MBNL1*; *miR-218* and *miR-372* as candidate repressors of *MBNL2*, and *miR-146b* and *miR-23b* as potential regulators of both.

In validation experiments, HeLa cells were transfected with the corresponding miRNA precursor sequences cloned into the *pCMV-MIR-GFP* vector. All candidate miRNAs confirmed the expected reduction in endogenous *MBNL1* and/or *MBNL2* mRNA levels (Fig. 1a, b), except for *miR-146b* that only significantly reduced *MBNL2* expression. Next, we used western blot quantification to confirm the Muscleblind-like protein downregulation by miRNAs (Fig. 1c–f). All mRNA reductions were thus confirmed at the protein level except for *miR-181c* on MBNL1 translation and *miR-146b*, which failed to repress both MBNL1 and MBNL2. Taken together, these results identified *miR-96*, *miR-23b*, and *miR-218* as new miRNAs that repress *MBNL1* and/or *MBNL2* expression both at the mRNA stability and protein levels.

Mapping of miRNA–mRNA binding sites in the 3′UTR of *MBNL1/2*. miRNAs generally act as post-transcriptional repressors by recognizing specific sequences in the 3′-UTR of target mRNAs[39]. To test if our three candidate miRNAs directly bind to the trailer regions of *MBNL1* and *MBNL2*, as predicted by miRanda[40] and TargetScan[41] (Fig. 2a, e), we performed reporter assays in HeLa cells. The 3′-UTR of each gene was fused to the Gaussian luciferase reporter (Gluc) so that any functional interaction of a regulatory miRNA and the reporter construct will reduce luminescence measurements. Cotransfection of miRNA target gene luciferase reporter constructs and miRNA plasmids in HeLa cells confirmed a significant decrease in the luciferase luminescence for all tested miRNAs (Fig. 2b, f).

miRNA–mRNA interaction strongly depends on the perfect complementarity between the target mRNA and the miRNA seed region at positions 2–8[39]. Next, we investigated direct binding of miRNAs to single or multiple *MBNL* 3′-UTR sequences. We made a series of miRNA target gene luciferase reporter plasmids with natural (WT), perfectly matched (PM), or absent (MUT) miRNA recognition sites. In these assays, WT versions of the 3′-UTR of *MBNL1* and *MBNL2* significantly reduced expression of the Gluc reporter when co-transfected with *miR-23b* or *miR-96* (*MBNL1*; Fig. 2c, d), and *miR-23b* or *miR-218* (*MBNL2*; Fig. 2g, h). In comparison, cotransfection with the corresponding mutant versions always abrogated the repressive effect of the miRNAs whereas PM versions had lower luciferase than WT constructs. Strikingly, deletion of any of the three *miR-218* recognition sites in *MBNL2* alleviated full repression of the Gluc reporter. Overall, we conclude that *miR-96*, *miR-218*, and *miR-23b*, directly regulate *MBNL1*, *MBNL2*, or both genes, respectively.

***miR-23b* and *miR-218* antagomiRs stabilize MBNL transcripts.** DM1 pathology depends on Muscleblind-like protein expression in muscle. A pre-requisite for the hypothesis that miRNAs fine-

tune MBNL1 and/or MBNL2 translation in muscle was that our candidate miRNAs were expressed there. We therefore measured levels of *miR-96*, *miR-23b*, and *miR-218* in muscle by qPCR. *miR-23b* and *miR-218* were highly expressed in cultured human DM1 myoblasts and muscle biopsies, whereas *miR-96* was found at negligible levels (Fig. 3a). To test this potential of *miR-23b* and *miR-218* as therapeutic targets for DM1, we designed antisense oligonucleotides (antagomiRs) that recognize these miRNAs. AntagomiRs are very stable and have cholesterol moieties to enhance their uptake into cells[42,43]. First, we characterized their toxicity profiles. The TC10 concentrations (at which at least 90% of cells remained viable) were 654.7 nM for antagomiR-23b and 347 nM for antagomiR-218 (Fig. 3b).

Visual confirmation of cell uptake was obtained with Cy3-labeled versions of antagomiRs at concentrations ranging 50–100 nM, but not at 10 nM (Supplementary Fig. 2). Having established the effective and non-toxic range for the antagomiRs, we tested the ability of antagomiR-23b and -218 to block their corresponding miRNA at concentrations at which cell uptake was confirmed (>50 nM), but well below TC10. DM1 myoblasts were transfected with antagonists and the mRNA levels of *MBNL1* and *MBNL2* were measured 48 and 96 h later. *MBNL1* and *MBNL2* transcripts in cells treated with antagomiR-218 increased in a dose-dependent manner at both time points and reached approximately 50% higher levels than in scramble control-treated DM1 cells (Fig. 3c, d). Of note, since silencing of *miR-218* enhanced *MBNL1* transcripts but did not bind to the *MBNL1* 3′-UTR reporter constructs (Supplementary Fig. 3) regulation by this miRNA might be indirect or dependent on sequences outside the 3′-UTR. In sharp contrast to *miR-218* blockers, the lower the concentration of antagomiR-23b the higher the increase in MBNL levels. *MBNL1* transcripts doubled in DM1 cells 96 h post-transfection with 50 nM of antagomiR-23b. Assuming a typical bell-shaped dose–response, these results suggested that working concentration for antagomiR-23b is 50 nM, or lower, and 200 nM or higher for antagomiR-218 (Fig. 3c, d). Importantly, levels of *miR-218* were not altered in cells treated with antagomiR-23b, suggesting a specific effect of the antagomiR on its target. *miR-23* family includes *miR-23a* and *miR-23b*, which are transcribed from different chromosomes, have identical seed sequences, and differ by only one nucleotide on their 3′ ends. As expected, antagomiR-23b also reduced the levels of *miRNA-23a* in the cells (Supplementary Fig. 4a, b).

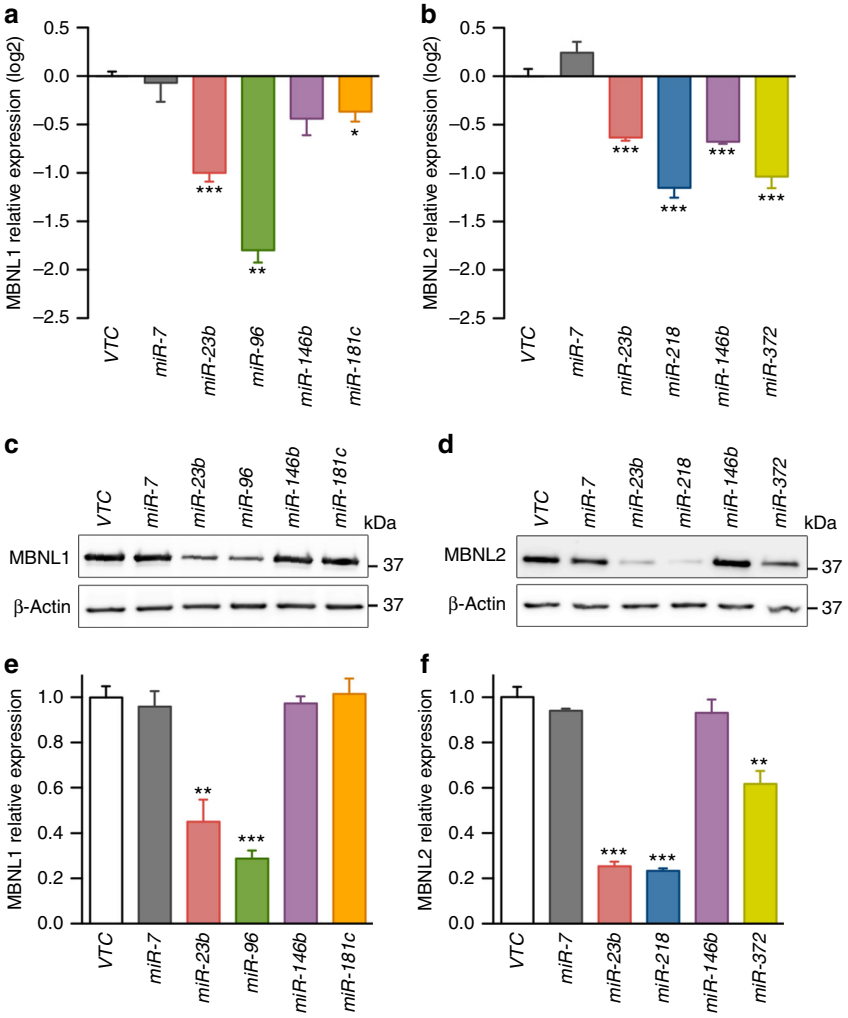

Fig. 1 Validation of candidate *MBNL1* and/or *MBNL2* regulatory miRNAs. Logarithmic representation on base 2 (log2) of the qRT-PCR quantification of *MBNL1* (**a**) and *MBNL2* (**b**) expression relative to *GAPDH* gene in HeLa cells transfected with the indicated *pCMV-MIR* plasmids. **c**–**f** Relative protein expression levels of MBNL1 (**c**, **e**) and MBNL2 (**d**, **f**) in HeLa cells transfected as above. β-ACTIN was the endogenous control. In all cases, empty *pCMV-MIR-GFP* plasmid (VTC) was used as reference value for relative quantification, *miR-372*[66] and *miR-7* were used as positive and negative controls, respectively. GFP was used as transfection control. ($n = 3$). Data are mean ± SEM. $^{*}p < 0.05$, $^{**}p < 0.01$, $^{***}p < 0.001$ according to Student's *t* test

In summary, we have confirmed the ability of *miR-23b* and *miR-218* antagonists to enter DM1 cells and enhance *MBNL1* and *MBNL2* mRNA levels, at concentrations well below their toxicity threshold.

***miR-23b* and *miR-218* silencing rescues defects in DM1 cells.** The best-known molecular alteration in DM1 is missplicing of defined subsets of muscle transcripts. To test whether higher amounts of *MBNL1* and *MBNL2* mRNA translate into rescue of the Muscleblind-dependent splicing events, we transfected DM1 cells using the optimal conditions determined above and verified improvement of missplicing events including *Bridging integrator 1* (*BIN1*)[44], *ATPase sarcoplasmic/endoplasmic reticulum* Ca^{2+} *transporting 1* (*ATP2A1*)[45], *Insulin receptor* (*INSR*)[46,47], and *Piruvate kinase M* (*PKM*)[48]. Exon inclusion (Percentage Spliced In; PSI) was significantly rescued for all four transcripts 96 h post-transfection (Fig. 3e; Supplementary Fig. 5) upon *miR-23b* or *miR-218* silencing (Fig. 3f, h). Similarly, *BIN1*, *ATP2A1*, and *PKM* splicing, but not *INSR*, was also rescued 48 h after antagomiR transfection (Supplementary Figs. 5 and 6). In contrast, increased levels of *MBNL1* and *MBNL2* in DM1 myoblasts did not significantly change the aberrant inclusion of exon 5 in the *Cardiac troponin T* (*cTNT*)[46] transcripts under any of the experimental conditions tested.

To test the specificity of antagomiRs-23b and -218, we quantified the inclusion of exon 8 of *CAPZB*, which depends on CUGBP Elav-like protein family member 1 (CELF1)[49], and observed that it was not rescued by the antagomiRs (Fig. 3e; Supplementary Figs. 5 and 6). Additionally, the regulated inclusion of exon 19 of *DLG1*, which is known to be *MBNL1* and *CELF1*-independent, did not change under any of the experimental conditions, thus discarding global effects on alternative splicing control upon antagomiR treatment (Fig. 3e; Supplementary Figs. 5, 6). Taken together, these results confirm Muscleblind-specific rescue of alternative splicing defects taking place in DM1 myoblasts as a result of antagomiR-mediated *MBNL1* and *MBNL2* derepression.

AntagomiRs-23b/-218 restore normal MBNL cell distribution. Since miRNAs can regulate gene expression at the mRNA

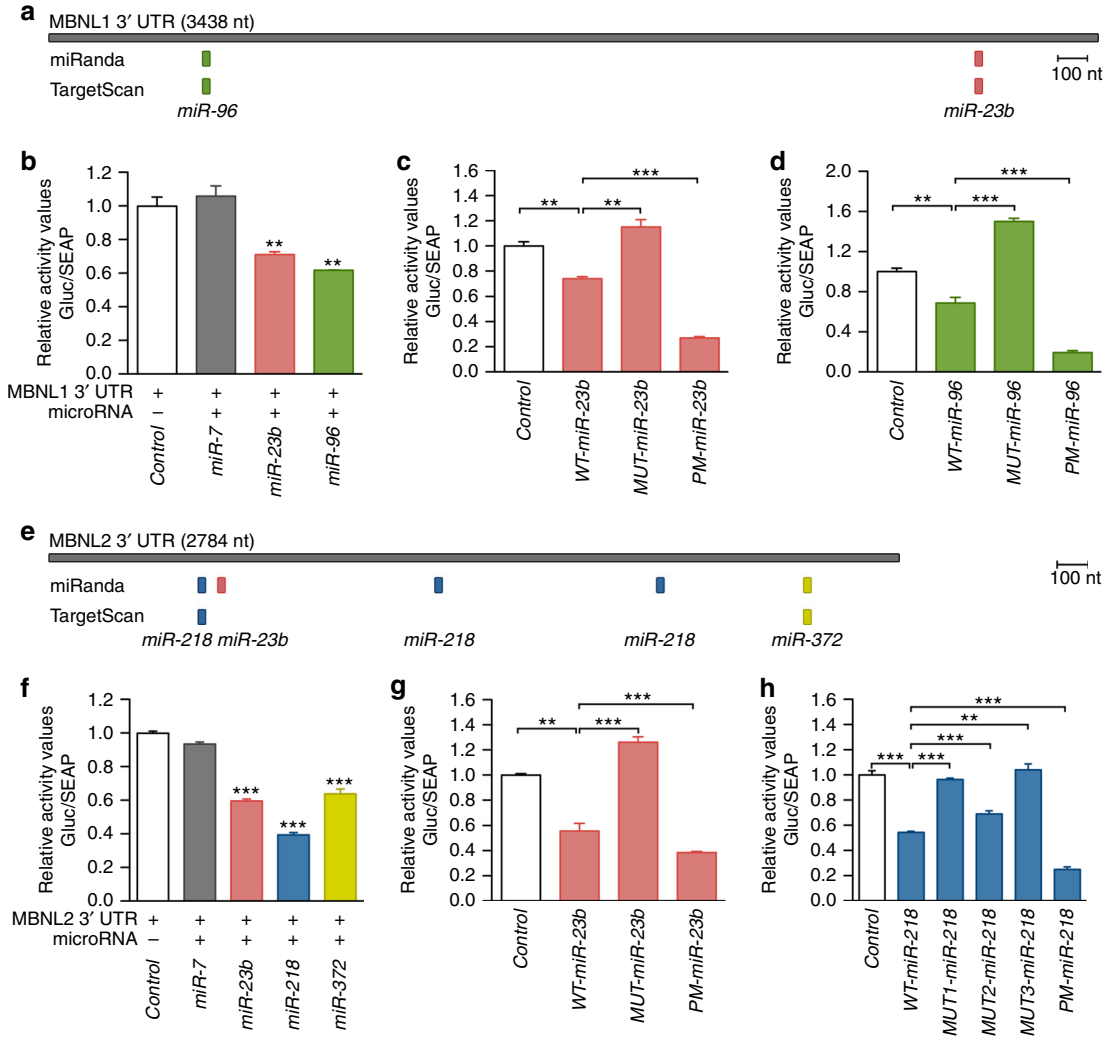

Fig. 2 Confirmation of miRNA binding to *MBNL1* and *MBNL2* 3′UTRs. **a**, **e** Scale representation of *MBNL1* (**a**) and *MBNL2* (**e**) 3′ UTRs and predicted miRNA binding sites according to miRanda and TargetScan algorithms. *MBNL1* (**b**–**d**) and *MBNL2* (**f**–**h**) 3′ UTR luciferase reporter assays of HeLa cells co-transfected with wild-type (**b**, **f**) or mutated (**c**, **d**, **g**, **h**) versions of 3′ UTR fused to Gaussia luciferase and miRNA plasmids ($n = 4$). *miR-7* was used as a negative control. Wild-type (WT) reporter plasmids had the natural sequence of the miRNA binding sites, mutated (MUT) constructs lacked a candidate miRNA seed region recognition site and the perfect match (PM) versions had the miRNA binding site replaced by the full complementary sequence. $^{**}p < 0.01$, $^{***}p < 0.001$ according to Student's *t* test. Data are mean ± SEM

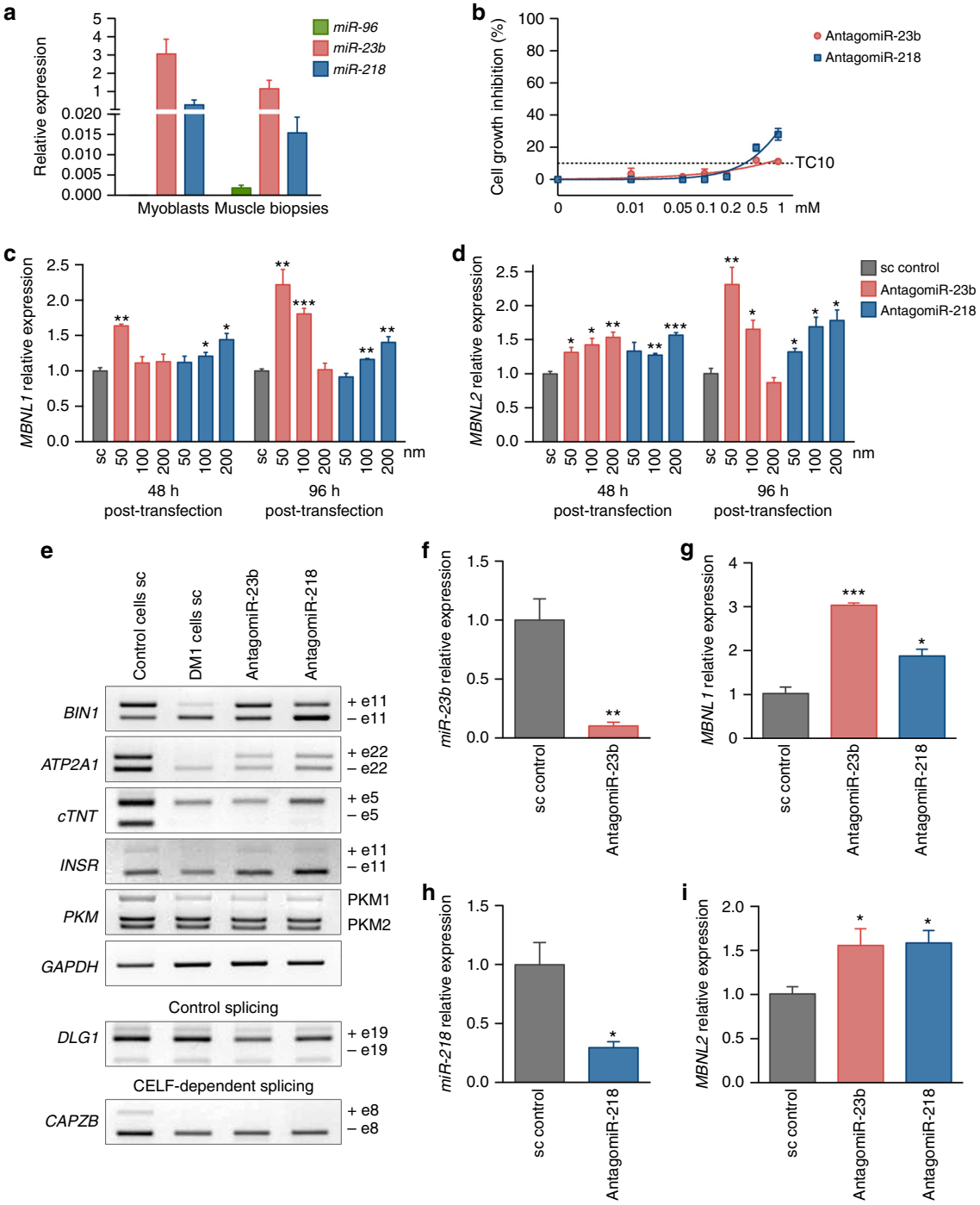

Fig. 3 AntagomiR-23b and -218 stabilize *MBNL* transcripts and rescue alternative splicing defects in DM1 myoblasts. **a** Real-time PCR quantification of *miR-96*, *miR-23b*, and *miR-218* expression in myoblasts and muscle biopsies from DM1 patients. *U1* and *U6* snRNAs were used as reference genes. **b** Cell growth inhibition assay by MTS method. Human normal myoblasts were transfected with increasing concentrations of antagomiRs against *miR-23b* and *miR-218* ($n = 4$). TC10 was obtained using the least squares non-linear regression model. **c**, **d** qRT-PCR quantification of *MBNL1* (**c**) and *MBNL2* (**d**) expression relative to *GAPDH* and *ACTB* genes in human DM1 myoblasts transfected with the indicated antagomiRs or scrambled control antagomiR (sc). **e** Semiquantitative RT-PCR analyses of splicing events altered in *BIN1* (exon 11), *ATP2A1* (exon 22), *cTNT* (exon 5), *INR* (exon 11), and *PKM* isoforms in DM1 cells. *GAPDH* was used as internal control. Inclusion of *DLG1* exon 9, which is not altered in DM1, and *CAPZB* exon 8, which is CELF1-dependent, were used as additional controls. **f**, **h** miRNA real-time PCR determination of available *miR-23b* (**f**) or *miR-218* (**h**) in DM1 myoblasts 96 h after transfection with 50 nM of antagomiR-23b or 200 nM of antagomiR-218. *U1* and *U6* snRNAs were used as reference genes in **f** and **h**. **g**, **i** qRT-PCR analyses of *MBNL1* (**g**) and *MBNL2* (**i**) expression relative to *GAPDH* and *ACTB* genes in human myoblasts 96 h after transfection with 50 nM of antagomiR-23b or 200 nM of antagomiR-218. ($n = 3$). Data are mean ± SEM. *$p < 0.05$, **$p < 0.01$, ***$p < 0.001$ according to Student's *t* test

stability and translation levels, we sought to determine the effect of antagomiRs on MBNL1 and MBNL2 protein expression. Upon antagomiR treatment, qPCR data confirmed a significant increase in the levels of *MBNL1* and *MBNL2* mRNA 96 h (Fig. 3g, i) or 48 h (Supplementary Fig. 6) post-transfection. At the protein level, these differences were further enhanced and western blots detected 4–5-fold more MBNL1, and 3–5-fold higher MBNL2 proteins, in DM1 myoblasts after 96 h (Fig. 4a, b, d, e) and 48 h (Supplementary Fig. 6) of antagomiR treatment. Of note, MBNL1 and MBNL2 protein levels remained unaltered in control and DM1 cells mock-transfected or transfected with a scrambled control antagomiR (Supplementary Fig. 7). In contrast, CELF1 protein levels remained unchanged upon *miR-23b* or *miR-218* silencing (Fig. 4c, f; Supplementary Fig. 6) and, consistently, *CAPZB* alternative splicing remained the same. Importantly, this increase was clearly visible by immunofluorescence. Whereas both MBNL1 and MBNL2 were sequestered in ribonuclear foci of DM1 myoblasts (Fig. 4h, l), antagomiRs-23b and -218 robustly increased the protein expression and restored their distribution in the cytoplasm and in the cell nucleus (Fig. 4i, j, m, n). The increase of MBNL1 and MBNL2 proteins in the cell nucleus was consistent with the previously shown splicing rescue. Because the relationship between MBNL proteins and CUGexp foci formation is complex, a potential undesirable side effect of boosting MBNL expression was an increase in the number of ribonuclear foci. To specifically test this hypothesis, we quantified foci in antagomiR-treated DM1 fibroblasts and found that remained unaltered (Fig. 4o–r).

***miR-23b* and *miR-218* are expressed in tissues relevant to DM1.** To obtain a broader view of the expression pattern and relative expression of these miRNAs, we turned to mouse tissue samples, using the reference FVB strain. We analyzed muscle (quadriceps, gastrocnemius), whole heart, and central nervous system (forebrain, cerebellum, hippocampus). All samples had robust expression of *miR-23b* and *miR-218*, whereas *miR-96* was again almost undetectable except in cerebellum (Fig. 5a). *miR-218* was expressed up to 80 times higher in brain tissues than in muscle-derived samples. *miR-23b* and *miR-218* are therefore strongly expressed in the tissues that are highly relevant to DM1 pathology (skeletal muscle, heart, brain) where they likely repress MBNL1 and/or MBNL2 translation. Since levels of MBNL proteins are limiting in DM1, *miR-23b* and *miR-218* may be contributing to the disease phenotypes and can be regarded as potential therapeutic targets.

AntagomiRs increase Mbnl expression in HSA^{LR} mouse muscle. Next, we investigated the activity of antagomiR-23b and -218 in the HSA^{LR} mouse DM1 model[31]. First, we evaluated the ability of antagomiRs to reach skeletal muscle. Cy3-labeled versions of the antagomiRs were administered to a 4-month-old HSA^{LR} mouse by a single subcutaneous injection. Four days post-injection, hind limb gastrocnemius and quadriceps muscles were processed to detect the labeled oligonucleotide. We observed the antagomiRs by anti-Cy3 immunofluorescence in a strong punctate pattern in nuclei and membrane of both muscles. The antagomiRs were also diffusely present throughout the cells (Fig. 5b–e). These data demonstrate that antagomiR oligonucleotides that block *miR-23b* or *miR-218* can reach the skeletal muscles of a DM1 mouse model.

We decided to inject unlabeled antagomiRs to nine additional DM1 animals, in three consecutive injections (12 h intervals) to a final dose of 12.5 mg kg^{-1}. The controls were injected with PBS1x ($n = 10$) or scrambled antagomiR ($n = 5$). Four days after the first injection, animals were sacrificed and quadriceps and gastrocnemius were obtained for histological and molecular analysis. We confirmed that *miR-23b* and *miR-218* were strongly silenced by their complementary antagomiRs. *miR-23b* was reduced to 30–40% and miR-218 to 50% of the levels measured in the untreated HSA^{LR} mice (Fig. 5f, g). As a result of miRNAs reduction, *Mbnl1* and *Mbnl2* increased at the transcript and protein levels in both muscle types (Fig. 5h, i, j, k, m, n). Importantly, levels of Celf1 protein were not altered by either treatment (Fig. 5l, o). In mice injected with PBS or with scrambled oligo as control, target microRNAs and the *Mbnl1* and *Mbnl2* transcript levels were indistinguishable (Supplementary Fig. 8a–d).

AntagomiRs rescue missplicing of muscle transcripts in mice. Given the robust increase in Mbnl1 and 2 in treated gastrocnemius and quadriceps muscles, we sought to confirm a rescue of Mbnl-dependent splicing events *Atp2a1, Chloride channel protein 1 (Clcn1)*, and Nuclear factor 1 X-type (*Nfix)* in HSA^{LR} mice (Fig. 6a, b; Supplementary Fig. 9). AntagomiR administration ameliorated aberrant exon choices for *Atp2a1* (exon 22) and *Nfix* (exon 7), and increased *Clcn1* exon 7a PSI in gastrocnemius but not in quadriceps of HSA^{LR} mice. To test the specificity of antagomiRs-23b and -218 on MBNL regulation, we quantified the inclusion of exon 8 of *Capzb*, Exon 21 of *Ank2*, and exon 3 of *Mfn2*, which depend on Celf1[49,50], and observed that they were not altered by treatment with antagomiRs.

In a routine test of transgene expression of HSA^{LR} mice, we discovered that CUG expression levels varied up to 0.5-fold among animals and that variation positively correlates with aberrant inclusion of alternative exons in gastrocnemius and quadriceps (Supplementary Fig. 10). To note *Atp2a1* exon 22 inclusion was bimodal. Two out of 10 mice that expressed low levels of transgene included exon 22 to levels significantly higher (closer to normal) than the rest of HSA^{LR} mice and were therefore excluded from the analysis (Supplementary Figs. 10 and 11). These data suggest that the lower the expression of CUG repeat RNA in muscles the less missplicing there is. In contrast, in the antagomiR-treated HSA^{LR} muscle samples splicing defects correlated with *Mbnl* mRNA levels, instead of repeat expression, which supported a causal role of these proteins in the rescue of the splicing events (Supplementary Fig. 10). Despite the intrinsic variability of the model, we conclude that both antagomiRs achieved similar levels of rescue in all gastrocnemius-missplicing events. However, antagomiR-23b rescued *Nfix* splicing to a greater extent than antagomiR-218 in quadriceps, which correlated with the lower upregulation of Mbnl1 and 2 protein levels achieved by antagomiR-218 in this muscle. Consistent with the unchanged levels of Celf1 protein in the muscles of treated HSA^{LR} mice, inclusion percentage of *Celf1*-dependent splicing events in gastrocnemius and quadriceps of treated and control mice was very similar (Fig. 6a, b and Supplementary Fig. 9). Importantly, the Mbnl1 and 2 protein levels and the splicing patterns of Mbnl- or Celf1-dependent events in mice injected with PBS or with scrambled oligo, as control, were indistinguishable (Supplementary Fig. 8e–i).

These results indicate that systemic delivery of antagomiRs was able to rescue muscle missplicing in vivo in a DM1 mouse model.

AntagomiRs improve muscle histopathology and reduce myotonia. Defective transitions of fetal to adult alternative splicing patterns have been proposed to originate DM1 muscle phenotypes[51]. In HSA^{LR} DM1 model mice, alterations in ionic currents cause repetitive action potentials, or myotonia, that can be quantified by electromyography. Before treatment, all DM1 mice had grade 3 or 4 myotonia, i.e., abundant repetitive

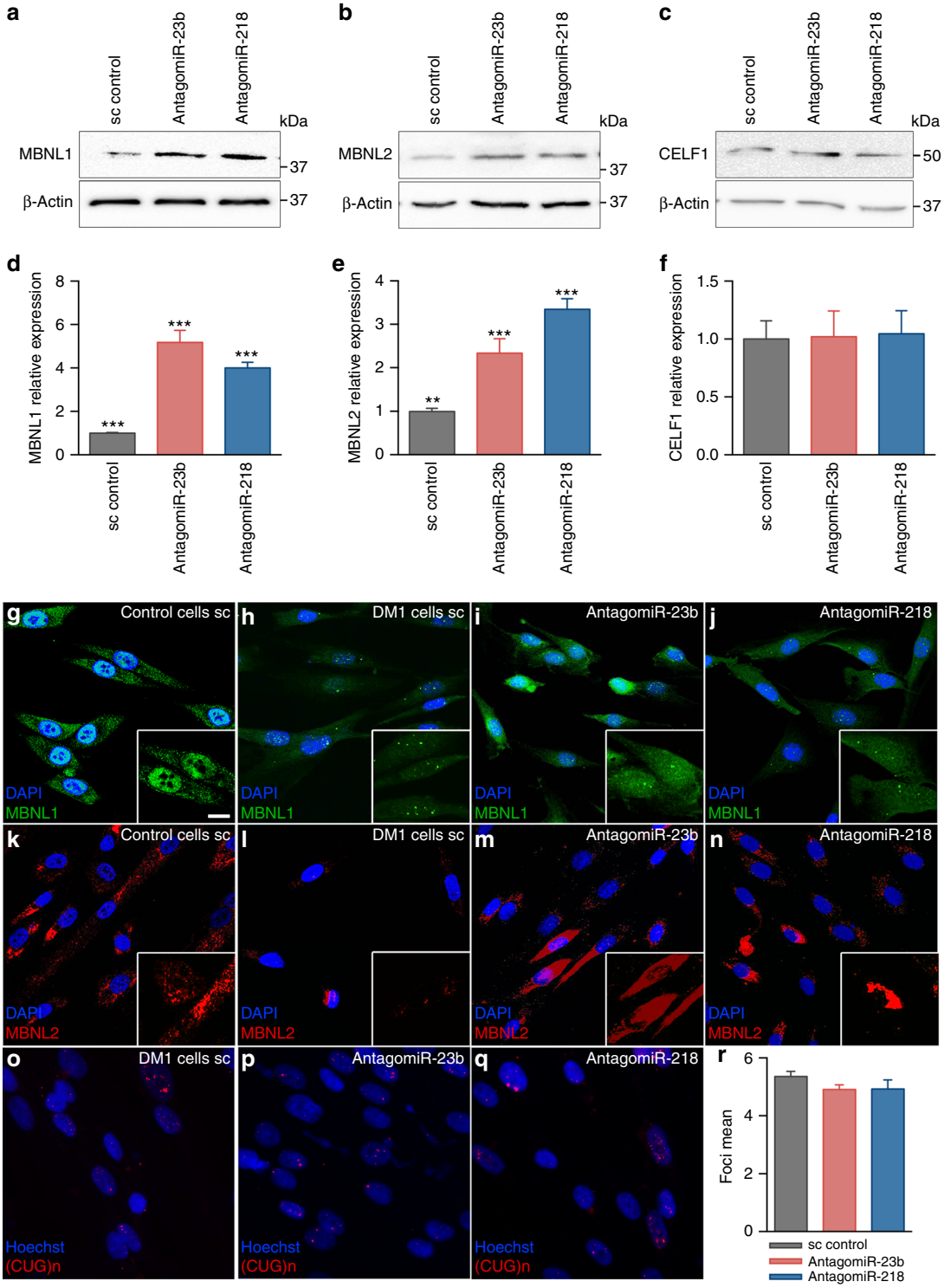

Fig. 4 Increase of MBNL1 and MBNL2 upon silencing of *miR-23b* or *miR-218* in human myoblast. **a**–**f** Western blot quantification of MBNL1 (**a**, **d**), MBNL2 (**b**, **e**), and CELF1 (**c**, **f**) expression levels in DM1 human myoblast 96 h after transfection with 50 nM of antagomiR-23b, 200 nM of antagomiR-218 or a scrambled control antagomiR (sc). β-ACTIN expression was used as endogenous control ($n = 3$). Data are mean ± SEM. $^{**}p < 0.01$, $^{***}p < 0.001$ in Student's *t* test. **g**–**n** Representative confocal images of MBNL1 (green) and MBNL2 (red) staining in healthy controls (control cells) and DM1 human myoblast 96 h after transfection with antagomiRs against *miR-23b* (50 nM) or *miR-218* (200 nM) and a scrambled control antagomiR (DM1 cells). Nuclei were counterstained with DAPI (blue). In DM1 cells, endogenous MBNL1 (**h**) and MBNL2 (**l**) were in nuclear aggregates (green and red puncta) and the total amount of both was reduced compared to control cells (**g**) and (**k**), respectively. In contrast, DM1 cells treated with antagomiRs against *miR-23b* or *miR-218* showed a robust increase in cytoplasmic and nuclear MBNL1 (**i**, **j**) and MBNL2 (**m**, **n**) levels compared to DM1 cells. **b**–**q** Representative fluorescence of FISH images showing (CUG)n RNA foci (red) in DM1 human fibroblasts transfected with antagomiRs against *miR-23b* (50 nM) or *miR-218* (200 nM) and a scrambled control antagomiR. Nuclei were counterstained with Hoechst (blue). AntagomiRs did not significant change the number of ribonuclear foci in DM1 fibroblasts (**r**). Scale bar = 20 μm

discharges with the vast majority of electrode insertions. Four days after, antagomiRs reduced myotonia to grade 2 (myotonic discharge in >50% of insertions) or grade 1 (occasional myotonic discharge) in 55% of the mice treated with antagomiR-218, and in 50% of the mice treated with antagomiR-23b, respectively (Fig. 6c).

A typical histological hallmark of DM1 and HSA^{LR} mouse muscle fibers is a central location of nuclei, which results from myopathic muscle attempting to regenerate[5]. Both antagomiRs caused decentralization of nuclei in both gastrocnemius and quadriceps muscles (Fig. 6d–h). In contrast, myotonia levels and number of central nuclei remained unaltered in mice treated with the scrambled antagomiR (Supplementary Fig. 8j–m).

Taken together, these results validate the potential of antagomiR-23b and -218 as a drug that suppresses CUG-repeat RNA-induced myopathy in mammals.

AntagomiR long-term treatment rescue functional phenotypes. In order to assess the long-term effects of the antagomiR treatments, we studied characteristic molecular and functional alterations in the HSA^{LR} mice in groups of mice treated with the same dose and posology as before but sacrificed 6 weeks after the antagomiR injections. The levels of *miR-23b* and *miR-218* in these mice were still significantly reduced 6 weeks after the initiation of the experiment, but the reduction was less pronounced than in the short-term treatment. In general, the reduction of target miRNAs was not enough to maintain the increased Mbnl transcript levels, as only Mbnl1 transcripts in quadriceps were significantly augmented 6 weeks after injection (Fig. 7a–d). Myotonia grade measured before injection (bi), in the halfway point (hp, 3 weeks after the injection) and in the final point (fp, before sacrifice) showed a clear tendency to decrease with time (Fig. 7e), and forelimb muscle force measured in the final point and normalized to body weight, increased in both treatments

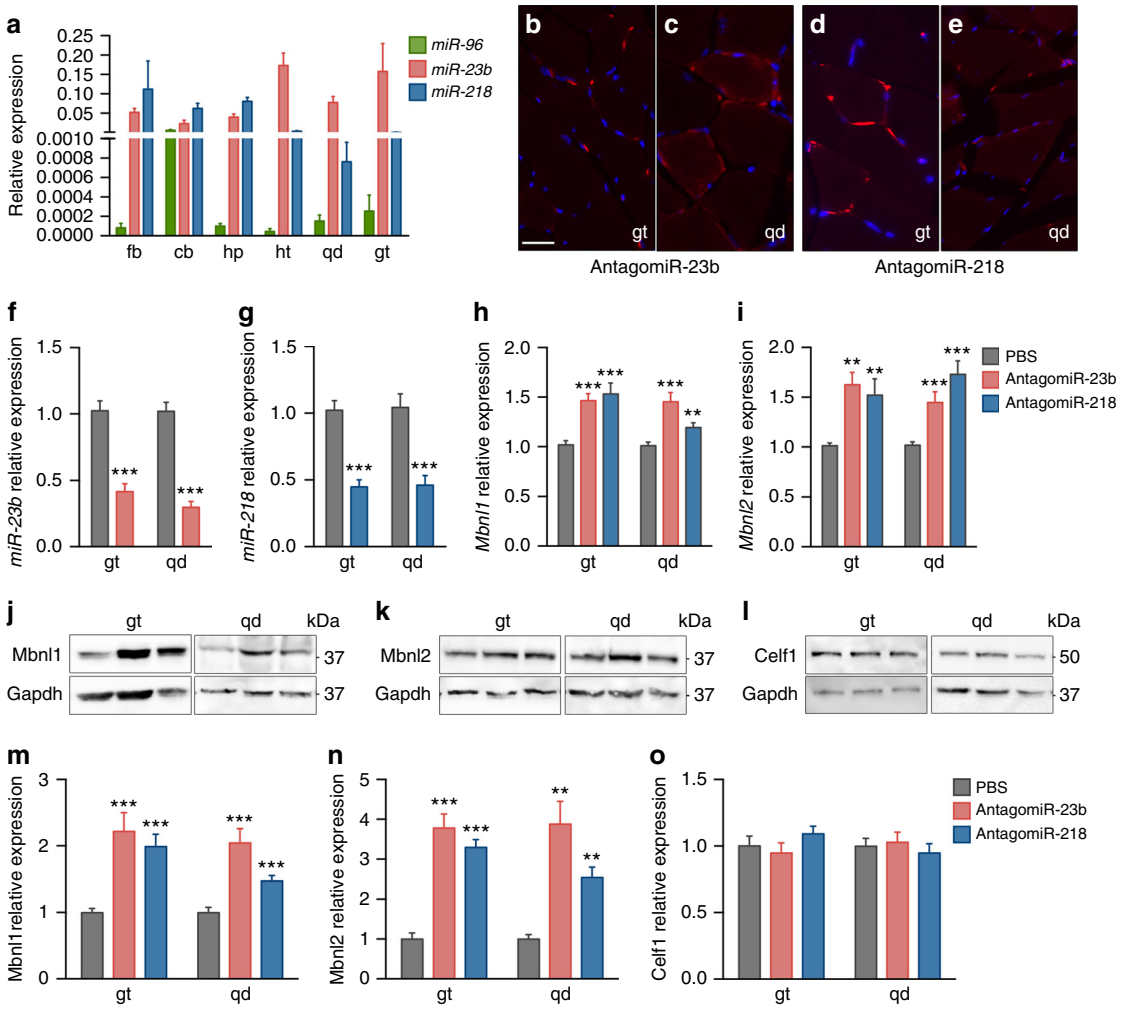

Fig. 5 Subcutaneous injection of antagomiR-23b or antagomiR-218 in HSA^{LR} mice reduced target miRNA levels and increased Mbnl1 and Mbnl2 without affecting levels of Celf1. **a** qPCR quantification of *miR-96*, *miR-23b*, and *miR-218* expression levels in forebrain (fb), cerebellum (cb), hippocampus (hp), heart (ht), and quadriceps (qd) and gastrocnemius (gt) muscles ($n = 3$). Average expression levels of *U1* and *U6* were used for normalization. **b–e** Immunodetection of Cy3-labeled antagomiRs in gastrocnemius (**b**, **d**) and quadriceps (**c**, **e**) cryosections of HSA^{LR} treated mice ($n = 1$). Myonuclei were counterstained with DAPI (blue). Scale bar = 50 µm. **f–g** Quantification of *miR-23b* and *miR-218* in gt and qd muscles of untreated mice (PBS, gray bars) or treated with antagomiR-23b (pink bars) or antagomiR-218 (blue bars). Relative values (to average of *U1* and *U6* expression) were further normalized to the levels in untreated mice. **h, i** Real-time PCR quantification of *Mbnl1* and *Mbnl2* transcript levels in gt and qd muscles. Expression levels relative to the endogenous *Gapdh* were normalized to the levels in untreated mice. **j–o** Western blotting analysis of Mbnl1 (**j**, **m**), Mbnl2 (**k**, **n**), and Celf1 (**l**, **o**) proteins in mouse gt and qd muscles. Representative blots used for quantification in (**m–o**) are shown in (**j–l**). The data were analyzed by unpaired Student's *t* test compared to untreated HSA^{LR} mice. Data are mean ± SEM. $^{*}p < 0.05$, $^{**}p < 0.01$, $^{***}p < 0.001$; HSA^{LR} PBS ($n = 10$ in **f–o**), HSA^{LR} antagomiR-23b ($n = 9$, in **f–o**). HSA^{LR} antagomiR-218 ($n = 9$, in **f–o**)

although the difference was only significant for antagomiR-218 (Fig. 7f).

Importantly, visual necropsy and biochemical blood parameters measured of the mice before sacrifice support a non-deleterious effect of the treatment with the antagomiRs, even after 6 weeks (Supplementary Data 2). The only parameters altered in these analyses were total bilirubin, which was decreased in all treated animals, potentially reflecting an increase in liver metabolic rate, and monocyte number, which increased also in all treated animals, suggesting activation of the immune system. Given that these two parameters were also altered in the scrambled-treated mice, the alterations might be caused by the oligo chemistry instead of specific microRNA inhibition.

Discussion

A largely unexplored therapeutic strategy for DM1 is therapeutic gene modulation (TGM), which pursues to raise or lower the expression of a given gene to alleviate a pathological condition. Examples of TGM are inhibition of CD44 in metastatic prostate cancer[52], or the pharmacological enhancement of *utrophin* expression to compensate lack of dystrophin in Duchenne Muscular Dystrophy[53]. Previous attempts to raise the critically low levels of Muscleblind in DM1 involved epigenetic upregulation of endogenous *MBNL1*[54] or derepression of *muscleblind* by sponge-mediated silencing of miRNAs in a *Drosophila* DM1 model[38]. Oligonucleotide-based modulation of miRNA activity has prompted great attention because of its efficacy in animal models of disease and the development of specialized chemistries[52,55,56].

In this study, we identified *miR-23b* and *miR-218* as inhibitors of *MBNL1* and *MBNL2* translation, and show that complementary antagomiRs robustly silence their target miRNAs in patient-derived myoblasts and HSA^{LR} mouse model. We found that antagomiRs are effective at doses lower than those previously reported in muscle[43,57,58]. By inhibiting *miR-23b* and *miR-218* in mouse muscle, we were able to upregulate MBNL1 and MBNL2 protein levels by approximately over 2-fold and 4-fold, respectively, without affecting CELF1 levels. Importantly, MBNL protein overexpression was previously shown to be well-tolerated in mouse models[34]. Accordingly, in our study, upregulation of MBNL proteins through *miR-23b* or *miR-218* silencing was not harmful, as mice showed no detrimental phenotype 6 weeks after the treatment. Similarly, *miR-23b* silencing in the heart of an inducible DM1 mice model caused no overt phenotype, despite producing CELF1 overexpression[59]. This data supports the safety of our therapeutic approach in DM. Although different effects of antagomiR-23b on CELF1 levels are reported in these two studies, antagomiR dose used or tissue-specific effects might explain this controversy. Given the tissue-specific expression of microRNAs, their targeting in TGM is also advantageous because it regulates genes only in the places where the regulator miRNAs are expressed, and the intensity of the upregulation will depend on the degree of repression by that microRNA.

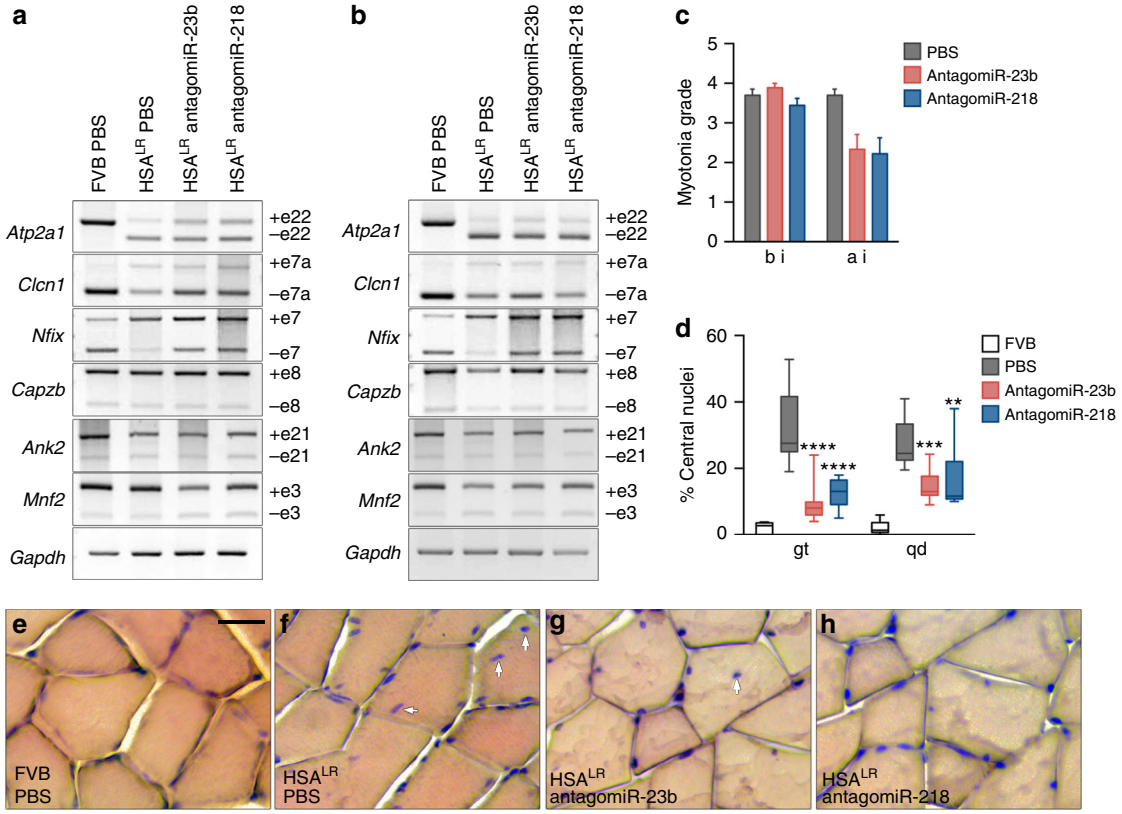

Fig. 6 Systemic delivery of antagomiRs improved missplicing of Mbnl-dependent transcripts, myotonia, and muscle histopathology in HSA^{LR} mice. **a**, **b** RT-PCR analyses of the splicing of *Atp2a1* exon 22, *Clcn1* exon 7a, *Nfix* exon 7, *Capzb* exon 8, *Ank2* exon 21, and *Mnf2* exon 3 in gastrocnemius (gt) (**a**) and quadriceps (qd) (**b**) muscles. *Gadph* values were used for normalization in the quantification of the exon inclusion in Supplementary Figs. 9 and 11. **c** Electromyographic myotonia grade in antagomiR (pink and blue bars) or PBS-treated (gray bars) HSA^{LR} mice before (bi) and 4 days after injection (ai). Data are mean ± SEM. **d** Quantification of the percentage of muscle fibers with central nuclei in gt and qd muscles of control FVB (white bar), and PBS (gray bar) or antagomiR-treated (pink and blue bars) HSA^{LR} mice. **e**–**h** Representative hematoxylin and eosin staining of gt muscles from all four groups of mice. Arrows point to examples of centrally located nuclei in muscle fibers. Scale bar = 50 μm. The data were analyzed by unpaired Student's *t* test compared to untreated HSA^{LR} mice. Data are media ± SEM. *$p < 0.05$; FVB ($n = 3$), HSA^{LR} PBS ($n = 5$), HSA^{LR} antagomiR-23b ($n = 4$) and HSA^{LR} antagomiR-218 ($n = 4$)

Several previous studies have reported that phenotypes of HSA^{LR} model mice are intrinsically variable[4,60]. This was suggested to stem from somatic instability of CUG repeats[4], but we found that the levels of expression of the HSA^{LR} transgene and the magnitude of missplicings have a strong positive correlation. Indeed, for some splice events such as *Atp2a1*, small changes in transgene expression translated into big changes in exon inclusion. We suggest that the quantification of the transgene expression is an important step in order to identify outliers.

It is well known that sequestration of MBNLs and activation of CELF1 block the developmental change from fetal to adult RNA transcripts in DM1 muscle. We demonstrate that upregulated MBNL1 and MBNL2 was sufficient to rescue several Muscleblind-dependent, but not the CELF1-dependent splice events, in DM1 myoblasts and HSA^{LR} DM1 model mice. Interestingly, a mere 2-fold increase of Mbnl2 (and a marginal increase in Mbnl1) protein in quadriceps was sufficient to strongly rescue *Nfix* missplicing. Thus, we found that a relatively small upregulation of the MBNL proteins can have a profound impact on DM1 phenotypes not only at the level of missplicing but also at histopathology (central nuclei) and functional (myotonia and muscle strength) levels. Overall our study highlights the use of oligonucleotide drugs to specifically de-repress the expression of the *MBNL1* and *MBNL2* genes as therapeutic approach for DM1.

Methods

Cell culture. HeLa cells were obtained from Dr. Francisco Palau (Sant Joan de Deu Hospital, Spain) and were grown in Dulbecco's Modified Eagle's Medium (DMEM) with 1 g L^{-1} glucose, 1% penicillin and streptomycin (P/S), and 10% fetal bovine serum (FBS; Sigma). Unaffected (control) and patient-derived cells (DM1 cells carrying 1300 CTG repeats quantified in the blood cells)[61] were kindly provided by Dr. Furling (Institute of Myology, Paris). Fibroblast cells were grown in DMEM with 4.5 g L^{-1} glucose, 1% P/S, and 10% FBS (Sigma). To transdifferentiate fibroblasts into myoblasts by inducing MyoD expression, the cells were plated in muscle differentiation medium (MDM) containing DMEM with 4.5 g L^{-1} glucose, 1% P/S, 2% horse serum, 1% apo-transferrin (10 mg ml^{-1}), 0.1% insulin (10 mg ml^{-1}), and 0.02% doxycycline (10 mg ml^{-1}). In all cases, the cells were grown at 37 °C in a humidified atmosphere containing 5% CO_2.

MicroRNA profiling. To search for miRNAs that regulate *MBNL1* and *MBNL2* in HeLa cells, the SureFIND Cancer miRNA Transcriptome PCR Array (Qiagen) was used according to the manufacturer's instructions. Briefly, a multiplex quantitative real-time PCR (qRT-PCR) assay was set up using the QuantiFast Probe PCR Kit reagent with TaqMan probes gene expression assays for human *MBNL1* and *MBNL2* (FAM-labeled probe) and *GAPDH* (MAX-labeled probe; Qiagen). qRT-PCR was performed using a StepOnePlus real-time thermal cycler and the results were analyzed using Excel-based data-analysis software provided with the SureFIND miRNA Transcriptome PCR Array. *MBNL1* and *MBNL2* gene expression was normalized to GAPDH.

Computational prediction of miRNA targets in MBNL1/2 3′ UTRs. Information about the predicted miRNA binding to *MBNL1* and *MBNL2* was obtained from miRecords[62] and miRDIP[63] databases. These databases integrate nine different programs (microT, MiRanda, MirTar2_V4.0, Mir Target2, Pic Tar, PITA, RNA hybrid, RNA 22, and TargetScan) that predict miRNA targets. A miRNA was considered as a candidate regulator if it was predicted by at least eight of these prediction algorithms. TargetScan (release 6.2) and MiRanda (release August 2010) were used to design the 3′UTR reporter assay, which allows analysis of the miRNA–mRNA binding sites.

AntagomiRs. Cy3-labeled and non-labeled oligonucleotides were synthesized by Creative Biogene. The antagomiR sequences were as follows:

5′-mG*mG*mUmAmAmUmCmCmCmUmGmGmCmAmAmUmGmU*mG*mA*mU*-3′-chol (antagomiR-23b)

5′-mA*mC*mAmUmGmGmUmAmGmAmUmCmAmAmGmCmA*mC*mA*mA*-3′-chol (antagomiR-218)

5′-mC*mA*mGmUmAmCmUmUmUmUmGmGmUmGmUmA*mC*mA*mA*-3′-chol (scramble control, SC)

where m denotes 2′-*O*-methyl-modified phosphoramidites, * denotes phosphorothioate linkages, and chol denotes cholesterol groups. Cy3-labeled oligonucleotides were used to visualize the distribution of the compound in cells and mouse tissues.

Cell transfection. HeLa cells and human myoblasts were transfected using X-tremeGENE™ HP (Roche) according to the manufacturer's protocols. For the miRNA overexpression assay, HeLa cells were seeded in 6-well plates at approximately 80% confluence and transfected with 1 µg of miRNA precursor sequences cloned into the *pCMV-MIR-GFP* vector (OriGene). At 48 h post-transfection, the cells were harvested for the qRT-PCR and western blot analyses. For the reporter assays, the cells were seeded in 24-well plates at approximately 80% confluence and transfected with MBNL1 and MBNL2 3′UTR luciferase constructs cloned into a *pEZX-MT05-Gluc* vector (GeneCopoeia). For each transfection, 500 ng of the appropriate reporter construct and 500 ng of the appropriate miRNA plasmids

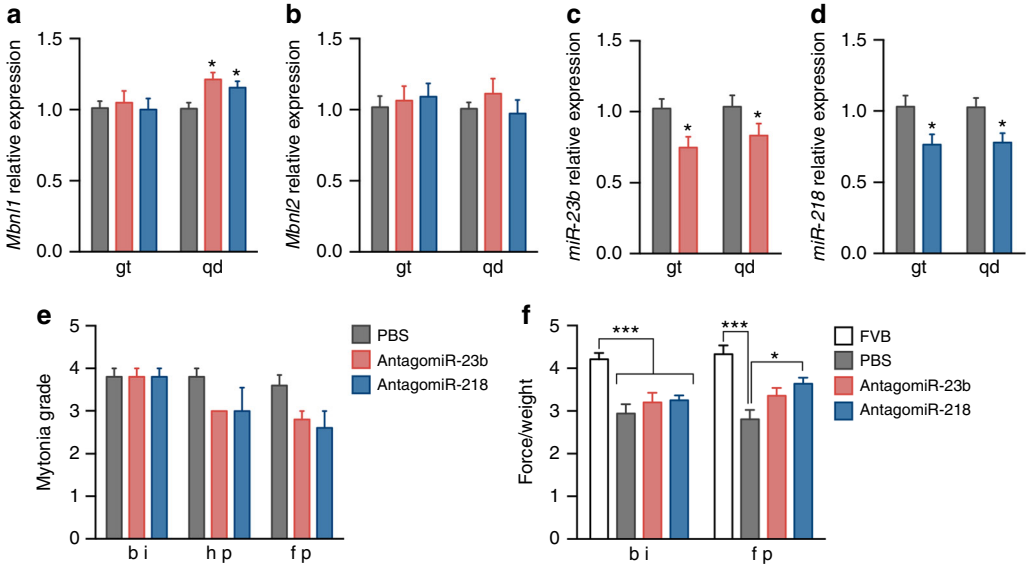

Fig. 7 Muscle function is improved in HSA^{LR} mice 6 weeks after injection of antagomiRs. **a**, **b** qRT-PCR quantification of *Mbnl1* and *Mbnl2* transcript levels in gt and qd muscles of untreated mice (PBS, gray bars) or treated with antagomiR-23b (pink bars) or antagomiR-218 (blue bars). **c**, **d** Real-time PCR quantification of *miR-23b* and *miR-218*. **e** Electromyographic myotonia grade in antagomiR (pink and blue bars) or PBS-treated (gray bars) HSA^{LR} mice before (bi), in the halfway-point (hp) and 6 weeks after injection (final point, fp). **f** Forelimb grip strength of mice treated with antagomiRs measured before injection (bi) and 6 weeks after injection (fp). The grip force was normalized with the body weight of each mouse. The data were analyzed by unpaired Student's *t* test compared to HSA^{LR} mice treated with the vehicle PBS. Data are mean ± SEM. *$p < 0.05$, ***$p < 0.001$; FVB ($n = 5$), HSA^{LR} PBS ($n = 6$), HSA^{LR} antagomiR-23b ($n = 5$) and HSA^{LR} antagomiR-218 ($n = 5$)

(OriGene) were used. In the case of *miR-23b*, *miR-96*, and *miR-218*, three types of constructs were tested, wild-type (WT), perfect match (PM), and constructs with a deletion in the seed region (MUT) predicted to disrupt binding. Both PM and MUT were provided by GeneCopoeia (see Supplementary Data 1). The supernatant was collected 48 h after transfection and the reporter activity was assayed.

Control fibroblasts were seeded into 96-well plates (1×10^5 cells per well), transfected with different antagomiR concentrations (from 1 nM to 1 µM) and transdifferentiated into myoblasts for 96 h in MDM medium; to analyze the toxicity. As a control to test the transfection levels, the Cy3-antagomiR was transfected in separate experiments under the same conditions. For the RT-PCR, qRT-PCR, and Western blot assays, control and DM1 fibroblasts were plated into petri dishes (1×10^6 cells per well), transfected with the appropriate antagomiR, and then differentiated for 48 or 96 h. Additionally, for the RT-PCR, control fibroblasts were plated into petri dishes (1×10^6 cells per well), transfected with the scrambled control antagomiR, and then differentiated for 48 or 96 h. Finally, for the immunofluorescence and foci assay, fibroblasts were seeded into 24-well plates (3×10^5 cells per well), transfected with the relevant antagomiRs, and transdifferentiated into myoblasts for 96 h.

Transgenic mice and antagomiR administration. Mouse handling and experimental procedures conformed to the European law regarding laboratory animal care and experimentation (2003/65/CE) and were approved by Conselleria de Agricultura, Generalitat Valenciana (Uso de bloqueadores de miRNAS como terapia potencial en distrofia miotónica, reference number 2016/VSC/PEA/00155). Homozygous transgenic HSA^{LR} (line 20 b) mice[31] were provided by Prof. C. Thornton (University of Rochester Medical Center, Rochester, NY, USA) and mice with the corresponding genetic background (FVB) were used as controls. Age-matched HSA^{LR} (<5 months old) male mice received three subcutaneous injections of 100 µl of 1× PBS (vehicle) ($n = 10$) or antagomiR (antagomiR-23b $n = 9$, antagomiR-218 $n = 9$, and antagomiR-SC $n = 5$) delivered to the interscapular area every 12 h. The overall quantity of antagomiR finally administered divided among the three injections was 12.5 mg kg^{-1}. For the long-term treatment, the same injection procedure was used in mice of 3.5 months in age (PBS, antagomiR-23b, antagomiR-218 and antagomiR-SC $n = 5$). Four days and 6 weeks after the first injection, the mice were sacrificed and the tissues of interest were harvested and divided into two samples each. One part was frozen in liquid nitrogen for the molecular analyses, and the other was fixed in 4% paraformaldehyde (PFA) and cryoprotected in 30% sucrose before histological processing. Cy3-labeled antagomiRs were administered in a single subcutaneous injection of 10 mg kg^{-1}.

RNA extraction, RT-PCR, and qRT-PCR. Total RNA from HeLa cells, human myoblasts, and murine muscle tissues was isolated using the miRNeasy Mini Kit (Qiagen; Valencia, CA) according to the manufacturer's instructions. One microgram of RNA was digested with DNase I (Invitrogen) and reverse-transcribed with SuperScript II (Invitrogen) using random hexanucleotides; 20 ng of cDNA was used in a standard PCR reaction with GoTaq polymerase (Promega). Specific primers were used to analyze the alternative splicing of *BIN1*, *ATP2A1*, *INR*, *PKM*, *cTNT*, *CAPZB*, and *DLG1* in control and DM1 human myoblasts, and *Atp2a1*, *Clcn1*, *Nfix*, *Capzb*[54], *Ank2, and Mfn2* in mouse samples (quadriceps and gastrocnemius). *GAPDH* and *Gapdh* were used as endogenous controls using 0.2 ng of cDNA. In the case of *PKM*, PCR products were digested with *Pst*I (Thermo Scientific™). PCR products were separated on a 2% agarose gel and quantified using ImageJ software (NIH). The primer sequences and exons analyzed are provided in Supplementary Table 2.

We used 1 ng of HeLa, human myoblast, or mouse tissue cDNA as a template for multiplex qRT-PCR using the QuantiFast Probe PCR Kit reagent. Commercial TaqMan probes (Qiagen) were used to detect human (*MBNL1* and *MBNL2*) or mouse (*Mbnl1* and *Mbnl2*; FAM-labeled probes) and reference (*GAPDH*; MAX-labeled probe) genes. Results from myoblasts were normalized to *GAPDH* and *ACTB* (TAMRA-labeled probe; Integrated DNA Technologies) whereas the mouse results were normalized to *Gapdh* only. HSA transgene expression levels were determined by qRT-PCR as described previously[64].

miRNA expression in human DM1 myoblasts, muscle biopsies, and murine tissues (muscle, heart, and central nervous system) was quantified using specific miRCURY™-locked nucleic acid microRNA PCR primers (Exiqon) according to the manufacturer's instructions. Relative gene expression was normalized to *U1* or *U6* snRNA.

Expression levels were measured using an Applied Biosystems StepOnePlus Real Time PCR System. Expression relative to the endogenous gene and control group was calculated using the $2^{-\Delta\Delta Ct}$ method. Pairs of samples were compared using two-tailed *t* tests ($\alpha = 0.05$), applying Welch's correction when necessary. The statistical differences were estimated by the Student's *t* tests ($p < 0.05$) on normalized data. Uncropped agarose gels are shown in Supplementary Figures 13 and 16.

Western blotting. For total protein extraction, HeLa and human myoblast cells were sonicated while mouse muscles (gastrocnemius and quadriceps) were homogenized in RIPA buffer (150 mM NaCl, 1.0% IGEPAL, 0.5% sodium deoxycholate, 0.1% SDS, 50 mM Tris–HCl, pH 8.0) supplemented with protease and phosphatase inhibitor cocktails (Roche Applied Science). Total proteins were quantified with a BCA protein assay kit (Pierce) using bovine serum albumin as a standard concentration range. For the immunodetection assay, 20 µg of samples were denatured for 5 min at 100 °C, electrophoresed on 12% SDS-PAGE gels, transferred onto 0.45 µm nitrocellulose membranes (GE Healthcare), and blocked with 5% non-fat dried milk in PBS-T (8 mM Na_2HPO_4, 150 mM NaCl, 2 mM KH_2PO_4, 3 mM KCl, 0.05% Tween 20, pH 7.4).

For HeLa cells, human myoblast, and murine samples, membranes were incubated overnight at 4 °C either with primary mouse anti-MBNL1 (1:1000, ab77017, Abcam) or mouse anti-CUG-BP1 (1:200, clone 3B1, Santa Cruz) antibodies. To detect MBNL2, mouse anti-MBNL2 (1:100, clone MB2a, Developmental Studies Hybridoma Bank) was used for human myoblast and mouse samples while rabbit anti-MBNL2 (1:1000, ab105331, Abcam) antibody was used for HeLa cells. All primary antibodies were detected using horseradish peroxidase (HRP)-conjugated anti-mouse-IgG secondary antibody (1 h, 1:5000, Sigma-Aldrich), except for the MBNL2 antibody in HeLa cell samples, which required a HRP-conjugated anti-rabbit-IgG secondary antibody (1 h, 1:5000, Sigma-Aldrich).

Loading controls were the anti-β-ACTIN antibody (1 h, 1:5000, clone AC-15, Sigma-Aldrich) for cell samples and anti-Gapdh (1 h, 1:5000, clone G-9, Santa Cruz) for mouse samples, followed by HRP-conjugated anti-mouse-IgG secondary antibody (1 h, 1:5000, Sigma-Aldrich). Immunoreactive bands were detected using an enhanced chemiluminescence Western Blotting Substrate (Pierce) and images were acquired with an ImageQuant LAS 4000 (GE Healthcare). Quantification was performed using ImageJ software (NIH), and statistical differences were estimated using Student's *t* test ($p < 0.05$) on normalized data. Uncropped westerns are shown in Supplementary Figures 13, 14, and 15.

Luciferase reporter assay. The activity of Gaussian luciferase (GLuc) and alkaline phosphatase (SEAP) were measured by quantifying the luminescence present in conditioned medium using the secreted-pair dual luminescence kit (GeneCopoeia) according to the manufacturer's protocols. Gaussian luciferase activity was normalized to alkaline phosphatase activity (GLuc/SEAP). The values of the luciferase activity were determined using a Tecan Infinite M200 PRO plate reader (Life Sciences). Statistical differences in the data were estimated using Student's *t* test ($p < 0.05$) on normalized data.

Cell proliferation assay. Cells were seeded at 10^5 cells per ml in 96-well plates and transfected with antagomiRs, as previously explained; 96 h post-transfection, cell proliferation was measured using the CellTiter 96® AQueous Non-Radioactive Cell Proliferation Assay (Promega) following the manufacturer's instructions. The TC_{10} and dose–response inhibition curves were calculated using non-linear least squares regression, and absorbance levels were determined using a Tecan Infinite M200 PRO plate reader (Life Sciences).

Immunofluorescence methods. For MBNL1 and MBNL2, myoblasts were fixed with 4% PFA for 15 min at room temperature (RT) followed by several washes in 1× PBS. Cells were then permeabilized with PBS-T (0.3% Triton-X in PBS) and blocked (PBS-T, 0.5% BSA, 1% donkey serum) for 30 min at RT, and incubated either with primary antibody mouse anti-MBNL1 (1:200, ab77017, Abcam) or rabbit anti-MBNL2 (1:200, ab105331, Abcam) at 4 °C overnight. After several PBS-T washes, the cells were incubated for 1 h with a biotin-conjugated secondary antibody, and anti-mouse-IgG (1:200, Sigma-Aldrich) to detect anti-MBNL1 or anti-rabbit-IgG (1:200, Sigma-Aldrich) to detect anti-MBNL2. The fluorescence signal was amplified with an Elite ABC kit (VECTASTAIN) for 30 min at RT, followed by PBS-T washes and incubation with either streptavidin-FITC (1:200, Vector) to detect anti-MBNL1 or streptavidin-Texas Red (1:200, Vector) to detect anti-MBNL2, for 45 min at RT. After several washes with PBS, the cells were mounted with VECTASHIELD® mounting medium containing DAPI (Vector) to detect the nuclei.

The Cy3 moiety was synthetically attached to the 5′ end of the oligonucleotide to visualize the distribution of the compound. Frozen sections (10 µm) of mouse tissues including heart, brain, gastrocnemius, and quadriceps were immunostained using anti-Cy3 antibody (1:50, Santa Cruz) followed by a secondary goat biotin-conjugated anti-mouse-IgG (1:200, Sigma-Aldrich). Cy3-labeled antagomiRs were directly detectable under a fluorescence microscope in myoblast cells. In all cases, the nuclei were stained with DAPI. Images of myoblast cells were taken on an Olympus FluoView FV100 confocal microscope and images of human myoblast and mouse tissues containing Cy3-antagomiR were obtained using a Leica DM4000 B LED fluorescence microscope. In all cases, the images were taken at a 40× magnification and processed with Adobe Photoshop software (Adobe System Inc.).

Fluorescent in situ hybridization. Fibroblasts were aliquoted into 8-well Cell Culture Slide (3×10^5 cells per well) and transfected with the antagomiRs. In situ detection was performed as previously described[65]. Images were taken and analyzed using an IN Cell Analyzer 2200 Imaging System (GE Healthcare).

Electromyography studies. Electromyography was performed before the treatment, at the halfway point and at the time of sacrifice under general anesthesia, as

previously described[32]. Briefly, five needle insertions were performed in each quadriceps muscle of both hind limbs, and myotonic discharges were graded on a five-point scale: 0, no myotonia; 1, occasional myotonic discharge in ≤50% of the needle insertions; 2, myotonic discharge in >50% of the insertions; 3, myotonic discharge in nearly all of the insertions; and 4, myotonic discharge in all insertions.

Muscle histology. Frozen 15 µm-sections of mouse gastrocnemius and quadriceps muscles were stained with haematoxylin eosin (H&E) and mounted with VECTASHIELD® mounting medium (Vector) according to standard procedures. Images were taken at a 100× magnification with a Leica DM2500 microscope. The percentage of fibers containing central nuclei was quantified in a total of 500 fibers in each mouse.

Forelimb grip strength test. The forelimb grip strength was measured with a Grip Strength Meter (BIO-GS3; Bioseb, USA). The peak pull force (measured in grams) was recorded on a digital force transducer when the mouse grasped the bar. The gauge of force transducer was reset to 0 g after each measurement. Tension was recorded by the gauge at the time the mouse released its forepaws from the bar. We performed three consecutive measurements at 30 s intervals. The bodyweight measurement was performed in parallel. The final value is obtained by dividing the average value of the grip force with the body weight of each mouse.

Data availability. All relevant data are available within the manuscript and its supplementary information or from the authors upon reasonable request. Please contact Rubén Artero (Ruben.artero@uv.es) for any inquire.

Received: 30 August 2017 Accepted: 30 May 2018
Published online: 26 June 2018

References

1. Foff, E. P. & Mahadevan, M. S. Therapeutics development in myotonic dystrophy type 1. *Muscle Nerve* **44**, 160–169 (2011).
2. Ebralidze, A., Wang, Y., Petkova, V., Ebralidse, K. & Junghans, R. P. RNA leaching of transcription factors disrupts transcription in myotonic dystrophy. *Science* **303**, 383–387 (2004).
3. Huichalaf, C. et al. Expansion of CUG RNA repeats causes stress and inhibition of translation in myotonic dystrophy 1 (DM1) cells. *FASEB J.* **24**, 3706–3719 (2010).
4. Jones, K. et al. GSK3beta mediates muscle pathology in myotonic dystrophy. *J. Clin. Invest.* **122**, 4461–4472 (2012).
5. Timchenko, L. Molecular mechanisms of muscle atrophy in myotonic dystrophies. *Int. J. Biochem. Cell Biol.* **45**, 2280–2287 (2013).
6. Kim, Y. K., Mandal, M., Yadava, R. S., Paillard, L. & Mahadevan, M. S. Evaluating the effects of CELF1 deficiency in a mouse model of RNA toxicity. *Hum. Mol. Genet.* **23**, 293–302 (2014).
7. Rau, F. et al. Misregulation of miR-1 processing is associated with heart defects in myotonic dystrophy. *Nat. Struct. Mol. Biol.* **18**, 840–845 (2011).
8. Krol, J. et al. Ribonuclease dicer cleaves triplet repeat hairpins into shorter repeats that silence specific targets. *Mol. Cell* **25**, 575–586 (2007).
9. Fernandez-Costa, J. M. et al. Expanded CTG repeats trigger miRNA alterations in *Drosophila* that are conserved in myotonic dystrophy type 1 patients. *Hum. Mol. Genet.* **22**, 704–716 (2013).
10. Kalsotra, A. et al. The Mef2 transcription network is disrupted in myotonic dystrophy heart tissue, dramatically altering miRNA and mRNA expression. *Cell Rep.* **6**, 336–345 (2014).
11. Du, H. et al. Aberrant alternative splicing and extracellular matrix gene expression in mouse models of myotonic dystrophy. *Nat. Struct. Mol. Biol.* **17**, 187–193 (2010).
12. Batra, R. et al. Loss of MBNL leads to disruption of developmentally regulated alternative polyadenylation in RNA-mediated disease. *Mol. Cell* **56**, 311–322 (2014).
13. Goodwin, M. et al. MBNL sequestration by toxic RNAs and RNA misprocessing in the myotonic dystrophy brain. *Cell Rep.* **12**, 1159–1168 (2015).
14. Lin, X. et al. Failure of MBNL1-dependent post-natal splicing transitions in myotonic dystrophy. *Hum. Mol. Genet.* **15**, 2087–2097 (2006).
15. Charizanis, K. et al. Muscleblind-like 2-mediated alternative splicing in the developing brain and dysregulation in myotonic dystrophy. *Neuron* **75**, 437–450 (2012).
16. Poulos, M. G. et al. Progressive impairment of muscle regeneration in muscleblind-like 3 isoform knockout mice. *Hum. Mol. Genet.* **22**, 3547–3558 (2013).
17. Choi, J. et al. Muscleblind-like 3 deficit results in a spectrum of age-associated pathologies observed in myotonic dystrophy. *Sci. Rep.* **6**, 30999 (2016).
18. Thornton, C. A., Wang, E. & Carrell, E. M. Myotonic dystrophy: approach to therapy. *Curr. Opin. Genet. Dev.* **44**, 135–140 (2017).
19. Konieczny, P. et al. Myotonic dystrophy: candidate small molecule therapeutics. *Drug Discov. Today* **22**, 1740–1748 (2017).
20. Garcia-Lopez, A., Llamusi, B., Orzaez, M., Perez-Paya, E. & Artero, R. D. In vivo discovery of a peptide that prevents CUG-RNA hairpin formation and reverses RNA toxicity in myotonic dystrophy models. *Proc. Natl. Acad. Sci. USA* **108**, 11866–11871 (2011).
21. Ketley, A. et al. High-content screening identifies small molecules that remove nuclear foci, affect MBNL distribution and CELF1 protein levels via a PKC-independent pathway in myotonic dystrophy cell lines. *Hum. Mol. Genet.* **23**, 1551–1562 (2014).
22. Hoskins, J. W. et al. Lomofungin and dilomofungin: inhibitors of MBNL1-CUG RNA binding with distinct cellular effects. *Nucleic Acids Res.* **42**, 6591–6602 (2014).
23. Warf, M. B., Nakamori, M., Matthys, C. M., Thornton, C. A. & Berglund, J. A. Pentamidine reverses the splicing defects associated with myotonic dystrophy. *Proc. Natl. Acad. Sci. USA* **106**, 18551–18556 (2009).
24. Coonrod, L. A. et al. Reducing levels of toxic RNA with small molecules. *ACS Chem. Biol.* **8**, 2528–2537 (2013).
25. Siboni, R. B. et al. Actinomycin D specifically reduces expanded CUG repeat RNA in myotonic dystrophy models. *Cell Rep.* **13**, 2386–2394 (2015).
26. Pandey, S. K. et al. Identification and characterization of modified antisense oligonucleotides targeting DMPK in mice and nonhuman primates for the treatment of myotonic dystrophy type 1. *J. Pharmacol. Exp. Ther.* **355**, 329–340 (2015).
27. Gao, Z. & Cooper, T. A. Antisense oligonucleotides: rising stars in eliminating RNA toxicity in myotonic dystrophy. *Hum. Gene Ther.* **24**, 499–507 (2013).
28. Mulders, S. A. et al. Triplet-repeat oligonucleotide-mediated reversal of RNA toxicity in myotonic dystrophy. *Proc. Natl. Acad. Sci. USA* **106**, 13915–13920 (2009).
29. Wheeler, T. M. et al. Targeting nuclear RNA for in vivo correction of myotonic dystrophy. *Nature* **488**, 111–115 (2012).
30. Madsen, A. Ionis reports setback on DMPKRx program for myotonic dystrophy. *MDA* https://strongly.mda.org/ionis-reports-setback-dmpkrx-program-myotonic-dystrophy/ (2017).
31. Mankodi, A. et al. Myotonic dystrophy in transgenic mice expressing an expanded CUG repeat. *Science* **289**, 1769–1773 (2000).
32. Kanadia, R. N. et al. Reversal of RNA missplicing and myotonia after muscleblind overexpression in a mouse poly(CUG) model for myotonic dystrophy. *Proc. Natl. Acad. Sci. USA* **103**, 11748–11753 (2006).
33. Lee, K. Y. et al. Compound loss of muscleblind-like function in myotonic dystrophy. *EMBO Mol. Med.* **5**, 1887–1900 (2013).
34. Chamberlain, C. M. & Ranum, L. P. Mouse model of muscleblind-like 1 overexpression: skeletal muscle effects and therapeutic promise. *Hum. Mol. Genet.* **21**, 4645–4654 (2012).
35. de Haro, M. et al. MBNL1 and CUGBP1 modify expanded CUG-induced toxicity in a *Drosophila* model of myotonic dystrophy type 1. *Hum. Mol. Genet.* **15**, 2138–2145 (2006).
36. Garcia-Lopez, A. et al. Genetic and chemical modifiers of a CUG toxicity model in *Drosophila*. *PLoS ONE* **3**, e1595 (2008).
37. Bargiela, A. et al. Increased autophagy and apoptosis contribute to muscle atrophy in a myotonic dystrophy type 1 *Drosophila* model. *Dis. Model Mech.* **8**, 679–690 (2015).
38. Cerro-Herreros, E., Fernandez-Costa, J. M., Sabater-Arcis, M., Llamusi, B. & Artero, R. Derepressing muscleblind expression by miRNA sponges ameliorates myotonic dystrophy-like phenotypes in *Drosophila*. *Sci. Rep.* **6**, 36230 (2016).
39. Bartel, D. P. MicroRNAs: target recognition and regulatory functions. *Cell* **136**, 215–233 (2009).
40. Betel, D., Koppal, A., Agius, P., Sander, C. & Leslie, C. Comprehensive modeling of microRNA targets predicts functional non-conserved and non-canonical sites. *Genome Biol.* **11**, R90 (2010).
41. Garcia, D. M. et al. Weak seed-pairing stability and high target-site abundance decrease the proficiency of lsy-6 and other microRNAs. *Nat. Struct. Mol. Biol.* **18**, 1139–1146 (2011).
42. Krutzfeldt, J. et al. Specificity, duplex degradation and subcellular localization of antagomirs. *Nucleic Acids Res.* **35**, 2885–2892 (2007).
43. Krutzfeldt, J. et al. Silencing of microRNAs in vivo with 'antagomirs'. *Nature* **438**, 685–689 (2005).
44. Fugier, C. et al. Misregulated alternative splicing of BIN1 is associated with T tubule alterations and muscle weakness in myotonic dystrophy. *Nat. Med.* **17**, 720–725 (2011).
45. Santoro, M. et al. Alternative splicing alterations of Ca2+ handling genes are associated with Ca2+ signal dysregulation in myotonic dystrophy type 1 (DM1) and type 2 (DM2) myotubes. *Neuropathol. Appl. Neurobiol.* **40**, 464–476 (2014).

46. Santoro, M. et al. Molecular, clinical, and muscle studies in myotonic dystrophy type 1 (DM1) associated with novel variant CCG expansions. *J. Neurol.* **260**, 1245–1257 (2013).
47. Savkur, R. S., Philips, A. V. & Cooper, T. A. Aberrant regulation of insulin receptor alternative splicing is associated with insulin resistance in myotonic dystrophy. *Nat. Genet.* **29**, 40–47 (2001).
48. Gao, Z. & Cooper, T. A. Reexpression of pyruvate kinase M2 in type 1 myofibers correlates with altered glucose metabolism in myotonic dystrophy. *Proc. Natl. Acad. Sci. USA* **110**, 13570–13575 (2013).
49. Koshelev, M., Sarma, S., Price, R. E., Wehrens, X. H. & Cooper, T. A. Heart-specific overexpression of CUGBP1 reproduces functional and molecular abnormalities of myotonic dystrophy type 1. *Hum. Mol. Genet.* **19**, 1066–1075 (2010).
50. Kalsotra, A. et al. A postnatal switch of CELF and MBNL proteins reprograms alternative splicing in the developing heart. *Proc. Natl. Acad. Sci. USA* **105**, 20333–20338 (2008).
51. Nakamori, M. et al. Splicing biomarkers of disease severity in myotonic dystrophy. *Ann. Neurol.* **74**, 862–872 (2013).
52. Liu, C. et al. The microRNA miR-34a inhibits prostate cancer stem cells and metastasis by directly repressing CD44. *Nat. Med.* **17**, 211–215 (2011).
53. Guiraud, S. et al. Second-generation compound for the modulation of utrophin in the therapy of DMD. *Hum. Mol. Genet.* **24**, 4212–4224 (2015).
54. Chen, G. et al. Phenylbutazone induces expression of MBNL1 and suppresses formation of MBNL1-CUG RNA foci in a mouse model of myotonic dystrophy. *Sci. Rep.* **6**, 25317 (2016).
55. Schober, A. et al. MicroRNA-126-5p promotes endothelial proliferation and limits atherosclerosis by suppressing Dlk1. *Nat. Med.* **20**, 368–376 (2014).
56. Ottosen, S. et al. In vitro antiviral activity and preclinical and clinical resistance profile of miravirsen, a novel anti-hepatitis C virus therapeutic targeting the human factor miR-122. *Antimicrob. Agents Chemother.* **59**, 599–608 (2015).
57. van Solingen, C. et al. Antagomir-mediated silencing of endothelial cell specific microRNA-126 impairs ischemia-induced angiogenesis. *J. Cell. Mol. Med.* **13**, 1577–1585 (2009).
58. Dey, B. K., Gagan, J., Yan, Z. & Dutta, A. miR-26a is required for skeletal muscle differentiation and regeneration in mice. *Genes Dev.* **26**, 2180–2191 (2012).
59. Kalsotra, A., Wang, K., Li, P. F. & Cooper, T. A. MicroRNAs coordinate an alternative splicing network during mouse postnatal heart development. *Genes Dev.* **24**, 653–658 (2010).
60. Brockhoff, M. et al. Targeting deregulated AMPK/mTORC1 pathways improves muscle function in myotonic dystrophy type I. *J. Clin. Invest.* **127**, 549–563 (2017).
61. Arandel, L. et al. Immortalized human myotonic dystrophy muscle cell lines to assess therapeutic compounds. *Dis. Model Mech.* **10**, 487–497 (2017).
62. Xiao, F. et al. miRecords: an integrated resource for microRNA-target interactions. *Nucleic Acids Res.* **37**, D105–D110 (2009).
63. Shirdel, E. A., Xie, W., Mak, T. W. & Jurisica, I. NAViGaTing the micronome—using multiple microRNA prediction databases to identify signalling pathway-associated microRNAs. *PLoS ONE* **6**, e17429 (2011).
64. Wheeler, T. M. et al. Reversal of RNA dominance by displacement of protein sequestered on triplet repeat RNA. *Science* **325**, 336–339 (2009).
65. Gonzalez, A. L. et al. In silico discovery of substituted pyrido[2,3-d] pyrimidines and pentamidine-like compounds with biological activity in myotonic dystrophy models. *PLoS ONE* **12**, e0178931 (2017).
66. Li, S. S. et al. Target identification of microRNAs expressed highly in human embryonic stem cells. *J. Cell. Biochem.* **106**, 1020–1030 (2009).

Acknowledgments

This work was funded by a grant from the Ministerio de Economía y Competitividad (SAF2015-64500-R, including funds from the European Regional Development Fund) to R.A. E.C.H. was supported by a predoctoral fellowship (BES-2013-064522) from the Ministerio de Economia y Competitividad. J.M.F.C. was supported by a postdoctoral fellowship (APOSTD/2017/088) from the Conselleria d' Educació, Investigació, Cultura i Esport (Generalitat Valenciana). Authors also thank Andres Rey Mellado for his technical help and Inmaculada Noguera, veterinary head of the animal facilities at the University of Valencia who performed the mouse necropsies.

Author contributions

R.A. provided the conceptual framework for the study. All the authors conceived and designed the experiments. E.C.H., M.S.A., N.M., J.M.F.C., and B.L.L. performed the experiments and analyzed data. E.C.H., J.M.F.C., and B.L.L. prepared the manuscript with input from M.P-A. and R.A.

Additional information

Supplementary Information accompanies this paper at https://doi.org/10.1038/s41467-018-04892-4.

Competing interests: The method described in this paper is the subject of a patent application (inventors: E.C.H., J.M.F.C., B.L.L., R.A.). The remaining authors declare no competing interests.

Reprints and permission information is available online at http://npg.nature.com/reprintsandpermissions/

Publisher's note: Springer Nature remains neutral with regard to jurisdictional claims in published maps and institutional affiliations.

-Resultados principales-

La presente tesis incluye el resumen de los resultados principales de tres articulos de los que soy primera autora y que comprenden los objetivos propuestos para la misma:

-Artículo 1- **Estefanía Cerro-Herreros**, Mouli Chakraborty, Manuel Pérez-Alonso, Rubén Artero, Beatriz Llamusí. 2017. " Expanded CCUG repeat RNA expression in *Drosophila* heart and muscle trigger Myotonic Dystrophy type 1-like phenotypes and activate autophagocytosis genes". Scientific Reports. 6;7(1):2843. doi: 10.1038/s41598-017-02829-3.

-Artículo 2- **Estefanía Cerro-Herreros**, Juan Manuel Fernández-Costa, María Sabater-Arcís, Beatriz Llamusí, Rubén Artero. 2016. "Derepressing muscleblind expression by miRNA sponges ameliorates myotonic dystrophy-like phenotypes in *Drosophila*. Scientific Reports. 2;6:36230. doi: 10.1038/srep36230.

-Artículo 3- **Estefania Cerro-Herreros**, Maria Sabater-Arcís, Juan Manuel Fernández-Costa, Nerea Moreno, Manuel Pérez-Alonso, Beatriz Llamusí, Rubén Artero. 2018. "*miR-23b* and *miR-218* silencing increase Muscleblind-like expression and alleviate myotonic dystrophy phenotypes in mammalian models" Nature Communications (en presa).

1. Caracterización funcional y molecular de un modelo muscular en *Drosophila* de Distrofia miotónica tipo 2.

Esta sección incluye el trabajo publicado en Cerro-Herreros et al. 2017. Este trabajo describe en detalle el efecto de la expresión de las expansiones CUG y CCUG en el músculo y corazón de *Drosophila*. En concreto, dentro de este artículo el trabajo relacionado con la presente tesis, se ha centrado en la caracterización de fenotipos musculares, mientras que la caracterización cardíaca forma parte de la tesis doctoral de Mouli Chakraborty, co-autora de dicho artículo.

Para estudiar las diferencias y las similitudes en la patogénesis de DM1 y DM2, se generaron moscas UAS-CTG y UAS-CCTG que portaban los transgenes con repeticiones expandidas CTG ([250]x) o CCTG ([1100]x) puras, respectivamente, y se las comparó con moscas control que contenían 20 repeticiones (C(C)TG ([20]x) o el reportero GFP. Estas expansiones se encuentran dentro del rango patológico de repeticiones e imitan el tamaño de expansión al menos 4 veces mayor en pacientes con DM2 en comparación con DM1 (Warf et al. 2007, Schoser et al. 2010). Tanto el reportero GFP, como dichas repeticiones CUG y CCUG fueron sobreexpresadas en el músculo, gracias al sistema de expresión UAS/Gal4 (Figura R-1). Para ello se cruzaron moscas que expresan el factor de transcripción de levaduras Gal4 con un patrón muscular (myosin heavy chain; Mhc-Gal4), por moscas que portan las secuencias de interés bajo el control de secuencias UAS, las cuales son reconocidas por Gal4 para activar su transcripción.

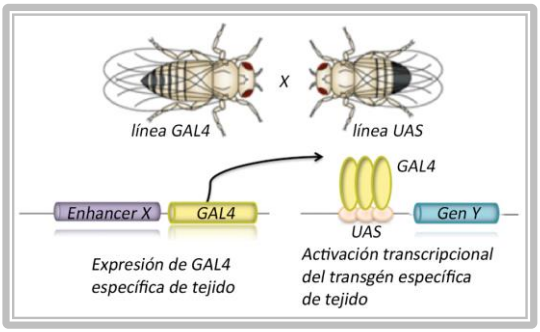

Figura R-1. Funcionamiento del sistema de expresión dirigida GAL4/UAS. La línea GAL4 expresa el factor de transcripcion de levadura GAL con el patrón de expresión determinado por "Enhancer X". Al cruzarla por la línea UAS la proteína GAL se unirá a la secuencia UAS y solo en ese momento se expresará el "Gen Y" con el mismo patrón de expresión que el enhancer.

Para la caracterización de los fenotipos DM2, las moscas F1 resultantes del cruce anterior se analizaron a distintos niveles.

1.1. La expresión de expansiones de repeticiones CCUG en el músculo de la mosca provoca el secuestro de Muscleblind en foci, afectando al *splicing* alternativo y al proceso autofágico

Un primer ensayo doble que combinaba análisis de hibridación fluorescente in situ (FISH) e inmunodetección en secciones de músculos indirectos del vuelo de *Drosophila*, reveló que los transcritos que contenían las expansiones patológicas CUG y CCUG eran retenidos en el núcleo celular en forma de *foci* ribonucleares, secuestrando a la proteína Muscleblind de unión al RNA. Por el contrario, el mismo ensayo en moscas que expresaban las versiones cortas de las repeticiones CUG o CCUG, desveló ausencia de foci ribonucleares y una localización en bandas sarcoméricas de la proteína Muscleblind típica de moscas adultas control.

El secuestro de Mbl en foci ribonucleares desencadena alteraciones en el metabolismo del RNA y particularmente en el control del *splicing* alternativo de un subconjunto de transcritos musculares en moscas *Mhc-Gal4>UAS-i(CTG)480* modelo de DM1 (Cerro-Herreros et al. 2016). A partir de homogeneizados de músculo de mosca que expresaban las repeticiones y la proteína GFP, se analizó mediante RT-PCR semicuantitativa la inclusión del exón 13 del gen *Serca* y el exón 16´ del gen *Fhos;* ambos eventos de *splicing* se encontraron alterados significativamente para ambos tipos de expansiones largas, pero no para las expansiones cortas o el control GFP. Este nos permitió confirmar que las expansiones largas CCUG producían alteraciones en el *splicing* de forma similar a lo que ocurría en moscas que expresaban las repeticiones CUG patológicas.

Un estudio previo realizado en el laboratorio con moscas modelo para DM1 (*Mhc-Gal4>UAS-i(CTG)480*) demostró que la expresión de repeticiones expandidas CTG induce la activación de la autofagia causando atrofia muscular, confirmándose este aumento por el incremento significativo de la expresión de genes relacionados con el proceso como son *Atg4*, *Atg7*, *Atg8a*, y *Atg9* en músculo de *Drosophila* (Bargiela et al. 2015). Al igual que en el estudio anterior las moscas que expresaban las repeticiones CUG y CCUG largas, mostraban niveles de expresión aumentados para los genes *Atg4*, *Atg7*, *Atg8a*, *Atg9* y *Atg12*, pero no para las repeticiones cortas y GFP, siendo de especial importancia el aumento del gen *Atg4*, previamente descrito como aumentado en músculo esquelético de pacientes DM1 (Fernandez-Costa et al. 2013). Este es el primer precedente que demuestra un aumento de autofagia en músculo de moscas modelo de DM2.

1.2. La expresión de expansiones CCUG en el músculo de mosca reduce el área muscular, la función motora y la supervivencia media.

Para el estudio de la atrofia muscular de las moscas modelo DM1 y DM2, se analizaron secciones dorsoventrales de tórax embebido en resina. La expresión de las expansiones de repeticiones CUG y CCUG en músculo de *Drosophila* originaba la atrofia muscular, observándose una disminución en el tamaño de los IFMs en estas moscas. Esta reducción en el tamaño de los paquetes musculares, provocaba a su vez, en las moscas modelo un detrimento en la capacidad de vuelo y escalada, presentado estas moscas mermada su capacidad locomotora. Por el contrario, tanto las moscas que expresan las repeticiones no expandidas CUG y CCUG, como las

que expresaban el reportero GFP, no presentaban fenotipo atrófico y por ende la capacidad de vuelo y escalada de estas moscas no estaba alterada.

En estudios anteriores se publicó como la expresión en músculo de las repeticiones CTG expandidas en moscas modelo DM1, tenía una importante contribución al fenotipo atrófico tanto a nivel de desarrollo como en el posterior mantenimiento de la masa muscular (Garcia-Lopez et al. 2008, Bargiela et al. 2015). Es por ello que, se pretendió averiguar qué tipo de contribución sobre el fenotipo atrófico ejercían las repeticiones expandidas CUG y CCUG, envejeciendo las moscas durante 30 días. De forma similar a lo que ocurría en moscas de 3 días, el área muscular de las moscas envejecidas que expresaban las expansiones patológicas estaba disminuida en comparación con las moscas control. Pero si comparábamos la reducción en área muscular de todos los genotipos de las moscas envejecidas respecto a las moscas de 3 días, la reducción era similar para todos los genotipos estudiados alrededor del 20%, lo que sugería que la fuerte reducción en área muscular observada en las moscas modelo DM1 y DM2 era debida en gran parte al efecto que ejercen las expansiones patológicas durante el desarrollo. Sin embargo, en las moscas envejecidas que expresaban las expansiones de repeticiones CUG o CCUG, observamos vacuolización, división de los músculos y ausencia ocasional de paquetes musculares, marcadores característicos de degeneración (Chelly et al. 2013). Tomados en conjunto, estos resultados sugerían que las repeticiones tóxicas interferían tanto en el desarrollo como en la homeostasis muscular.

La esperanza de vida se encuentra significativamente reducida en pacientes de DM1, no tanto en DM2 (Mathieu et al. 1999, Meola et al. 2017). Para estudiar si el efecto de las repeticiones CUG y CCUG expandidas provocaba un detrimento en la tasa de supervivencia en las moscas modelo de DM1 y DM2, se llevaron a cabo análisis de supervivencia en moscas de diferentes genotipos. De manera similar a lo que ocurre en pacientes de DM1, observamos que la supervivencia promedio de las moscas que expresan repeticiones CUG o CCUG expandidas se redujo significativamente en comparación con las moscas control que expresan la repeticiones cortas o GFP.

Tanto la atrofia como la degeneración muscular, el *splicing* alterado y la supervivencia media reducida que presentan las moscas que expresan la repeticiones CUG ([250]x) y CCUG ([1100]x), son congruentes con la descripción previa realizada en moscas *Mhc-Gal4>UAS-i(CTG)480* modelo de DM1 (Garcia-Lopez et al. 2008, Bargiela et al. 2015). Estos resultados revelan por primera vez que las expansiones CCUG tienen una toxicidad potencial in *vivo* similar a la de las expansiones CUG en tejidos musculares de *Drosophila* a diferencia que lo que ocurre en humanos donde los fenotipos son más leves, haciendo a estas moscas modelo DM2 un buen sistema en el que investigar los factores moduladores de la toxicidad en pacientes de DM2.

2. Desrepresión de Muscleblind mediante silenciamiento de miRNAs represores en un modelo en *Drosophila* de Distrofia miotónica tipo 1: Prueba de concepto

Esta segunda sección incorpora el trabajo publicado en Cerro-Herreros et al. 2016. Este artículo demuestra la regulación al alza de las proteínas Muscleblind endógenas en *Drosophila* mediante el secuestro de miRNAs que modulan negativamente su expresión, concretamente mediante el uso de construcciones “sponge” o señuelo.

Varias observaciones sugieren que la sobreexpresión de MBNL1 es una terapia potencial para tratar la patología DM1. En primer lugar, la administración de la proteína recombinante Mbnl1 al modelo murino HSA^{LR} de DM1, rescata la miotonía y las alteraciones del *splicing* características de la DM1 (Kanadia et al. 2006). En segundo lugar, en el laboratorio demostramos que la sobreexpresión de una isoforma C de Muscleblind rescata parcialmente la atrofia muscular en un modelo en *Drosophila* para DM1 (Bargiela et al. 2015). Finalmente, la sobreexpresión de MBNL1 humano es bien tolerada en el músculo esquelético en ratones HSA^{LR} y FVB causando cambios menores en el *splicing*, pero ningún efecto sobre la longevidad (Chamberlain et al. 2012).

Puesto que el papel principal de los microRNAs es como reguladores de la expresión génica, en este estudio de prueba de concepto, se utilizó un modelo en *Drosophila* de DM1 (*Mhc-Gal4>UAS-i(CTG)480*) para explorar el potencial terapéutico de silenciar miRNAs específicos, para así aumentar la expresión endógena de *muscleblind*.

Para identificar qué miRNAs reprimían la expresión de *mbl*, seleccionamos una serie de miRNAs candidatos y bloqueamos su actividad utilizando construcciones "sponge" las cuales están bajo el control del sistema Gal4/UAS para expresión especifica de tejido (Fulga et al. 2015, Figura R-2).

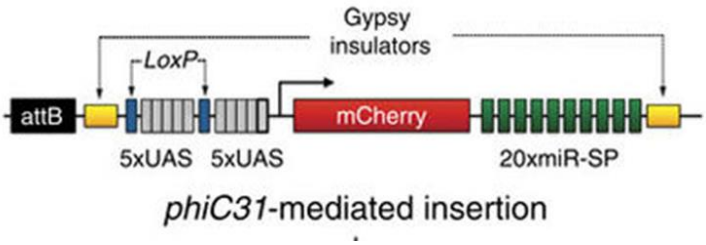

Figura R-2. Esquema de las construcciones "sponge". Estos "sponges" o señuelos están constituidos por una construcción que expresa un RNA que contiene 20 dianas para un miRNA dado situadas en la región 3 'no traducida del reportero mCherry. La construcción está bajo el control del sistema GAL4 generando falta de función de un miRNA concreto en un tejido específico. (Tomado de (Fulga et al. 2015)

2.1. El silenciamiento de *dme-miR-277* o *dme-miR-304* desreprime la expresión de Muscleblind en el músculo de *Drosophila*

Cinco miRNAs fueron los seleccionados como posibles reguladores de *mbl*: *dme-miR-92a*, *dme-miR-100* y *dme-miR-124* en base a los datos generados con anterioridad en nuestro laboratorio y su ortología con miRNAs humanos, y *dme-miR-277* y *dme-miR-304* exclusivos de mosca pero con buenas predicciones bioinformáticas de unión al 3'UTR de Muscleblind. Las moscas que portaban la construcción señuelo correspondiente UAS-miR-XSP y UAS-Scramble-SP como control, fueron cruzadas por la línea Gal4 de elección, en nuestro caso Myosin heavy chain (Mhc)-Gal4, para su expresión en musculatura. Sólo el silenciamiento específico de dos de los miRNAs del juego inicial, *dme-miR-277* o *dme-miR-304*, dio lugar al efecto directo deseado consistente en un aumento de los transcritos de *mbl* cuando alguno de estos miRNAs disminuía.

2.2. *dme-miR-277* y *dme-miR-304* regulan diferentes isoformas de Muscleblind

Para determinar qué isoformas de *muscleblind* estaban reguladas por *dme-miR-277* o *dme-miR-304*, se utilizó el algoritmo de predicción MiRanda (Enright et al. 2003) con la finalidad de identificar los sitios de reconocimiento de *dme-miR-277* y *dme-miR-304* en la región 3'UTR de las isoformas de *muscleblind*. Es importante destacar que MiRanda solo realizaba la búsqueda en los transcritos de *mblA*, *mblB*, *mblC* y *mblD*, siguiendo la nomenclatura utilizada por (Begemann et al. 1997), pero no incluía las isoformas identificadas recientemente, *mblH*, *mblH'*, *mblJ* y *mblK* (Irion 2012). Este análisis predijo un sitio de reconocimiento potencial de *dme-miR-277* en la isoforma *mblA* y dos en *mblB* y *mblD*. En el caso *dme-miR-304*, se encontró un sitio de reconocimiento en la región 3'UTR de *mblC* y otro para *mblD*.

Un análisis de expresión de los niveles de las isoformas de *muscleblind*, determinó que la expresión de mblB aumentó significativamente cuando se bloqueó *dme-miR-277*, mientras que la expresión de *mblD* se redujo en las moscas *Mhc-Gal4>UAS-miR-277SP* y no se detectaron diferencias significativas en *mblA* cuando se comparaba con las moscas control que expresaban la construcción Scrambled-SP. Por otro lado, el bloqueo *dme-miR-304* provocó una regulación al alza en *mblD* y *mblC*, siendo de especial importancia el aumento de los niveles de *mblC*, la isoforma más expresada en moscas adultas (Vicente et al. 2007).

El hecho de que el silenciamiento de *dme-miR-277* y *dme-miR-304* originara cambios en los niveles de expresión específicos de cada isoforma de *muscleblind* sugería una regulación directa sobre transcritos de *mbl* mediada por estos miRNAs. Para confirmar la unión directa de estos miRNAs a los correspondientes 3 'UTRs de las diferentes isoformas de *mbl*, se realizaron ensayos de gen reportero luciferasa en células HeLa. En estos estudios, el 3 'UTR de los diferentes transcritos de *mbl* se clonó aguas abajo del reportero luciferasa de Gaussia. La interacción de los microRNAs a sus respectivos 3´UTR, se detectó como una disminución en las mediciones de luminiscencia. Estos experimentos confirmaron la unión directa de *dme-miR-277* al 3 'UTR de las isoformas *mblB* y *mblD* y la unión directa de *dme-miR-304* a las isoformas *mblC* y *mblD*.

Teniendo en cuenta que un miRNA puede actuar típicamente a nivel de estabilidad del mRNA o del bloqueo de su traducción, se decidió analizar los niveles de la proteína Muscleblind con los miRNAs reguladores candidatos. Con este objetivo, se utilizó un anticuerpo anti-Mbl para detectar la regulación al alza de las proteínas MblA, MblB y MblC (Houseley et al. 2005, Vicente-Crespo et al. 2008). Los análisis de Western blot revelaron un aumento en los niveles de la proteína Muscleblind sólo en las moscas Mhc-Gal4 miR-304SP. Congruente con las determinaciones por RT-qPCR, la banda detectada en la transferencia western correspondía a la proteína MblC.

Con el fin de analizar la distribución subcelular de la proteína Muscleblind por el efecto del silenciamiento de *dme-miR-277* o *dme-miR-304*, se tiñeron secciones longitudinales de IFMs. Previamente en el laboratorio se había demostrado que la proteína endógena Muscleblind se localiza principalmente en las bandas sarcoméricas Z y H del músculo (Llamusi et al. 2013). En consonancia con ello, las imágenes confocales obtenidas de dichas secciones permitieron detectar las proteínas Muscleblind preferentemente en las bandas de los sarcómeros musculares en las moscas control que expresaban la construcción Scrambled-SP. Curiosamente,

la reducción en la función de *dme-miR-277* y *dme-miR-304* tuvo diferentes efectos sobre la distribución de las proteínas Muscleblind: mientras el silenciamiento de *dme-miR-277* aumentó la señal de la proteína Muscleblind en las bandas sarcoméricas, en las moscas *Mhc-Gal4>UAS-miR-304SP* se detectó una fuerte localización nuclear.

2.3. El silenciamiento de *dme-miR-277* y *dme-miR-304* potencia la expresión de Muscleblind y rescata cambios en la expresión génica de transcritos definidos en moscas modelo de DM1

Puesto que las isoformas endógenas de Muscleblind pueden ser reguladas al alza mediante el bloqueo de la actividad inhibidora de *dme-miR-277* y *dme-miR-304* en músculo, decidimos utilizar las construcciones miR-277SP y miR-304SP en moscas *Mhc-Gal4>UAS-i(CTG)480* modelo de DM1. Al igual que en los apartados anteriores el descenso en la expresión de *dme-miR-277* o *dme-miR-304*, provocó un aumento de los niveles tanto de la proteína Muscleblind como del correspondiente mRNA. De forma similar que en moscas *Mhc-Gal4>UAS-miR-304SP*, el bloqueo de la actividad de *dme-miR-304* aumento los niveles de proteína MblC en las moscas DM1. El silenciamiento de *dme-miR-277* o *dme-miR-304* también tuvo un efecto sobre la localización subcelular de la proteína Muscleblind en IFMs de moscas modelo de DM1, liberándola de los foci ribonucleares (característicos de la enfermedad) y aumentando sus niveles en núcleo y citoplasma.

La espliceopatía es el principal hito bioquímico de la DM1 y el único que ha sido vinculado directamente con los síntomas. Para probar si el aumento de Muscleblind, provocado por el silenciamiento de *dme-miR-277* o *dme-miR-304*, era suficiente para rescatar las alteraciones en el *splicing* en las moscas modelo de DM1, se estudiaron algunos eventos de *splicing* característicamente alterados como son la exclusión del exón 16´ del gen *Fhos* y la inclusión del exón 13 del gen *Serca*, ambos eventos regulados por MblC. Además, se comprobó qué sucedía con otra función molecular descrita para Mbl, la de regulador de la expresión génica, y concretamente se cuantificó la expresión del gen *CyP6W1* alterado en moscas modelo de DM1 (Picchio et al. 2013) y dependiente de MblC. La expresión de miR-304SP en moscas *Mhc-Gal4>UAS-i(CTG)480* consiguió rescatar el *splicing* alterado de *Fhos* y *Serca* y normalizo la expresión del gen CyP6W1. Por el contrario, la expresión de miR-277SP, no modificó estos eventos de *splicing*, ni la expresión del gen CYP6W1. Este hecho es posiblemente debido a que el silenciamiento de *dme-miR-304* en el músculo provocó un fuerte aumento en los niveles de *mblC* una isoforma que previamente se había demostrado que actuaba como regulador nuclear del *splicing* (Vicente et al. 2007), mientras que el silenciamiento de *dme-miR-277* rescató la expresión Muscleblind en el citoplasma y redujo los niveles de expresión de *mblC*.

2.4. El silenciamiento de *dme-miR-277* o *dme-miR-304* mejora la atrofia muscular, la locomoción y la supervivencia de las moscas modelo de DM1

Este aumento de Muscleblind en mosca *Mhc-Gal4>UAS-i(CTG)480* también tuvo efecto a nivel funcional, puesto que el silenciamiento de *dme-miR-277* o *dme-miR-304* era capaz de aumentar el área muscular, rescatando el fenotipo atrófico característico de la enfermedad. Asimismo, la inhibición de *dme-miR-277* o *dme-miR-304* en las moscas modelo DM1 en las que se llevó a cabo el ensayo mostraron una mejora funcional en los ensayos de vuelo y de escalada, mejorando así su actividad locomotora, lo cual se correlacionaba con la mejora en el área muscular.

Para estudiar si el silenciamiento de *dme-miR-277* o *dme-miR-304* era capaz de rescata la tasa de supervivencia reducida de las moscas modelo de DM1, se obtuvieron análisis de curvas supervivencia. La expresión de miR-277SP o miR-304SP en las moscas modelo incrementó la vida media de estas moscas, uno de los aspectos más interesantes a destacar del estudio. En paralelo, estos ensayos funcionales fueron llevados a cabo en un contexto muscular no patológico y al igual que en ratón (Chamberlain et al. 2012) la sobreexpresión de Mbl en moscas *(Mhc-gal4>UAS-miR-277SP* y *Mhc-gal4>UAS-miR-304SP*) fue en general bien tolerada. Solo el silenciamiento de *dme-miR-277*, uno de los microRNAs más expresados en músculo (Fulga et al. 2015), causó una pequeña reducción pero significativa en el área de músculo, que se correlaciona con una disminución en la capacidad de vuelo de las moscas.

A la luz de los resultados, esta prueba de concepto en *Drosophila* demuestra que el silenciamiento de miRNAs represores específicos provoca un incremento de los niveles de Muscleblind suficiente para rescatar diferentes aspectos moleculares y fisiológicos de la patología en moscas DM1. Estos resultados son prometedores puesto que abren la puerta al siguiente nivel de análisis en modelos murinos y humanos.

3. Silenciamiento de miRNAs represores específicos de la expresión de MBNL1 y MBNL2 en un modelo celular y murino de DM1

Este tercer apartado incorpora el trabajo publicado en Cerro-Herreros et al. 2018. En este artículo se demuestra que el silenciamiento de *miR-23b* y *miR-218* mediado por antagonistas contra los mismos, mejora los niveles de las proteínas MBNL1/2 y rescata eventos de *splicing* alterados en mioblastos DM1. De forma análoga, la administración sistémica de estos "AntagomiRs" en ratones HSA^{LR} estimula la expresión de Mbnl1 y Mbnl2 y mejora fenotipos característicos de DM1 como son las alteraciones en el *splicing*, la histopatología muscular y la miotonía.

3.1. Identificación de miRNAs reguladores de *MBNL1* y *MBNL2*

Dado que la regulación al alza de MBNL es una terapia prometedora y que el silenciamiento de miRNAs específicos en moscas DM1 provoca un aumento de los niveles de Muscleblind suficiente para rescatar varias características moleculares y fisiológicas de la enfermedad (Cerro-Herreros et al. 2016, Chen et al. 2016), el trabajo se centró en la regulación de *MBNL1* y *MBNL2* por miRNAs. Para llevar a cabo una descripción detallada de la regulación de *MBNL1* y *MBNL2* realizamos un *screening* piloto empleando el kit comercial SureFIND Transcriptome array (Qiagen). Este estudio permitió identificar en células HeLa 19 microRNAs potenciales represores de *MBNL1* y 9 microRNAs potenciales represores de *MBNL2*. Como control positivo *miR-372* reprimía la expresión *MBNL2*, lo cual ya se había confirmado con anterioridad en células madre (Li et al. 2009). A partir del *screening* y bases de datos bioinformáticas como miRecords (Xiao et al. 2009) y miRDIP (Shirdel et al. 2011) se seleccionaron solo 6 miRNAs a validar en células HeLa: *miR-96* y *miR-181c* como potenciales represores de *MBNL1*, *miR-218* y *miR-372* de *MBNL2* y *miR-146b* y *miR-23b* de ambos genes.

En un experimento de validación posterior, se transfectó células HeLa con versiones de los microRNAs seleccionados contenidos en el vector pCMV-MIR-GFP. Como control se utilizó dicho vector vacío y *miR-7,* pues éste no resulto positivo en el *screening* inicial. Cuatro de los miRNAs iniciales resultaron positivos para este ensayo de validación (*miR-96*, *miR-23b* y *miR-*

218 y *miR-372*), pero solo tres, *miR-96*, *miR-23b* y *miR-218* eran nuevos miRNAs represores de la expresión de *MBNL1* y / o *MBNL2* tanto a nivel de mRNA como de proteína.

3.2. Mapeo de los sitios de unión miRNA-mRNA al 3'UTR de *MBNL1 / 2*

Los microRNAs actúan a nivel post-transcripcional para ejercer su función como represores génicos mediante la unión a la 3´ UTR del mRNA al que regulan (Bartel 2009). Para comprobar que los tres microRNAs pre-seleccionados se unían a las dianas predichas en el 3´UTR de MBNL1 y 2, realizamos ensayos de reportero en células HeLa. En estos estudios, el 3 'UTR de ambos genes se encontraba fusionado al gen reportero luciferasa de Gaussia (Gluc), de modo que cuando se produce la interacción entre microRNA y mRNA, esta es detectada como una disminución en la luminiscencia. La co-transfección en células HeLa de la construccion 3´UTR del mensajero y el plásmido con el miRNA apropiado, confirmó una disminución significativa en la actividad luciferasa para todos los miRNAs del ensayo (*miR-96*, *miR-23b* y *miR-218*).

La interacción miRNA-mRNA depende en gran medida de la complementariedad perfecta entre el mRNA diana y la región de semilla del miRNA situada entre las posiciones 2-8 del mismo (Bartel 2009). Puesto que un microRNA puede tener varias dianas de unión en un mismo 3´UTR diseñamos una serie de 3´UTR-X-Gluc adicionales, para la mejor comprensión del mecanismo de unión miRNA-mRNA. Basándonos en predicciones bioinformáticas para cada uno de los microRNAs candidatos, se diseñaron versiones con sitios de reconocimiento natural (WT), versiones donde la secuencia semilla estaba ausente (MUT) y versiones con complementariedad perfecta por el microRNA (PM). Al igual que anteriormente, en los ensayos donde se co-transfecto las versiones WT del 3'-UTR de *MBNL1* y *MBNL2* con los plásmidos *miR-23b* o *miR-96* y *miR-23b* o *miR-218*, respectivamente, se redujo significativamente la expresión del reportero Gluc. En comparación con las construcciones WT, la co-transfección de todos los miRNAs con sus correspondientes versiones MUT, eliminó el efecto represor de los miRNAs observándose un aumento en los niveles de Gluc, mientras que las versiones PM generaron el efecto contrario y los niveles de luminiscencia resultaron menores que con construcciones WT. A partir de estos resultados, se pudo concluir que *miR-96*, *miR-218* y *miR-23b* regulan directamente los genes *MBNL1*, *MBNL2* o ambos, respectivamente.

3.3. El silenciamiento de *miR-23b* y *miR-218* estabiliza los transcritos de *MBNL1/2* y rescata los defectos en el *splicing* en mioblastos DM1

Si bien es importante comprobar la capacidad represora de los miRNAs, también lo es analizar si estos se expresan en los tejidos donde se manifiestan los síntomas de la enfermedad. Por lo tanto, medimos los niveles de *miR-96*, *miR-23b* y *miR-218* en tejido muscular por RT-qPCR. *miR-23b* y *miR-218* se expresaban en mioblastos humanos DM1 cultivados y biopsias musculares, mientras que *miR-96* lo hacía a niveles insignificantes. Ante los bajos niveles de expresión de *miR-96* el trabajo se centró únicamente en *miR-23b* y *miR-218* como dianas terapéuticas en DM1.

Para la inhibición de *miR-23b* y *miR-218,* diseñamos oligonucleótidos antisentido de tipo antagomiR siguiendo el precedente de (Gomez et al. 2015). Estos oligonucleótidos de cadena sencilla y secuencia completamente complementaria a la del miRNA a silenciar, contenían distintas modificaciones químicas del esqueleto fosfodiester (2 enlaces fosforotioato en 5´ y 4

enlaces fosforotioato en 3´), nucleotidos con la modificación 2´-metoxi en todas las pentosas, y cuatro grupos colesterol en 3´. Un antagomiR con secuencia al azar (antagomiR-SC) fue utilizado como control.

Inicialmente, caracterizamos el perfil de toxicidad y captación celular de los antagomiRs, estableciendo así un rango de concentraciones que va de 50 nM a 200 nM no tóxico. El rango de concentraciones arriba mencionado fue testado en mioblastos DM1 para ambos antagomiRs y se midió el nivel de mRNA *MBNL1* y *MBNL2*. El análisis de RT-qPCR reveló un aumento de los transcritos de *MBNL1 y 2* con ambos antagomiR. En el caso del antagomiR-218 el aumento era mayor para *MBNL1 y 2* a la dosis 200 nM, mientras que para el antagomiR-23b este aumento en la expresión de ambos genes de forma general era mayor a la concentración 50 nM. Remarcable era lo que ocurría con el silenciamiento de *miR-218* que aumentaba los transcritos de *MBNL1* pero no se unía al 3´UTR de *MBNL1*. Probablemente esta regulación sea indirecta o por unión a otra/s secuencia/s fuera del 3´UTR.

Una de las principales funciones de las proteínas MBNL es la de reguladores del *splicing*, siendo las alteraciones moleculares en este procesado alternativo de exones una de las afectaciones más estudiadas en la patología. Por tanto, llegados a este punto se comprobó si cantidades mayores de mRNA de *MBNL1* y *MBNL2* se traducían en un rescate de eventos de *splicing* típicamente alterados en músculo de pacientes de DM1 como son *BIN1*, *ATP2A1, INSR* y *PKM (Savkur et al. 2001, Fugier et al. 2011, Gao et al. 2013, Santoro et al. 2013, Santoro et al. 2014)*. Para ello se transfectaron mioblastos DM1 usando las condiciones óptimas de antagomiR determinadas con anterioridad y se analizaron sus transcritos por RT-PCR semicuantitativa. El porcentaje de inclusión (PSI) de los exones alterados de *BIN1*, *ATP2A1*, I*NSR* y *PKM* se rescató significativamente cuando *miR-23b* y *miR-218* eran silenciados. Con la finalidad de probar la especificidad de los antagomiRs-23b y -218 en la regulación del *splicing*, cuantificamos la inclusión del exón 8 de *CAPZB,* el cual es un evento de *splicing* dependiente CELF1 y del exón 19 de DLG1, siendo este último un evento de *splicing* independiente de la regulación por MBNL1 y CELF1. Ambos eventos no sufrieron ningún cambio por el tratamiento con antagomiRs. Por tanto, estos resultados en conjunto confirmaban un rescate de defectos de *splicing* alternativo específicos de mioblastos DM1 como resultado de la desrepresión de *MBNL1* y *MBNL2* mediada por los antagomiRs.

3.4. Los AntagomiRs-23b y -218 restauran la distribución subcelular normal de las proteínas MBNL

Dado que los miRNAs están implicados en la regulación de la expresión génica tanto a nivel de la estabilidad del mRNA como a nivel de la traducción, se procedió a determinar qué efecto tenían estos antagomiRs a nivel de las proteínas MBNL1 y MBNL2. Mediante análisis de western blot se detectó un aumento de 4 a 5 veces más proteína MBNL1, y de 3 a 4 veces más proteína MBNL2, en mioblastos DM1. Por el contrario, los niveles de proteína CELF1 no se vieron alterados tras el silenciamiento de *miR-23b* o *miR-218* siendo este dato congruente con lo descrito para el *splicing* alternativo de CAPZB, el cual permaneció sin modificaciones. Este aumento de proteína también fue detectado mediante inmunofluorescencia. Considerando que tanto la proteína MBNL1 como MBNL2 son secuestradas en foci ribonucleares en mioblastos DM1, el tratamiento con el antagomiR-23b y -218 produjo un aumento significativo de la expresión de ambas proteínas y restauró su distribución a nivel de núcleo y citoplasma en

mioblastos DM1. Este aumento de las proteínas MBNL1 y MBNL2 en el núcleo celular era consistente con el rescate de *splicing* mostrado anteriormente.

3.5. La administración sistémica de AntagomiRs en ratones HSA^{LR} aumenta la expresión muscular de Mbnl

Partiendo de la expresion confirmada de *miR-23b* y *miR-218* en músculo de ratón, se decidió administrar los antagomiRs a ratones modelo de la enfermedad (HSA^{LR}) con la finalidad de investigar su actividad *in vivo*. En un primer momento se evaluó la capacidad de dichos antagomiRs para llegar a músculo esquelético. Para ello administramos a ratones de 4 meses de edad la versión marcada con Cy3 de los antagomiRs mediante inyección subcutánea. Cuatro días después de la inyección, en secciones musculares se confirmó la presencia de los antagomiRs, por tanto, éstos eran capaces de llegar a grastocnemio y cuádriceps.

El mismo modo de administración fue el elegido para inyectar los antagomiRs sin marcar a nueve ratones modelo de DM1 adicionales a una dosis final de 12,5 mg/kg. Los ratones HSA^{LR} control del experimento fueron inyectados con PBS1x y con el antagomiR-SC. Cuatro días después de la inyección los animales fueron sacrificados y se obtuvieron muestras de gastrocnemio y cuádriceps para los análisis histológicos y moleculares.

En un primer ensayo se conformó el silenciamiento mediante RT-qPCR de *miR-23b* y *miR-218* respecto a los ratones control. Como resultado de la disminución de los miRNAs por el tratamiento con antagomiRs, los niveles de *Mbnl1* y *Mbnl2* aumentaron tanto a nivel de transcripción como de proteína en ambos tipos de músculo. A diferencia de lo que ocurría con las proteinas Mbnl1 y 2 tras el tratamiento con los antagomiRs, los niveles de la proteína Celf1 no se vieron alterados por ninguno de los tratamientos.

3.6. Los AntagomiRs rescatan los defectos en el *splicing* muscular en ratones HSA^{LR}

Dado el fuerte aumento de Mbnl1 y 2 en los músculos gastrocnemio y cuádriceps tratados, se intentó confirmar si también algunos de los eventos de *splicing* dependientes de Mbn1 como son *Atp2a1*, *Clcn1* y *Nfix* en ratones HSA^{LR} eran rescatados por los antagomiRs. La administración de los AntagomiRs rescató la inclusión alterada de los exones alternativos en ambos músculos para los genes *Atp2a1* (exón 22) y *Nfix* (exón 7), y mejoro la inclusión del exón 7a para los transcritos de *Clcn1* en gastrocnemio pero no en cuádriceps de ratones HSA^{LR} con el antagomiR-218. Para probar la especificidad de antagomiRs-23b y -218 en la regulación de Mbnl, se cuantificó la inclusión del exón 8 de *Capzb*, el exón 21 de *Ank2* y el exón 3 de *Mfn2*, todos ellos *splicings* dependientes de Celf 1 (Kalsotra et al. 2008, Koshelev et al. 2010), no viéndose ninguno de ellos alterado.

A pesar de la variedad intrínseca existente entre los ratones HSA^{LR}, estos datos demostraron como la administración sistémica de los antagomiRs era capaz de rescatar en músculo de ratones modelo DM1 la espliceopatía característica de la enfermedad.

3.7. El silenciamiento de *miR-23b* y *miR-218* rescata la histopatología muscular y reduce la miotonía en ratones HSA^{LR}

En los ratones modelo de DM1 HSA^{LR}, las alteraciones en las corrientes iónicas son la causa de potenciales de acción repetitivos, o miotonía, eventos que pueden ser cuantificados mediante electromiografía. Antes del tratamiento, todos los ratones DM1 tenían miotonía de grado 3 o 4, es decir, abundantes descargas repetitivas cuando se insertaba el electrodo en el músculo. Tras cuatro días de tratamiento, los antagonistas redujeron la miotonía al grado 2 (descarga miotónica en> 50% de las inserciones) o grado 1 (descarga miotónica ocasional) en los ratones tratados con los antagomiR-218 y antagomiR -23b.

Una de las principales características histopatológicas que presentan las fibras musculares de ratones HSA^{LR}, es una ubicación central de los núcleos en las fibras, producto del intento del músculo miopático por intentar regenerarse (Timchenko 2013). Ambos antagomiRs disminuyeron el número de núcleos centrales tanto en gastrocnemio como en cuádriceps.

Tomados en conjunto todos estos resultados validan el potencial de antagomiR-23b y -218 como fármacos para suprimir la miopatía en ratones modelo de DM1.

3.8. El tratamiento con AntagomiRs rescata a largo plazo fenotipos funcionales y no produce efectos deletéreos

Con el fin de evaluar los efectos a largo plazo del tratamiento con los antagomiRs, se realizó un estudio a nivel molecular y funcional en ratones HSA^{LR} tratados durante 6 semanas con la misma dosis y posología. Tras seis semanas de tratamiento, los niveles de expresión de *miR-23b* y *miR-218* todavía estaban significativamente disminuidos pero de una forma menos pronunciada que con el tratamiento a corto plazo. De hecho, esta reducción en los miRNAs era insuficiente para aumentar los niveles de transcripción de *Mbnl1* y *2*. Sin embargo, sí que se observó un efecto de los antagomiRs a largo plazo sobre la miotonía y la fuerza muscular, mostrando dichos ratones a tiempo final, una miotonía disminuida y una fuerza muscular de los miembros delanteros aumentada.

Un análisis independiente de necropsia visual y bioquímica sanguínea en ratones tratados revelo que no existían efectos deletéreos tras seis semanas de tratamiento. Los únicos parámetros alterados fueron la bilirrubina total y el número de monocitos en todos los animales tratados. Dado que estos dos parámetros también se vieron alterados en ratones tratados con el antagomiR-SC, es posible que esta alteración sea debida a la modificación química de los antagomiRs y no al silenciamiento de *miR-23* y *miR-218*.

-Discusión general-

El papel de la proteínas MBNL humanas se ha relacionado con diversas enfermedades degenerativas mediadas por RNAs expandidos como son DM1, DM2, ataxia espinocerebelar 8, enfermedad de Huntington o tipo Huntington 2 y distrofia corneal (Fuchs endothelial corneal dystrophy; FECD) (Li et al. 2010, Mykowska et al. 2011, Irion 2012, Fiszer et al. 2013, Du et al. 2015). De forma más concreta en la DM1 y la DM2, estos RNAs tóxicos se pliegan en forma de horquillas secuestrando a las proteinas MBNL, lo que desencadena alteraciones en el metabolismo del RNA y particularmente en el control del *splicing* alternativo de subconjuntos de transcritos musculares, cardiacos y de SNC. Por tanto, entender la regulación que ejercen ciertos microRNAs sobre la expresión génica de Muscleblind nos puede servir para el desarrollo de terapias efectivas basadas en TGM para este tipo de enfermedades.

1. Las moscas modelo de DM2 son una importante herramienta in vivo donde probar nuevos enfoques terapéuticos para la distrofia miotónica tipo 2

Las distrofias miotónicas tipo 1 y 2 son trastornos genéticos neuromusculares causados por la expansión patológica de los microsatélites CUG y CCUG respectivamente, en regiones no traducidas del genoma. Aunque se ha descrito un origen similar para ambas enfermedades, clínicamente los pacientes con DM2 experimentan de forma general una progresión las lenta y menos grave de la enfermedad que los pacientes con DM1. Sin embargo, estas características clínicas más leves son contradictorias a nivel molecular, puesto que la expresión del gen *CNBP* portador de la expansiones CCUG es de 4 a 8 veces mayor que la del gen *DMPK* portador de las expansiones CUG (Mankodi et al. 2003, Mele et al. 2015, Uhlen et al. 2015). Además, el tamaño promedio de las expansiones de repeticiones generalmente es más alto en DM2 en comparación con DM1 (Liquori et al. 2001), donde el mayor número de repeticiones CUG tóxicas esta correlacionado con un mayor secuestro de las proteínas MBNL, ocasionando alteraciones en el metabolismo del RNA y por ende mayor gravedad de la enfermedad (Wagner et al. 2016, Thomas et al. 2017). Sin embargo, una diferencia en la afinidad de las proteínas MBNL por las expansiones de repeticiones CUG frente a las repeticiones CCUG no puede explicar la menor gravedad de DM2, dado que las proteínas MBNL se unen con mayor afinidad a las expansiones CCUG que a las CUG de modo que sería esperable un mayor secuestro de las proteínas en la DM2 que en la DM1(Kino et al. 2004).

Con la finalidad de profundizar sobre esta paradoja, en el presente trabajo de tesis se estudiaron los fenotipos musculares provocados por ambos tipos de expansiones en *Drosophila*. En particular se esperaban fenotipos más leves para las expansiones CCUG (DM2) si eran intrínsecamente menos toxicas que las repeticiones CUG (DM1); mientras que por el contrario se esperaban fenotipos similares si la toxicidad es modulada en humanos por factores específicos de CCUG.

A diferencia de lo que ocurre en humanos (Udd et al. 2012), se observó una reducción en tamaño de los músculos, de la función locomotora y de la supervivencia muy grave en moscas modelo DM2, de forma similar a lo que ocurre en moscas DM1. Además, las moscas modelo DM2 mostraron a nivel molecular fenotipos de tipo DM1 incluyendo la sobreexpresión de genes relacionados con autofagia, alteraciones en el *splicing* alternativo y la agregación de Muscleblind

en foci ribonucleares. Por tanto, ambos modelos de mosca, DM1 y DM2, presentan fenotipos similares en un contexto no humano, proporcionado este hecho evidencias de la elevada toxicidad potencial que tienen las repeticiones CCUG *in vivo* en tejidos afectados en la enfermedad (Cerro-Herreros et al. 2017). Estos resultados sugieren la existencia de factores específicos en humanos que inhiben la toxicidad de las repeticiones CCUG en pacientes con DM2, convirtiendo esto a *Drosophila* en buen modelo en el que investigar dichos factores moduladores de la toxicidad. En este sentido un artículo de reciente publicación apunta a las proteínas de unión a RNA rbFOX como las posibles moduladoras de la patología (Sellier et al. 2018). Dichas proteínas compiten con las proteínas Muscleblind por la unión a las repeticiones CCUG expandidas tanto en células musculares DM2 como en moscas que expresan las repeticiones CCUG, pero no por la unión a repeticiones CUG típicas de DM1. Concretamente, en moscas modelo de DM2 la sobreexpresión de rbFOX1 es capaz de rescatar parcialmente la atrofia muscular, eventos de *splicing* alterados y la supervivencia reducida, ejerciendo estas proteínas una función amortiguadora del efecto tóxico de las repeticiones CCUG *in vivo* (Sellier et al. 2018).

A pesar de la existencia de modelos musculares de DM2 tanto en ratón, mosca y cultivo celular estos presentan fenotipos de muy leves a inexistentes. Los ratones DM2-HSAtg modelo para DM2 presentan una patología muscular muy leve y miotonía, pero carecen de defectos en *splicing*, estando estos fenotipos dentro de una ventana terapéutica muy estrecha con la que trabajar (Udd et al. 2011). Por el contrario, las moscas modelo de DM2 que expresan 106 repeticiones CCTG, sí que presentan defectos en *el splicing*, pero carecen de fenotipo atrófico (Yenigun et al. 2017). Por último, las líneas celulares de mioblastos inmortalizados DM2 existentes, ni presentan defectos en el *splicing*, ni en la capacidad de fusión celular para formar miotubos, estando esta capacidad de fusión directamente relacionada con regeneración muscular (Arandel et al. 2017). Por tanto, en este trabajo de tesis doctoral se describe por primera vez, un modelo animal de DM2 que reproduce gran parte de los defectos musculares presentes en los pacientes (Cerro-Herreros et al. 2017). Puesto que *Drosophila* ha demostrado ser un sistema modelo eficaz para el estudio de las enfermedades humanas, este modelo es un potencial sistema donde testar nuevas estrategias terapéuticas para la DM2 (Cerro-Herreros et al. 2016).

Puesto que está ampliamente aceptado que las proteinas MBNL son una diana terapeútica de primer orden en la DM1 y la DM2, decidimos explorar una aproximacion terapeútica novedosa basada en la modulación terapéutica de la expresión génica de Muscleblind mediada por microRNAs como una posible terapia para DM. Dichos estudios han sido llevado a cabo en diferentes modelos de la enfermedad previamente descritos y caracterizados, moscas modelo DM1 (Garcia-Lopez et al. 2008), mioblastos de pacientes DM1 (Arandel et al. 2017) y ratones modelo HSA^{LR} (Mankodi et al. 2000).

2. El silenciamiento de *dme-miR-277* y *dme-miR-304* potencia la expresión de Muscleblind y rescata alteraciones moleculares y funciones típicas de DM1 en *Drosophila*

En un primer momento y siendo conocedores de que los miRNAs son pequeñas moléculas ampliamente conocidas por su función como represores de la expresión génica, se propuso

aumentar la expresión endógena de Muscleblind por medio del silenciamiento de miRNA en un modelo muscular de DM1 en *Drosophila* (*Mhc-Gal4>UAS-i(CTG)480*) como prueba de concepto. Para generar la falta de función del microRNA en estas moscas se ultilizaron construcciones "sponge", dichas construcciones se componen de muchas dianas en tándem para un miRNA dado, de tal forma que el miRNA se une a estas diana y se genera un silenciamiento del mismo. Sólo la disminución especifica comprobada de dos de los miRNAs de un juego inicial de partida, *dme-miR-277* o *dme-miR-304*, ocasionaron el aumento de los niveles tanto del mensajero como de la proteína Mbl (Cerro-Herreros et al. 2016).

Un análisis cuantitativo específico de isoformas reveló que cada construcción esponja daba lugar a la elevación de los niveles de diferentes isoformas de *muscleblind*, mientras que mediante ensayos de reportero luciferasa se confirmó que esta regulación estaba mediada por la unión directa de los miRNAs al 3 'UTR de las diferentes isoformas *muscleblind*. Se confirmó la unión directa de *dme-miR-277* al 3 'UTR de las isoformas *mblB* y *D* y la unión directa de *dme-miR-304* a las isoformas *mbl C* y *D*. Curiosamente, ambas construcciones esponja, miR-277SP y miR-304SP, fueron capaces de regular negativamente la expresión de las isoformas *mblB* y *mblC*, respectivamente, en lugar de aumentar la expresión, lo que sugiere algún tipo de regulación inter-isoforma, tal como se ha demostrado previamente para las proteínas MBNL (Terenzi et al. 2010, Kino et al. 2015). Este hecho, ayudó al replanteamiento de la identificación en las células humanas no solo de miRNAs que reprimieran la expresión de MBNL1 o MBNL2, sino que reprimieran la expresión de ambos a la vez, para controlar posibles efectos reguladores o compensatorios entre ambas proteínas.

De forma paralela, los ensayos de inmunodetección de la proteína en el tejido muscular de moscas que expresaban una de las construcciones esponja, *Mhc-gal4>UAS-miR-304SP* o *Mhc-gal4>UAS-miR-277SP*, demostraron la sobreexpresión de Muscleblind en ambos casos, aunque en diferentes localizaciones subcelulares: miR-277SP provocó un incremento preferentemente en bandas sarcoméricas y miR-304SP en los núcleos. De igual forma el silenciamiento de *dme-miR-277* o *dme-miR-304* en moscas *Mhc-Gal4>UAS-i(CTG)480* produjo un aumento de Muscleblind en citoplasma y núcleo, pero además tuvo un efecto sobre la distribución subcelular liberándolo de las expansiones. De forma congruente con los conocimientos previos que indican que la isoforma MblC se localiza en el núcleo y con la regulación preferencial de la expresión de MblC por parte de miR-304SP, pudo confirmase como la expresión de miR-304SP permitió rescatar una serie de eventos de *splicing* y transcritos alterados dependientes de Muscleblind (Cerro-Herreros et al. 2016).

El efecto que ejerce el silenciamiento de ambos microRNAs en la atrofia muscular también fue analizado. Previamente se demostró como la sobreexpresión de MblC rescataba parcialmente la atrofia muscular en moscas modelo DM1 (Bargiela et al. 2015). En consonancia con esta observación la expresión de miR-304SP en moscas modelo también rescató la atrofia muscular. Sin embargo, la expresión miR-277SP, que no consiguió rescatar los eventos de *splicing* alterados, sí que era capaz de rescatar la atrofia en las moscas modelo DM1, pudiendo estar otras isoformas, además de MblC, implicadas en el proceso atrófico. En ambos casos esta reversión del proceso atrófico está correlacionada a nivel funcional con la mejora de la supervivencia y de la capacidad de escalada y vuelo de las moscas DM1 (Cerro-Herreros et al. 2016).

A pesar de que el silenciamiento de *dme-miR-277* causó una reducción pequeña en el area muscular en en moscas *Mhc-Gal4>UAS-miR-277SP*, pero significativa; en las moscas con fondo *Mhc-Gal4>UAS-i(CTG)480,* la expresión de cualquiera de las construcciones esponja provocó efectos beneficiosos, lo que sugiere que la sobreexpresión de otros transcritos dianas naturales adicionales de los miRNAs bloqueados es insignificante en comparación con los efectos positivos de estimular la expresión de Muscleblind en un contexto patogénico. Estos resultados se convierten en un respaldo para la estrategia de intentar inhibir / silenciar / disminuir / la actividad de miRNAs específicos implicados en la regulación negativa de las proteínas MBNL1/2 en mamíferos.

De igual forma que en moscas modelo DM1, nuestra idea era utilizar estas construcciones miR-277SP y miR-304SP en moscas modelo para DM2 y así demostrar que la desrepresión endógena de Mbl mediada por el silenciamiento de *dme-miR-277* y *dme-miR-304* también era potencialmente terapéutica en el caso de DM2. Sin embargo, este trabajo todavía no ha podido ser llevado a cabo debido a una serie de problemas que han surgido en la generación del recombinante *Mhc-Gal4>UAS-(CCUG)1100*. Lo que sí se ha podido llevar a cabo en este modelo de DM2 en *Drosophila* es sobreexpresar MBNL1 humano, siendo la sobreexpresión de esta proteína suficiente para rescatar diferentes aspectos moleculares y fisiológicos de la patología(Sellier et al. 2018). Estos resultados apoyan el potencial terapéutico que puede tener el aumento Muscleblind como terapia para la DM2.

3. El silenciamiento de *miR-23b* y *miR-218* incrementa la expresión de las proteínas MBNL rescatando fenotipos característicos de DM1 en modelos mamíferos.

Partiendo del primer precedente de regulación al alza de las proteínas Muscleblind endógenas en *Drosophila* mediante el silenciamiento de miRNAs que modulan negativamente su expresión (Cerro-Herreros et al. 2016), se llevó a cabo, el siguiente paso en el estudio investigando en modelos mamíferos de la enfermedad. Para ello se usaron oligonucleótidos inhibidores de microRNAs de tipo antagomiR, un método terapéutico atractivo debido que actúan a nivel de todos transcritos maduros de los genes MBNL1/2.

En este estudio se observó que la administración en mioblastos DM1 y ratón HSA^{LR} del antagomiR-23b y antagomiR-218 silenciaba la expresión de sus respectivos miRNAs diana, logrando un aumento en la expresión de Mbnl1 y Mbnl2 tanto a nivel de RNA como de proteína. Los niveles de proteína Celf1 no se vieron afectados por el tratamiento con antagomiR en ninguno de los casos, a pesar de que se ha descrito un efecto del antagomiR-23b sobre los niveles de Celf1 en corazón de ratón. La dosis de antagomiR utilizada (mayor dosis) o los efectos específicos de tejido podrían explicar esta controversia (Kalsotra et al. 2010). Se consiguió un elevado nivel de silenciamiento con ambos antagomiRs, a pesar de utilizar una cantidad de este tipo de oligonucleótidos bastante menor a lo que suele utilizarse en ratón para este tipo de ensayos (Krutzfeldt et al. 2005, van Solingen et al. 2009, Dey et al. 2012). Tanto la sobrexpresión de Mbnl1/2 (Chamberlain et al. 2012) como la infraexpresión de *miR-23b* y *miR-218* fueron bien toleradas en ratón, pues no se observó ningún fenotipo deletéreo ni en los ratones tratados durante cuatro días, ni en los tratados durante seis semanas con los antagomiRs (Cerro-Herreros et al. 2018).

Trabajos previos sugieren la existencia de modificadores genéticos que pueden tener efectos sobre la inestabilidad de las repeticiones CTG en ratones HSA^{LR} dando lugar a diferencias entre ratones de una misma camada (Jones et al. 2012, Brockhoff et al. 2017). En relación con esta variabilidad en los fenotipos, decidimos comparar el nivel de expresión del transgén que contiene las repeticiones y el porcentaje de inclusión de los exones alternativos alterados en ratones HSA^{LR}. Una fuerte correlación positiva entre la menor expresión del transgén y un fenotipo más leve a nivel de *splicing* en los ratones fue observada, lo que permitió en el caso del *splicing* alterado de *Atp2a1,* excluir a 2 ratones del análisis. Por tanto, sugerimos que la cuantificación de la expresión transgénica es un paso importante previo para identificar valores atípicos (Cerro-Herreros et al. 2018).

Se sabe que en la DM1 el secuestro de las proteínas MBNL y la activación de CELF1 conducen al mantenimiento de patrones de *splicing* alternativo fetales, en vez de los propios de adultos, en transcritos musculares. A lo largo de este estudio, se observó como el aumento de MBNL1/2 por silenciamiento específico de miRNAs reguladores, era suficiente para rescatar algunos de estos sucesos críticamente alterados en mioblastos DM1 y ratones HSA^{LR} y que son dependientes de MBNL1 y MBNL2, pero no de CEFL1. Son las alteraciones en el *splicing* las que se han relacionado directamente con los síntomas, por ejemplo alteraciones en el *splicing* del canal de cloro (*CLCN1*) humano en músculo explican la miotonía (Charlet et al. 2002, Kino et al. 2009). Curioso era lo que se observó en cuádriceps para del *splicing* de *Clcn1* y la miotonía después de la inyección con el antagomiR-218, donde observamos un rescate de esta alteración funcional similar a la que veíamos con el antagomiR-23b, a pesar de no observarse una mejora significativa en la exclusión del exón 7a como la mostrada cuando *miR-23b* era silenciado. Ya se ha descrito con anterioridad que la miotonía en ratones HSA^{LR} adultos no se debe exclusivamente a una canalopatía del canal de Cl, sino al mosaico existente en la expresión del CLCN1 entre las fibras musculares y la afectación de otros canales iónicos (canales de Na^+ y canales de K^+) (DiFranco et al. 2013), pudiendo ser esta una posible explicación a la mejoría que encontramos con el AntagomiR-218 para la miotonía.

Tomados en conjunto, estos resultados demuestran un rescate específico de los transcritos alterados tanto en mioblastos DM1, como en músculo de ratones HSA^{LR}, pero también a nivel funcional en ratones, como resultado del aumento de las proteínas MBNL mediada por el tratamiento con antagomiRs.

Puesto que se confirmó la expresión *miR-23b* y *miR-218* en otros tejidos importantes para la patología como son corazón y SNC, es de espera que el aumento en las proteínas MBNL1 y MBNL2 por la administración sistémica de los antagomiRs pueda rescatar fenotipos en estos tejidos, de la misma forma que lo hacía el aumento de MblC en corazón de *Drosophila* (Chakraborty et al. 2018). En general, este estudio remarca el uso de fármacos oligonucleotídicos para desreprimir específicamente la expresión de las proteínas MBNL1 y MBNL2 como enfoque terapéutico para DM1 (Figura D-1).

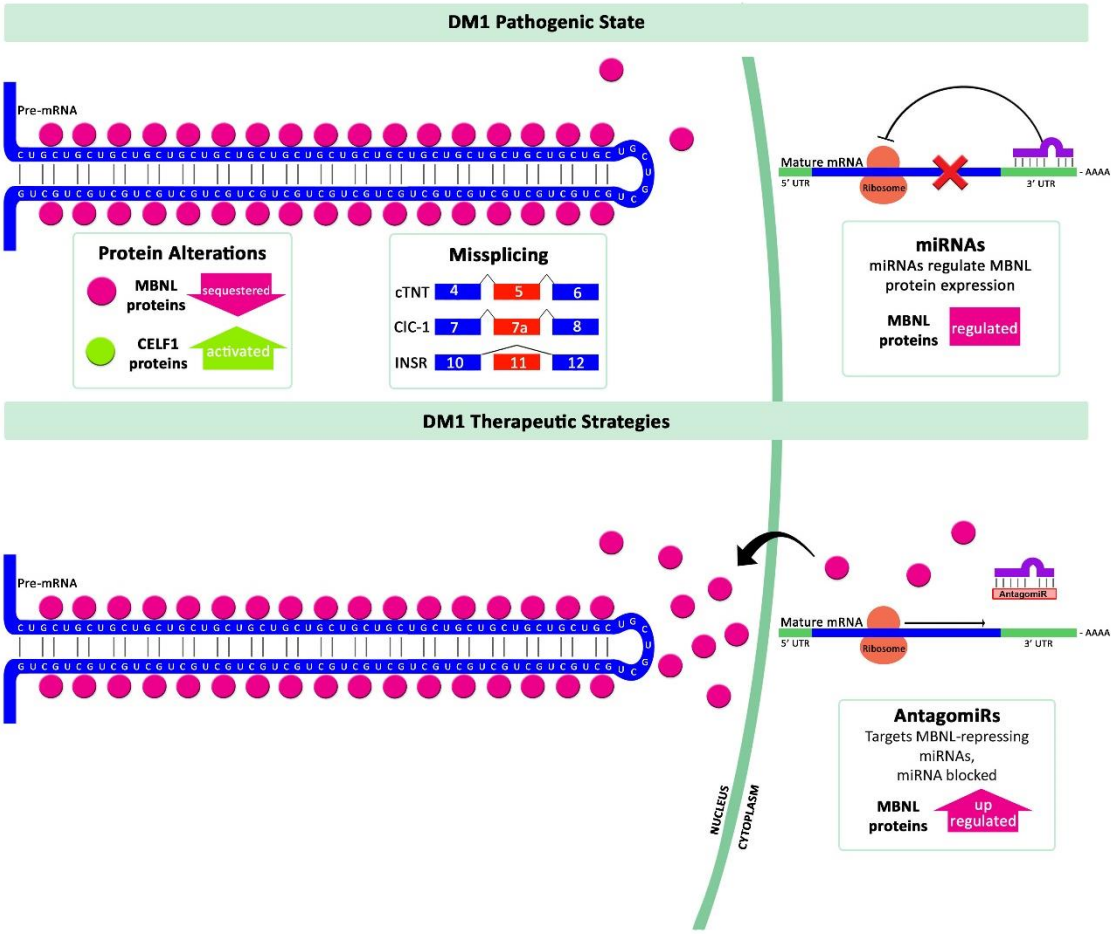

Figura D-1. Terapia basada en AntagomiRs en la distrofia miotónica. (Arriba) Estado patogénico de DM1 donde se incluye el secuestro de proteínas MBNL por los transcritos tóxicos de DMPK, la activación de proteínas CELF y patrones de splicing de tipo fetal alterados. En este estado de DM1 los microRNAs regulan post- transcripcionalmente la expresión de las proteínas MBNL. (Abajo) Se muestra la estrategia terapéutica basada en antagomiRs, donde los antagomiRs diseñados para bloquear la función del miRNA, levantan la represión que ejerce éste sobre el mRNA diana, aumentado la expresión de las proteínas MBNL (Tomado de (Overby et al. 2018).

-Conclusiones-

Las conclusiones que pueden extraerse de los resultados presentados en esta tesis docotoral son las siguientes:

1. La expresión de repeticiones largas de CCTG en músculo de *Drosophila* reproduce varios aspectos de la enfermedad humana tales como: la atrofia muscular, presencia de foci ribonucleares, alteraciones en el *splicing*, limitaciones en la capacidad motora y reducción de la vida media.

2. A diferencia de lo que ocurre en pacientes de DM2, la expresión de expansiones CCUG tiene un potencial de toxicidad *in vivo* en mosca similar al de las expansiones CUG en tejidos musculares, lo que sugiere la existencia de factores moduladores específicos en humanos que inhiben la toxicidad de dichas repeticiones en pacientes con DM2.

3. A pesar de la existencia de diferentes modelos musculares de DM2, la generación de un nuevo modelo de DM2 en *Drosophila* contribuye a la mejor comprensión la patología y proporciona una excelente plataforma donde testar nuevas estrategias terapéuticas *in vivo*.

4. A partir del estudio de prueba de concepto llevado a cabo en moscas modelo de DM1 se consiguió aumentar la expresión endógena de Muscleblind mediante el silenciamiento específico de 2 microRNAs, *dme-miR-277* y *dme-miR-304* identificados en el contexto de este trabajo.

5. La desrepresión de Muscleblind provocada por el silenciamiento de *dme-miR-277* y *dme-miR-304* en moscas modelo de la enfermedad, es suficiente para rescatar de forma significativa diferentes eventos de *splicing* alterados en DM1 y características funcionales tan importantes como la vida media.

6. Un estudio en células HeLa, identificó a *miR-23b* y *miR-218* entre otros microRNAs, como represores de la transcripción y traducción de MBNL1 y MBNL2.

7. El silenciamiento de *miR-23b* y *miR-218* mediado por antagomiRs en mioblastos DM1 desencadena un aumento de los niveles de proteína MBNL1 y MBNL2 y rescata eventos de *splicing* típicamente alterados en la patología.

8. La administración sistémica de estos antagomiRs consigue llegar a músculo de ratones HSA^{LR} DM1 aumentando las proteínas Mbnl1 y Mbnl2 y mejora fenotipos típicos de la enfermedad, incluidas las alteraciones de *splicing*, la histopatología y la miotonía.

9. Un aumento de 2 veces en la expresión de las proteínas Mbnl1 y Mbnl2 es suficiente para rescatar fenotipos en ratones HSA^{LR}, a diferencia de resultados previos en los que se había sobreexpresado mucho más MBNL1.

10. A pesar de que el silenciamiento de *miR-23b* y *miR-218* por el tratamiento con antagomiRs puede tener un efecto deletéreo sobre diversos mRNAs diana, sus beneficios en condiciones patológicas superon a las alteraciones que podía provocar este silenciamiento sobre los mRNAs no deseados.

-Bibliografía -

Adereth, Y., et al. (2005). "*RNA-dependent integrin alpha3 protein localization regulated by the Muscleblind-like protein MLP1.*" Nature Cell Biology **7**(12): 1240-1247.

Ambros, V. (2004). "*The functions of animal microRNAs.*" Nature **431**(7006): 350-355.

Arandel, L., et al. (2017). "*Immortalized human myotonic dystrophy muscle cell lines to assess therapeutic compounds.*" Dis Model Mech **10**(4): 487-497.

Artero, R., et al. (1998). "*The muscleblind gene participates in the organization of Z-bands and epidermal attachments of Drosophila muscles and is regulated by Dmef2.*" Developmental Biology **195**(2): 131-143.

Bargiela, A., et al. (2015). "*Increased autophagy and apoptosis contribute to muscle atrophy in a myotonic dystrophy type 1 Drosophila model.*" Dis Model Mech **8**(7): 679-690.

Bargiela, A., B. Llamusi, E. Cerro-Herreros y R. Artero (2014). "*Two enhancers control transcription of Drosophila muscleblind in the embryonic somatic musculature and in the central nervous system.*" PLoS One **9**(3): e93125.

Bartel, D. P. (2009). "*MicroRNAs: target recognition and regulatory functions.*" Cell **136**(2): 215-233.

Batra, R., et al. (2014). "*Loss of MBNL leads to disruption of developmentally regulated alternative polyadenylation in RNA-mediated disease.*" Mol Cell **56**(2): 311-322.

Batra, R., et al. (2017). "*Elimination of Toxic Microsatellite Repeat Expansion RNA by RNA-Targeting Cas9.*" Cell **170**(5): 899-912 e810.

Begemann, G., et al. (1997). "*muscleblind, a gene required for photoreceptor differentiation in Drosophila, encodes novel nuclear Cys3His-type zinc-finger-containing proteins.*" Development **124**(21): 4321-4331.

Bohnsack, M. T., K. Czaplinski y D. Gorlich (2004). "*Exportin 5 is a RanGTP-dependent dsRNA-binding protein that mediates nuclear export of pre-miRNAs.*" RNA **10**(2): 185-191.

Bouhour, F., M. Bost y C. Vial (2007). "*[Steinert disease].*" Presse Med **36**(6 Pt 2): 965-971.

Brennecke, J., A. Stark, R. B. Russell y S. M. Cohen (2005). "*Principles of microRNA-target recognition.*" PLoS Biol **3**(3): e85.

Brockhoff, M., et al. (2017). "*Targeting deregulated AMPK/mTORC1 pathways improves muscle function in myotonic dystrophy type I.*" J Clin Invest **127**(2): 549-563.

Brook, J. D., et al. (1992). "*Molecular basis of myotonic dystrophy: expansion of a trinucleotide (CTG) repeat at the 3' end of a transcript encoding a protein kinase family member.*" Cell **69**(2): 385.

Buj-Bello, A., et al. (2002). "*Muscle-specific alternative splicing of myotubularin-related 1 gene is impaired in DM1 muscle cells.*" Hum Mol Genet **11**(19): 2297-2307.

Burnett, J. C. y J. J. Rossi (2012). "*RNA-based therapeutics: current progress and future prospects.*" Chem Biol **19**(1): 60-71.

Carthew, R. W. y E. J. Sontheimer (2009). "*Origins and Mechanisms of miRNAs and siRNAs.*" Cell **136**(4): 642-655.

Castanotto, D., et al. (2015). "*A cytoplasmic pathway for gapmer antisense oligonucleotide-mediated gene silencing in mammalian cells.*" Nucleic Acids Res **43**(19): 9350-9361.

Cech, T. R. y J. A. Steitz (2014). "*The Noncoding RNA Revolution-Trashing Old Rules to Forge New Ones.*" Cell **157**(1): 77-94.

Cerro-Herreros, E., et al. (2017). "*Expanded CCUG repeat RNA expression in Drosophila heart and muscle trigger Myotonic Dystrophy type 1-like phenotypes and activate autophagocytosis genes.*" Sci Rep **7**(1): 2843.

Cerro-Herreros, E., et al. (2016). "*Derepressing muscleblind expression by miRNA sponges ameliorates myotonic dystrophy-like phenotypes in Drosophila.*" Sci Rep **6**: 36230.

Cerro-Herreros, E., et al. (2018). "*miR-23b and miR-218 silencing increase Muscleblind-like expression and alleviate myotonic dystrophy phenotypes in mammalian models.*" Nature Communications. Nat Commun. 26;9(1):2482.

Cirak, S., et al. (2011). "*Exon skipping and dystrophin restoration in patients with Duchenne muscular dystrophy after systemic phosphorodiamidate morpholino oligomer treatment: an open-label, phase 2, dose-escalation study.*" Lancet **378**(9791): 595-605.

Coonrod, L. A., et al. (2013). "*Reducing levels of toxic RNA with small molecules.*" ACS Chem Biol **8**(11): 2528-2537.

Creugny, A., A. Fender y S. Pfeffer (2018). "*Regulation of primary microRNA processing.*" FEBS Lett.

Chakraborty, M., et al. (2018). "*Daunorubicin reduces MBNL1 sequestration caused by CUG-repeat expansion and rescues cardiac dysfunctions in a Drosophila model of myotonic dystrophy.*" Dis Model Mech **11**(4).

Chamberlain, C. M. y L. P. Ranum (2012). "*Mouse model of muscleblind-like 1 overexpression: skeletal muscle effects and therapeutic promise.*" Hum Mol Genet **21**(21): 4645-4654.

Chan, J. H., S. Lim y W. S. Wong (2006). "*Antisense oligonucleotides: from design to therapeutic application.*" Clin Exp Pharmacol Physiol **33**(5-6): 533-540.

Charizanis, K., et al. (2012). "*Muscleblind-like 2-mediated alternative splicing in the developing brain and dysregulation in myotonic dystrophy.*" Neuron **75**(3): 437-450.

Charlet, B. N., et al. (2002). "*Loss of the muscle-specific chloride channel in type 1 myotonic dystrophy due to misregulated alternative splicing.*" Mol Cell **10**(1): 45-53.

Chelly, J. y I. Desguerre (2013). "*Progressive muscular dystrophies.*" Handb Clin Neurol **113**: 1343-1366.

Chen, G., et al. (2016). "*Phenylbutazone induces expression of MBNL1 and suppresses formation of MBNL1-CUG RNA foci in a mouse model of myotonic dystrophy.*" Sci Rep **6**: 25317.

Chery, J. (2016). "*RNA therapeutics: RNAi and antisense mechanisms and clinical applications.*" Postdoc J **4**(7): 35-50.

Cho, D. H. y S. J. Tapscott (2007). "*Myotonic dystrophy: emerging mechanisms for DM1 and DM2.*" Biochim Biophys Acta **1772**(2): 195-204.

de Haro, M., et al. (2006). "*MBNL1 and CUGBP1 modify expanded CUG-induced toxicity in a Drosophila model of myotonic dystrophy type 1.*" Human Molecular Genetics **15**(13): 2138-2145.

de Haro, M., et al. (2006). "*MBNL1 and CUGBP1 modify expanded CUG-induced toxicity in a Drosophila model of myotonic dystrophy type 1.*" Hum Mol Genet **15**(13): 2138-2145.

Deiuliis, J. A. (2016). "*MicroRNAs as regulators of metabolic disease: pathophysiologic significance and emerging role as biomarkers and therapeutics.*" Int J Obes (Lond) **40**(1): 88-101.

Dey, B. K., J. Gagan, Z. Yan y A. Dutta (2012). "*miR-26a is required for skeletal muscle differentiation and regeneration in mice.*" Genes Dev **26**(19): 2180-2191.

DiFranco, M., C. Yu, M. Quinonez y J. L. Vergara (2013). "*Age-dependent chloride channel expression in skeletal muscle fibres of normal and HSA(LR) myotonic mice.*" J Physiol **591**(5): 1347-1371.

Dixon, D. M., et al. (2015). "*Loss of muscleblind-like 1 results in cardiac pathology and persistence of embryonic splice isoforms.*" Sci Rep **5**: 9042.

Djuranovic, S., et al. (2010). "*Allosteric regulation of Argonaute proteins by miRNAs.*" Nat Struct Mol Biol **17**(2): 144-150.

Dowdy, S. F. (2017). "*Overcoming cellular barriers for RNA therapeutics.*" Nat Biotechnol **35**(3): 222-229.

Du, H., et al. (2010). "*Aberrant alternative splicing and extracellular matrix gene expression in mouse models of myotonic dystrophy.*" Nat Struct Mol Biol **17**(2): 187-193.

Du, J., et al. (2015). "*RNA toxicity and missplicing in the common eye disease fuchs endothelial corneal dystrophy.*" J Biol Chem **290**(10): 5979-5990.

Ebralidze, A., et al. (2004). "*RNA leaching of transcription factors disrupts transcription in myotonic dystrophy.*" Science **303**(5656): 383-387.

Eisenberg, I., et al. (2007). "*Distinctive patterns of microRNA expression in primary muscular disorders.*" Proc Natl Acad Sci U S A **104**(43): 17016-17021.

Enright, A. J., et al. (2003). "*MicroRNA targets in Drosophila.*" Genome Biol **5**(1): R1.

Exondys 51 FDA. (2016). "https://www.accessdata.fda.gov/drugsatfda_docs/appletter/2016/206488Orig1s000ltr.pdf."

Fardaei, M., et al. (2002). "*Three proteins, MBNL, MBLL and MBXL, co-localize in vivo with nuclear foci of expanded-repeat transcripts in DM1 and DM2 cells.*" Human Molecular Genetics **11**(7): 805-814.

Fernandez-Costa, J. M. y R. Artero (2010). "*A conserved motif controls nuclear localization of Drosophila Muscleblind.*" Mol Cells **30**(1): 65-70.

Fernandez-Costa, J. M. y R. Artero (2010). "*A conserved motif controls nuclear localization of Drosophila Muscleblind.*" Molecules and Cells **30**(1): 65-70.

Fernandez-Costa, J. M., et al. (2013). "*Expanded CTG repeats trigger miRNA alterations in Drosophila that are conserved in myotonic dystrophy type 1 patients.*" Hum Mol Genet **22**(4): 704-716.

Fernandez-Costa, J. M., M. B. Llamusi, A. Garcia-Lopez y R. Artero (2011). "*Alternative splicing regulation by Muscleblind proteins: from development to disease.*" Biological Reviews of the Cambridge Philosophical Society

Ferrari, N., et al. (2006). "*Characterization of antisense oligonucleotides comprising 2'-deoxy-2'-fluoro-beta-D-arabinonucleic acid (FANA): specificity, potency, and duration of activity.*" Ann N Y Acad Sci **1082**: 91-102.

Filipowicz, W., S. N. Bhattacharyya y N. Sonenberg (2008). "*Mechanisms of post-transcriptional regulation by microRNAs: are the answers in sight?*" Nat Rev Genet **9**(2): 102-114.

Fiorillo, A. A., et al. (2015). "*TNF-alpha-Induced microRNAs Control Dystrophin Expression in Becker Muscular Dystrophy.*" Cell Rep **12**(10): 1678-1690.

Fiszer, A. y W. J. Krzyzosiak (2013). "*RNA toxicity in polyglutamine disorders: concepts, models, and progress of research.*" J Mol Med (Berl) **91**(6): 683-691.

Francois, V., et al. (2011). "*Selective silencing of mutated mRNAs in DM1 by using modified hU7-snRNAs.*" Nat Struct Mol Biol **18**(1): 85-87.

Fu, Y. H., et al. (1992). "*An unstable triplet repeat in a gene related to myotonic muscular dystrophy.*" Science **255**(5049): 1256-1258.

Fugier, C., et al. (2011). "*Misregulated alternative splicing of BIN1 is associated with T tubule alterations and muscle weakness in myotonic dystrophy.*" Nat Med **17**(6): 720-725.

Fulga, T. A., et al. (2015). "*A transgenic resource for conditional competitive inhibition of conserved Drosophila microRNAs.*" Nat Commun **6**: 7279.

Gambardella, S., et al. (2010). "*Overexpression of microRNA-206 in the skeletal muscle from myotonic dystrophy type 1 patients.*" J Transl Med **8**: 48.

Gao, Z. y T. A. Cooper (2013). "*Reexpression of pyruvate kinase M2 in type 1 myofibers correlates with altered glucose metabolism in myotonic dystrophy.*" Proc Natl Acad Sci U S A **110**(33): 13570-13575.

Garber, K. (2017). "*Worth the RISC?*" Nat Biotechnol **35**(3): 198-202.

Garcia-Alcover, I., et al. (2014). "*Development of a Drosophila melanogaster spliceosensor system for in vivo high-throughput screening in myotonic dystrophy type 1.*" Dis Model Mech **7**(11): 1297-1306.

Garcia-Lopez, A., et al. (2011). "*In vivo discovery of a peptide that prevents CUG-RNA hairpin formation and reverses RNA toxicity in myotonic dystrophy models.*" Proceedings of the National Academy of Sciences of the United States of America **108**(29): 11866-11871.

Garcia-Lopez, A., et al. (2008). "*Genetic and chemical modifiers of a CUG toxicity model in Drosophila.*" PLoS One **3**(2): e1595.

Gates, D. P., L. A. Coonrod y J. A. Berglund (2011). "*Autoregulated splicing of muscleblind-like 1 (MBNL1) Pre-mRNA.*" J Biol Chem **286**(39): 34224-34233.

Geary, R. S., D. Norris, R. Yu y C. F. Bennett (2015). "*Pharmacokinetics, biodistribution and cell uptake of antisense oligonucleotides.*" Adv Drug Deliv Rev **87**: 46-51.

Goers, E. S., et al. (2010). "*MBNL1 binds GC motifs embedded in pyrimidines to regulate alternative splicing.*" Nucleic Acids Research **38**(7): 2467-2484.

Goers, E. S., R. B. Voelker, D. P. Gates y J. A. Berglund (2008). "*RNA binding specificity of Drosophila muscleblind.*" Biochemistry **47**(27): 7284-7294.

Gomes-Pereira, M., T. A. Cooper y G. Gourdon (2011). "*Myotonic dystrophy mouse models: towards rational therapy development.*" Trends Mol Med **17**(9): 506-517.

Gomes-Pereira, M., et al. (2007). "*CTG trinucleotide repeat "big jumps": large expansions, small mice.*" PLoS Genet **3**(4): e52.

Gomez, I. G., et al. (2015). "*Anti-microRNA-21 oligonucleotides prevent Alport nephropathy progression by stimulating metabolic pathways.*" J Clin Invest **125**(1): 141-156.

Gonzalez-Barriga, A., et al. (2013). "*Design and analysis of effects of triplet repeat oligonucleotides in cell models for myotonic dystrophy.*" Mol Ther Nucleic Acids **2**: e81.

Goodwin, M., et al. (2015). "*MBNL Sequestration by Toxic RNAs and RNA Misprocessing in the Myotonic Dystrophy Brain.*" Cell Rep **12**(7): 1159-1168.

Greco, S., et al. (2012). "*Deregulated microRNAs in myotonic dystrophy type 2.*" PLoS One **7**(6): e39732.

Gregory, R. I., T. P. Chendrimada, N. Cooch y R. Shiekhattar (2005). "*Human RISC couples microRNA biogenesis and posttranscriptional gene silencing.*" Cell **123**(4): 631-640.

Grimson, A., et al. (2007). "*MicroRNA targeting specificity in mammals: determinants beyond seed pairing.*" Mol Cell **27**(1): 91-105.

Guiraud, S., et al. (2015). "*Second-generation compound for the modulation of utrophin in the therapy of DMD.*" Hum Mol Genet **24**(15): 4212-4224.

Guo, H., N. T. Ingolia, J. S. Weissman y D. P. Bartel (2010). "*Mammalian microRNAs predominantly act to decrease target mRNA levels.*" Nature **466**(7308): 835-840.

Hale, M. A., et al. (2018). "*An engineered RNA binding protein with improved splicing regulation.*" Nucleic Acids Res **46**(6): 3152-3168.

Hammond, S. M., et al. (2001). "*Argonaute2, a link between genetic and biochemical analyses of RNAi.*" Science **293**(5532): 1146-1150.

Harley, H. G., et al. (1992). "*Expansion of an unstable DNA region and phenotypic variation in myotonic dystrophy.*" Nature **355**(6360): 545-546.

Haro, M. D., et al. (2006). "*MBNL1 and CUGBP1 modify expanded CUG-induced toxicity in a Drosophila model of Myotonic Dystrophy Type 1.*" Human Molecular Genetics.

Harper, P. (2001). Myotonic dystrophy. London, Saunders.

Hebert, S. S. y B. De Strooper (2009). "*Alterations of the microRNA network cause neurodegenerative disease.*" Trends Neurosci **32**(4): 199-206.

Higham, C. F., et al. (2012). "*High levels of somatic DNA diversity at the myotonic dystrophy type 1 locus are driven by ultra-frequent expansion and contraction mutations.*" Hum Mol Genet **21**(11): 2450-2463.

Ho, T. H., et al. (2004). "*Muscleblind proteins regulate alternative splicing.*" EMBO Journal **23**(15): 3103-3112.

Ho, T. H., et al. (2005). "*Colocalization of muscleblind with RNA foci is separable from mis-regulation of alternative splicing in myotonic dystrophy.*" Journal of Cell Science **118**(Pt 13): 2923-2933.

Hoskins, J. W., et al. (2014). "*Lomofungin and dilomofungin: inhibitors of MBNL1-CUG RNA binding with distinct cellular effects.*" Nucleic Acids Res **42**(10): 6591-6602.

Houseley, J. M., et al. (2005). "*Myotonic dystrophy associated expanded CUG repeat muscleblind positive ribonuclear foci are not toxic to Drosophila.*" Hum Mol Genet **14**(6): 873-883.

Huguet, A., et al. (2012). "*Molecular, physiological, and motor performance defects in DMSXL mice carrying >1,000 CTG repeats from the human DM1 locus.*" PLoS Genet **8**(11): e1003043.

Irion, U. (2012). "*Drosophila muscleblind codes for proteins with one and two tandem zinc finger motifs.*" PLoS One **7**(3): e34248.

Jauvin, D., et al. (2017). "*Targeting DMPK with Antisense Oligonucleotide Improves Muscle Strength in Myotonic Dystrophy Type 1 Mice.*" Mol Ther Nucleic Acids **7**: 465-474.

Jiang, H., et al. (2004). "*Myotonic dystrophy type 1 is associated with nuclear foci of mutant RNA, sequestration of muscleblind proteins and deregulated alternative splicing in neurons.*" Hum Mol Genet **13**(24): 3079-3088.

Jin, J., et al. (2009). "*GSK3beta-cyclin D3-CUGBP1-eIF2 pathway in aging and in myotonic dystrophy.*" Cell Cycle **8**(15): 2356-2359.

Jones, K., et al. (2012). "*GSK3beta mediates muscle pathology in myotonic dystrophy.*" J Clin Invest **122**(12): 4461-4472.

Kalsotra, A., et al. (2014). "*The Mef2 transcription network is disrupted in myotonic dystrophy heart tissue, dramatically altering miRNA and mRNA expression.*" Cell Rep **6**(2): 336-345.

Kalsotra, A., K. Wang, P. F. Li y T. A. Cooper (2010). "*MicroRNAs coordinate an alternative splicing network during mouse postnatal heart development.*" Genes Dev **24**(7): 653-658.

Kalsotra, A., et al. (2008). "*A postnatal switch of CELF and MBNL proteins reprograms alternative splicing in the developing heart.*" Proceedings of the National Academy of Sciences of the United States of America **105**(51): 20333-20338.

Kalsotra, A., et al. (2008). "*A postnatal switch of CELF and MBNL proteins reprograms alternative splicing in the developing heart.*" Proc Natl Acad Sci U S A **105**(51): 20333-20338.

Kamsteeg, E. J., et al. (2012). "*Best practice guidelines and recommendations on the molecular diagnosis of myotonic dystrophy types 1 and 2.*" Eur J Hum Genet **20**(12): 1203-1208.

Kanadia, R. N., et al. (2003). "*A muscleblind knockout model for myotonic dystrophy.*" Science **302**(5652): 1978-1980.

Kanadia, R. N., et al. (2006). "*Reversal of RNA missplicing and myotonia after muscleblind overexpression in a mouse poly(CUG) model for myotonic dystrophy.*" Proc Natl Acad Sci U S A **103**(31): 11748-11753.

Kanadia, R. N., et al. (2003). "*Developmental expression of mouse muscleblind genes Mbnl1, Mbnl2 and Mbnl3.*" Gene Expression Patterns **3**(4): 459-462.

Ketley, A., et al. (2014). "*High-content screening identifies small molecules that remove nuclear foci, affect MBNL distribution and CELF1 protein levels via a PKC-independent pathway in myotonic dystrophy cell lines.*" Hum Mol Genet **23**(6): 1551-1562.

Khvorova, A. y J. K. Watts (2017). "*The chemical evolution of oligonucleotide therapies of clinical utility.*" Nat Biotechnol **35**(3): 238-248.

Kim, D. H., et al. (2005). "*HnRNP H inhibits nuclear export of mRNA containing expanded CUG repeats and a distal branch point sequence.*" Nucleic Acids Res **33**(12): 3866-3874.

Kimura, T., et al. (2005). "*Altered mRNA splicing of the skeletal muscle ryanodine receptor and sarcoplasmic/endoplasmic reticulum Ca2+-ATPase in myotonic dystrophy type 1.*" Hum Mol Genet **14**(15): 2189-2200.

Kino, Y., et al. (2004). "*Muscleblind protein, MBNL1/EXP, binds specifically to CHHG repeats.*" Hum Mol Genet **13**(5): 495-507.

Kino, Y., et al. (2015). "*Nuclear localization of MBNL1: splicing-mediated autoregulation and repression of repeat-derived aberrant proteins.*" Hum Mol Genet **24**(3): 740-756.

Kino, Y., et al. (2009). "*MBNL and CELF proteins regulate alternative splicing of the skeletal muscle chloride channel CLCN1.*" Nucleic Acids Res **37**(19): 6477-6490.

Koebis, M., et al. (2013). "*Ultrasound-enhanced delivery of morpholino with Bubble liposomes ameliorates the myotonia of myotonic dystrophy model mice.*" Sci Rep **3**: 2242.

Koebis, M., et al. (2011). "*Alternative splicing of myomesin 1 gene is aberrantly regulated in myotonic dystrophy type 1.*" Genes Cells **16**(9): 961-972.

Konieczny, P., et al. (2017). "*Myotonic dystrophy: candidate small molecule therapeutics.*" Drug Discov Today **22**(11): 1740-1748.

Koshelev, M., et al. (2010). "*Heart-specific overexpression of CUGBP1 reproduces functional and molecular abnormalities of myotonic dystrophy type 1.*" Hum Mol Genet **19**(6): 1066-1075.

Krol, J., et al. (2007). "*Ribonuclease dicer cleaves triplet repeat hairpins into shorter repeats that silence specific targets.*" Mol Cell **25**(4): 575-586.

Krutzfeldt, J., et al. (2005). "*Silencing of microRNAs in vivo with 'antagomirs'.*" Nature **438**(7068): 685-689.

Kubowicz, P., D. Zelaszczyk y E. Pekala (2013). "*RNAi in clinical studies.*" Curr Med Chem **20**(14): 1801-1816.

Kuyumcu-Martinez, N. M., G. S. Wang y T. A. Cooper (2007). "*Increased steady-state levels of CUGBP1 in myotonic dystrophy 1 are due to PKC-mediated hyperphosphorylation.*" Molecular Cell **28**(1): 68-78.

Lai, E. C. (2002). "*Micro RNAs are complementary to 3' UTR sequence motifs that mediate negative post-transcriptional regulation.*" Nat Genet **30**(4): 363-364.

Latronico, M. V. y G. Condorelli (2009). "*MicroRNAs and cardiac pathology.*" Nat Rev Cardiol **6**(6): 419-429.

Lee, J. E., C. F. Bennett y T. A. Cooper (2012). "*RNase H-mediated degradation of toxic RNA in myotonic dystrophy type 1.*" Proc Natl Acad Sci U S A **109**(11): 4221-4226.

Lee, J. E. y T. A. Cooper (2009). "*Pathogenic mechanisms of myotonic dystrophy.*" Biochem Soc Trans **37**(Pt 6): 1281-1286.

Lee, K. S., R. M. Squillace y E. H. Wang (2007). "*Expression pattern of muscleblind-like proteins differs in differentiating myoblasts.*" Biochemical and Biophysical Research Communications **361**(1): 151-155.

Lee, K. Y., et al. (2013). "*Compound loss of muscleblind-like function in myotonic dystrophy.*" EMBO Mol Med **5**(12): 1887-1900.

Lee, S. T., et al. (2011). "*Altered microRNA regulation in Huntington's disease models.*" Exp Neurol **227**(1): 172-179.

Lee, Y., et al. (2004). "*MicroRNA genes are transcribed by RNA polymerase II.*" EMBO J **23**(20): 4051-4060.

Lee, Y. S., et al. (2004). "*Distinct roles for Drosophila Dicer-1 and Dicer-2 in the siRNA/miRNA silencing pathways.*" Cell **117**(1): 69-81.

Leger, A. J., et al. (2013). "*Systemic delivery of a Peptide-linked morpholino oligonucleotide neutralizes mutant RNA toxicity in a mouse model of myotonic dystrophy.*" Nucleic Acid Ther **23**(2): 109-117.

Leroy, O., et al. (2006). "*Brain-specific change in alternative splicing of Tau exon 6 in myotonic dystrophy type 1.*" Biochim Biophys Acta **1762**(4): 460-467.

Lewis, B. P., et al. (2003). "*Prediction of mammalian microRNA targets.*" Cell **115**(7): 787-798.

Li, L. B. y N. M. Bonini (2010). "*Roles of trinucleotide-repeat RNA in neurological disease and degeneration.*" Trends Neurosci **33**(6): 292-298.

Li, S. S., et al. (2009). "*Target identification of microRNAs expressed highly in human embryonic stem cells.*" J Cell Biochem **106**(6): 1020-1030.

Lim, L. P., et al. (2005). "*Microarray analysis shows that some microRNAs downregulate large numbers of target mRNAs.*" Nature **433**(7027): 769-773.

Lin, X., et al. (2006). "*Failure of MBNL1-dependent post-natal splicing transitions in myotonic dystrophy.*" Human Molecular Genetics **15**(13): 2087-2097.

Lin, X., et al. (2006). "*Failure of MBNL1-dependent postnatal splicing transitions in myotonic dystrophy.*" Hum Mol Genet.

Liquori, C. L., et al. (2001). "*Myotonic dystrophy type 2 caused by a CCTG expansion in intron 1 of ZNF9.*" Science **293**(5531): 864-867.

Liu, C., et al. (2011). "*The microRNA miR-34a inhibits prostate cancer stem cells and metastasis by directly repressing CD44.*" Nat Med **17**(2): 211-215.

Liu, N., et al. (2012). "*microRNA-206 promotes skeletal muscle regeneration and delays progression of Duchenne muscular dystrophy in mice.*" J Clin Invest **122**(6): 2054-2065.

Loro, E., et al. (2010). "*Normal myogenesis and increased apoptosis in myotonic dystrophy type-1 muscle cells.*" Cell Death Differ **17**(8): 1315-1324.

Llamusi, B., et al. (2013). "*Muscleblind, BSF and TBPH are mislocalized in the muscle sarcomere of a Drosophila myotonic dystrophy model.*" Dis Model Mech **6**(1): 184-196.

Machuca-Tzili, L., et al. (2006). "*Flies deficient in Muscleblind protein model features of myotonic dystrophy with altered splice forms of Z-band associated transcripts.*" Hum Genet **120**: 487-499.

Madsen A, M. (2017). "https://strongly.mda.org/ionis-reports-setback-dmpkrx-program-myotonic-dystrophy/."

Mahadevan, M., et al. (1992). "*Myotonic dystrophy mutation: an unstable CTG repeat in the 3' untranslated region of the gene.*" Science **255**(5049): 1253-1255.

Mahadevan, M. S., et al. (2006). "*Reversible model of RNA toxicity and cardiac conduction defects in myotonic dystrophy.*" Nature Genetics **38**(9): 1066-1070.

Mankodi, A., et al. (2000). "*Myotonic dystrophy in transgenic mice expressing an expanded CUG repeat.*" Science **289**(5485): 1769-1773.

Mankodi, A., et al. (2002). "*Expanded CUG repeats trigger aberrant splicing of ClC-1 chloride channel pre-mRNA and hyperexcitability of skeletal muscle in myotonic dystrophy.*" Mol Cell **10**(1): 35-44.

Mankodi, A., et al. (2003). "*Ribonuclear inclusions in skeletal muscle in myotonic dystrophy types 1 and 2.*" Annals of Neurology **54**(6): 760-768.

Martorell, L., et al. (1998). "*Progression of somatic CTG repeat length heterogeneity in the blood cells of myotonic dystrophy patients.*" Hum Mol Genet **7**(2): 307-312.

Masuda, A., et al. (2012). "*CUGBP1 and MBNL1 preferentially bind to 3' UTRs and facilitate mRNA decay.*" Sci Rep **2**: 209.

Mathieu, J., et al. (1999). "*A 10-year study of mortality in a cohort of patients with myotonic dystrophy.*" Neurology **52**(8): 1658-1662.

Matranga, C., et al. (2005). "*Passenger-strand cleavage facilitates assembly of siRNA into Ago2-containing RNAi enzyme complexes.*" Cell **123**(4): 607-620.

Mele, M., et al. (2015). "*Human genomics. The human transcriptome across tissues and individuals.*" Science **348**(6235): 660-665.

Melo, S. A. y M. Esteller (2011). "*Dysregulation of microRNAs in cancer: playing with fire.*" FEBS Lett **585**(13): 2087-2099.

Mendell, J. R., et al. (2013). "*Eteplirsen for the treatment of Duchenne muscular dystrophy.*" Ann Neurol **74**(5): 637-647.

Meola, G. y R. Cardani (2015). "*Myotonic dystrophies: An update on clinical aspects, genetic, pathology, and molecular pathomechanisms.*" Biochim Biophys Acta **1852**(4): 594-606.

Meola, G. y R. Cardani (2017). "*Myotonic dystrophy type 2 and modifier genes: an update on clinical and pathomolecular aspects.*" Neurol Sci **38**(4): 535-546.

Meola, G. y R. T. Moxley, 3rd (2004). "*Myotonic dystrophy type 2 and related myotonic disorders.*" J Neurol **251**(10): 1173-1182.

Meola, G. y V. Sansone (1996). "*A newly-described myotonic disorder (proximal myotonic myopathy--PROMM): personal experience and review of the literature.*" Ital J Neurol Sci **17**(5): 347-353.

Meola, G., et al. (1996). "*A family with an unusual myotonic and myopathic phenotype and no CTG expansion (proximal myotonic myopathy syndrome): a challenge for future molecular studies.*" Neuromuscul Disord **6**(3): 143-150.

Michalowski, S., et al. (1999). "*Visualization of double-stranded RNAs from the myotonic dystrophy protein kinase gene and interactions with CUG-binding protein.*" Nucleic Acids Research **27**(17): 3534-3542.

Miller, J. W., et al. (2000). "*Recruitment of human muscleblind proteins to (CUG)(n) expansions associated with myotonic dystrophy.*" EMBO J **19**(17): 4439-4448.

Monckton, D. G., L. J. Wong, T. Ashizawa y C. T. Caskey (1995). "*Somatic mosaicism, germline expansions, germline reversions and intergenerational reductions in myotonic dystrophy males: small pool PCR analyses.*" Hum Mol Genet **4**(1): 1-8.

Mooers, B. H., J. S. Logue y J. A. Berglund (2005). "*The structural basis of myotonic dystrophy from the crystal structure of CUG repeats.*" Proc Natl Acad Sci U S A **102**(46): 16626-16631.

Morales, F., et al. (2012). "*Somatic instability of the expanded CTG triplet repeat in myotonic dystrophy type 1 is a heritable quantitative trait and modifier of disease severity.*" Hum Mol Genet **21**(16): 3558-3567.

Mulders, S. A., et al. (2009). "*Triplet-repeat oligonucleotide-mediated reversal of RNA toxicity in myotonic dystrophy.*" Proc Natl Acad Sci U S A **106**(33): 13915-13920.

Mykowska, A., et al. (2011). "*CAG repeats mimic CUG repeats in the misregulation of alternative splicing.*" Nucleic Acids Res **39**(20): 8938-8951.

Nakamori, M., et al. (2008). "*Aberrantly spliced alpha-dystrobrevin alters alpha-syntrophin binding in myotonic dystrophy type 1.*" Neurology **70**(9): 677-685.

Nakamori, M., et al. (2013). "*Splicing biomarkers of disease severity in myotonic dystrophy.*" Ann Neurol **74**(6): 862-872.

Nakamori, M., et al. (2016). "*Oral administration of erythromycin decreases RNA toxicity in myotonic dystrophy.*" Ann Clin Transl Neurol **3**(1): 42-54.

Nielsen, C. B., et al. (2007). "*Determinants of targeting by endogenous and exogenous microRNAs and siRNAs.*" RNA **13**(11): 1894-1910.

Obad, S., et al. (2011). "*Silencing of microRNA families by seed-targeting tiny LNAs.*" Nat Genet **43**(4): 371-378.

Oddo, J. C., et al. (2016). "*Conservation of context-dependent splicing activity in distant Muscleblind homologs.*" Nucleic Acids Res **44**(17): 8352-8362.

Osborne, R. J. y C. A. Thornton (2006). "*RNA-dominant diseases.*" Hum Mol Genet **15 Spec No 2**: R162-169.

Ottosen, S., et al. (2015). "*In vitro antiviral activity and preclinical and clinical resistance profile of miravirsen, a novel anti-hepatitis C virus therapeutic targeting the human factor miR-122.*" Antimicrob Agents Chemother **59**(1): 599-608.

Overby, S., E. Cerro-Herreros, B. Llamusi y R. Artero (2018). "*RNA-Mediated Therapies in Myotonic Dystrophy* " Drug Discovery Today (aceptado).

Pandey, S. K., et al. (2015). "*Identification and characterization of modified antisense oligonucleotides targeting DMPK in mice and nonhuman primates for the treatment of myotonic dystrophy type 1.*" J Pharmacol Exp Ther **355**(2): 329-340.

Parkesh, R., et al. (2012). "*Design of a bioactive small molecule that targets the myotonic dystrophy type 1 RNA via an RNA motif-ligand database and chemical similarity searching.*" J Am Chem Soc **134**(10): 4731-4742.

Paul, S., et al. (2006). "*Interaction of muscleblind, CUG-BP1 and hnRNP H proteins in DM1-associated aberrant IR splicing.*" EMBO Journal **25**(18): 4271-4283.

Peng, Y. y C. M. Croce (2016). "*The role of MicroRNAs in human cancer.*" Signal Transduct Target Ther **1**: 15004.

Perbellini, R., et al. (2011). "*Dysregulation and cellular mislocalization of specific miRNAs in myotonic dystrophy type 1.*" Neuromuscul Disord **21**(2): 81-88.

Perfetti, A., et al. (2014). "*Plasma microRNAs as biomarkers for myotonic dystrophy type 1.*" Neuromuscul Disord **24**(6): 509-515.

Peter, M. E. (2010). "*Targeting of mRNAs by multiple miRNAs: the next step.*" Oncogene **29**(15): 2161-2164.

Picchio, L., et al. (2013). "*Novel Drosophila model of myotonic dystrophy type 1: phenotypic characterization and genome-wide view of altered gene expression.*" Hum Mol Genet **22**(14): 2795-2810.

Poulos, M. G., et al. (2013). "*Progressive impairment of muscle regeneration in muscleblind-like 3 isoform knockout mice.*" Hum Mol Genet **22**(17): 3547-3558.

Ranum, L. P. y J. W. Day (2004). "*Myotonic dystrophy: RNA pathogenesis comes into focus.*" Am J Hum Genet **74**(5): 793-804.

Ranum, L. P., et al. (1998). "*Genetic mapping of a second myotonic dystrophy locus.*" Nat Genet **19**(2): 196-198.

Rau, F., et al. (2011). "*Misregulation of miR-1 processing is associated with heart defects in myotonic dystrophy.*" Nat Struct Mol Biol **18**(7): 840-845.

Ravel-Chapuis, A., et al. (2012). "*The RNA-binding protein Staufen1 is increased in DM1 skeletal muscle and promotes alternative pre-mRNA splicing.*" J Cell Biol **196**(6): 699-712.

Ricker, K., et al. (1994). "*Proximal myotonic myopathy: a new dominant disorder with myotonia, muscle weakness, and cataracts.*" Neurology **44**(8): 1448-1452.

Rzuczek, S. G., M. R. Southern y M. D. Disney (2015). "*Studying a Drug-like, RNA-Focused Small Molecule Library Identifies Compounds That Inhibit RNA Toxicity in Myotonic Dystrophy.*" ACS Chem Biol **10**(12): 2706-2715.

Salisbury, E., et al. (2008). "*Ectopic expression of cyclin D3 corrects differentiation of DM1 myoblasts through activation of RNA CUG-binding protein, CUGBP1.*" Exp Cell Res **314**(11-12): 2266-2278.

Santoro, M., et al. (2013). "*Molecular, clinical, and muscle studies in myotonic dystrophy type 1 (DM1) associated with novel variant CCG expansions.*" J Neurol **260**(5): 1245-1257.

Santoro, M., et al. (2014). "*Alternative splicing alterations of Ca2+ handling genes are associated with Ca2+ signal dysregulation in myotonic dystrophy type 1 (DM1) and type 2 (DM2) myotubes.*" Neuropathol Appl Neurobiol **40**(4): 464-476.

Savkur, R. S., A. V. Philips y T. A. Cooper (2001). "*Aberrant regulation of insulin receptor alternative splicing is associated with insulin resistance in myotonic dystrophy.*" Nat Genet **29**(1): 40-47.

Savkur, R. S., et al. (2004). "*Insulin receptor splicing alteration in myotonic dystrophy type 2.*" Am J Hum Genet **74**(6): 1309-1313.

Schara, U. y B. G. Schoser (2006). "*Myotonic dystrophies type 1 and 2: a summary on current aspects.*" Semin Pediatr Neurol **13**(2): 71-79.

Schober, A., et al. (2014). "*MicroRNA-126-5p promotes endothelial proliferation and limits atherosclerosis by suppressing Dlk1.*" Nat Med **20**(4): 368-376.

Schoser, B. y L. Timchenko (2010). "*Myotonic dystrophies 1 and 2: complex diseases with complex mechanisms.*" Curr Genomics **11**(2): 77-90.

Sellier, C., et al. (2018). "rbFOX1/MBNL1 competition for CCUG RNA repeats binding contributes to myotonic dystrophy type 1/type 2 differences." Nat Commun 9(1): 2009).

Sen, S., et al. (2010). "*Muscleblind-like 1 (Mbnl1) promotes insulin receptor exon 11 inclusion via binding to a downstream evolutionarily conserved intronic enhancer.*" Journal of Biological Chemistry **285**(33): 25426-25437.

Sergeant, N., et al. (2001). "*Dysregulation of human brain microtubule-associated tau mRNA maturation in myotonic dystrophy type 1.*" Hum Mol Genet **10**(19): 2143-2155.

Seznec, H., et al. (2001). "*Mice transgenic for the human myotonic dystrophy region with expanded CTG repeats display muscular and brain abnormalities.*" Hum Mol Genet **10**(23): 2717-2726.

Seznec, H., et al. (2000). "*Transgenic mice carrying large human genomic sequences with expanded CTG repeat mimic closely the DM CTG repeat intergenerational and somatic instability.*" Hum Mol Genet **9**(8): 1185-1194.

Shirdel, E. A., W. Xie, T. W. Mak y I. Jurisica (2011). "*NAViGaTing the micronome--using multiple microRNA prediction databases to identify signalling pathway-associated microRNAs.*" PLoS One **6**(2): e17429.

Siboni, R. B., et al. (2015). "*Actinomycin D Specifically Reduces Expanded CUG Repeat RNA in Myotonic Dystrophy Models.*" Cell Rep **13**(11): 2386-2394.

Sobczak, K., T. M. Wheeler, W. Wang y C. A. Thornton (2013). "*RNA interference targeting CUG repeats in a mouse model of myotonic dystrophy.*" Mol Ther **21**(2): 380-387.

Soutschek, J., et al. (2004). "*Therapeutic silencing of an endogenous gene by systemic administration of modified siRNAs.*" Nature **432**(7014): 173-178.

Spinraza FDA (2016). "*https://www.accessdata.fda.gov/drugsatfda_docs/nda/2016/209531Orig1s000Approv.pdf.*"

Suenaga, K., et al. (2012). "*Muscleblind-like 1 knockout mice reveal novel splicing defects in the myotonic dystrophy brain.*" PLoS One **7**(3): e33218.

Tang, Z. Z., et al. (2012). "*Muscle weakness in myotonic dystrophy associated with misregulated splicing and altered gating of Ca(V)1.1 calcium channel.*" Hum Mol Genet **21**(6): 1312-1324.

Teplova, M. y D. J. Patel (2008). "*Structural insights into RNA recognition by the alternative-splicing regulator muscleblind-like MBNL1.*" Nature Structural & Molecular Biology **15**(12): 1343-1351.

Terenzi, F. y A. N. Ladd (2010). "*Conserved developmental alternative splicing of muscleblind-like (MBNL) transcripts regulates MBNL localization and activity.*" RNA Biology **7**(1): 43-55.

Thomas, J. D., et al. (2017). "*Disrupted prenatal RNA processing and myogenesis in congenital myotonic dystrophy.*" Genes Dev **31**(11): 1122-1133.

Thornton, C. A., R. C. Griggs y R. T. Moxley, 3rd (1994). "*Myotonic dystrophy with no trinucleotide repeat expansion.*" Ann Neurol **35**(3): 269-272.

Thornton, C. A., E. Wang y E. M. Carrell (2017). "*Myotonic dystrophy: approach to therapy.*" Curr Opin Genet Dev **44**: 135-140.

Tian, B., et al. (2000). "*Expanded CUG repeat RNAs form hairpins that activate the double-stranded RNA-dependent protein kinase PKR.*" RNA **6**(1): 79-87.

Timchenko, L. (2013). "*Molecular mechanisms of muscle atrophy in myotonic dystrophies.*" Int J Biochem Cell Biol **45**(10): 2280-2287.

Timchenko, N. A., et al. (2001). "*RNA CUG repeats sequester CUGBP1 and alter protein levels and activity of CUGBP1.*" Journal of Biological Chemistry **276**(11): 7820-7826.

Tran, H., et al. (2011). "*Analysis of exonic regions involved in nuclear localization, splicing activity, and dimerization of Muscleblind-like-1 isoforms.*" J Biol Chem **286**(18): 16435-16446.

Udd, B. y R. Krahe (2012). "*The myotonic dystrophies: molecular, clinical, and therapeutic challenges.*" Lancet Neurol **11**(10): 891-905.

Udd, B., et al. (1997). "*Proximal myotonic dystrophy--a family with autosomal dominant muscular dystrophy, cataracts, hearing loss and hypogonadism: heterogeneity of proximal myotonic syndromes?*" Neuromuscul Disord **7**(4): 217-228.

Udd, B., et al. (2011). "*Myotonic dystrophy type 2 (DM2) and related disorders report of the 180th ENMC workshop including guidelines on diagnostics and management 3-5 December 2010, Naarden, The Netherlands.*" Neuromuscul Disord **21**(6): 443-450.

Uhlen, M., et al. (2015). "*Proteomics. Tissue-based map of the human proteome.*" Science **347**(6220): 1260419.

van Solingen, C., et al. (2009). "*Antagomir-mediated silencing of endothelial cell specific microRNA-126 impairs ischemia-induced angiogenesis.*" J Cell Mol Med **13**(8A): 1577-1585.

Vicente-Crespo, M., et al. (2008). "*Drosophila muscleblind is involved in troponin T alternative splicing and apoptosis.*" PLoS One **3**(2): e1613.

Vicente, M., et al. (2007). "*Muscleblind isoforms are functionally distinct and regulate alpha-actinin splicing.*" Differentiation **75**(5): 427-440.

Vicente, M., et al. (2007). "*Muscleblind isoforms are functionally distinct and regulate alpha-actinin splicing.*" Differentiation **75**(5): 427-440.

Vihola, A., et al. (2003). "*Histopathological differences of myotonic dystrophy type 1 (DM1) and PROMM/DM2.*" Neurology **60**(11): 1854-1857.

Wagner, S. D., et al. (2016). "*Dose-Dependent Regulation of Alternative Splicing by MBNL Proteins Reveals Biomarkers for Myotonic Dystrophy.*" PLoS Genet **12**(9): e1006316.

Wallace, L. M., S. E. Garwick-Coppens, R. Tupler y S. Q. Harper (2011). "*RNA interference improves myopathic phenotypes in mice over-expressing FSHD region gene 1 (FRG1).*" Mol Ther **19**(11): 2048-2054.

Wang, E. T., et al. (2012). "*Transcriptome-wide regulation of pre-mRNA splicing and mRNA localization by muscleblind proteins.*" Cell **150**(4): 710-724.

Wang, G. S., et al. (2009). "*PKC inhibition ameliorates the cardiac phenotype in a mouse model of myotonic dystrophy type 1.*" J Clin Invest **119**(12): 3797-3806.

Warf, M. B. y J. A. Berglund (2007). "*MBNL binds similar RNA structures in the CUG repeats of myotonic dystrophy and its pre-mRNA substrate cardiac troponin T.*" RNA.

Warf, M. B., J. V. Diegel, P. H. von Hippel y J. A. Berglund (2009). "*The protein factors MBNL1 and U2AF65 bind alternative RNA structures to regulate splicing.*" Proc Natl Acad Sci U S A **106**(23): 9203-9208.

Warf, M. B., et al. (2009). "*Pentamidine reverses the splicing defects associated with myotonic dystrophy.*" Proceedings of the National Academy of Sciences of the United States of America **106**(44): 18551-18556.

Wheeler, T. M., et al. (2012). "*Targeting nuclear RNA for in vivo correction of myotonic dystrophy.*" Nature **488**(7409): 111-115.

Wheeler, T. M., et al. (2007). "*Correction of ClC-1 splicing eliminates chloride channelopathy and myotonia in mouse models of myotonic dystrophy.*" The Journal Of Clinical Investigation **117**(12): 3952-3957.

Wu, C., et al. (2016). "*BioGPS: building your own mash-up of gene annotations and expression profiles.*" Nucleic Acids Res **44**(D1): D313-316.

Wu, S., et al. (2010). "*Multiple microRNAs modulate p21Cip1/Waf1 expression by directly targeting its 3' untranslated region.*" Oncogene **29**(15): 2302-2308.

Xiao, F., et al. (2009). "*miRecords: an integrated resource for microRNA-target interactions.*" Nucleic Acids Res **37**(Database issue): D105-110.

Yamashita, Y., et al. (2014). "*LDB3 splicing abnormalities are specific to skeletal muscles of patients with myotonic dystrophy type 1 and alter its PKC binding affinity.*" Neurobiol Dis.

Yamashita, Y., et al. (2012). "*Four parameters increase the sensitivity and specificity of the exon array analysis and disclose 25 novel aberrantly spliced exons in myotonic dystrophy.*" J Hum Genet **57**(6): 368-374.

Yenigun, V. B., et al. (2017). "*(CCUG)n RNA toxicity in a Drosophila model of myotonic dystrophy type 2 (DM2) activates apoptosis.*" Dis Model Mech **10**(8): 993-1003.

Yu, Z., et al. (2015). "*A fly model for the CCUG-repeat expansion of myotonic dystrophy type 2 reveals a novel interaction with MBNL1.*" Hum Mol Genet **24**(4): 954-962.

Zanetta, C., et al. (2014). "*Molecular therapeutic strategies for spinal muscular atrophies: current and future clinical trials.*" Clin Ther **36**(1): 128-140.